Advances in Functional Materials 2023

7th International Conference

'Development of Functional Materials for a Better World'

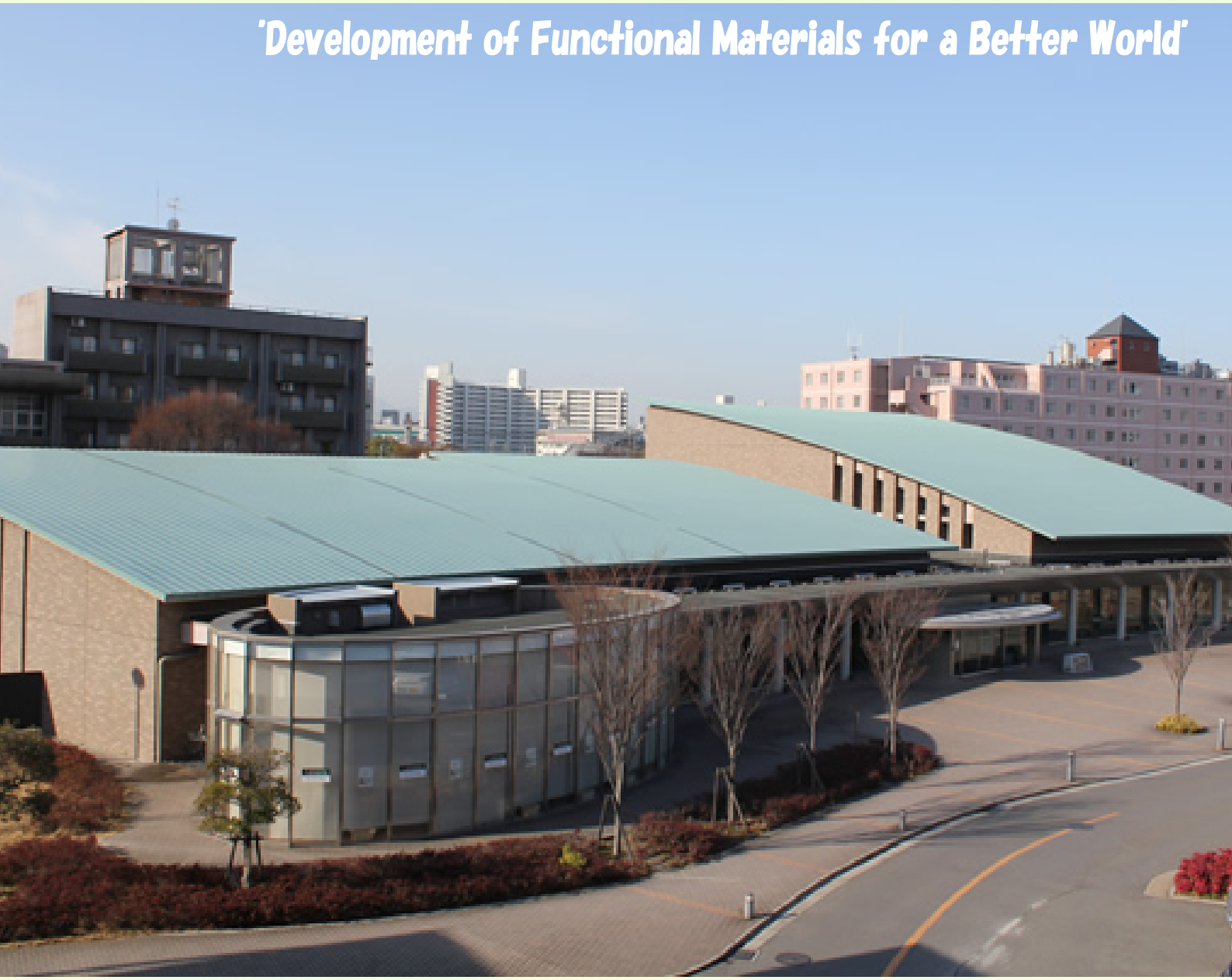

Program Book

AFM 2023 : January 09-12, 2023

'Development of Functional Materials for a Better World'

https://functionalmaterials.org/afm2022/

International Advisory Committee

Following well-known names in the field of advanced functional materials is part of our organizing committee.

SeungNam Cha Sungkyunkwan, Korea
Zhong Lin Wang Georgia Tech, USA
Hui-Ming Cheng Chinese Academy of Sciences, China
Kazuhiro Takanabe King Abdullah University of Science and Technology (KAUST)
Vivek Polshettiwar Tata Institute of Fundamental Research (TIFR), India
Arindam Ghosh Indian Institute of Science, India
Li Zhang The Chinese University of Hong Kong
Xiangfeng Duan University of California Los Angeles
Arun Kumar Amity University, Noida, India
Michael De Volder University of Cambridge, UK
Jose Rodriguez Brookhaven National Laboratory Upton, NY, USA
Rajeev S. Assary Argonne National Laboratory, Lemont IL, USA
Bin Zhu KTH, Stockholm, Sweden
N. Ali Chairman CNC Coatings, UK
Mohamed Bououdina University of Bahrain
Jean-Marie Basset Director, KAUST Catalysis Research Center
Fuat Celik Rutgers University, New Jersey, USA
Chang-Yong Nam Brookhaven National Lab, BNL
Prof. Dae Joon Kang Sungkyunkwan University, Jangan-gu Suwon, Korea
Prof. Imran Shakir King Saud University, Saudi Arabia

Local Organizing Committee

Professor Masaharu Shiratani Kyushu University, LOC Chair
Professor Kenshi Hayashi Kyushu University
Professor Atsushi Masuda Niigata University
Doctor Shota Nunomura National Institute of Advanced Industrial Science and Technology (AIST)
Professor Tamiko Ohshima Sasebo National College of Technology
Professor Giichiro Uchida Meijo University

AFM2023 Welcome Message

Welcome to AFM2023

Advances in Functional Materials (AFM) Conference is held at The Kyushu University School of Medicine Centennial Hall, Kyushu, Japan from January 0-12, 2023. AFM is an annual conference started in 2015, supported by a number of universities in the world. In particular, AFM is one of the well-reputed conferences on the advancement of functional materials science and technology, a meaningful occasion to confirm major research results and up-to-date research trends in the world, increase exchanges among researchers in relevant fields, and materialize the results of research. AFM Conference attendees include engineers, scientists, educators, and students who seek to establish fruitful research relationships with global and international partners for future collaboration.

Fukuoka is the ideal surrounding to meet and discuss equally intriguing functional materials in an relaxed atmosphere, enjoying the high-quality scientific program of AFM2023. The Organizing Committee of AFM2023 welcome all of the participants.

白谷正治

Masaharu Shiratani
Local Organizing Committee Chairman of AFM2023
Senior Vice President,
Director of Center of Plasma Nano-interface Engineering,
Distinguished Professor, Graduate School of Information Science and Electrical Engineering,
Kyushu University, Japan

Date: Monday, 09/Jan/2023

3:00pm - 5:00pm Exchange Lobby	**Registration: Registration** Location: **Exchange Lobby**	

Date: Tuesday, 10/Jan/2023

8:40am - 3:00pm Exchange Lobby	**Registration-1: Registration** Location: **Exchange Lobby I**	
8:50am - 9:00am Main Hall	**Open Cerem: Opening Ceremony** Location: **Main Hall**	
9:00am - 9:45am Main Hall	**Plen Sess: Plenary Session** Location: **Main Hall**	P1
9:45am - 10:00am	**Coffee Break-1: Coffee Break**	
10:00am - 12:06pm Main Hall	**Invited Talk-1: Invited Talk** Location: **Main Hall**	P2-4
12:00pm - 1:15pm	**Lunch Break-1: Lunch Break**	
1:15pm - 2:15pm Main Hall	**Keynote Session-1: Keynote Session** Location: **Main Hall**	P5
2:30pm – 4:18pm Main Hall	**Oral Talk-9: Oral Talk** Location: **Main Hall**	P6-9
2:30pm – 4:18pm Hall 1&2	**Oral Talk-3: Oral Talk** Location: **Hall 1&2**	P10-13
2:30pm – 4:18pm Hall 3	**Oral Talk-1: Oral Talk** Location: **Hall 3**	P14-17
3:30pm - 5:00pm Exchange Hall and Exchange Lobby	**Poster Session-1: Poster Session** Location: **Exchange Hall and Exchange Lobby**	P18-38

Date: Wednesday, 11/Jan/2023

8:40am - 3:00am Exchange Lobby	**Registration-2: Registration** Location: **Exchange Lobby**	
8:45am - 10:45am Main Hall	**Keynote Session-2: Keynote Session** Location: **Main Hall**	P39-40
10:45am - 11:00am	**Coffee Break-2: Coffee Break**	
11:00am - 11:54pm Main Hall	**Invited Talk-2: Invited Talk** Location: **Main Hall**	P41
12:00pm - 1:15pm	**Lunch Break-2: Lunch Break**	
1:15pm – 2:40pm Main Hall	**Invited Talk-3: Invited Talk** Location: **Main Hall**	P42-43
1:15pm – 3:51pm Hall 1&2	**Oral Talk-2: Oral Talk** Location: **Hall 1&2**	P44-48
1:15pm - 3:51pm Hall 3	**Oral Talk-4: Oral Talk** Location: **Hall 3**	P49-53
2:40pm – 4:04pm Main Hall	**Oral Talk-10: Oral Talk** Location: **Main Hall**	P54-56
3:30pm – 5:00pm Exchange Hall and Exchange Lobby	**Poster Session-2: Poster Session** Location: **Exchange Hall and Exchange Lobby**	P58-77

Date: Thursday, 12/Jan/2023

8:40am - 12:00pm Exchange Lobby	**Registration-3: Registration** Location: **Exchange Lobby**	
8:45am - 10:45am Hall 1&2	**Keynote Session-3: Keynote Session** Location: **Hall 1&2**	P78-79
8:45am - 10:45am Hall 3	**Oral Talk-5: Oral Talk** Location: **Hall 3**	P80-83
10:45am - 11:00am	**Coffee Break-3: Coffee Break**	
11:00am - 12:36pm Hall 1&2	**Oral Talk-11: Oral Talk** Location: **Hall 1&2**	P84-86
11:00am - 12:36pm Hall 3	**Oral Talk-6: Oral Talk** Location: **Hall 3**	P87-89
12:40pm - 2:00pm	**Lunch Break-3: Lunch Break**	
2:00pm - 3:36pm Hall 1&2	**Oral Talk-7: Oral Talk** Location: **Hall 1&2**	P90-92
2:00pm - 3:36pm Hall 3	**Oral Talk-8: Oral Talk** Location: **Hall 3**	P93-95

Presentations

Plen Sess: Plenary Session

Time: Tuesday, 10/Jan/2023: 9:00am – 9:45am · *Location:* Main Hall

9:00am - 9:45am

Wide bandgap and ultrawide bandgap semiconductors

Hiroshi Amano

Nagoya University, Nagoya, Japan; amano@nuee.nagoya-u.ac.jp

I would like to focus on the necessity of the research and development of wide bandgap and ultrawide bandgap semiconductors, especially GaN, AlN and their alloys as examples. The contributions of GaN and related materials in LED lighting for energy savings are huge. The applications of these materials systems are not limited to lighting. By replacing Si-based power IGBTs with GaN-based power devices, we can expect at least a 10% reduction in the total electricity consumption. GaN-based high-voltage power devices should become the key devices in establishing renewable-energy-based electricity grids because of their high-speed switching and high-voltage capability. GaN-based high-frequency and high-power transistors will provide a unique solution for realizing millimeter-wave and even THz wireless communication systems. By spatially modifying the alloy composition while maintaining the coherent growth, we can realize either a p-type or n-type layer without any impurity doping. These new types of doping, called distributed polarization doping (DPD), were applied to p-type AlGaN with high Al composition, for which it had long been very difficult to realize a highly conducting p-layer by Mg doping. By a conventional Mg doping method, the emission wavelength of III-nitrides LDs was limited to 338 nm, while with the DPD method, LDs with emission wavelengths as short as 271.8 nm have been realized [1]. Recently, the continuous-wave operation of DUV LDs has been achieved [2]. Using the DPD method, it is also possible to realize a p-n junction diode without any impurity-doped layer [3]. Fabrication of DUV LDs is conducted under the collaborative research with Asahi Kasei.

Funding: This work was supported by MEXT-Program for Creation of Innovative Core Technology for Power Electronics Grant Number JPJ009777 and JSPS KAKENHI under Grant No. JP22H00213.

References:

[1] Z. Zhang, M. Kushimoto, T. Sakai, N. Sugiyama, L. J. Schowalter, C. Sasaoka, and H. Amano, Appl. Phys. Exp., 12, 124003 (2019).

[2] Z. Zhang, M. Kushimoto, A. Yoshikawa, K. Aoto, L. J. Schowalter, C. Sasaoka, and H. Amano, Appl. Phys. Exp., 15, 041007 (2022).

[3] T. Kumabe, S. Kawasaki, H. Watanabe, S. Nitta, Y. Honda, and H. Amano, Physica Status Solidi RRL, 2200127 (2022).

Invited Talk-1: Invited Talk

Time: Tuesday, 10/Jan/2023: 10:00am - 12:06pm · *Location:* Main Hall

10:00am - 10:18am

Development of the new multi-structured hybrid photocatalysts for water splitting and purification

Rak Hyun Jeong[1,2], Ji Won Lee[1,2], Jin-Hyo Boo[1,2]

[1]Department of Chemistry, Sungkyunkwan University, Suwon 440-746, Korea.; [2]Institue of Basic Science, Sungkyunkwan University, Suwon 440-746, Korea.; jhboo@skku.edu

As the industrial development improves, environmental issues are also on the rise, and many studies have been proposed to solve them [1]. Photocatalysts are active materials based on solar energy, an infinite resource that can be easily obtained, and have optimal conditions for solving environmental problems such as solar energy conversion (Hydrogen Evolution) and eco-friendly decomposition of pollutants (Water and Air Treatment) [2-4]. In this study, synthesis and characterization of the new photocatalysts were studied by establishing synthetic parameters under mild conditions, and presented as follows. First, a Ti-based peroxo (Ti-OOH) complex was successfully synthesized by oxidizing the surface of a metallic titanium hydride (TiH2) precursor using hydrogen peroxide (H2O2), which is easy to react even under mild oxidizing conditions as a green oxidizing agent.

Additionally, 2D materials have the fast mobility due to 2-dimensional Massless Dirac Fermions, Klein Tunneling, Half-Integer Quantum Hall Effect, but has good electrical properties even though it is difficult to control. The Red Phosphorus (RP) substance that composes phosphorene consists of a single element with an atomic number of 15, and belongs to the non-metal group. There are many naturally occurring and basically, it is highly reactive and various allotropes exist. Allotropes of phosphorus have different crystal structures and different properties. It is possible to design materials with various properties through the combination and control between allotropes.

Based on this, we successfully synthesized the new RP allotropes composite that will dramatically increase the hydrogen generation effect of Ti-OOH complex. Through this, organic pollutant decomposition experiments were conducted under visible light, and eco-friendly energy research, which has the advantages that only water and carbon dioxide are formed as a by-product, such as volatile organic compound oxidation characteristics, was also carried out. Various optical and physico-chemical properties were analyzed at the interface between RP allotropes composite and Ti-OOH complex, and as a result, it was confirmed that high photocatalytic hydrogen evolution efficiency in visible light was obtained by increasing the life time of the light induced carrier (electron-hole pairs). In addition, optimal efficiency increase was achieved by designing materials with desired properties through control of RP allotropes composite.

10:18am - 10:36am

New Copper Sulfide Electrodes for Electronics and Optoelectronics Applications

Sangyeon Pak

School of Electronic and Electrical Engineering, Hongik University; spak@hongik.ac.kr

We introduce a new class of covellite copper monosulfide (CuS) nanosheet film as a promising candidate for transparent, flexible conductive electrodes, which can be employed in various flexible and wearable electronic and optoelectronic devices. Especially, the presentation will cover its employment as the source-drain electrode materials for 2D MoS2 channel. We achieved record high electron mobility up to 100 cm2V-1s-1 at room temperature in a back-gate device configuration. We will also cover effective doping method to tune its electrical and optical properties.

10:36am - 10:54am

Externally-stimulated Metal-Insulator-Transition of Vanadium Dioxide Thin Films on Flexible Glass Substrate

Min Kyun Sohn[1], Hardeep Singh[2], Ha Young Choi[2], Dae Joon Kang[2]

[1]Department of Physics and Institute of Basic Science, Sungkyunkwan University, 2066 Seobu-ro, Jangan-gu, Suwon, Gyeonggi-do 16419, Republic of Korea; [2]Department of Physics, Sungkyunkwan University, 2066 Seobu-ro, Jangan-gu, Suwon 16419, Gyeonggi-do, Republic of Korea; djkang@skku.edu

Vanadium dioxide (VO2) is an archetypal solid-state system that undergoes the first-order phase transition near room temperature (~ 68 ℃) concurrently with structural distortion. Since lattice strain could effectively control the order parameters such as lattice, spin, charge, and orbital, many reports are focused on strain manipulation using external and interfacial strain. Earlier studies utilized the lattice mismatch between substrate and thin films to induce the strain effect, but the strain in thin films is limited to deposition conditions and substrate selection specifically. In addition, post-annealing, doping, and ion implantation were carried out to reveal the systematic effect of strain in thin films. However, these strategies are not reversible to control the phase transition in VO2 thin films. Even though reversible phase transition through external strain in nanobeams or nanowires has been demonstrated, their mechanical strength limits practical applicability. In this study, we demonstrate reversible phase transition in VO2 thin films grown on the flexible glass substrate through external strain. The electrical property tuned through external strain reveals excellent stability and reversibility of phase transition behavior. In addition, structural and optical properties show similar behavior even after repeatedly applied external strain, showing excellent mechanical stability. These results not only provide essential knowledge for understanding the correlation between external strain and VO2 thin film properties but also suggest applicability to strain-based phase change devices.

10:54am - 11:12am

Development of HEMT-based hydrogen sensor and Study of its standard-based test method

Kyung-Ho Park[1], Chu-Young Cho[1], Sang Hyun Jung[1], Jong Hyuk Yim[2], Hosang Lee[2]

[1]Convergence Technology Division, Korea Advanced Nano Fab Center (KANC), Suwon 16229, South Korea; [2]Netmics Co., Seongnam, Gyeonggi-do, South Korea; kyungho.park@kanc.re.kr

Hydrogen is colorless, odorless, non-toxic, and the lightest gas under atmospheric conditions. Also, hydrogen is a flammable gas, and the flammability range (between 4% and 75% in air) is very wide compared to other fuels. Therefore, to ensure the safe use of hydrogen, developing highly sensitive hydrogen sensors and properly testing their performance is essential.

AlGaN/GaN HEMT (high electron mobility transistor) typically shows the extremely sensitive nature of the adsorption on the gate surface. For the use of this property as a sensing mechanism, we fabricated a hydrogen sensor using a conventional HEMT fabrication process with a thin Pt layer as a sensing material and gate contact. The HEMT hydrogen sensor shows two possible operational modes of the negative shift of threshold voltage and the increase of gate leakage-current as H2 exposure. Using the threshold voltage shift mode, we observed the HEMT hydrogen sensor characteristics of a very high sensitivity of 109 % and a relatively short response time of 6 sec at 0.5% hydrogen concentration and room temperature. It was also observed the HEMT hydrogen sensor has good gas selectivity to CO and CH4 gases.

In this study, we report the development results of AlGaN/GaN HEMT hydrogen sensor and also discuss the test method of HEMT hydrogen sensor based on present International Standards for hydrogen sensors.

11:12am -11:30pm

Nanostructured Copper Sulfide Electrode Materials for Electrochemical Energy Storage Performance

John Hong

Kookmin University, Korea, Republic of (South Korea); johnhong@kookmin.ac.kr

Managing the structure and morphology of transition metal sulfide electrodes plays a crucial role in determining the physical and electrochemical characteristics of energy-storing applications. Usually, electrochemical performance is related to the interaction between electrode materials and electrolyte ions at the surface of electrodes. Therefore, properly structured electrode morphology can show high electrochemical performance due to its high surface area, short ion path, and structural robustness, which can enhance high specific capacitance, favorable ion diffusion kinetics, and stable cyclability. A variety of synthetic methods for nanostructured electrodes have demanded multiple time-consuming processes, different synthetic input energies (heat of electric current), and various precursor solutions. Here we introduce a new and practical synthetic route to design the hierarchically structured transition copper sulfide electrodes by using a direct exposure method on highly active sulfide solution (Ammonium Sulfide). The major synthetic process with the solution is that the ammonium sulfide solution can rapidly react with Cu, and the Cu ions emanating due to the activity of ammonium ions. The dissolved Cu and sulfur ions in the solution can converted to the copper sulfide materials. By controlling the parameters of synthesis, the diverse structures of copper sulfide electrodes are induced, and the different electrochemical performance has been characterized. This synthetic method ensures a facile and efficient approach to fabricating scalable and hierarchical copper sulfide nanostructures, highlighting the uniqueness of the solution-based sulfur activation method.

11:30pm - 11:48pm

A Magnetic Iron Oxide Nanoneedles for the Catalytic Reduction of 4-Nitrophenol

Hyokyung Jeon[1], Ha-Jin Lee[2]

[1]Western Seoul Center, Korea Basic Science Institute, 150 Bugahyun-ro, Seoudaemun-gu, Seoul 03759, Republic of Korea; [2]Division of Chemistry and Bio-Environmental Sciences, Seoul Women's University, Seoul 01797, Republic of Korea; hajinlee@swu.ac.kr

Designing catalyst systems with high catalytic activity and sustainability is highly desired. Here we present the preparation of hierarchical nanostructured magnetic iron oxide nanoneedles (mIO) and their application as catalysts for nitrophenol reduction. The hierarchical magnetic nanoneedles were prepared by a successive coating of polydopamine, metal nanoparticles, and iron oxide nanoneedles on a magnetic core. The thickness of the polydopamine layer can be controlled by varying the concentration of dopamine precursor. In addition, by controlling the composition of metal ion precursors, multi-metallic nanoparticle embedded mIO could be prepared (M-mIO). The M-mIO exhibited excellent performance of catalytic activity for the reduction of 4-nitrophenol showing the reduction was completed within 3 min. The M-mIO catalysts significantly improved the catalytic activity through the synergistic effect of iron oxide and multi-metallic nanoparticles. Furthermore, the magnetically recyclable nanocatalysts were readily separated using an external magnet and reused up to 5 times without any loss of the catalytic activity.

This work was supported by a research grant from Seoul Women's University (2021-0409) and Nano·Material Technology Development Program through the National Research Foundation of Korea(NRF) funded by the Ministry of Science, ICT and Future Planning. (2009-0082580).

11:48pm - 12:06pm

Diamond-based electronic tongues system: from CVD growth to applications

Shinya Ohmagari

Sensing System Research Center, National Institute of Advanced Industrial Science and Technology, Japan;
shinya.ohmagari@aist.go.jp

An electronic tongue (e-tongue) is a system made of sensors responding to some tastes of foods, cosmetics, and biochemical solutions through the transduction of a pattern of spectrum thanks to a pattern-recognition software system [1]. While general-purpose sensors are good at selectively detecting and quantifying specific “targeted” components, e-tongues handle input signals with a mixture of chemical components characterized statistically by machine learning, neural network, and so on. Diamond chemical sensors made from conductive boron-doped diamond films have the widest potential windows among materials, and their excellent chemical stability enables highly sensitive electrochemical detection with small background currents. They attract much attention as electrodes for chemical sensors that can detect environmental pollutants, as well as for bio- and health-care monitoring [2]. Here, we propose an e-tongue system made from diamond chemical sensors which enables a prompt analysis (one minute and one drop) of food/beverage, life science, and environmental monitoring. Key issues developing diamond-based electronic tongues including CVD growth will be presented in the talk.

Acknowledgment

This work was partially supported by JST SCORE Team Promotion Type, Grant Number JPMJST2133 and Adaptable and Seamless Technology transfer Program through Target-driven R&D (A-STEP) from Japan Science and Technology Agency (JST) Grant Number JPMJTR22R2.

References

[1] A. Riul et al., “Recent advances in electronic tongues”, Analyst, 135, 2481 (2010).

[2] Y. Einaga, “Development of Electrochemical Applications of Boron-Doped Diamond Electrodes”, Bull. Chem. Soc. Jpn. 91, 1752 (2018)

Keynote Session-1: Keynote Session

Time: Tuesday, 10/Jan/2023: 1:15pm - 2:15pm · *Location:* Main Hall

1:15pm - 1:45pm

Hybridisation of perovskite nanocrystals with organic molecules for X-ray sensing

Hyunsik Im, Hyungsang Kim

Department of Physics and Semiconductor Science, Dongguk University, Seoul 04620, Korea *Email: hyunsik7@dongguk.edu; hyunsik7@dongguk.edu

A hybrid liquid scintillator could be used in low-dose radiation detectors for use in imaging applications and scientific research. Highly sensitive X-ray detection is increasingly being used in industrial and military applications and for fundamental scientific research. Although liquid scintillators are more resilient to damage from exposure to intense radiation than crystalline or plastic scintillators, they have relatively low density and low radioluminescence quantum yields, both of which are critical for achieving high resolution and contrast in X-ray imaging.

Here, a new generation of highly efficient and low-cost liquid scintillators constructed by surface hybridisation of colloidal metal halide perovskite CsPbA3 (A: Cl, Br, I) nanocrystals (NCs) with organic molecules (2,5-diphenyloxazole) is presented. Experimental and theoretical analyses suggest that the enhanced quantum yield is associated with X-ray photon-induced charge transfer from the organic molecules to the NCs. High-resolution X-ray imaging is demonstrated using a hybrid CsPbBr3 NC-based liquid scintillator. The novel hybrid scintillator device could see use in a wide range of X-ray technologies that require high-performance detectors and imagers.

1:45pm - 2:15pm

Electrical-driven spin synapsis and neuron networks in HM/FM material layer stacks for artificial intelligence applications

Jin Pyo Hong

Hanyang University, Korea, Republic of (South Korea); jphong@hanyang.ac.kr

One long-standing goal in the emerging field of neuromorphic system is to build up a generic computing architecture ensuring low energy consumption, fault tolerant, and massively parallel computation. In this regard, artificial neuron and synapses emulating intelligent functions of human brain have emerged as alternative options for efficient computation, learning, and memory. Herein, we address typical AI trends and concept of and spin dynamics-based-AI functions by using spin transfer/orbit torques. Synaptic short-term functions including the reversible facilitation, potentiation, and depression were clearly identified, along with the achievement of long-term potentiation under repeated stimuli. Based on the extensive analyses of electrical/structural findings, we describe a possible mechanism for the observed synaptic/neuron features.

Oral Talk-9: Oral Talk

Time: Tuesday, 10/Jan/2023: 2:30pm – 4:18pm · *Location:* Main Hall

2:30pm – 2:42pm

High electrical conductivity LiAlGePO films deposited by plasma co-sputtering for Li-ion battery application

Giichiro Uchida, Junki Hayashi, Yuma Habu, Kenta Nagai

Meijo University/Japan, Japan; uchidagi@meijo-u.ac.jp

Li-ion battery has the advantages of high capacity, long cycle life, and low environmental pollution, which is attributable to the serious safety issues caused by the volatile and flammable organic liquid electrolyte, such as electrolyte leakage and fire hazard. Currently, it is an effective approach to solve the above problem by developing All-solid-state Li-ion batteries which replace the liquid electrolytes with the inorganic solid electrolytes. Recently, we have reported high-capacity Ge anodes fabricated by high-pressure plasma sputtering in the sub-Torr range [1]. In this study, we developed LiAlGePO solid electrolyte material in low-temperature plasma process, in order to apply it to all-solid-state Li-ion batteries with high-capacity Ge anode.

LiAlGePO films were deposited by using RF magnetron co-sputtering with 1-inch targets of Li3PO4 (source 1) and Li1.5Al0.5Ge1.5(PO4)3 (source 2). The pressure of Ar discharge gas was 0.5 Pa. The rf power density of source 1 (Li3PO4 sputtering target) was varied from 0 to 9.8 W/cm2. On the other hand, the power density of source 2 (Li1.5Al0.5Ge1.5(PO4)3 sputtering target) was fixed to be 3.9 W/cm2. We performed a combinatorial deposition: a total of five substrates were set in the radial direction (r) to the targets at r = –30～30 mm, where r = 0 denotes the center position of substrate holder.

The P/Ge content ratio in the LiAlGePO film markedly changed at the substrate positions and rf power density, and was successfully controlled in the wide range from 1.6 to 23. We obtained the ionic conductivity over 10-6 S/cm in LiAlGePO film with adequate P/Ge content ratio at room temperature. The relationship between the chemical composition and ionic conductivity of the LiAlGePO film will be discussed in detail.

2:42pm - 2:54pm

High performance-highly flexible, hierarchical metal network transparent conducting electrodes for Cu(In, Ga)Se2 thin-film solar cell

Seoin Kang, Eunyeong Yang, Choong-Heui Chung

Hanbat National University, Korea, Republic of (South Korea); kseoin0116@gmail.com

In optoelectronic devices such as touch screen panels, solar cells, and light emitting diodes, the transparent conductive layer is the most important element controlling the input and output of light. Therefore, such a transparent conducting electrodes (TCEs) requires high transmittance and, at the same time, high conductivity and strong durability against mechanical stress. Indium tin oxide (ITO), which is currently the most widely used transparent electrode material in industry, can be easily applied to various substrates using physical vapor deposition (PVD), but it is difficult to use as an electrode material requiring flexibility due to brittleness. As a result, metal mesh and metal nanowires are being explored as potential replacements for ITO. Metal mesh has the advantage of being able to flexibly control light transmittance and electrical conductivity according to the network formation method, and silver nanowires have high thermal and chemical stability and can be solution-processed, enabling mass synthesis. In this study, we fabricated a hierarchical silver network using silver micromesh as the primary framework and silver nanowires as secondary framework. Silver nanowires provide a local path for electric current to flow into adjacent layers, while micromesh provides a major path for electric current to flow throughout the network. This hierarchical network had a higher figure of merit than ITO, and the resistance increase was negligible at 2.7% even after 150 bends. When applied to Cu(In, Ga)Se2 thin film solar cells, the hierarchical network performance was better than that of individual TCEs. Silver nanowires can be better incorporated into devices without sacrificing the transmittance of the highly conductive micromesh. Consequently, the hierarchical network can be the best choice as an efficient TCE for Cu(In, Ga)Se2 thin-film solar cells.

2:54pm – 3:06pm

Gas visualization by SERS substrate fabricated by a simple sputtering method

lin chen, Takuya Matsuo, Fumihiro Sassa, Kenshi Hayashi

Kyushu University, Japan; chen.lin.658@s.kyushu-u.ac.jp

Gas sensors with high sensitivity and selectivity are vital in the detection of low concentration gas. Surface-Enhanced Raman Scattering (SERS) technique has been increasingly used for fabricating gas sensors due to its excellent selectivity, ultra-sensitive and rapid-detection performance1,2. In this work, a SERS gas sensor was developed by a simple sputtering method and its application of gas visualization was achieved.

Gas visualization could be realized by using its Raman signals after it's detected by the SERS sensor. Herein, two types of SERS sensors were fabricated by sputtering Ag nanoparticles (AgNPs) on the glass substrate (substrate 1) and annealing the Ag-sputtered substrate (substrate 2) (Fig 1 (a)). The size of AgNPs was roughly similar on substrate 1, large and small size nanoparticles were simultaneously observed on substrate 2 (Fig 1 (b)). Smaller AgNPs were sputtered into the middle of the larger AgNPs (substrate 2), which could shorten the distances of nanogaps and increase the numbers of hot spots between the larger and surrounding smaller AgNPs. In Fig 1 (c), the intensities of characteristic peaks in the Raman spectrum of acetophenone gas obtained from substrate 1 were higher and more homogeneous. Hence, the intensity values of the peak at 1006 cm-1 collected by scanning the sensor were used for gas visualization. Due to the flowability of gas, the amounts of gas molecules adsorbed varied from the positions on the SERS sensor, thus intensity values were different. Gas adsorption mainly occurs in the middle of the sensor (Fig 1 (d)). Our future plan includes the development of mixture gases visualization through the different distinct characteristic Raman peaks of the gases.

3:06pm – 3:18pm

Plasmonic Library Based on Substrate-Supported Au@Ag Core-shell Nanoparticles

Hao Guo, Fumihiro Sassa, Kenshi Hayashi
Department of Electronics, Graduate School of Information Science and Electrical Engineering, Kyushu university;
guo.hao.097@s.kyushu-u.ac.jp

Noble gold nanoparticles (NPs), such as gold (Au) and silver (Ag), exhibit unique optical properties arising from localized surface plasmon resonance (LSPR), which can be applied for biosensing, imaging, biomedicine, and surface-enhanced Raman scattering (SERS), etc. Bimetallic nanoparticles such as Au@Ag Core-shell NPs are particularly attention due to Ag not only being more attractive for optoelectronics, photovoltaics, and sensing but also coupling between Au and Ag can exhibit better performance than single metal.

In this research, we demonstrate a seed-mediated synthesis that is able to generate Ag shells over substrate-immobilized Au nano seeds by light irradiation. Prior to this study, the adaptation of light-driven seed-mediated growth modes to substrate-immobilized seeds have relied on single Au material [1,2], we extend this approach to the synthesis of bimetallic NPs. As light-driven growth mode, Ag shell thickness could be tuned by simply controlling the light irradiation time or light intensity, therefore, by adding a simple grayscale gradient photomask to the light source, different intensities of light can be irradiated in different areas of one substrate. By this means, Au@Ag Core-shell NPs of various sizes can be fabricated on one substrate, which is called “plasmonic library”. In 2014, Mareen and co-workers were the first to demonstrate the concept of “plasmonic library” and fabricated the corresponding substrate [3], further developed research focused on Au nano-stars libraries for SERs application was proposed in 2021 [4]. Therefore, the Au@Ag Core-shell plasmonic library substrate fabricated in this research is expected to be an excellent candidate for SERS-based analytical.

3:18pm - 3:30pm

Micro and nanoarchitecture of 3D printed ceramic scaffolds for osteoconduction and bone augmentation.

Franz E. Weber
University of Zurich, Switzerland; franz.weber@zzm.uzh.ch

In the last decades, advances in bone tissue engineering mainly based on osteoinduction and on stem cell research. Only recently, new efforts by others and us focused on the micro- and nanoarchitecture needed to improve and accelerate bone regeneration. By the use of additive manufacturing, libraries of diverse microarchitectures were produced and tested to identify the ideal pore size or rod distance for osteoconduction to occur. Presently, we try to elucidate the dependency of osteoconduction on microporosity and expand our view on micro- and nanoarchitecture of bone substitutes for optimal bone augmentation.

For the production of scaffolds, we applied for titanium-based scaffolds selective laser melting and for ceramics the CeraFab 7500 from Lithoz, a lithography-based additive manufacturing machine. As in vivo test model, we used a calvarial defect and a bone augmentation model in rabbits.

The histomorphometric analysis showed that bone formation was significantly increased with pores between 0.7-1.2 mm in diameter. Best microarchitecture for osteoconduction and bone augmentation are different. Moreover, microporosity appeared to be a strong driver of osteoconduction and influenced osteoclastic degradation for tri-calcium phosphate based scaffolds. For hydroxyapatite based scaffolds, however, microporosity appears to influence osteoconductivity to a lesser extent.

In essence, additive manufacturing enables to generate libraries of microarchitectures to search for the most osteoconductive microarchitecture for orthopaedics and the ideal microarchitecture for bone augmentation purposes. Moreover, additive manufacturing appears as a promising tool for the production of personalized bone tissue engineering scaffolds to be used in cranio-maxillofacial surgery, dentistry, and orthopaedics.

3:30pm -3:42pm

Self-healing chemiresistor gas sensor component with healing agent supply mechanism

Takumi Takesue, Fumihiro Sassa, Kenshi Hayashi
Kyushu Univ., Japan; takesue.takumi.679@s.kyushu-u.ac.jp

In recent years, one of important application of gas sensors is to monitor the health condition from the gas emitted by a person. As a gas sensor that is compatible with this application, there is a chemiresistor gas sensor that is lightweight, flexible, and easy to increase the number of channels. However, one of the obstacles to putting this gas sensor into practical use is that the degradation of gas response due to long-term use. Self-healing material which can be recover mechanical property from damage have been reported in recent years. To extend the idea, we are developing electronic components with self-healing function. In this work, we developed a self-healing gas sensor system with active chemical healing processing to extend the life of the chemiresistor.

A chemiresistor is an electrical resistance element that responds to chemical substances and is made by mixing a conductive material with an insulating solvent. Adsorption of chemicals causes the polymer to swell and change the conductive path in the mixed material, resulting in a change in its conductivity. By this feature, it is used as a gas sensor by measuring the change in electrical resistance that occurs in the mixed material when an odor substance is adsorbed.

However, if it is used continuously for a long time, the distribution of the conductive material in the chemiresistor will be biased and the gas response ability will be degraded. We have confirmed that this degradation can be restored by dropping ethanol as healing agent, on the gas sensing material. And more, we have developed a microfluidic mechanism to automatically perform this healing process. This mechanism consists of three layers: an acrylic reservoir for storing the healing agent, an Au micro-heater sputtered on a polypropylene adhesive tape to trigger the discharge of the healing agent, and a chemiresistor gas sensor formed by inkjet printing on photographic paper with hydrophobic flow channel. When we want to supply the solution, we apply electric current to the micro heater via silver ink printed on photographic paper, and the resulting high temperature make a pin hole on the adhesive tape. Finally, the healing agent in reservoir is discharged. We will also evaluate the functional recovery efficiency of gas responsiveness by this healing mechanism and the extension of the life as a sensor.

3:42pm – 3:54pm

Stretch-Insensitive E-Skin based on Hybrid Response Pressure Sensors (HRPS)

Nanshu Lu

The University of Texas at Austin, United States of America; nanshulu@utexas.edu

Soft pressure sensors can be applied on e-tattoos for mechanophysiology measurements or as e-skins on human-mimetic robotics. After decades of research on soft capacitive pressure sensors, their sensitivity has been significantly improved at low pressures but still decays drastically as the pressure increases.[1] To overcome this bottleneck, we have engineered a hybrid response pressure sensor (HRPS) by laminating a barely electrically conductive porous nanocomposite (PNC) with an ultrathin (500-nm-thick) insulating layer. The HRPS was measured to have a sensitivity of 3.13 /kPa within 0-1 kPa, 1.65 /kPa within 1-5 kPa, 1.16 /kPa within 5-10 kPa, 0.68 /kPa within 10-30 kPa, and 0.43 /kPa within 30-50 kPa of pressure ranges, representing up to 423% improvement over existing capacitive pressure sensors. It is the first capacitive pressure sensor that benefits from both piezoresistivity and piezocapacitivity. The mechanism of HRPS was fully understood through a simplified circuit model, which has been validated by experimental measurements and could be used to determine the optimal f-CNT doping concentration.[2] With improvement in the fabrication process, HRPS could be made stretchable, which we call SHRPS (stretchable hybrid response pressure sensor). We found that given the enormous pressure sensitivity, the capacitance change of SHRPS due to out-of-plane pressure is significantly larger than that due to in-plane stretch. Therefore, SHRPS is insensitive to stretch and has been applied as an intrinsically stretchable pressure sensor with 4 x 4 electrodes on an inflatable robotic finger. When the robotic finger is inflated, it is stiff and curved, which is ideal for pulse checking, even with wrist movement. When the robotic finger is deflated, it is soft and flat, which is ideal for grabbing both stiff and soft brittle materials without causing any damage.[3] SHRPS is the first intrinsically stretchable but stretch-insensitive e-skin that can endow highly deformable soft robots with accurate haptic sensation.

[1] Ha, K.-H., Huh, H., Li, Z., and Lu, N.: 'Soft capacitive pressure sensors: trends and challenges', ACS Nano (invited perspective by Rising Star Awardee), 2021, submitted.

[2] Ha, K.-H., Zhang, W., Jang, H., Kang, S., Wang, L., Tan, P., Hwang, H., and Lu, N.: 'Highly sensitive capacitive pressure sensors over wide pressure range enabled by the hybrid responses of a highly porous nanocomposite', Adv Mater, 2021, pp. 2103320

[3] Ha, K.-H., Huh, H., Li, Z., Kim, S., Kang, S., Wang, Z., Scalco de Vasconcelos, L., and Lu, N.: 'E-Skin based on Stretchable Hybrid Response Pressure Sensors (SHRPS)', 2021, in preparation

3:54pm – 4:06pm

Chemical synthesis of acid-resistant β-Ga2O3 disperse particles for photocatalytic applications

Ilya Mikhailovich Sosnin, Lilia Sokura, Alexei Evgenievich Romanov

ITMO University, Russian Federation; sim.nanosci@gmail.com

The main reason of the high relevance of photocatalytic methods for the effective treatment of wastewater and industrial air-exhausts is the possibility of complete removal of toxic impurities (even of low concentrations) without by-product formation. The most important is purification of acidic wastewater and exhaust, where the crucial issue is the choice of a semiconductor material, which is resistant to harsh environment and displays photocatalytic activity under chosen range of electromagnetic radiation.

Monoclinic modification of gallium oxide (β-Ga2O3) does correspond these criteria. For example, Zhao and Zhang in Ref. [1] described the oxidation of perfluorooctanoic acid, Asakura et al. in Ref. [2] presented the example of photocatalytic air purification from nitrogen oxides. Moreover, it is β-Ga2O3 that demonstrates the highest activity in comparison with other gallium oxide allotropic modifications. Hou et al. reported in Ref. [3] that the rate of photocatalytic oxidation decreases in the series β-Ga2O3 > α-Ga2O3 > γ-Ga2O3.

Since the structure of β-Ga2O3 is described by the space group C2/m, there is anisotropy of all physical properties of this crystalline phase, including the anisotropy of photocatalytic activity. Therefore, the photocatalytic activity of dispersed β-Ga2O3 particles with different morphologies but with the same specific surface area will differ. The correlation between the anisotropy of the structure and the rate of photocatalysis is known for various semiconductors [4, 5].

In our work, fabrication of dispersed particles having different morphology is implemented by the methods of colloid chemistry. These methods make it possible to synthesize particles in the micro- and nanometer size range. The formation of particles occurs because of chemical reactions in a liquid phase. The conditions of chemical synthesis, in particular the composition of the reaction mixture, directly impact the morphology, size, and defective structure of the formed particles. Usually, the chemical synthesis of metal oxide crystals is based on the interaction of the precursors of these metals and alkali.

In conclusion, we have demonstrated the influence of synthesis conditions on the morphology of β-Ga2O3 dispersed particles and on their catalytic activity.

4:06pm – 4:18pm

Effects of Dispersion Solvent-Ionomer Interactions on Selective CO2 Electrolysis to C2+ Products over Copper-Coated Gas Diffusion Electrodes

Mohamed Nazmi Idros[1], Yuming Wu[1], Timothy Duignan[1], Mengran Li[1,2], Thomas Edward Rufford[1]

[1]the University of Queensland, Australia; [2]Delft University of Technology; m.idros@uq.edu.au

Electrolysis powered by renewable electricity is a promising approach to converting carbon dioxide (CO2) into valuable fuel and feedstocks. A major challenge associated with this technology is the limited supply of CO2 to the catalyst where the electrochemical CO2 reduction (CO2RR) occurs. This limits the CO2RR reactivity and selectivity. By tuning the structure and composition of the catalyst layer (CL), the supply of CO2 to the catalyst can be enhanced, and CO2RR performance and stability can be improved. Ionomers are a common component in the CL and are typically dispersed in a catalyst ink solvent during CL fabrication. While this solvent quickly

evaporates, the solvent can still impact the final ionomer conformation in the CL.[1, 2] Here, we demonstrate the role of ionomer-solvent interaction in diluted and concentrated catalyst ink and its impact on CO2RR performance.

In this study, we chose Aquivion® (a type of perfluorinated sulfonic acid, PFSA) as the ionomer model and compared acetone and methanol as the solvents. We show that acetone exhibits stronger interaction with the ionomer backbone than methanol, resulting in a more continuous catalyst layer with greater film hydrophobicity than the CL formed using methanol dispersion. This is attributed to acetone's lower solubility parameter, which induces greater Aquivion® backbone mobility than methanol. Consequently, the CL made with acetone yields greater selectivity to C2 products at high current density, up to 30% higher than CL derived with methanol at 200 mA cm-2. Predominantly, the C2 primary product is ethylene, with ethylene faradaic efficiency reaching up to 39.8 ± 2.4 % for the CL prepared from acetone compared to 27.8 ± 8.0 % for CL prepared with methanol at 200 mA cm-2. With a more continuous and hydrophobic ionomer film due to acetone, CL is modulated to show a high local pH and improved gas transport, synergistically promoting the formation of C2 products. However, the acetone-derived CL displays a higher overpotential at all current densities due to the high surface coverage of Aquivion's non-conductive backbone on CL, limiting the electron transfer. Our findings demonstrate the potential of an alternative strategy for optimising the local reaction environment, which will benefit all electrochemical designs.

[1] B. A. W. Mowbray, D. J. Dvorak, N. Taherimakhsousi, and C. P. Berlinguette, How Catalyst Dispersion Solvents Affect CO2 Electrolyzer Gas Diffusion Electrodes, Energy & Fuels, 35, 19178-19184

[2] C. M. Johnston, K.-S. Lee, T. Rockward, A. Labouriau, N. Mack, and Y. S. Kim, Impact of Solvent on Ionomer Structure and Fuel Cell Durability, ECS Transactions, 25, 1617-1622,

4:18pm - 4:30pm

Luminescence thermometry – beyond the Boltzmann dependence

Eugeniusz Zych, Paulina Bolek, Dagmara Kulesza, Justyna Zeler, Joanna Jedon, Joanna Trojan-Piegza

University of Wroclaw, Poland; eugeniusz.zych@chem.uni.wroc.pl

The emerging technologies require the development of novel methods of remote temperature measuring, which might offer spatial resolution below micron-size and even down to nanometers. Resistance to disturbances caused by external electric or magnetic fields is also crucial. Luminescence thermometry is considered one of the most prospective techniques for remote temperature measurements which may fulfill the needs of future technologies.

Designing wide-range luminescence thermometers that might be used in the aerospace industry, space research, nuclear plants, etc. poses a real challenge, however. Practically all phosphors present a dependence of their emissions on temperature. This does not yet make them luminescence thermometers. In this presentation In this presentation, we shall discuss the possibilities of designing wide-range high-sensitivity and good-accuracy luminescent thermometers in which Pr3+ ions are the emitting centers. The methods to manage such phosphors' properties will be in the core interest of this work.

Oral Talk-3: Oral Talk

Time: Tuesday, 10/Jan/2023: 2:30pm - 4:18pm · *Location:* Hall 1&2

2:30pm - 2:42pm

Film thickness dependence of alternating spin current generated via gyromagnetic effect of surface acoustic waves

Ryo Shinozaki[1], Ryusei Toba[1], Kazuto Yamanoi[1], Yukio Nozaki[1,2]

[1]Keio University, Yokohama, Japan; [2]Center for Spintronics Research Network, Keio University, Yokohama, Japan; sr0723@keio.jp

Spin current, i.e. a flow of electron spin, has been widely used in a variety of spintronic devices. However, to generate it, we need ferromagnets and/or rare metals with strong spin orbit interaction (SOI) so far. Recently, some novel SOI-free methods have been demonstrated. One of these methods utilizes a gyromagnetic effect (GME) that enables a conversion between macroscopic rotation and microscopic electron spin according to a conservation of angular momentum [1]. Indeed, we have succeeded to demonstrate an excitation of spin wave resonance (SWR) caused by the GME of Rayleigh-type surface acoustic wave (R-SAW) [2]. Moreover, highly nonlinear frequency variation appeared in the spin current generation [3]. In this study, we have examined the thickness of spin current produced via the GME in NiFe/Pt bilayer, whose amplitude is expected to depend not only on the distribution of SAW amplitude but also on the spin transport properties, e.g. spin diffusion length.

Our experimental setup to observe the spin wave excited via GME of the SAW is as follows. We prepared a pair of interdigital transducer (IDTs) and a rectangle of NiFe(20 nm)/Pt(tPt) bilayer between them. The SAW attenuation owing to the SWR was measured by a vector network analyzer. An excitation frequency of the SAW was fixed at 1.33 GHz. We measured the SAW attenuation at resonant magnetic field of the spin wave with frequency correspond to that of the SAW.

Figure 1 shows that a rapid increase in the SAW attenuation □Pnorm appears when tPt is 40 nm. It is known that the R-SAW decays exponentially along the depth direction and the decay length is comparable to its wavelength. It is sub □m in this experiment, which is much larger than tPt . In contrast, a spin diffusion length of the Pt is approximately 10 nm [4] which is shorter than tPt where □Pnorm rapidly increases. For discussion of □Pnorm, we evaluated the spin current at NiFe/Pt interface numerically by solving the spin diffusion equation in consideration of the GME. Here, the spin diffusion length of the Pt was assumed as 7 nm. Figure 2 shows the square of spin current amplitude, which is in proportion to the excitation of the spin wave. It is noted that the square of spin current is maximized around 40 nm as shown similarly in the experiment. This may be attributed to a convolution of different characteristic lengths for spin diffusion and decay of the SAW. Our findings are significant for spintronic application of the acoustic waves.

2:42pm - 2:54pm

Gas Sensor Array System Using Microgravimetric and Amperometric Sensors Coated with Room Temperature Ionic Liquid to Enhance Isomers Separation

Anifatul Faricha, Parthojit Chakraborty, Tso-Fu Mark Chang, Masato Sone, Takamichi Nakamoto

Tokyo Institute of Technology, Japan; anifatulfaricha@gmail.com

In a gas measurement, to distinguish among the isomers are challenge due to the same molecular formula and identical molar mass. The Quartz Crystal Microbalance (QCM), one of the most popular sensors used due to good stability and commercial availability, has difficulty to separate the isomers because it follows the microgravimetric principle. We developed the sensor array system composed of two kind of sensors i.e., microgravimetric and amperometric sensors coated with the same sensing film. The different mechanism of those two kind of sensors are expected to enhance the isomers separation. In this study, three microgavimetric sensors such as QCMs and three amperometric sensors based on Interdigitated Array Electrodes (IDAs) were used. Furthermore, three kinds of Room Temperature Ionic Liquids (RTILs) were used for sensing film i.e., 1-ethyl-3-methylimidazolium trifluoromethane sulfonate, 1-ethyl-3-methylimidazolium dicyanamide, and 1-ethyl-3-methylimidazolium bis(trifluoromethy-lsulfonyl) imide, abbreviated as [C2mim][otf], [C2mim][dca], and [C2mim][T2fN] respectively. Two kind of isomers i.e., propanol and butanol isomers, summarized in Table 1, were used in this study. In the experiment, the solenoid valve-based gas delivery system with its nitrogen carrier gas at the flow rate of 200 mL/min was used [1]. The sensor array recorded the signal from the compounds, where the sensor responses from QCMs and IDAs coated with RTILs were extracted from frequency changes and cyclic voltammogram (CV) curves respectively. For the IDAs sensor, the forward scan with voltage from -1V to +1V, was applied. In addition, the region of interest related to voltage slicing where the compounds can be discriminated well, was investigated. Briefly, an IDA coated with certain sensing film provided five dimensional data. The Wilks lambda was applied to measure the separation power among the compounds numerically. The lower the Wilks lambda (Λ) is, the better the separation is [1]. Table 2 summarizes the Wilks lambda for several sensor combinations. In this study, the combination employing two types of sensors, the combination was limited to simplify the situation i.e., only consisting of one QCM and one IDA coated with certain sensing film. According to Table 2, the lowest Wilks lambda was achieved by the QCM and IDA coated with [C2mim][dca] and [C2mim][otf] respectively. Furthermore, Figure 1 visualizes the comparison of sensor configuration for compounds separation using linear discriminant analysis (LDA). According to Figure 1, the discriminant capability among compounds was enhanced using two types of sensors i.e., QCM coated with [C2mim][dca] and IDA coated with [C2mim][otf] compared only applying one type of sensor i.e., QCMs coated with different sensing films.

2:54pm - 3:06pm

Improved surface morphology and crystalline quality of InAlN epilayer with AlN interlayers grown by PMOCVD

Yingda Qian[1,2], Lingyu Wan[2], Xinwei Zhao[1], Zhe Chuan FENG[3]

[1]Tokyo University of Science, Japan; [2]School of Physics Science and Technology, Guangxi University; [3]Southern Polytechnic College of Engineering and Engineering Technology, Kennesaw State University; 1221708@ed.tus.ac.jp

With its high breakdown field and high electron drift, InAlN is one of the most promising material for transistors. In this study, InAlN/GaN heterostructure was grown on c-plane sapphire with GaN buffer by pulsed-metal organic chemical vapor deposition (PMOCVD) aimed

for transistor. Ga atom diffusion from the buffer layer to the epitaxy layer was observed by angle resolved XPS. Ga doped in the InAlN layer caused the valence band shift and reduce the surface quality. By inducing AlN interlayer between InAlN and GaN, the epitaxy layer Ga ratio decreased to 0.7 at%. 2 nm AlN interlayer can efficiently reduce the roughness of the epitaxy layer from 3.2 nm to 2.1 nm and block the Ga atom diffusion from GaN buffer layer. To further investigate the effect of the Ga motion, the stability of samples with and without AlN interlayer was compared by varied temperature ellipsometry measured from 300K to 800K. Varshni equation fitting results show that bandgap shift depend on temperature is more stable. This work proved that 2 nm AlN insertion layer can efficiently improve the InAlN film quality and revealed the Ga diffusion damage to the stabilization and surface topography of InAlN layer.

3:06pm – 3:18pm

Large-Area, Active Thin-Film Resonator for Dynamic Coloration Based on Redox Reaction of Polyaniline

Serim Kim, Joo Hwan Ko, Young Min Song

Gwangju Institute of Science and Technology, Korea, Republic of (South Korea); serim0106@gm.gist.ac.kr

Optically active materials, which reversibly change their optical properties (i.e., refractive index and extinction coefficient), have attracted attention as an active medium for dynamic responses in photonic structures due to their fine tunability and reversibility. Representatively, optically active materials include inorganic materials (e.g., phase change materials (PCM) and transition metal oxide) and organic materials (e.g., polyaniline (PANI) and poly-(3,4-ethylenedioxythiophene) (PEDOT), and polypyrrole (PPy)) [1]. Since the long-term durability and thermal/chemical stability of PCMs, they have been widely used for reconfigurable photonics. However, PCMs suffer from slow transition time and energy limitations. On the other hand, conducting polymers (CPs) provide advantages such as cost-effectiveness, a simple manufacturing process, and low operating power [2]. In addition, the optical properties of CPs can be electrically controlled, encouraging to be utilized in tunable color display, metasurface, or wavefront modulator.

PANI, one of CPs, is interestingly explored in several research fields. PANI has a high current density, low power consumption, and it also realizes reversible optical properties change with a low voltage range (-0.2 V ~ 0.8 V) in the visible region. However, there is a limit to the expression of full color only by a single materials substrate. To overcome the obstacle, optical resonators (e.g., plasmonics, photonic crystal, and metasurface) combined with PANI have been extensively studied [3]. In this study, an ultra-thin film resonator (i.e., Pr-Ge on Au) was adopted to realize full-color tuning through potential and Pr-Ge modulation.

As depicted in Figure 1a, the proposed active thin film resonator was fabricated by synthesizing PANI on ITO and then depositing Pr-Ge and Au. The basic mechanism of an active thin film resonator is that the oxidation by potential causes proton and electron loss, and then the molecular structure is converted, resulting in changing refractive index. When the voltage varies from -0.2 V to 0.8 V, oxidation occurs twice in the entire cycle, the PANI sate is replaced by leucoemeraaldine to emeraldine (Figure 1c). Consequently, we can get a wide color range shown Figure 1d, and the Pr-Ge thickness modulation can also contribute color diversification. Figure 1e is an experiment result, showing the rich color tuning of the active thin film resonator according to the voltage variation. Therefore, our structure allows rich color expression subject to voltage control, and so it can be utilized as a display.

3:18pm – 3:30pm

Localized Surface Plasmon Resonance Sensors for Vapors Detection

Bin Chen[1], Lin Chen[2], Cong Wang[1], Kenshi Hayashi[2]

[1]Southwest University, China.; [2]Kyushu University, Japan.; chenbin121@swu.edu.cn

Localized surface plasmon resonance (LSPR) results from the plasmonic resonance of noble metallic nanoparticles (NPs), and is sensitive to changes in the surrounding refractive index (RI). The high local sensitivity of this sensing mechanism arises from the strong evanescent field, which decays within the 6-30 nm from the surface of nanoparticles (NPs). Therefore, LSPR sensors can detect a very low concentration of chemicals and biomolecules, which are mainly concentrated near the metal surface where the plasmonic field are strongest. While in the practical application, it is difficult to concentrate the volatile molecules into the most sensitive range of NPs. In our works, polymer films were fabricated on the surface of NPs through spin-coating method, and according to the experimental results, a relative uniformly distributed film on NPs surface was generate [1]. Organic acid vapors can be identified and distinguished via imprinting the target molecules during the polymer synthesis process. While the spin-coating method is easy to affect the original distribution of NPs on the surface of substrate. Additionally, the surface of polymer film fabricated through the spin-coating method is plat and smooth. Hence, we further proposed a direct silica coating method through hydrolyzing tetraethylorthosilicate (TEOS) in ethanol to fabricate Au NUs@SiO2 particles on substrates. The larger surface provided by the Au NUs@SiO2 sensors makes gas molecules facile to anchor and interact with the plasmonic field.

3:30pm - 3:42pm

Microscopic analysis of single crystalline Zn1-xMgxO thin films on sapphire grown via inverted Stranski-Krastanov mode

Naoto Yamashita[1], Daichi Takahashi[1], Takamasa Okumura[1], Kunihiro Kamataki[1], Kazunori Koga[1,2], Masaharu Shiratani[1], Naho Itagaki[1]

[1]Kyushu University, Japan; [2]National Institutes of Natural Sciences; yamashita.naoto.952@m.kyushu-u.ac.jp

Zn1-xMgxO is a strong candidate for optoelectronic devices due to its large exciton binding energy and the bandgap tunability[1-3] over the range of 3.4–4.15 eV[4]. A useful substrate is a c-plane sapphire, but the large lattice mismatch limits the crystal quality. Recently, a new crystal growth mode ‘inverted Stranski-Krastanov (inverted SK) mode’ has been demonstrated and a single-crystalline ZnO film is grown on the c-plane sapphire substrate[5]. In the demonstration, a ZnO buffer layer consisting of relaxed 3D islands was fabricated on the c-plane sapphire substrate followed by a two-dimensional (2D) growth of high-quality single-crystalline ZnO film. If Zn1-xMgxO film also grows on the cutting-edge buffer layer in the inverted SK mode, the films will get a single crystal of high quality. Here, we demonstrate the inverted SK growth of single-crystalline Zn1-xMgxO films on the ZnO buffer layers.

C-plane sapphire substrates and two ZnO targets were prepared for the fabrication of ZnO buffer layers. The substrate temperature was set to 780°C. The gas flow rate of N2 and Ar were 1.0 and 24 sccm, respectively, and the pressure was 0.35 Pa during the deposition. After depositing the ZnO for 10 nm, the Zn1-xMgxO films were fabricated on the buffer layer using another ZnO target and a MgO target

at a substrate temperature of 800°C. The gas flow of O2 and Ar were 5.0 and 45 sccm, respectively. The total gas pressure was 0.7 Pa. As a control experiment, a ZnMgO film was fabricated directly on the same substrate without a ZnO buffer layer.

The high-quality Zn1-xMgxO crystal was grown on the ZnO buffer, which was confirmed from the surface morphologies of the films. Zn0.78(0.79)Mg0.22(0.21)O film was formed on the substrate with (without) the ZnO buffer layer. To examine the nature of the inverted SK mode, transmission electron microscopic images of these films were observed as shown in Fig. 1. These Zn1-xMgxO films showed a patchy pattern, which was ascribable to the condition of the TEM. The difference between these films was the line patterns only appeared in the Zn1-xMgxO film deposited without any buffer layers. Thus, we successfully visualized the difference between the growth modes. The origin of the line pattern is the crystal grains that grow vertically from the substrate via conventional SK mode since the Zn1-xMgxO film formed a polycrystal.

This work was supported by JSPS KAKENHI Grant Numbers JP21H01372, JP21K18731, NTT collaborative research, Toyota Riken Scholar, and The Murata Science Foundation.

3:42pm - 3:54pm

Modulation of spin transport in Dy film with different magnetic phases

KAZUTO YAMANOI[1], Yukio Nozaki[1,2]

[1]Department of Physics, Keio University, Yokohama, 223-8522, Japan.; [2]Center for Spintronics Research Network, Keio University, Yokohama 223-8522, Japan.; k.yamanoi@keio.jp

4f-electronlanthanide materials are essential elements for the next generation of spintronic devices and permanent magnets because of strong spin-orbit coupling. In the 4f-electronlanthanide series of elements, Dy is one of the most important materials because two separate transitions, between the ferromagnetic (FM) and antiferromagnetic (AFM) phases and the AFM and paramagnetic (PM) phases, appear at Curie (TC) and Neel (TN) temperatures, respectively. In this work, we have study on the spin transport properties for Dy film with different magnetic orders by using them as a spin sink layer for the spin pumping effect.

We firstly investigated the temperature dependence of the magnetic properties for Dy film. A Ta (2 nm)/Dy (50 nm)/Ta (2 nm) continuous multilayer was deposited on Si/ SiO2 substrate using magnetron sputtering system. In this study, the Ta layes were employed to prevent the oxidization of the Dy film. During Dy film's deposition, the substrate temperature was fixed at 350 deg. C. The temperature dependence of the magnetization in the Dy film was performed at a fixed external magnetic field of 200 mT with the temperature range of 15-270 K. To investigate the spin-pumping efficiency of the Dy film, we sputtered a Ta(2 nm)/Dy(50 nm)/NiFe(20 nm)/SiO2(30 nm) continuous multilayer on Si/SiO2 substrate. By means of laser lithography and Ar-ion milling, the multilayer was formed in a rectangle with a lateral dimension of 6 x 280 □m2. A Ti (3 nm)/Au (70 nm)-coplanar waveguide (CPW), which generates an orthogonal microwave field to excite ferromagnetic resonance, was deposited on the rectangle using a lift-off technique with EB-evaporation. The CPW was connected to a vector-network analyzer (VNA). The CPW microwave reflection coefficient was measured as a function of frequency.

Fig. 1 shows the temperature dependence of Dy-film magnetization. A rapid decrease in magnetization with an increasing temperature appears approximately at 130 K. This behavior indicated that the transition temperature from the FM to the AFM phases.

The magnetization of Dy film shows a local maximum around 176 K. Such a local maximum is attributable to the increase in thermal spin fluctuation in AFM ordering.

Fig. 2 shows the value of effective Gilbert damping constant □eff as a function of temperature of the Dy/NiFe bilayer and NiFe monolayer, respectively. The values of □eff for the NiFe monolayer gradually decreases with temperature down to 130 K. This temperature behavior of □eff in NiFe monolayer can be explained by intra-band scattering caused by spin-orbit interaction. The temperature dependent of □eff for Dy/NiFe bilayer shows a local maximum of □eff owing to a growth of magnetization fluctuation appears at TN. Interestingly, □eff was remarkably reduced at the AFM phase followed by a rapid increase at TC. In our presentation, we will also discuss the relationship between the strong suppression of □eff and spin transport property.

3:54pm – 4:06pm

Nanocarbon-based Ohmic Electrodes for Diamond electronics: Adhesion and Corrosion Resistance Investigations

Sreenath Mylo Valappil[1,2], Shinya Ohmagari[1,3], Abdelrahman Zkria[1], Phongasaphak Sittimart[1,2], Eslam Abubakar[1], Hiromatsu Kato[3], Tsuyoshi Yoshitake[1]

[1]Sensing System Research Center, National Institute of Advanced Industrial Science and Technology (AIST), 807-1 Shuku-machi, Tosu, Saga 841-0052, Japan; [2]Department of Applied Science for Electronics and Materials, Kyushu University, Kasuga-Koen, Kasuga, Fukuoka 816-8580, Japan; [3]3Advanced Power Electronics Research Center, National Institute of Advanced Industrial Science and Technology (AIST), 1-1-1 Umezono, Tsukuba 305-8568, Japan; sreenath_mylovalappil@kyudai.jp

Diamond-based electronic devices are exploring new operational regimes in the fields of power conversion, quantum sensing, radiation detecting, etc. The operational efficiency of the diamond-based electronic device is limited due to the ON resistance (RON) from the metal/diamond interface and less carrier activation at room temperature making ohmic contact formation on diamond films a crucial component in diamond electronics research. Indeed, an ideal ohmic contact should satisfy good material and interfacial properties like mechanical adhesion, corrosion resistance, chemical, and thermal stability, etc. In this work, we are introducing a new contact strategy for phosphorus-doped n-type single-crystalline diamond films through the high-temperature direct fabrication of nanocarbon electrodes using coaxial arc plasma deposition (CAPD).

The nanocarbon electrodes fabricated by CAPD are analyzed for their specific contact resistance (ρc) through circular transmission line model (cTLM) theory and have shown an active declination in ρc (~10-3 Ωcm2) when compared with the Ti/Mo/Au electrodes (ρc ~10-2 Ωcm2). The interfacial stability and the corrosion resistance of the ohmic electrodes were analyzed by 250oC acid removal with an H2SO4+HNO3 (3:1) solution. The nanocarbon electrode shows high interfacial adhesion and durability under acid removal, unlike conventional Ti/Mo/Au electrodes.

4:06pm – 4:18pm

Orthorhombic Distortion Induced Insulator-to-Metal Transition Behavior of VO2/TiO2 Bilayer Films on (1-100) α-Al2O3

Binjie Chen[1], Gowoon Kim[1], Hai Jun Cho[1,2], Hiromichi Ohta[1,2]

[1]Graduate School of Information Science and Technology, Hokkaido University, Sapporo, 060-0814, Japan; [2]Research Institute for Electronic Science, Hokkaido University, Sapporo, 001-0020, Japan; nclearlove@gmail.com

Vanadium dioxide (VO2) has been widely investigated in the past few decades, due to its temperature induced insulator-to-metal transition (IMT), accompanied with abrupt changes in electric and optical properties. These intriguing changes make it become a competitive candidate for the core material of memory, sensor, smart window etc. However, the IMT of bulk VO2 usually occurs around 68 °C with obvious thermal hysteresis, which is adverse to its practical application. Numerous efforts have been made to modulate the IMT behavior of VO2. And it has been repeatedly verified that the transition temperature (Tc) can be reduced to room temperature when rutile TiO2 is used as the substrate [1]. However, the limited size of Verneuil-grown TiO2 crystal is unreal to achieve large-scale applications. In this study, we used α-Al2O3 single crystal as the substrate to deposit VO2 film. By inserting the rutile TiO2 as the buffer layer, the Tc of VO2 film was significantly reduced to a near room temperature of 32°C. Meanwhile, by controlling the thickness of VO2 and TiO2 layer, the IMT behavior can also be regularly modulated. Based on this, we further discovered the relationship between orthorhombic distortion and the IMT behavior of VO2.

3:18pm - 3:30pm

Oxygen Reduction Reaction and Electronic Properties on PrO and LaO Terminated Surfaces of Pr2NiO4 and La2NiO4

Aleksandar Staykov

International Institute for Carbon Neutral Energy Research (WPI-I2CNER), Kyushu University, Japan; alex@i2cner.kyushu-u.ac.jp

Frist-principal calculations were performed to elucidate the origin of catalytic activity of the pristine AO-terminated surface of two Ruddlesden Popper phase oxides of industrial interest. The direct comparison of molecular oxygen interaction with La2NiO4 and Pr2NiO4 allowed us to evaluate the electronic effect on the oxygen reduction reaction energetics. We have further addressed the surface catalytic activity as a function of interstitial oxygen occupancy in the rock salt layer and provided a possible explanation for the limits of the interstitial oxygen concentration. The oxide ion transport in the rock salt layer was compared for La2NiO4.125 and Pr2NiO4.125. The diffusion difference was attributed to the electronic structure of the valence shells of Pr and La. The different polarizability of those elements would lead to opposite effect on the transition states stability. In depth understanding of the La2NiO4 and Pr2NiO4 (including La2NiO4.125 and Pr2NiO4.125) electronic properties allowed us to refer electronic and hole conductivities to the computed band gaps and the electronic structure of the valence bands. Our study shows that while La2NiO4 and Pr2NiO4 share similar crystallographic structure, the most important properties, such as surface catalytic activity, ionic diffusivity, and electron transport, are direct consequence of the valence shell structure of the A site cations: La and Pr.

Oral Talk-1: Oral Talk

Time: Tuesday, 10/Jan/2023: 2:30pm - 4:18pm · *Location:* Hall 3

2:30pm - 2:42pm

Fabrications and Properties of Fluoride and Halide Scintillator Crystals with Eutectic Morphology

Yuui Yokota[1,2], Takahiko Horiai[1], Masao Yoshino[2], Akira Yoshikawa[1,2]

[1]Institute for Materials Research, Tohoku University, Japan; [2]New Industry Creation Hatchery Center (NICHe), Tohoku University, Japan; yui.yokota.a5@tohoku.ac.jp

Scintillators with an eutectic morphology (eutectic scintillator) have been developed for applications of X-ray imaging with great spatial resolution. Eutectic structure composed of two phases can be self-organized by the unidirectional solidification from the melt at an eutectic point in a pseudo-binary phase diagram. The unidirectional solidification of a material including one phase with small volume ratio self-organizes a rod phase in a matrix phase. When the rod phase is scintillator material and the matrix phase have a high refractive index, the scintillation light in the rod phase under irradiation can be reach to the opposite side for detector with total reflections. Ce-doped GdAlO3 (GAP)-Al2O3 [GAP/Al2O3] eutectic scintillator is composed of GAP scintillator rod phase in the Al2O3 matrix phase and scintillation light in the GAP scintillator is transported along the rod direction by a total reflection mode. The GAP/Al2O3 eutectic scintillator achieved high resolution on the X-ray imaging because of the excellent light guiding properties compared to the CsI columnar film.

In this study, we focused on the fluoride and halide scintillator materials with the eutectic morphology. Fluoride scintillators containing Li are expected to be applied for neutron scintillator with high stopping power to neutron. In contrast, there is a possibility of great eutectic scintillator composed of halide scintillator with higher light yield and greater energy resolution compared to oxide scintillators.

We grew the LiF/LiLuF4 fluoride eutectic scintillators by a micro-pulling-down method. SEM images and chemical composition analyses by EDX indicated that the eutectic configuration was composed of a LiF rod phase in the LiLuF4 matrix phase. In addition, the phase diagram of BaI2-LuI3 was created by XRD and DSC, and undoped and Ce-doped BaI2/LuI3 eutectic scintillators were fabricated at the eutectic point. In the X-ray radioluminescence spectrum of the polished Ce:BaI2/LuI3 specimen, a broad emission peak was observed, and the broad peak could be divided into two peaks at 470 and 520 nm. Details of growth and properties for the eutectic scintillators will be reported.

2:42pm – 2:54pm

Drift velocity and mobility of electrons and light holes in thermal SiO2

Ravi Kumar Chanana

Retired, India; ravikumarchanana@yahoo.co.in

The electron and light hole effective masses meff, in amorphous thermal SiO2 has been determined by the MIS characterization as 0.42m and 0.58m respectively at 300 K temperature, where m is the free electron mass [1-2]. The electron mass of 0.42m is established since 1969 [3], and the hole mass of 0.58m found by the author in a group study has been confirmed recently utilizing a 4H-SiC-MOS device [7]. It has also been confirmed by the author utilizing n-channel polysilicon-gated Silicon MOSFETs [8-11]. The average drift velocity of the light hole in thermal SiO2 at 300 K temperature can be determined using the equation (1/2)(meff)(vth)^2 = (3/2)kT, with the thermal energy of (3/2) kT at 300 K of 0.0388 eV, keeping in mind that the thermal velocity is nearly equal to the average drift velocity of the particles at saturation in semiconductors and insulators. The vth in the above equation is therefore equated to vd in the equation vd=μEe. It is calculated to be 0.153 x 108 cm/s. An average field Ee of about 1 MV/cm across the oxide causes the electron or light hole to reach the above saturation drift velocity [5]. Using the second equation, the mobility of light hole in SiO2 μ, is found to be about 15.3 cm2/V-s at 300 K. Similarly, with the meff of electron in SiO2 as 0.42m, vd and μ is found to be about 0.180 x 108 cm/s and 18.0 cm2/V-s, respectively at 300 K. A value of about 20 cm2/V-s is reported for electron mobility in SiO2 from a Monte Carlo simulation study [12]. The effect of increasing temperature can be seen by using equation (dE/E)=(dm/m). When the temperature increases from 300 K to 400 K, the differential thermal energy dE becomes 0.0129 eV, and the effective mass increases by 25% with the total thermal energy E as 0.0517 eV. The effective mass of the kinetic electron or light hole becomes 1.25meff at 400 K. The drift velocity vd of the light hole and electron reduces to 0.137 x 108 cm/s and 0.161 x 108 cm/s, respectively at 400 K as compared to 300 K temperature. The mobility of the light hole and electron also reduces to 13.7 cm2/V-s and 16.1 cm2/V-s. It can be observed that the decrease in drift velocity and particle mobilities in SiO2 for a 100oC increase in temperature is small. The effect of decreasing temperature from 300 K to 200 K is similar, when the effective masses of the conducting particles decrease by 25% to 0.75meff, thereby causing a small increase in their drift velocity and mobility at 200 K as compared to that at 300 K temperature. This effect of temperature on the drift velocity of electron is calculated by the author with the above theory in Silicon also. It was found that the calculated and observed drift velocities at 200, 300, and 400 K temperatures in Silicon matched very closely to within 10% [13]. The effect is non-linear below 300 K [6]. The above theory can be used to find the drift velocity in semiconductors in a particular direction in which the effective mass is known.

2:54pm – 3:06pm

A new method to determine longitudinal effective mass of electron in semiconductors having anisotropy in mobility

Ravi Kumar Chanana

Retired, India; ravikumarchanana@yahoo.co.in

The MIS characterization can lead to the determination of the intrinsic Fermi level Ei in the semiconductors having significant intrinsic defects density [1-2]. Of particular interest are three semiconductors:4H-SiC, 6H-SiC, and GaN in which anisotropy in the mobility exists depending on the directions of electron flow. From the ratio of the intrinsic Fermi Level-Conduction band (CB) energy difference to the bandgap energy, the effective mass in the longitudinal direction can be obtained given that the (0001) surface is used to fabricate the MOS device using the relation dE/E equals dm/m. Here, m is the free electron mass, dE is the differential potential energy of the electron from Ei to the semiconductor CB, or differential kinetic energy of the electron when excited from Ei to the semiconductor CB,

and dm is the differential or effective mass in the semiconductor or insulator material. E is the semiconductor bandgap as the total potential energy of the electron [3]. The longitudinal electron effective masses of the above three semiconductors are presented in Table I below. Different sources give different values for the longitudinal effective mass in 6H-SiC of which one value matches closely to the value presented in the Table I below.

Table I. Longitudinal effective masses of electrons in anisotropic semiconductors

Semiconductor,

(0001) oriented Bandgap, Eg, in eV Intrinsic Fermi Level from the Conduction Band, in eV, Ref. [2]. Longitudinal effective mass, parallel to the [0001] direction.

4H-SiC 3.26 0.97 0.297m

6H-SiC 3.02 0.80 0.264m

GaN (Wurtzite) 3.4 (Γ=0 Valley) 0.95 0.279m

GaN (Wurtzite) 4.35 (L-Valley) 0.95 0.218m

GaN (Wurtzite) 4.7 (A-Valley) 0.95 0.202m

The value of the longitudinal electron effective mass can give a clue to the fabrication of, for example, the 4H-SiC-MOSFET, where fabricating the MOSFET on (1120) surface will result in the electron flow parallel to the [0001] direction having a mass of 0.297m, and thus result in a larger mobility than in the MOSFET fabricated on the (0001) oriented surface where the electron flow will be in the transverse direction perpendicular to [0001] direction having a mass of 0.42m. A peak field effect mobility of 57 cm2/V-s is observed on a 4H-SiC MOSFET fabricated on (1120) oriented surface as compared to a mobility of 45 cm2/V-s in MOSFET fabricated on (0001) oriented surface [4]. The ratio of the mobilities in the two MOSFETs of 1.26 matches closely to the ratio of transverse to longitudinal effective masses in 4H-SiC of 1.41 confirming the relation between the effective masses and the peak field-effect mobilities. Electron effective masses in wurtzite GaN are presented above, and the A and L-valley masses matches with the cyclotron mass determined to be 0.20m to 0.22m utilizing the Γ=0 valley differential energy dE of 0.95 eV found by the author by MIS characterization [5-6].

3:06pm – 3:18pm

Enhanced UV photosensing properties by field-induced polarization in ZnO-modified (Bi0.93Gd0.07)FeO3 ceramics

Pin-Yi Chen[1], Jin-Ping Wang[1], Haidee Mana-ay[1], Rhys Hinampas Montecillo[1], Cheng-Sao Chen[2], Kuei-Chih Feng[1], Chi-Shun Tu[3]

[1]Ming Chi University of Technology, Taiwan; [2]Hwa Hsia University of Technology, Taiwan; [3]Fu Jen Catholic University, Taiwan; pinyi@mail.mcut.edu.tw

Self-powered photodetection was studied using x wt% ZnO-modified

Bi0.93Gd0.07)FeO3 (abbreviated as B7GFO-xZn) ferroelectric ceramics. The ITO/B7GFO-xZn ceramic/Au photovoltaic (PV) cell was constructed for photosensing study at ultraviolet-A (λ = 360 nm) and near-ultraviolet (λ = 405 nm). The + 2kV/cm poled

PV cell using B7GFO-1 wt%Zn ceramic under 360-nm irradiation displays maximal photocurrent density of ~364 μA/cm2 at 102 mW/cm2. Furthermore, a remarkable photosensing performance was observed with photoresponsivity (R) of ~3.02 × 10 2A/W, specific detectivity (D*) of ~2.27 × 1012 Jones, and photo conductive gain (G) of ~10.4%. A sensitive photosensing response time (rise time, r) of ~9 ms was acquired under illumination from the 360-nm laser at 102 mW/cm2. The enhanced photodetection performance originated from the collective influence of the narrower bandgap, enhanced p-n junction effect, E-field modulated energy band tilt, and improved photocurrent generation due to the local conductive pathways formed by the interconnected domain walls and grain boundaries. This work provides an extensive analysis to elucidate the photovoltaic mechanisms in BiFeO3-based ceramics and explores their potential in self powered UV photosensing.

3:18pm – 3:30pm

Ferroelectric N:HfO2 characterization by synchrotron XPS and electrical analysis and the application on non-volatile ferroelectric field-effect transistor memory

Chong-Jhe Sun[1], Shih-Hao Chen[1], Guang-Li Luo[2], Yung-Chun Wu[1]

[1]National Tsing Hua University, Hsinchu, Taiwan; [2]Taiwan Semiconductor Research Institute, Hsinchu, Taiwan; jj199658@gmail.com

In this study, we have investigated the ferroelectricity of 5 nm N:HfO2¬ thin film which fabricated by Atomic Layer deposition (ALD) HfO2 with a following NH3 plasma treatment. First, the non-destructive X-ray photoelectron spectroscopy (XPS) depth analysis was achieved by using energy adjustable synchrotron X-ray radiation. Since the lower incident X-ray energy could only excite the photoelectron from the shallower surface. We have used two incident X-ray energy (500 eV and 750 eV) for investigating the thin film bonding state in different depth. The XPS of N 1s of two spectra with different incident X-ray energy reveals that after the NH3 plasma treatment, a small amount of nitrogen was doped in HfO2. Although there is a less intensity of N 1s spectrum with the 750 eV incident energy than the 500 eV, but a more obvious N-Hf bonding peak can be observed, showing that the doped nitrogen atom bond with HfO2 in deeper level of HfO2 thin film.

For ferroelectricity characterization, the PUND pulse analyze was used. The current with two consecutive negative triangular pulses was measured. The current of the first pulse is larger than the second, which is attributed to the polarization switching current. Also, the results were then converted into the polarization-applied voltage relation showing that the fabricated N:HfO2 has a 2 remnant polarization (2Pr) of 1.14 uC/cm2.

Finally, we applied the proposed ferroelectric N:HfO2 thin film as the gate insulator on a SiGe channel Fin Field-Effect Transistor (FinFET) structure device with a 60 nm Fin height, 60 nm Fin width and 500 nm gate length. The drain current (ID) to gate voltage (VG) characteristic of the fabricated ferroelectric FET (FeFET) with both forward and reverse sweeps was measured at. The DC ID-VG curve with VG measuring from + 4 V ~ - 4 V and VD = -0.1 V shows an iconic FeFET clockwise characteristic and a large memory window of

about 1.5 V, where the threshold voltage was extracted at ID of 10-7 A/um. The proposed ferroelectric N:HfO2 is highly potential for the future non-volatile FeFET memory.

3:30pm - 3:42pm

Ferroelectric transition and structural modulation in Sr2Na(Nb1−xTax)5O15 tungsten bronze ceramics

Ying Wang[1], Tu Lai Sun[2], Xiao Li Zhu[1], Lu Liu[1], Xiang Ming Chen[1]

[1]Zhejiang University; [2]Zhejiang University of Technology; wangying7313@qq.com

Tetragonal tungsten bronze (TTB) compounds constitute the second-largest class of dielectric family next to perovskites. The coexistence of cations, their distribution in A1 and A2-sites, and the related structure modulation played a crucial role to dominate the ferroelectric nature in tetragonal tungsten bronze systems. As an important issue, the effects of B-site substitution on the physical properties in TTB compounds have been attracting increasing attention.

In the present work, effects of Ta5+ in B-site on the crystal structure, dielectric and ferroelectric properties were investigated together with the phase transitions in Sr2Na(Nb1-xTax)5O15(x = 0, 0.1, 0.2, 0.25, 0.5) ceramics. With increasing Ta-content, the crystal structure of the present system changed from non-centrosymmetric P4bm to centrosymmetric P4/mbm. With Ta-substitution for Nb, the frequency- and temperature-dependent dielectric permittivity and dielectric loss curves exhibited typical relaxor features, and the saturated polarization-electric field (P-E) hysteresis loop changed gradually to a slim one and eventually to a linear one, though a commensurate structure modulation was determined by the selected area electron diffraction (SAED) patterns for all compositions. Raman spectra indicated changes of the B–O vibrations during the transition from normal to relaxor ferroelectrics, reflecting the different electron configuration of Nb and Ta and the different bonding of Nb and Ta with O. This work not only provides a new approach for modifying the ferroelectric properties but also deepens the physical understanding of the crystal structure-ferroelectricity relationship in tungsten bronze ceramics.

3:42pm - 3:54pm

Hybrid improper ferroelectricity in A-site cation ordered Li2La2Ti3O10 ceramic with triple-layer Ruddlesden-Popper structure

Zhang Bihui, Liu Xiaoqiang, Chen Xiangming

Zhejiang University, China, People's Republic of; zhangbh@zju.edu.cn

Hybrid improper ferroelectricity has been extensively studied in the double-layer Ruddlesden-Popper oxides in recent years. Although the hybrid improper ferroelectricity could be created among triple-layer Ruddlesden-Popper oxides with an ordered A-site cation predicted by the first-principles calculations, no experimental result has been reported yet. In the present work, the room-temperature ferroelectricity has been observed in Li2La2Ti3O10 ceramic with A-site cation ordered triple-layer Ruddlesden-Popper structure. The polar phase P21ab has been determined by combining the first-principles calculation and the powder diffraction analysis at room temperature. The hybrid improper ferroelectricity was induced by the triple-coupled irreps including the A-site cation ordering. The variable temperature DSC measurements and dielectric responses indicate no evidence of phase transition over the temperature range of 200 - 1080 K. The present work sheds light on designing the hybrid improper ferroelectrics in A-site ordered triple-layer Ruddlesden-Popper compounds.

3:54pm – 4:06pm

Local structure and dynamics of tungsten oxide-based glasses: insights from concurrent neutron diffraction and Compton scattering

Maciej Krzystyniak[1], Kacper Druzbicki[2,3], Istvan Tolnai[4], Margit Fabian[4]

[1]STFC, United Kingdom; [2]Materials Physics Centre, Paseo Manuel de Lardizabal, 5—E-20018 Donostia, San Sebastián, Spai; [3]Centre of Molecular and Macromolecular Studies, Polish Academy of Sciences, Sienkiewicza 112, 90-363 Lodz, Poland; [4]Centre for Energy Research, 1121 Budapest, Konkoly Thege Miklós st. 29-33., Hungary; matthew.krzystyniak@stfc.ac.uk

In this work, following our previous work on molybdate glasses [1], here we employ a combination of neutron diffraction and neutron Compton scattering, augmented by ab initio harmonic lattice dynamics and Reverse Monte Carlo modelling to characterise the force-constant disorder in the tungsten oxide-based glasses [2]. Specifically, we discuss the correlations between the average interatomic force constant magnitudes inferred from neutron Compton scattering and the glass formation ability, measured in terms of the value of the glass transition temperature, as well as the average bond-lengths and interatomic distances obtained from diffraction data analysis. Moreover, we provide a comparative analysis of the widths of force-constant distributions of individual atomic species in glasses and their precursor metal oxides based on the distributions of the widths of nuclear momentum distributions. Furthermore, we assess the degree of softening of atom-projected vibrational densities of states induced by the force-constant disorder in the glasses.

[1] Matthew Krzystyniak et al 2020 J. Phys. Commun. 4 095027

[2] Matthew Krzystyniak et al 2021 J. Phys. Commun. 5 075013

4:06pm – 4:18pm

Magnetic Foam as Potential Tactile Sensor

Gildas Diguet[1,2], Joerg Froemel[1,2], Masanori Muroyama[3], Koichi Ohtaka[4]

[1]AIMR, Tohoku university, Sendai, Japan; [2]Division for the Establishment of Frontier Sciences, Organization for Advanced Studies, Tohoku University, Sendai, Japan; [3]Department of Electrical and Electronic Engineering, Faculty of Engineering, Tohoku Institute of Technology, Sendai; [4]Microsystem integration center, Sendai, Japan; gildas.diguet.d4@tohoku.ac.jp

Introduction

This abstract is studying a foam-based magnetic composite for sensing application. Existing sensors with deformable magnetic composite and coils array are already demonstrated [1], but that system was functioning based on deformable bi-layer: a magnetic layer on top of a non-magnetic layer, coils were placed below. Sensing was then detecting the reducing distance between the magnetic layer to the coils. The system presented below is directly measuring the deformation by a single magnetic layer.

This layer was based on a polyurethane (PU) Foam, that is extremely lightweight, with low density, and permitting large compression scale. Moreover, this material is cheap and easy to process (molding). Addition of magnetic particles to compressible foam, produced a magnetic composite that was changing its magnetic properties with deformation. This simple material in combination with coils, was then designed for deformation/compression sensing device. This was used as a sensing skin onto robotic hand.

Experimental

Spherical Carbony Iron Particles (CIP-CS, BASF, Tokyo, Japan) with D50 = 6-7 µm, were mixed to a commercial polyurethane (CM-218, PROST, Toride, Japan) with a mass ratio mCIP/mPU =80%. The particles were added to the liquid PU, hand-stirred for 5 minutes, before the curing agent was injected. Next, the mixture was inserted into a slab mold with controllable thickness. Slab was cured at room temperature for 20 minutes. Slab was cut into square shape of 20 mm × 20 mm ×1.4 mm.

Coils array used for detection was composed of four coils printed onto a Flexible PCB (P-ban, Tokyo). Size of the Flexible PCB was similar to the foam composite (Figure 1a). The sensor was then attached by a double-side tape onto a 3D-printed actuated hand (Figure 1b) for demonstration. Coils arrays was connected to an inductance-to-digital converter (LDC1614EVM, Texas Instruments Corp., USA) and measurement of inductance signals was recorded.

Results and discussion

The sensor placed on the robotic finger was tested to test its ability to record any pressure applied on it. In Figure 1b), the robotic hand is shown in the two tested positions: when the finger was applying a pressure and when it was released. This process of tightening and loosening was repeated several. The corresponding inductance measured with time by a coil was then showing a pattern that revealed the succession of increase and decrease of pressure applied on the sensor.

Conclusion

The magnetic foam can be easily deformed by pressure. This deformation was changing magnetic properties which was detected by an array of coil placed below the composite. Application of a succession of pressure was successfully recorded by this system.

4:18pm - 4:30pm

Continuous Synthesis of Pdop@Urease@Amorphous ZIF-8 for Enhanced Movement and Protection of Nano-motor

byung kwon kaang, Dong-Pyo Kim

postech, Korea, Republic of (South Korea); kangbk@postech.ac.kr

The enzyme-based micro-/nano-motor has recently been in the spotlight as promising use in various bio-field by its features such as bio-compatibility and fuel-bioavailability. However, enzyme-based motors have a disadvantage in that is denatured and their function is lost by their active site shape if enzyme are exposed to harsh external environments (pH, temperature, etc.). Here, we report a continuous flow synthesis of enzyme based amorphous ZIF-8 nano-motor (Pdop@urease@aZIF-8) for enhanced movement and protection of substrate (Pdop) and enzyme of nano-motor. The Polydopamine (Pdop, size: 200 nm) were pre-synthesized in batch and the triple laminar flow in continuous flow-reactor allows efficient self-assembly of amorphous ZIF-8 on Pdop and then, enzyme was encapsulated in a serial flow process. The obtained Pdop@urease@aZIF-8 (meso-pore: 2-8 nm) had an improved enzyme activity than the crystal ZIF-8 based Pdop@urease@cZIF-8 (micro-pore: <2 nm) prepared in batch. In particular, the enzyme activity and photothermal therapy function of Pdop were maintained even after 5 days reuse as aZIF-8 protects the weak points of enzyme and Pdop based motor, which are vulnerable to external environment. The enhanced enzyme activity and sequential phothermal therapy of Amotor (Pdop@urease@aZIF-8) was confirmed by 2D cellular membrane. Biocompatible Amotor showed improved membrane transmigration (>80%) compared to bare Pdop nanoparticle (<30%) and Cmotor (<50%) by enhanced Brownian motion, which had a powerful effect on cell uptake and photothermal therapy for bladder cancer cells (T-24). Enhanced protection for substrate (Pdop) and enzyme without loss of function would be successfully harnessed for treatment in the various human environments as a drug delivery carrier.

Poster Session-1: Poster Session

Time: Tuesday, 10/Jan/2023: 3:30pm - 5:00pm · *Location:* Exchange Hall and Exchange Lobby

p1-1 Synthesis and Characterization of an Ionic Polyacetylene by the Catalyst-free Polymerization of 2-Ethynylpyridine using 1-(3-Bromo-1-propynyl)naphthalene

Y. S Gal[1], S. H. Jin[2], J. Park[3], K. T. Lim[4], D.-Y. Shin[4], T. Kim[5], S. Y. Klm[5]

[1]Kyungil University, Korea, Republic of (South Korea); [2]Pusan National University; [3]Kyunghee University; [4]Pukyong National University; [5]KAIST; ysgal@kiu.kr

The polyacetylene polyelectrolytes have been studied as silver nanocomposites for photoinduced patterning, ultrathin films using the layer-by-layer deposition technicues, unpolar write-once-read-many times (WORM) memory devices, light-emitting diodes, cathode interfacial layers of organic solar cells, etc.1,2 Now, we report a new polyelectrolytic polyacetylene via the non-catalyst polymerization of 2-ethynylpyridine using 1-(3-bromo-1-propynyl)naphthalene. The polymerization proceed well in homogeneous manner without any additional initiator or catalyst to give the corresponding polymer in high yield. The polymerization behaviors are similar to that of the similar polymerization using propargyl bromide.

The analytical data on polymer structure revealed that the polymer have the polyacetylene backbone with the designed substituents. The FT-IR spectrum of polymer did not show the C□C bond stretching (2110 cm-1) and □C-H bond stretching (3293 cm-1) frequencies of starting material, 2-ethynylpyridine. On the other hand, the C=C stretching peaks of polymer backbone around 1582-1675 cm-1 became more intense. The polymer exhibited irreversible electrochemical behaviors between the doping and undoping peaks. The UV-visible spectrum of polymer showed a characteristic absorption peak in the visible region, which is strong evidence for the presence of the polyacetylene backbone system. The photoluminescence peak of polymer was observed at 548 nm, which is corresponding to the photon energy of 2.27 eV.

P1-2 Enhanced Photovoltaic Performance of Benzothiadiazole-Based Donor-Acceptor Type Polymers by Modulating Electron-Withdrawing Substituents

Dinda Fariesta Nugraha, Juan Anthony Prayogo, Geun Ryun Ma, Jaewon Chang

Department of Industrial Chemistry, Pukyong National University, Busan 48513, Republic of Korea; dinda.nugraha@gmail.com

In this study, a series of benzothiadiazole-based D-A type conjugated polymers with the strong electron-withdrawing substituents were designed and synthesized to be used for polymer solar cells (PSCs). The electron-donating benzodithiophene (BDT) unit was linked to the electron-accepting benzothiadiazole derivatives through thiophene or thieno[3,2-b]thiophene linkers under Stille condition. In addition, the strong electron-withdrawing fluorine atom and cyano units were systematically incorporated on the benzothiadiazole acceptor to investigate their effects on various properties of the polymers. All polymers are well soluble in common organic solvents such as tetrahydrofuran, chloroform, and toluene. Once several fundament properties such as optical, electrochemical, and structural features were analyzed, the photovoltaic properties of the polymers were examined by fabricating the inverted-type devices with a configuration of indium tin oxide/ZnO/active layer/MnO3/Ag. In an active layer of the device, the well-known small molecule of Y6 was used as a nonfullerene-type acceptor. Notably, the replacement fluorine atom with cyano unit can significantly reduce the bandgap and the energy level of the highest occupied molecular orbital of the polymers. Moreover, it was found the photovoltaic performances of the polymers are strongly correlated with the existing electron-withdrawing substituents and type of π-bridges. Therefore, these finding provide meaningful insight into the structure-property relationships of the benzothiadiazole-based D-A type conjugated polymers for photovoltaic applications.

P1-3 Paclitaxel Loaded Porous Hydroxyapatite Microspheres for Targeting Cancer Treatment

Meng-Ying Wu[1], Wan-Ru Hsieh[2], Yi-Jyun Tseng[1], Jiunn-Wang Liao[2], *Shiow-Kang Yen[1]

[1]Department of Materials Science and Engineering, National Chung Hsing University, Taichung.; [2]Graduate Institute of Veterinary Pathobiology, National Chung Hsing University, Taichung.; skyen@dragon.nchu.edu.tw

Synthesis of hydroxyapatite (HAp) by wet-chemical method using (NH4)H2PO4 and Ca(NO3)2·4H2O as a source of calcium and phosphate ions, with the addition of biopolymer to form HAp microspheres which is proved to be more osteoconductive than commercial products of fibrin glue and Osteoset® Bone Graft Substitute [2]. SEM shows the HAp is round and porous with spikes on the surface. Firstly, PTX was mixed with 0% (C0) and 0.125% (C1) chitosan solutions and HAp powders then stirred at 80 rpm for 48 hours. The drug entrapment efficiency of each sample is around 58%. In drug release tests, cumulative releases of C0 is over 75% and that of C1 reaches 55% after six months immersion in phosphate buffered saline. In vitro experiment by MTT assay, the viability of human osteosarcoma cell line G292 for C0 are 39% and 20%, while 96.6% and 22% for C1 on days 1 and 14 respectively. In vivo experiment, female BALB/c nude mice weight about 20 g were separated into five groups: PTX-HAp high dose (600 μg in C1), lose-dose (300 μg in C1), intravenous (IV) injection (20 mg/kg), unloaded HAp and control group, with 5 mice in each group. Subcutaneous xenograft model of G-292 human osteosarcoma cells was established on every mouse. Once the tumor volume reach 0.1 cm3, various treatments were given, and the weight and the tumor size of the mice were recorded for 15 days [3]. The average tumor volume in high-dose or low-dose group keeps constant while it increases 50% in the control one. No side effects are observed in organs of PTX-HAp-treated mice while multifocal white-swelling lesions accompanied by increased number of apoptosis cells are found in spleen for the IV group, indicating that PTX-HAp targeting treatment may be an alternative way of cancer therapy.

P1-4 A Low-Frequency Mechanical Energy Harvester Based on Ion Transport through Layered Hydrogel

Merreta Noorenza Biutty, Seong Il Yoo
Pukyong National University, Korea, Republic of (South Korea); merretaenbe@gmail.com

Extracting electricity from low-frequency mechanical vibrations is one of the challenges in many energy-harvesting techniques. [1,2] To address this issue, we developed an ionic hydrogel-based energy harvester, which is capable to convert low-frequency mechanical vibrations into electricity by taking advantage of slow diffusion of ions. We fabricated three-layered hydrogels, which are composed of soft and hard hydrogels separated by ion-selective one. When mechanical stress was applied to the layered hydrogels, each hydrogel was compressed to a different degree depending on its stiffness. In consequence, the dissolved ions transported through stacked structure from soft to hard hydrogels. By inserting cation-selective hydrogel in the middle layer, the selective transport of cation can be realized, resulting in charge separation between top and bottom layers for power generation. Based on this principle, the mechanical energy can be converted to electricity. This mechanical-to-electrical energy conversion was engineered under a number of experimental conditions such as the compressional volume, the vibrational frequency, and the type of hydrogel/electrolyte.

P1-5 3D nanocomposite hydrogel composed of skeletal muscle and HA-AuNPs for motion enhanced biohybrid robot

Minkyu Shin, Dongyeon Kim, Jeong-Woo Choi
sogang university, Korea, Republic of (South Korea); mkshin91@sogang.ac.kr

Due to the potential of detection, reaction, and adaption to environmental change, the biological component and soft materials-based biohybrid robot is developed. Biohybrid robots can be used in various fields such as drug screening and toxicity evaluation. However, the muscle cell of biohybrid robot have low contraction force, so it is difficult to evaluate drug and toxicological effect of muscle cell. To overcome this limitation, in this study, hyaluronic acid modified gold nanoparticles (HA-AuNPs) were introduced into the skeletal muscle cell using extracellular matrix (ECM) hydrogel (3D nanocomposite hydrogel). In particular, HA was biocompatible component that has advantage in regeneration of tissue. The differentiation of skeletal muscle cells and electrical conductivity of 3D nanocomposite hydrogel were enhanced due to the HA-AuNPs. The 3D nanocomposite hydrogel showed enhanced motion performance compared with that of without HA-AuNPs. To develop the two-tailed structure of biohybrid robot, polydimethylsiloxane (PDMS) scaffold was fabricated by 3D printed mold. Then, biohybrid robot was developed by combination of two 3D nanocomposite hydrogel and PDMS scaffold. Developed biohybrid robot was swum by contraction of 3D nanocomposite hydrogel with electrical stimuli. In addition, the developed biohybrid robot indicated a considerable change in motion with the addition of inotropic drugs. The proposed biohybrid robot can be utilized to neuromuscular disease drug screening by integrating motor neuron spheroid and brain organoids. Acknowledgments: This research was supported by the National Research Foundation of Korea (NRF) grant funded by the Korea government (MSIT) (No.2019R1A2C3002300).

P1-6 A novel alloy with high corrosion resistance developed for biomaterial applications

Kuang-Fu Lee, Meng-Shiun Tsai, *Shiow-Kang Yen
National Chung Hsing University, Taiwan; miles199919@gmail.com

In this study, the dynamic polarization tests of the multi-component CoCrFeGexNi (x = 0.05, 0.1, 0.25, 0.5) high entropy alloys (HEAs) in 3.5 wt. % NaCl aerated aqueous Solution were carried out for investigating the related passivation behaviors. The surface of the alloy after corrosion was observed by FE-SEM, and its crystal structure was analyzed by XRD. The multi-stage corrosion mechanism of the alloy was analyzed respectively from the view of ion release and passive film by combining redox equilibrium potential with, ICP-MS and XPS. The alloy design theory was proposed for these lection and addition ratio of the fifth element of the high corrosion resistance of HEAs.

All CoCrFeNiGex (x ≤ 0.5) HEAs present single phase FCC structures after annealing at 1100°C for 48 hours, while CoCrFeNiGex (0.25 ≤ x ≤ 0.5) HEAs reveal better passivation performance, ascribed to the early formation of germanium(IV) oxide (GeO2) in air further stabilizing and densifing the original chromium-rich passive film and even durable at potential 1.0 V for the formation of more valent chromium(VI) oxide (CrO3), chromate (CrO42-), germanate (GeO32-) and NiOOH. For the biomaterial applications, dynamic polarization tests of CoCrFeNiGex (x=0.1, 0.25) HEAs were also conducted in Hank's aerated aqueous solution. Both alloys show the better corrosion resistance than CoCrMo. Finally, a series of in vitro cytotoxicity tests using L929 were performed for CoCrFeNiGe0.25 to evaluate the biocompatibility. Like 316L (ASTM-F55) and CoCrMo (ASTM-F1537), no toxicity is identified by ISO 10993-5 and ISO 10993-12.

P1-7 A phlorotannins-laden acellular matrix film modulates post-implantation inflammatory responses

Tae-Hee Kim[1,2], Seong-Yeong Heo[3], Gun-Woo Oh[4], Il-Whan Choi[5], Kwon-Hoo Kim[6], Won-Kyo Jung[1,2]
[1]Major of Biomedical Engineering, Division of Smart Healthcare, College of Information Technology and Convergence and New-Senior Healthcare Innovation Center (BK21 Plus), Pukyong National University, Busan, Republic of Korea.; [2]Marine Integrated Biomedical Technology Center, The National Key Research Institutes in Universities, Pukyong National University, Busan 48513, Korea; [3]Jeju Marine Research Center, Korea Institute of Ocean Science & Technology (KIOST), Jeju, Korea.; [4]National Marine Biodiversity Institute of Korea (MABIK), Seochun, Chungcheongnam, Korea.; [5]Department of Microbiology, College of Medicine, Inje University, Busan, Korea.; [6]Major of Metallurgical Engineering, College of Engineering, Pukyung National University, Busan, Korea.; wkjung@pknu.ac.kr

Peritendinous adhesion (PA) mainly occurs between proliferating fibrous tissues and adjacent normal organs after surgery. Many physical barriers are applied to the implanted site to prevent PA. However, these barriers often trigger inflammatory responses. Therefore, our study sought to develop phlorotannins (PT)-loaded cartilage acellular matrix (CAM) films as a physical barrier and

investigate their inhibitory effect on inflammatory responses. Our findings indicated that incorporating PT into the CAM film did not affect its unique characteristics. Moreover, the PT-loaded CAM films suppressed the expression of inflammatory mediators on RAW 264.7 macrophages stimulated using lipopolysaccharides and exhibited an anti-inflammatory effect when implanted subcutaneously in rats. Therefore, our results highlight the potential of PT-loaded CAM films as a promising physical barrier to prevent postoperative peritendinous adhesion.

P1-8 Advanced plasma processing for silicon surface passivation improvement

Shota Nunomura, Isao Sakata

National Institute of Advanced Industrial Science and Technology, Japan; s.nunomura@aist.go.jp

The surface passivation of crystalline silicon (c-Si) plays an important role in optoelectronic devices such as solar cells and image sensors. The surface passivation is usually obtained by the formation of wide-gap materials over the c-Si surface. Among a large variety of wide-gap materials, hydrogenated amorphous silicon (a-Si:H), prepared by plasma enhanced chemical vapor deposition (PECVD), is known to yield an excellent property of the passivation. However, the details of surface passivation, associated with defect creation and band structure at the a-Si:H/c-Si interface, are not fully understood.

In this presentation, we show the surface passivation property during growth of a-Si:H and epitaxial silicon (epi-Si), in terms of the defect creation as well as band structure [1]. In the experiments, the growth mode of the passivation layer is changed from epitaxial to amorphous, by varying the hydrogen dilution during PECVD. The passivation property is monitored in real time via the photocurrent measurement of c-Si during PECVD and post-annealing [2].

The following results are found [1]. For the a-Si:H growth over c-Si, the passivation is maximized via the formation of a large valence band offset at the a-Si:H/c-Si interface. For the epi-Si layer growth, the passivation is deteriorated with an ultrathin layer of epi-Si, because the H-mediated defects are created in the c-Si bulk near the surface. In addition, the band bending is not fully formed near the epi-Si/SOI interface. Thus, the suppression of the bulk Si defects as well as the formation of the band offset are important for the passivation.

This work was supported by JSPS KAKENHI (Grant Number 18K03603) and New Energy and Industrial Technology Development Organization (NEDO).

[1] S. Nunomura et al., J. Appl. Phys. 128, 033302 (2020).

[2] S. Nunomura et al., Appl. Phys. Exp. 12, 051006 (2019).

P1-9
Advancement of X-Ray shielding of Polyethylene/Boron composites: thermal and mechanical properties

Juana Abenojar[1,2], Eva Paz[3], Sara López de Armentia[3], Juan Carlos del Real[3], Miguel Angel Martinez[1], Iñaki Prieto[4]

[1]Universidad Carlos III de Madrid, Spain; [2]Universidad Pontificia Comillas de Madrid, Spain; [3]Universidad Pontificia Comillas de Madrid, IIT, Spain; [4]Policlínica Gipuzkoa, San Sebastian, Spain; abenojar@ing.uc3m.es

Every day we are all exposed to different types of radiation. These radiations can cause a biological effect and their somatic effects depend directly on the doses received, producing diseases at very high doses, between 500 and 1000 mSv. Some examples of radiation doses are those from the natural background which is 0.01 mSv/day, a chest X-ray emits 0.1 mSv, while the dose of a heart computed tomography angiography is between 6.5 and 13 mSv. The threshold value per year is 300 mSv for the thyroid gland, 150 mSv for the eye, and 500 mSv for the hand, these values should not be exceeded by surgeons, radiologists, or patients.

Personal shielding is required to be used by the staff to be protected against X-ray exposure, which depends on the work type and the distance to X-ray source. However, it must be remembered that the shielding is only relative, and most shields do not entirely attenuate the X-ray beam. Wearing a lead collar reduces radiation exposure to the thyroid gland while the lead gloves did not protect the surgeon's fingers [1]. These radiations can be measured by thermo luminescent dosimeters, that are placed behind the protective equipment, such as aprons, gloves, or collars.

When an X-ray tube emits 100 kV and 1 mA on a patient who is placed at 1 meter from the X-ray tube, the surgeon receives 1.2 mSV / hour. Previous studies have shown that a 40 kV lamp can be shielded by a 1 mm plate made of polyethylene composite with 60% of amorphous boron [2]. The objective of this work is to study the necessary thickness of composite to shield 100 kV radiation provides by X-ray equipment (Philips-Azurion Clarity IQ), with the purpose of manufacturing protective material for healthcare personnel and patients. Therefore, a study of its mechanical and thermal properties is also necessary.

Keywords: composite material, X-ray shielding, polyethylene, boron

[1] MECHLENBURG, I., DAUGAARD H., & SØBALLE K. 2009. Radiation exposure to the orthopaedic surgeon during periacetabular osteotomy. Int Orthop (SICOT), 33,1747–1751

[2] Abenojar, J., López de Armentia, S., Gálvez, P., Martínez, M.A. 2020. Polyethylene/boron composite materials in X-ray attenuation. Revista de la Asociación Española de Materiales Compuestos (AEMAC), 4/2, 103-107.

P1-10
AFM Observation for Apatite-Forming Process in SBF on Akermanite Surface Synthesized from Solid State Reaction

Jaeeun Go, Jong Kook Lee

Chosun University, Korea, Republic of (South Korea); go_98@naver.com

Bioactive akermanite (Ca2MgSi2O7) was synthesized by the solid state reaction and attrition milling and investigated its bioactivity through in vitro test in simulated body fluid (SBF). Calcium carbonate (CaCO3), magnesium carbonate (MgCO3) and silicon dioxide (SiO2) were mixed by ball milling and heat-treated to induce the solid state reaction. Synthesized akermanite powder was analyzed by XRD, SEM and TEM, and evaluated its bioactivity by apatite-forming ability in SBF through AFM observation with immersion

period. Microstructural evolution, morphology and forming period for apatite precipitation on akermanite surface were dependent on the synthesized temperature, related with the difference in dissolution rate in SBF among powders due to the grain growth and intra-granular sintering.

P1-11
Artificial bio-eye composed of photosensitive protein/chlorophyll a/Ni@TiO2 nanoparticles for biohybrid robot

Joungpyo Lim, Minkyu Shin, Jeong-Woo Choi
Sogang University, Korea, Republic of (South Korea); jpim92@sogang.ac.kr

Due to its applicability to various fields, the development of biohybrid robots composed of functional biomolecules is being actively conducted. However, the biohybrid robots reported to date do not have the ability to transmit signals to cells by sensing external stimuli. In this study, artificial bio-eye composed of photosensitive protein (bacteriorhodopsin, bR), chlorophyll a (Chl), and nickel/titanium dioxide hybrid nanoparticles (Ni@TiO2 NP) was developed to induce motion activity of the biohybrid robot. Light-sensitive biomolecules, bR and Chl, absorbed the light (435~660 nm) of wavelength in visible light to generate a photocurrent. Besides, the signal of generated photocurrent was amplified by Ni@TiO2 NP. Muscle cells that cultured on the artificial bio-eye were differentiated from C2C12 cells. By applying light stimulation, the photocurrent generated by artificial bio-eye was transferred to the muscle cells, inducing the change of membrane potential of muscle cell, which caused the movement of muscle cells. Biohybrid robot was fabricated by combining artificial bio-eye and muscle cells on a tripod-shaped polydimethylsiloxane (PDMS). Based on contraction/relaxation movements induced by changes in the membrane potential of muscle cells with the photocurrent of artificial bio-eye, the constructed biohybrid robot was moved by applying of the light stimulation. The proposed artificial bio-eye can be applied as a visual sensor in biohybrid robot with sensory detection/adjustment function of light stimulus.

Acknowledgments: This research was supported by the National Research Foundation of Korea (NRF) grant funded by the Korea government (MSIT) (No.2019R1A2C3002300).

P1-12 Assessment of Trapping Layer Control in Synaptic Transistor for Neuromorphic Computing

Eunseo Jo, Youseung Rim
Sejong university, Korea, Republic of (South Korea); joeunseo29@gmail.com

Neuromorphic computing has been required recently due to the nature of the von Neumann structure, which causes high power consumption and more time to require the process of big data and deep learning tasks [1].

In new hardware architectures, two terminal-based neuromorphic devices have been studied widely but the regarding leakage current, reduction of Snake path has still been challenged [2]. On the other hand, synapse transistors have been attracting attentions in the substitute technology to overcome the leakage current and control the weight of the synapse independently [3].

Here, we conducted to create synapse transistors with potentiation and depression, which were consisted of high mobility IGZO transistors with Ga2O3 charge trap layer using a solution process.

As the trapping layer thickness increased (10, 20 and 40nm), there was a difference in EPSC/IPSC performance seen in the device.

In this study, we explained the difference and showed the process of finding the optimal pulse conditions accordingly.

The magnitude of charge trapping in transistors highly depend on inducing pulse numbers and frequencies of applied voltages. We studied this aspect of trap control and guide how to approach optimal condition of own devices as function of pulse time, input voltage, and initialization.

High linearity was obtained by utilizing the characteristics of the high mobility channel and optimizing the gate pulse.

This leads to high deep learning accuracy, and differences according to trapping layer thickness can also be confirmed.

As a result, we were able to implement neuromorphic devices with high learning rates through multilayer synaptic structures.

Acknowledgements

This work was supported by the National Research Foundation of Korea (NRF) grant funded by the Korea government (MSIT) (No. 2020R1A2C1013693), and Korea Institute for Advancement of Technology (KIAT) grant funded by the Ministry of Trade, Industry & Energy (MOTIE, Korea) (P0020966, HRD Program for Industrial Innovation).

[1] Yu Liu1, Xiawa Wang1, Wenjie Chen, Linyuan Zhao, Wei Zhang, Weijun Cheng, Ziting Zhuo, Jing Wang, Tian-Ling Ren, Jun Xu. 2019. IGZO/Al2O3 based depressed synaptic transistor: Superlattices and Microstructures, 128 , 177-180.

[2] Geoffrey W. Burr, Robert M. Shelby, Abu Sebastian, Sangbum Kim, Seyoung Kim, Severin Sidler, Kumar Virwani, Masatoshi Ishii, Pritish Narayanan, Alessandro Fumarola, Lucas L. Sanches, Irem Boybat, Manuel Le Gallo, Kibong Moon, Jiyoo Woo, Hyunsang Hwang & Yusuf Leblebici. 2017. Neuromorphic computing using non-volatile memory: Taylor & Francis 2, 89-124.

[3] Yeojin Lee, Hyerin Jo, Kooktae Kim, Hyobin Yoo, Hyeonjun Baek, Dong Ryeol Lee, and Hongseok Oh. 2022. IGZO synaptic thin-film transistors with embedded AlOx charge-trapping layers: Applied Physics Express 15(6), 061005.

P1-13 Biosynthesis of silver nanoparticles using sericin and investigation of its biological activities

GITISHREE DAS[1], SU-JIN SEO[2], HAN-SEUNG SHIN[2], JAYANTA KUMAR PATRA[1]

[1]Research Institute of Integrative Life Sciences, Dongguk University-Seoul, Goyang-si, Republic of Korea.; [2]Department of Food Science and Biotechnology, Dongguk University-Seoul, Goyang-si, Republic of Korea.; jkpatra@dongguk.edu

Sericin is a biological waste material from the silk gland of silkworm. It is removed as a waste material from the silk cocoon during the extraction of silk fibers for making silk. This silk protein possesses numerous bioactive properties and has ample applications in the field of pharmaceutical, biomedical, cosmetic and food industries. The high-molecular weight sericin protein are usually used in the biomedical, wound dressing and enzyme immobilization applications, whereas the low molecular weight sericin protein has enormous applications including anti-oxidant, anti-elastase and anti-tyrosinase properties. Considering the enormous potential of the sericin protein, in the current investigation, an attempt has been made to use this extracted sericin in the synthesis of silver nanoparticles by bio-reduction method, characterize them and study its biopotential in terms of antimicrobial and antioxidant properties. After extracting the sericin from the silk cocoon of Bombyx mori by the degumming method, it was subjected to purification using the cellulose tubing dialysis membrane with a molecular weight cutoff of 12 kDa, followed by freeze-drying. Synthesis of silver nanoparticles are carriedout by using sericin extract as the reducing agent. Following synthesis, it was characterized by UV-Vis spectroscopy, Fourier-transform infrared spectroscopy and Transmission electron microscopy- Energy-dispersive X-ray spectroscopy, Particle size and Zeta potential analysis. Further, the biopotential of the sericin-based silver nanoparticles are studied against a number of Gram-positive and Gram-negative foodborne pathogenic bacteria and its activity was recorded in terms of diameter of inhibition zones. The minimum inhibitory concentrations and the minimum bactericidal concentrations were also calculated. Zentamycin was taken as the positive control. The antioxidant potential of the sericin-based silver nanoparticles was evaluated in terms of the DPPH assay, ABTS assay and the reducing power assay.

Acknowledgment: This work was supported by the National Research Foundation of Korea (NRF) grant funded by the Korea government (MSIT) (No. 2020R1G1A1004667), the Republic of Korea.

Keywords: Silk cocoon; Sericin; silver nanoparticles; antibacterial; antioxidant

P1-14 Carbon capture from air using photo-thermal adsorbent with carbon black composite

Taishi Kataoka, Yasuhiko Orita, Yusuke Shimoyama

Tokyo Institute of Technology, Japan; yshimo@chemeng.titech.ac.jp

Negative carbon technology that can remove CO2 from the atmosphere is needed to prevent global warming according to the Intergovernmental Panel on Climate Change (IPCC) report. Direct air capture (DAC) technology is one of the most attractive negative carbon technologies, where adsorbents that support polyamine are often used for rapid CO2 capture from the ambient air. However, the DAC process consumes a large amount of heat energy that accounts for over 80 % of the total required energy. Therefore, a reduction in the heat energy could be reduced the cost of the operation of the DAC process. In this work, we combined the polyethyleneimine (PEI)-based silica adsorbent and a photo-thermal conversion material applied for the photo-thermal adsorbent for an energy-saving DAC process. The photo-thermal system has been reported to reduce the heat energy in some processes, such as steam generation, where carbon materials are used as light-absorbing material for photo-thermal conversion.

To fabricate the photo-thermal adsorbent, a slurry of methanol containing PEI, fumed silica (FS), and carbon black (CB) was prepared, where the mass fraction of PEI:(FS+CB) was 1:2. The dried adsorbent was obtained by heating evaporation of methanol in the slurry under a N2 atmosphere at 90 ˚C. The flow rate of N2 gas was 200 mL min-1. After the obtained sample was ground, a CO2 adsorption test was carried out for 6 h at 25 ˚C, where the inlet concentration of CO2 was approximately 400 ppm. The CO2 concentration of the outlet gas was analyzed by a CO2 probe. After the adsorption, the light of 3 kW m-2 intensity was irradiated to the adsorbent in the glass bottle for 90 min.

There is no difference in CO2 adsorption between the adsorbents, suggesting the CB content does not have much effect on CO2 adsorption. The result of the desorption test. The adsorbent with CB desorbed 42.5 mg-CO2 g-1 under light irradiation, while the adsorbent without CB desorbed a slight amount of CO2, 0.56 mg-CO2 g-1. Additionally, the light irradiation led to an increase in the temperature to 59.3 ˚C at the adsorbent with CB. Therefore, it can be concluded that the photo-thermal conversion occurred in the adsorbent by adding CB particles, resulting in successful CO2 desorption under light irradiation.

P1-15 Cartilage acellularized matrix derived highly porous hydrogels with reduction and NIR light dual-responsive drug release properties

Yi-Jun Jo, Soo-Bin Joo, Ji Hyun Park, Jung Ha Kim, Chul-Woong Oh, Sang-Hyuk Park, Kwon Taek Lim

Pukyong National University, Korea, Republic of (South Korea); ktlim@pknu.ac.kr

We report novel stimuli responsive hydrogels composed of a highly biocompatible cartilage acellularized matrix (CAM) and a diselenide bridge-containing water-soluble cross-linker by using norbornene (Nb)-tetrazine (Tz) click chemistry. The cross-linking reaction between Nb groups of the CAM and Tz groups of the cross-linker evolved nitrogen gas and resulted in injectable hydrogels with highly porous structures. The synthesized hydrogels demonstrated high drug loading efficiencies (up to 93%), good swelling ratios, and better mechanical properties. The doxorubicin (DOX)-loaded hydrogels released minimal amounts of DOX in simulated physiological medium, however, sustained release of DOX was detected in reducing conditions, revealing more than 90% DOX release after 96 h. Interestingly, the indocyanine green (ICG) incorporated hydrogels produced reactive oxygen species upon exposure to NIR light and exhibited burst release (> 50% DOX release) of DOX during the first 4 h, followed by a sustained release phase. The in vitro cytocompatibility studies showed that the synthesized CAM-Nb and hydrogels are essentially non-toxic to HFF-1 fibroblast cells and HT-29 colon cancer cells, indicating their excellent bio-orthogonality and biocompatibility. Furthermore, DOX-loaded and DOX+ICG-loaded hydrogels inhibited the metabolic activities of HT-29 cells after GSH or NIR exposure, and induced anti-tumor effects, which were similar to that of free DOX. Therefore, these biocompatible and reduction responsive injectable

hydrogels, possessing on-demand drug release properties after NIR exposure, could be promising candidates for minimally invasive local delivery of cancer therapeutics.

P1-16 Characterization of Killer Defects in Schottky Barrier Diodes Fabricated on Heteroepitaxial Diamond Substrates

Phongsaphak Sittimart[1,2], Tomoki Iwao[1,2], Ryohei Yamaguchi[3], Hitoshi Umezawa[4], Tsuyoshi Yoshitake[2], Shinya Ohmagari[1,4]

[1]Sensing System Research Center, National Institute of Advanced Industrial Science and Technology (AIST), 807-1 Shuku-machi, Tosu, Saga 841-0052, Japan; [2]Department of Applied Science for Electronics and Materials, Kyushu University, 6-1 Kasuga-koen, Kasuga, Fukuoka 816-8580, Japan; [3]Department of Electrical Engineering and Electronics, Kyushu Institute of Technology, 1-1 Sensui, Tobata, Kitakyushu 804-8550, Japan; [4]Advanced Power Electronics Research Center, National Institute of Advanced Industrial Science and Technology (AIST), 1-8-31 Midorigaoka, Ikeda, Osaka 563-8577, Japan; phongsaphak_sittimart@kyudai.jp

An issue of diamond electronics development for switching-sensing applications is a limitation of enlargement of effective area in diamond devices due to crystalline dislocation. In this work, large-area (diameter > 1 mm) diamond Schottky barrier diodes (SBDs) were successfully fabricated utilizing metal-assisted termination (MAT) technique. The large-area SBD exhibited good rectifying action with a high rectifying ratio exceeding 109 at ± 3 V. Specific on-resistance (RonA) was 0.31 Ωcm2. Ideality factor and Schottky barrier height were 1.11 and 0.85 eV, respectively. Low leakage current (~10-12 A) was obtained, indicating that dislocation density, which is a source of killer defects, was suppressed using MAT technique. According to Murphy plot, killer defect density of the large-area SBD (A = 7.85×10-3 cm2) was evaluated to be approximately 104 cm-2. From the temperature-dependent study, reverse characteristic of the SBD obeyed thermionic field emission associated with barrier lowering (TFE+BL) regime. This work is demonstrating the success of effective-area enlargement of diamond SBD without degrading device properties.

P1-17 CO2 gas sensing using thin-film transistors with co-sputtered In2O3/CaO reactive channel

Ayumu Nodera, Shun Mori, Shinya Aikawa

Kogakuin University, Japan; c418084@ns.kogakuin.ac.jp

Recently, CO2 detection is strongly demanded for agricultural-, environmental-, and medical-uses, including daily life nowadays [1]. Although there are various kinds of CO2 gas sensors, semiconductor type has some advantages in terms of small size and cost effective. Since CO2 is very stable, low sensitivity and high operation temperature above 300 °C are critical issue in a conventional resistive-type sensor [2]. To improve the sensor responses, basic oxides or alkaline earth oxides, which show strong interaction with CO2, have been utilized [3]. Because typical thin-film transistor (TFT) structure has large surface area and the surface expose to the ambient, it is suitable for use of gas sensor applications. In2O3-based materials are commonly used as a TFT channel and has unique features such as structural flexiblity, which can incorporate impurities with different ionic radius into their matrix [4,5]. In addition, because they have active surfaces [6], high sensitive NOx gas sensor operated at room temperature has been demonstrated [7]. However, there are still difficult to detect CO2 gas with highly sensitivity. Here, we fabricated TFTs with both normal In2O3 and co-sputtered In2O3/CaO (In2O3:Ca) channel, and compared their I-V characteristics under CO2 ambient. Because CaO is a basic oxide, co-sputtered In2O3/CaO thin film is expected for strong interaction to CO2 gas.

A bottom-gate TFT was fabricated on a Si/SiO2 substrate (SiO2 thickness: 200 nm). The channel layer (20 nm) was deposited using RF magnetron sputtering co-sputtered with an In2O3 target and CaO pellets. Then, Cu source/drain electrode (50 nm) was deposited by electron beam evaporation. The fabricated TFTs were measured in a vacuum prober in an inert N2 and then CO2 atmosphere. The TFT was heated at 150 °C during electrical characterization.

Figure 1 shows the I-V characteristics of In2O3:Ca TFT under N2 and CO2 ambient. In the N2 condition, the maximum drain current (Id,max) and the hysteresis (Vhys) were 0.76 μA and 18.6 V, respectively. On the other hand, those were 2.23 μA and 9.1 V, respectively, in the CO2 condition. The Id,max was increased about 3.8 times and Vhys was decreased about 9.5 V under the CO2 compared to the N2 ambient. This result indicate that CO2 gas was successfully detected. We suggest that increase in the Id,max under CO2 ambient is due to desorption of surface oxygen, which acts as electron traps [8]. When CO2 molecules adsorbed on the surface, they react with O2− and then become CO32− [9]. During this reaction, density of surface oxygen reduces on the channel. This trend is consistent with the decrease in the Vhys as shown in Fig. 1. Furthermore, the clockwise hysteresis is attributed to electron trap in the TFT channel, and the trapped electron leads to induce screening effect [10,11]. Thus, the turn-off voltage was shifted to the negative direction and the Id,max was enhanced.

P1-18 Detailed Investigation Of Floating Catalyst Chemical Vapor Deposition Mechanisms Toward Highly Crystalline Single-walled Carbon Nanotubes

Haolu Lin, Mitsuaki Maetani, Hiroo Suzuki, Takeshi Nishikawa, Yasuhiko Hayashi

Okyama university, Japan; psyk6uyo@s.okayama-u.ac.jp

The floating catalyst chemical vapor deposition process (FCCVD) is an important technology to synthesize highly crystalline single-walled carbon nanotubes (SWCNTs) through the reasonable control of the synthesis parameters. In this research, we investigated how the molar ratio of iron and sulfur in the ferrocene solution, as a catalyst, introduced into the CVD furnace and the flow rate of the carrier gas (H2 and Ar mixed gas) affect the synthesis of SWCNTs.

(I) As an adjuvant, sulfur helps increase the iron particles' catalytic activity. However, if there is too much sulfur, it will deactivate the iron catalyst [1], and in our experiments, SWCNT films with the Raman intensity ratio of G band (~1350cm-1) to D band (~1590cm-1) ratio as high as 72 were prepared by adjusting the ratio of iron/sulfur elements. (II) The flow rate of mixed gas was changed while the hydrogen concentration was kept constant during CVD growth. The results show the increase of crystallinity of SWCNTs with the increase in gas flow rate. Based on Computational Fluid Dynamics simulation, vortex flow can be reduced with an increase in

the flow rate and prevent iron particles from being repeatedly coated by carbon atoms under the action of vortex flows, leading to a reduction of reactivity

P1-19
Developing Prediction of Key Process Parameters and Sputtering Conditions for Amorphous and high Mobility ITO/In2O3 Films via Machine Learning

Kunihiro KAMATAKI[1], Yuta Mido[1], Iori Nagao[1], Daisuke Yamashita[1], Takamasa Okumura[1], Naoto Yamashita[1], Kazunori Koga[1,2], Naho Itagaki[1], Masaharu Shiratani[1]

[1]Kyushu University, Japan; [2]National Institute of Natural Sciences; kamataki@plasma.ed.kyushu-u.ac.jp

In semiconductor manufacturing, plasma processes of CVD, sputtering, and etching, play central roles. These processes have dozens of tuning parameters and multiple objective variables for product evaluation. Relations between the tuning parameters and objective variables are highly complicated and thus are hard to be interpreted. Since plasma process has a non-linear relationship between these tuning parameters and plasma parameters and a complex relationship between the plasma and material interface/property of material, to identify important experimental tuning parameter for the quick production of the desired material requires considerable efforts by well-established researchers and can be a bottleneck of the research and development. In this study, the estimation of key tuning parameter in plasma process is partially overcome by utilizing the state-of-the-art ensemble learning algorithm. We used one of the ensemble learning, gradient boosting decision trees (GBDT) [1], for estimating feature importance. Moreover, we perform classification and regression analysis for crystallinity and mobility of a-ITO film in order to predict the optimal sputtering conditions for fabricating high mobility a-ITO/In2O3 film. For classification of crystallinity, support vector machine (SVM) is used. For regression of mobility, GBDT is used.

In this abstract, we discuss classification between amorphous and crystal films. For the classification of crystallinity, we used SVM with radial base function kernel which was non-linear, and logistic regression model which was linear. SVM in machine learning is supervised learning models with associated learning algorithms that analyze data used for classification and regression analysis. The number of all labels is 124, and 89 of which are amorphous and 35 are crystalline. These results show the classification is successful and films tend to become amorphous when N2/Ar flow ratio and d(T-S) increase. The trained classification model is useful for predicting the crystallinity of not measured data and future experiment with probability as confidence level. We will discuss details at the conference. This work was partly supported by JSPS KAKEN HI (Grant No. JP19K03809 and JP20H00142)

P1-20
Development and properties of hybride B4C-Cf-GNPs composites prepared by spark plasma sintering

Pavol Hvizdos

Institute of Materials Research, Slovak Republic; phvizdos@saske.sk

Boron carbide (B4C) ceramics are interesting for low weight and high temperature applications. The addition of carbon structures can be used to reduce the density and to modify the properties of the ceramic matrix. Carbon fibers (Cf) and graphene nanoplatelets (GNP) reinforced B4C matrix composites were fabricated by spark plasma sintering. B4C-based hybride high-temperature ceramic composites containing 30 vol. % of Cf and 0.5 wt. % of GNPs with SiC and TiB2 sintering additives were prepared by SPS. The microstructure, ablation, and oxidation of the prepared materials were tested under different exposition times in a oxyacetylene torch and infrared laser ray. The significant difference in ablation behavior was mostly attributed to different exposition time and different additive. Different responses to the torch and laser ray testing were recorded depending on sort of additive, and final porosity which ranged between 5 and 15%. Cracks in the composite matrix resulted from high thermal residual stresses generated during the cooling process from the sintering temperature due to the thermal expansion coefficient mismatch between fiber and matrix. Microstructure of the prepared materials was studied by electron and light microscopies, their mechanical properties of the composites were evaluated by (nano) indentation methods. Fibers provided non-catastrophic fracture behavior of the composites as evidenced by the stress-displacement curves and fracture surface of the composites. Interdiffusion transition regions formed between Cf, GNPs and B4C matrix under high sintering temperature, which were responsible for the balanced strength and ductility of the composites. The addition of carbon fibers and graphene nanoplatelets results in smaller crack sizes indicating an improvement in fracture toughness.

P1-21 Development of dyeable PTFE surface using surface fluorination

Mizuki Kobayashi, Jae-Ho Kim, Susumu Yonezawa

University Fukui, Japan; mi210325@g.u-fukui.ac.jp

Polytetrafluoroethylene (PTFE) is the most widely used fluoropolymer, and has various functionalities such as heat resistance, chemical resistance, and abrasion resistance, as well as non-adhesiveness. However, PTFE is difficult to be dyed because it has high water repellency. To solve it, the surface should be modified. For example, hydrophilic modifications are beneficial for dyeing, metal plating, and other coating needs. In this study, Au vapor deposited PTFE plates were modified to hydrophilic surface by introducing fluorine gas. Polytetrafluoroethylene (PTFE) plate (10mm × 10mm) was used as a sample. PTFE plate was washed with ethanol before use. And Au coating was deposited on PTFE by ion coater. The deposited Au layer was dissolved with royal water, and then the PTFE surface was fluorinated using fluorine gas. The fluorination conditions were room temperature (25 °C), fluorine pressure of 13.3-101.3 kPa, and time of 1 h. The surface-modified PTFE was characterized by XPS, AFM, and contact angle measurements. Fig.1 shows the XPS results of untreated PTFE and fluorinated PTFE samples. Comparing with the untreated sample, the fluorinated samples showed almost no C-F peak (294 eV) belong to PTFE. And the intensity of C-C peak was increased. Also, the intensity of C-O peaks (289 eV) was increased with increasing F2 pressure. From the result (Fig. 2) of dyeing tests with MB (methylene blue), the dye staining on the surface of fluorinated PTFE samples was confirmed. Consequently, the PTFE surface can be hydrophilized using surface fluorination skill, and the hydrophilized PTFE can be applied for dyeing, metal plating, and other coating needs.

P1-22 Development of Plasma Assisted Reactive Process for Uniform Formation of High Mobility Oxide Semiconductor Thin Film Transistors over Large Areas

Kosuke Takenaka[1], Tomoki Yoshitani[1], Susumu Toko[1], Giichiro Uchida[2], Akinori Ebe[3], Yuichi Setsuhara[1]
[1]Osaka University, Japan; [2]Meijo University, Japan; [3]EMD Corporation, Japan; k_takenaka@jwri.osaka-u.ac.jp

In recent years, flat panel displays are rapidly becoming larger and higher resolution. Therefore, thin film transistors (TFTs), which are the driving elements of pixels, are required to have higher performance. An amorphous oxide semiconductor, a-InGaZnOx (a-IGZO), have attracted the considerable attentions to serve as the channel layer of TFTs since a-IGZO can deposit a film with high mobility at a low substrate temperature. In this study, a-IGZO thin films are fabricated by plasma-assisted reactive sputtering. We have studied the uniform formation of high-mobility oxide semiconductor thin films over a large area at low temperature by optimizing the film formation process and low-temperature post-processing (plasma annealing) with a view to uniform TFT formation on large-area substrates. The variation of the in-plane uniformity of the film formation rate when distance between substrate to target (DST) and DC voltage are varied have been investigated. With increasing DST, the in-plane uniformity improved. When the DST was increased to 220 mm, good in-plane uniformity was obtained. Therefore, the deposition condition, which gave the best in-plane uniformity, was used as the film forming condition for TFT fabrication. The in-plane distribution of field-effect mobility of IGZO TFTs treated by plasma annealing have been studied. The in-plane distribution of field-effect mobility of IGZO TFTs after plasma treatment was almost uniform at □FE = 32~35 cm2/Vs.

P1-23
Development of quantum nanostructures for suppression of recombination losses in intermediate band solar cells

Yasushi Shoji
National Institute of Advanced Industrial Science and Technology (AIST), Japan; y.shoji@aist.go.jp

Intermediate-band solar cells (IBSCs) have attracted attention as novel photovoltaic devices to achieve a high conversion efficiency that exceeds the Shockley–Queisser limit. In the IBSCs, photocurrent increases due to two-step optical transitions through the sub-bandgap IB, which can absorb photons with energies smaller than the bandgap of the host materials. Quantum dots (QDs) superlattices are expected as one of the means to form IBs. The photocurrent generated by two-step optical transitions through quantum states has been confirmed, however, its production and conversion efficiency are still small. One of the causes is that QDs trap the photogenerated carriers. To address this problem, in this study, we fabricated a quantum nanostructure to prevent the photogenerated carriers from flowing into QDs. In this study, 10-layer stacked GaSb QDs were grown into p-i-n structured solar cells using the Stranski-Krastanov growth method. AlAsSb layers with a wide energy gap were formed around the GaSb QDs to suppress the process of photogenerated carriers being captured by the QDs. Samples were grown via solid-source molecular-beam epitaxy. Growing AlAsSb cover layers on GaSb QDs increased the size of the QDs without changing the density. This result indicates that AlAsSb cover layers were grown with GaSb QDs as nuclei. The current-voltage curves of the GaSb QDSCs, which were measured under airmass 1.5 global solar spectrum illumination. AlAsSb cover layers improved the cell performance—the short-circuit current density increased from 4.33 to 5.75 mA/cm2. This result suggests that the AlAsSb cover layers suppress carrier capture into GaSb QDs.

P1-24
Dissolution and Apatite-precipitation in SBF Solution on Diopside Synthesized by Sol-gel Method

Hyunjung Park, Jong Kook Lee
Chosun University, Korea, Republic of (South Korea); gkgk1120@naver.com

Diopside is considered to have potential as biomaterials for artificial bone graft materials for dental and orthopaedic applications. In this study, bioactive diopside was synthesized by sol-gel method and investigated its bioactivity via in vitro test in SBF solution from AFM, SEM and TEM observation. Diopside sol was synthesized by hydrolyzing a mixed solution of Ca(NO3)2·4H2O, MgCl2·6H2O, Si(OC2H5)4 and ethanol. Dried diopside gel was heat-treated at temperature range from 1000 to 1500 ℃ to verify the relation with dissolution and apatite-forming-ability in SBF solution. The change of microstructural evolution and surface morphology during immersion period were observed by AFM, SEM, TEM and XRD. Dissolution and apatite precipitation on diopside surface were dependent on the heat-treated temperature, considering by the dissolution difference in SBF solution due to the formation of large grains and strong agglomerates by partial sintering during heat-treatment.

P1-25 Effect of Counter Anions of The Interlayer Materials on The Photovoltaic Properties

RAHMATIA FITRI BINTI NASRUN, DONG HWAN SON, SABRINA AUFAR SALMA, QURROTUN AYUNI KHOIRUN NISA, JOO HYUN KIM
PUKYONG NATIONAL UNIVERSITY, Korea, Republic of (South Korea); rahmatiaf@pukyong.ac.kr

A series of polyelectrolytes based on dimethylaminopropyl fluorene and naphthalene diimide (PFN-NDI) was synthesized. In addition to the side chain modification using hydroxyl groups, we also convert the amine group to quaternary ammonium salt using a variety of counter anion (CA) types, including bromide and iodide. The ionic functionality at the end of the side chain in these materials produces a favorable interface dipole, and the polar hydroxyl groups improve the magnitude of interface dipole. The addition of polyelectrolytes as the interlayer increased the power conversion efficiency (PCE). In comparison to the device with pure ZnO, the PCE of the PFN-NDI-based device with acetic acid addition as the interlayer increased from 8.40% to 8.51%. Due to the significant improvement in FF, the PCE of the device based on PFN-NDI-Br was increased up to 9.02%. Due to the synergistic effect on the interface dipole moment, the incorporation of extra hydroxyl groups raises the PCE by up to 9.15%. Additionally, a PCE improvement of up to 9.41% was achieved utilizing PFN-NDI-I as the interlayer, primarily due to the Jsc enhancement. This study suggests a relation between device performance and ionic functionality modification.

P1-26 Effect of Electron-Withdrawing Fluorine and Chlorine Substituents on the Photovoltaic Properties of Mono-Cyanated Quinoxaline-Based Polymers

Yu Kyung Lee, Soo Yeon Lee, Jaewon Chang
Pukyong National University, Korea, Republic of (South Korea); dldbrud0550@gmail.com

Herein, a series of mono-cyanated quinoxaline-based D-A type conjugated polymers with the strong electron-withdrawing substituents were developed for polymer solar cells (PSCs). The electron-donating benzodithiophene (BDT) derivatives were coupled with the electron-accepting mono-cyanated quinoxaline units through thiophene bridge under Stille coupling condition. On the basic building block of the polymers, the strong electron-withdrawing fluorine and chlorine atom were systematically introduced to clarify their influence on diverse properties of the polymers. Owing the existing multiple alkyl chains, all polymers were well soluble in common organic solvents such as tetrahydrofuran, chloroform, and toluene. Once, the structural, optical, and electrochemical features of the polymers were clarified, the photovoltaic characteristics of the polymers were investigated by using the inverted-type devices with a configuration of indium tin oxide/ZnO/active layer/MnO3/Ag. The well-known n-type molecule of Y6 was adopted as a nonfullerene acceptor in an active layer of the device. Interestingly, the incorporation of fluorine and chlorine atom on the mono-cyanated quinoxaline-based D-A type conjugated polymers can induce the significant alternations in diverse aspects of the polymers such as optical, electrochemical, and photovoltaic properties. Hence, these results can offer valuable knowledge on the structure-property relationships of quinoxaline-based D-A type conjugated polymers for photovoltaic applications.

P1-27 Effect of microarchitectural surface of polycaprolactone by reactive ion etching on bone differentiation

Inho Bae, Byung-Hoon Kim, Ji-Hun Seok
Chosun University, Korea, Republic of (South Korea); ihbae@chosun.ac.kr

Plasma reactive ion etching (RIE) is well-known as a very effective technique for modifying the surface of biomaterials. The aim of this study was to compare the cytocompatibility and osteodifferentiation of polycaprolactone (PCL) surfaces with Spiky and hill and valley (H-a-V) topologies fabricated by plasma technology. The RIE process was performed with a low-pressure RF discharge plasma apparatus. The RIE process was performed under the conditions of 100 W plasma power and 100 mTorr pressure using 100 sccm oxygen for 3 min (for Spiky) and 5 min [(for hill-and-valley (H-a-V)] topology. This process was repeated for the designated time period, and each process was cooled for 3 min. After RIE treatment, changes in PCL surface chemistry were analyzed by X-ray photoelectron spectroscopy, atomic force microscopy and contact angle analysis, respectively. Then, cell proliferation and osteogenic differentiation of C3H10T1/2 cell was investigated by XTT and western blotting analysis. Focal cell adhesion was observed at 24 hrs of culture through Vinculin and Paxillin staining. As results, XPS analysis showed that the carbon (C1s) peak decreased slightly and the oxygen peak (O1s) shifted from 531 eV to 533 eV. The surface roughness of PCL was increased with increasing RIE process time. As expected, the RIE-treated group showed a significantly lower contact angle than the control group. Focal cell adhesion and migration were increased in the H-a-V group compared to the Spiky group. As well as cell proliferation in H-a-V group showed a slightly higher than that of the Spiky group at early period of cultivation. Moreover, cell differentiation values were statistically significantly improved in H-a-V compared to that of Spiky (16.7%, $p = 0.031$ and 23.1%, $p = 0.017$, respectively). Western blot analysis demonstrated that H-a-V promoted cell differentiation compared to spiky [for ALP (17.8%, $p = 0.042$), for Runx-2 (19.7%, $p = 0.038$, and for OPN (10.9%, $p = 0.463$, respectively]. Taken together, these results suggest that grooved surfaces are more favorable for cytocompatibility and differentiation rather than pointed surfaces. (No. NRF-2021R1A4A1030243).

P1-28 Effect of Plasma Treatment to Electron Transport Layer on Perovskite Solar Cells

Kohei Yamamoto, Takurou N. Murakami, Yuji Yoshida
AIST, Japan; kohei-yamamoto@aist.go.jp

Perovskite solar cells (PSCs) have been reported the high power conversion efficiency (PCE) over 25%, and their R&D are still underway for mass-production because of the technical issues for cost effective mass-production and high durability. The electron transport layer of PSCs are often introduced metal oxides such as titanium oxide and tin oxide. These layers are commonly used after cleaning with wet process such as sonication in organic solvent and ultrapure water, and/or with dry process such as plasma and UV-ozone treatment. Also, these processes are widely used as the pretreatment for adjusting the work function of the layers in addition to the cleaning. These pretreatment processes are widely used from the R&D to the mass production process. The problem of previous pretreatment process is that these processing times take several minutes to 0.5 hours. To speed up the pretreatment process, it is necessary to establish a cleaning method on mass production of PSCs with metal oxides for their substrates. Both Sheet to Sheet and Roll to Roll processes require high-speed cleaning processes to enable PSCs mass production at low cost. To speed up the pretreatment process, we develop a cleaning method of oxygen plasma with controlled composition ratio in plasma. Device structure of our PSCs is Au / Spiro-OMeTAD / Cs0.05(FA0.89MA0.11)0.95Pb(I0.89Br0.11)3 / SnO2 / FTO / Glass. The surface pretreatment methods of SnO2 were investigated as the comparing between (a) oxygen plasma treatment with optimized composition ratio in plasma for 30 seconds and (b) UV-ozone treatment for 20 minutes. The current density-voltage (J-V) characteristics and parameters are presented in Fig. 1. The PSCs with oxygen plasma treatment showed higher open circuit voltage (Voc) than that of the PSCs with UV-ozone treatment. These result indicate that the interface condition of SnO2- Cs0.05(FA0.89MA0.11)0.95Pb(I0.89Br0.11)3 was optimized by introducing oxygen plasma with short treatment. To investigate device stability by difference pretreatment, we evaluated the light stability test with encapsulation under continuous Light irradiation, as shown Figure 2. PSCs with UV-ozone treatment was very low, for example, the PCE dropped to 20 % after irradiation with 1 Sun for 24 hours. On the other hand, the PCE with oxygen plasma maintained 90% of the initial value after 3000 hours. We found that the use of a oxygen plasma treatment for PSCs leads to not only the improved pretreatment time, but also good light stability.

P1-29
Effects of Amplitude Modulation Discharge on Ion Energy and Angular Distributions studied by PIC-MCC method

Iori Nagao[1], Akihiro Yamamoto[1], Kunihiro Kamataki[1], Daisuke Yamashita[1], Takamasa Okumura[1], Naoto Yamashita[1], Naho Itagaki[1], Kazunori Koga[1,2], Masaharu Shiratani[1]

[1]Kyushu University, Japan; [2]National Institute of Natural Sciences, Japan; i.nagao@plasma.ed.kyushu-u.ac.jp

Insulating films such as SiO2 in 3D structures are generally fabricated by plasma enhanced chemical vapor deposition (PECVD). The conventional PECVD often shows poor film quality on side walls of trenches. This is due to insufficient ion bombardment on the side walls. High-precision control of the ion energy distribution function (IEDF) and ion angular distribution function (IADF) [1] is important for such deposition in trenches. Moreover, it is difficult to measure IEDF and IADF simultaneously in experiments. Here, we focus on amplitude modulation (AM) discharge method [2] to improve film quality on side walls of trenches. We investigated effects of amplitude modulation frequency(fAM) on IEDF and IADF in capacitively coupled discharge plasma using Particle-In-Cell Monte-Carlo-Collision (PIC-MCC) method [3].

Axisymmetric PIC-MCC model was used to analyze an asymmetric capacitive discharge. RF frequency (13.56 MHz) voltage was applied between the parallel plate electrodes. The amplitude of RF voltage was modulated by sin wave in frequency range of 10 kHz to 100 kHz and compared to continuous waveform (CW) discharge.

The gas was Ar. The gas pressure was 1.33 Pa. IEDF and the IADF were analyzed at the surface of lower grounded electrode.

The electron density at the center region is constant of 2.30×1015 m-3 in the CW discharge. In the AM discharges, the electron density at center region varies from 1.27×1015 to 2.60×1015 m-3 for fAM = 10 kHz and from 1.93×1015 to 2.14×1015 m-3 for fAM = 100 kHz. The variation of electron density decreases with increasing the modulation frequency.

IADF show that most ions impinge onto the substrate at 90 degree. There is a small angular difference represented by the full width at half maximum (FWHM) of IADF, depending on the modulation frequency. FWHM of IADF ranges from 1.94 to 2.19 degrees for CW discharges and from 1.56 to 2.98 degrees for AM discharges. The results suggest the AM discharge has potential to improve the film quality on side walls of trenches. Details will be discussed in the conference. This study was partly supported by JSPS KAKENHI Grant Number JP20H00142.

Keywords: IEDF, IADF, Amplitude Modulation discharge, High Aspect Ratio

[1] De-Qi Wen, et al., Plasma Process Polymer, Vol.14, No.4 201600100 (2017)

[2] K.Kamataki, et al., Appl. Phys. Express 4 105001 (2011)

[3] Zoltán Donkó, et al., Plasma Sources Sci. Technol. 30 095017 (2021)

P1-30
Effects of Gas Pressure on Deposition Characteristics of Hydrogenated Amorphous Carbon Films Produced by Ar + CH4 Capacitively Coupled Plasma

Shinjiro Ono[1], Sung Hwa Hwang[1], Daichi Yoshikawa[1], Takamasa Okumura[1], Kunihiro Kamataki[1], Naoto Yamashita[1], Naho Itagaki[1], Kazunori Koga[1,2], Masaharu Shiratani[1]

[1]Kyushu University; [2]National Institutes of Natural Sciences; s.ono@plasma.ed.kyushu-u.ac.jp

Plasma chemical vapor deposition (CVD) has been widely employed to deposit hydrogenated amorphous carbon (a-C:H) films which can control the flux of precursors and ions, and the energy of ions impinging to the films. The gas pressure has been a control parameter of deposition which change the generation of the precursors and the ion energy, leading to change the deposition characteristics such as deposition rate, mass density, and film structure. Here we employed a capacitively coupled plasma CVD method to examine the effects of the gas pressure [1-4]. Si (100) substrates of 10 mm × 10 mm were placed on the grounded electrode 30 mm below the powered electrode. The gas flow rates of Ar and CH4 were 95 and 3.8 sccm, respectively. The pressure was set a range from 0.5 to 7 Torr. A 28 MHz discharge voltage of 170 Vpp was supplied to generate the plasma. The self-bias voltage Vdc was −47.5 V. A deposition rate was measured using an ellipsometer. The mass density of the films was obtained using the mass of the films and the film thickness. The structure of the deposited a-C:H films were analyzed by Raman spectroscopy (excitation laser at 532 nm) and X-ray diffraction (XRD). The deposition rate increased monotonically with increasing the pressure while the mass density was constant. The Raman spectra of our films showed three peaks around 1300, 1600, and 1450 cm-1. The peak around 1300 cm-1 was recognized as N and/or D band of a-C:H films. It around 1600 cm-1 was as G+, G- and/or D´ bands [5]. In our previous research, we recognized the peak at 1450 cm-1 was G- band [4]. However, we found that curve fitting by Voigt function was not work well to the peak that we have recognized as G- band. Thus, it suggests that the existence of another structure to the a-C:H film. Tarrant et al. reported that the Raman spectra of a thick graphitic-amorphous carbon film have a peak around 1450 cm-1. According to their simulated Raman spectra, transverse bond motions of C-C bonds by the series of linearly aggregated 6-membered aromatic ring systems contribute to the peak at 1450 cm-1 [6]. Another possibility was the presence of nanocrystals, but the XRD pattern showed the structure of the films is amorphous. These results suggests that our a-C:H films might consist of a material linearly aggregated hexagonal aromatic ring. The intensity ratios among the peaks around 1300 cm-1, 1450 cm-1 and 1600 cm-1 depends on the pressure. This result suggests that gas pressure is a key parameter to control structure of a-C:H films and incorporation of the other carbon materials.

P1-31
Effects of lower discharge frequency on plasma parameters in capacitively coupled plasmas studied by particle-in-cell/Monte Carlo collision method

Toshiaki Arima[1], MIchihiro Otaka[1], Iori Nagao[1], Kunihiro Kamataki[1], Daisuke Yamashita[1], Naoto Yamashita[1], Naho Itagaki[1], Takamasa Okumura[1], Kazunori Koga[1,2], Masaharu Shiratani[1]

[1]Kyushu University, Japan; [2]National Institutes of Natural Sciences; t.arima@plasma.ed.kyushu-u.ac.jp

Capacitively Coupled Plasma (CCP) is widely used in deposition process of semiconductor manufacturing. the driving frequency used in CCP is usually 13.56 MHz, and it is known that the plasma density tends to increase as the driving frequency increases [1]. Therefore, higher driving frequency is generally utilized in plasma processing for semiconductor device manufacturing. In constant, low frequency, e.g. 400 kHz trends to be applied as a bias power source in PECVD processes. However, there are small number of literatures [2] reported effects of driving frequency below 13.56MHz. In this study, effects of the driving frequency on plasma parameters in capacitively coupled discharge plasmas was investigated using the Particle-In-Cell/Monte Carlo Collision (PIC/MCC) model.

A one-dimensional axisymmetric PIC/MCC model was used to analyze an asymmetric capacitive discharge with a blocking capacitor. RF voltage were applied between the parallel plate electrodes. The electrode gap was 20 mm. Gas was Ar. The gas pressure was 1Torr. The rf amplitude Vrf was fixed at 400 V. Effects of the driving frequency frf on the electron and ion densities were examined from 2, 3.39, 6.78 and 13.56MHz.

The electron and ion densities in bulk plasma increase with increasing the driving frequency from 2.00 MHz to 13.56 MHz. The electron density at bulk plasma were ~ 4.5×1015 m-3 at frf =2.00 MHz, ~ 1.1×1016 m-3 at frf = 3.39 MHz, ~ 3×1016 m-3 at frf = 6.78 MHz, and ~ 7×1016 m-3 at frf = 13.56 MHz, respectively. Ion densities in bulk plasma are almost the same as electron densities. The profile of electron density between the electrodes becomes wider with increasing the rf frequency from 2.00 MHz to 13.56 MHz. For the driving frequency below 3.39 MHz, which is close to ion plasma frequency, the ion density profile oscillates with the period of the driving frequency. Eventually, the plasma density decreases due to collapse of plasma bulk at such low frequency. Details will be presented at the conference.

This study was partly supported by JSPS KAKENHI Grant Number 20H00142.

P1-32
Effects of RF powers on the crystal quality and surface morphology of single crystalline ZnO films deposited by magnetron sputtering

Ryo Mitsuishi[1], Naoto Yamashita[1], Daichi Takahashi[1], Takamasa Okumura[1], Kunihiro Kamataki[1], Kazunori Koga[1,2], Masaharu Shiratani[1], Naho Itagaki[1]

[1]Kyushu University, Fukuoka, Japan; [2]National Institutes of Natural Sciences, Tokyo, Japan; r.mitsuishi@plasma.ed.kyushu-u.ac.jp

Zinc oxide (ZnO) is recognized as a candidate for ultraviolet light emitting diodes and laser diodes due to its wide band gap (3.37 eV) and large exciton binding energy of 60 meV[1]. An important technology for the industry is fabrication of high-quality single crystalline ZnO thin film on commercially useful sapphire substrates. The main challenge faced by researchers is the large lattice mismatch of 18% between ZnO and sapphire. We have recently developed a new technology using inversed Stranski-Krastanov (ISK) mode[2]; a thin buffer layer consisting of tiny 3D islands grow and relax the strain, and these islands rapidly coalesce and form a flat 2D layer. The essence of the ISK mode is the surface energy during the deposition, which depends on the surface morphology and the atmosphere. Despite the importance of the flux density in the surface morphology, there has been no detailed investigation. Here, we study the influence of RF power on the surface morphology of ZnO thin films fabricated on the buffer layer consisting of 3D islands.

All films were fabricated by RF magnetron sputtering using two ZnO targets with the purity of 99.99 %. First, 10-nm thick ZnO buffer layers were deposited on c-plane sapphire substrates in Ar/N2 atmosphere at 780°C. The flow rates of Ar and N2 were fixed to 24 and 1 sccm, respectively. The total gas pressure was 0.35 Pa. The RF power was fixed to 100 W. Then, 500-nm-thick ZnO films were deposited on the buffer layers in Ar/O2 atmosphere at 800°C. The flow rates of Ar and O2 were fixed at 45 and 5 sccm, respectively. The total gas pressure was 0.70 Pa. The RF power was varied from 20 W to 70 W. The surface morphologies were examined using atomic force microscope (AFM) and the lateral correlation length ξ of these ZnO films were examined.

The RF power dependence of ξ is shown in Fig. 1. ZnO film deposited at the power of 40 W provided the highest ξ of 1084 nm. At lower RF powers, ξ decreased. We assumed that the adsorbed atoms easily reached the thermodynamically stable position and the efficient fusion of crystal grains occurs at the optimal power of 40 W, whilst the atoms hardly reached the stable position and ended up with less ξ at different powers. More detail mechanism of the ISK mode will be discussed in the presentation.

This work was supported by JSPS KAKENHI Grant Numbers JP21H01372, 21K18731, NTT collaborative research, Toyota Riken Scholar, The Murata Science Foundation.

P1-33 Effects of surface fluorination on the oxidation resistance of Cu metal and its mechanism

Miho Fujihashi, Jae-Ho Kim, Susumu Yonezawa

University of Fukui, Japan; mi210392@g.u-fukui.ac.jp

Printed electronics (PE) refers to the technology that allows the fabrication of an electronic device through a printing process and to the respective devices manufactured in such a way. It appeared as a solution to pollutant and time-consuming deposing/etching techniques traditionally used as a circuits-making method. Commonly, gold (Au) and silver (Ag) have been the most used metals in the fabrication of metal-based inks for PE. Taking into account that the solid metal-based inks contain high metal loadings (above 20 wt.%), the current challenge is to substitute silver particles by other cheaper conductive metals, such as copper (Cu) with high electroconductivity. However, copper nanoparticles are subject to rapid oxidation during sintering, resulting in a significant decrease in conductivity. In previous studies [1], we attempted to improve the oxidation resistance of metal nanoparticles by surface fluorination with F2 gas. In case of Cu particles, a copper oxyfluoride (CuOxFy) layer formed on Cu particles could play a role to

prevent the surface oxidation of Cu particles even at 200℃. However, it is difficult to establish optimal fluorination conditions for the formation of the CuOxFy layer. Because the Cu particles have usually a non-uniform shape and particle size, it may be reasoned for various states of oxide layer on Cu particles. In this study, we tried to prove the CuOxFy layer using copper plates with uniform oxide films after surface fluorination.

Fig. 1 shows the XPS result of various Cu samples. After fluorination, two new peaks were observed; CuF2 at 687 eV and CuOxFy at 683 eV. The formation of CuOxFy was especially enhanced in the case of the fluorine-oxygen mixture and the stepwise inputting of O2 and F2 gases, which can be regarded as the optimum fluorination condition.

The conductivity results of each sample after heating are shown in Fig. 2. The surface conductivity of the Cu sample fluorinated with fluorine-oxygen mixture gas was about 100 times higher than that of the untreated or pure fluorine surface-treated sample. From these results, it is considered that the fluorine-oxygen mixture is suitable for the formation of CuOxFy layer with high oxidation resistance. Other information about CuOxFy and its relationship with film thickness will be explained in the poster presentation.

P1-34
Effects of thermal treatment of ZnO substrates on epitaxial growth of (ZnO)x(InN)1-x films fabricated by magnetron sputtering

Ryota Narishige, Naoto Yamashita, Kunihiro Kamataki, Takamasa Okumura, Kazunori Koga, Masaharu Shiratani, Naho Itagaki

Kyushu University, Japan; r.narishige@plasma.ed.kyushu-u.ac.jp

(ZnO)x(InN)1-x (called “ZION” hereinafter), pseudo-binary alloys of ZnO and InN, are promising materials for optoelectronic devices[1] since they have high exciton binding energies of 30–60 meV. Recently, we have succeeded in epitaxial growth of ZION films by radio-frequency (rf) magnetron sputtering on 1.6%-lattice mismatched ZnO substrates[2]. However, they turned out to have large root-mean-square (RMS) roughness around 7 nm. Here, to improve the surface morphology of ZION films, we investigated effects of the surface morphology of substrates on that of ZION films. The morphological data, obtained by atomic force microscopy (AFM), are analyzed statistically deriving the surface height distribution, RMS roughness, Rq, and skewness, Rsk. The last one is a third moment of the height distribution means the magnitude of asymmetry of the distribution.

Two types of ZnO substrates with different surface morphologies were prepared; one was not annealed, and another was annealed at 1000°C in air for 10 hours. ZION films were deposited on the O-polar surface of the substrates by rf magnetron sputtering in Ar/N2/O2 atmosphere at 450°C.

Figure 1 shows surface height distribution of ZION films, and the insets show AFM images of ZION films. The ZION film on non-annealed ZnO substrate has rough surface with the Rq of 7.09 nm. While, the ZION film on annealed ZnO substrate has flat surface with the Rq of 2.75 nm. We consider that this difference is attributed to the Rq and the Rsk of substrate. The Rq of ZION film decreases with decreasing the Rq of the substrates from 2.3 to 0.2 nm. Rsk affects migration of adatoms. The spikes on the surface, which appears as tail components in the height distribution, hamper the migration of adatoms and leads to secondary nucleation (Rq, an even order function of the height distribution, is insensitive to the odd order function). On the annealed substrate with small Rsk of 0.75, secondary nucleation might be suppressed. We also found that the ZION film grew coherently for more than 15 monolayers (ML) on the annealed ZnO substrate and had an atomically sharp interface with substrate by observing the cross sections using a high-resolution transmission electron microscopy. This research made an important contribution to the realization of device-grade ZION films.

This work was supported by JSPS KAKENHI Grant Numbers JP21H01372, JP21K18731, NTT collaborative research, Toyota Riken Scholar, The Murata Science Foundation.

P1-35
Electrical Properties of Li-doped and Undoped p-NiOx Double-layers on β-Ga2O3 Schottky Barrier Diodes

Jiyoung Min, Youseung Rim

Sejong University, Korea, Republic of (South Korea); mjy0539@gmail.com

Recently, beta gallium oxide (β-Ga2O3, 4.7–4.9eV), which has a wide band gap than SiC and GaN, has been attracting attentions in the field of power electronic applications.[1] The Baliga’s figure of merit(B-FOM) of Ga2O3 is about 3000, which is 4 times that of GaN and 10 times that of SiC, and is expected to achieving high breakdown voltage at low on-resistance in the power device.[2] Several devices structures, such as Schottky barrier diodes (SBD), Metal-semiconductor field-effect transistor (MESFET), and metal-oxide-semiconductor field-effect transistor (MOSFET) have been studied as power devices in recent years. However, despite these high numbers, the actual reported performance of the power unit is much lower than expected. This is because it is difficult to implement p-type Ga2O3, which can be used as PN junction termination to improve breakdown voltage value.[3] As a strategy to compensate for this is to construct p–n heterojunctions by integrating n-type Ga2O3 with other p-type semiconductors if the interface quality is controlled in an appropriate manner.[4]

In this study, a device was fabricated using NiO, a material with p-type conductivity.[5] Among p-type oxide families, the wide-bandgap NiO material has promising potentials in the applications of various optoelectronic and power devices due to its high visible spectral transparency and p-type conductivity stemming from nickel vacancies or monovalent impurities.[6] It was confirmed that the p-type NiOx was inserted between the β-Ga2O3 and the Ni Schottky junction to ensure the p-n characteristics and thus the depletion layer expanded. In addition, the conductivity control of nickel oxide was attempted by lithium doping. It was to improve the characteristics of the diode by lithium doping and oxygen concentration control. Furthermore, a diode was manufactured using a double-layer design of lithium doped and undoped NiOx by adjusting the hole concentration. As a result, compared to SBD and a diode without controlling a hole concentration, a double-layer diode provided an effective approach for improving the breakdown voltage and reducing the leakage current.

Acknowledgment

This work was supported by Korea Institute for Advancement of Technology (KIAT) grant funded by By the Ministry of Trade, Industry & Energy (MOTIE, Korea) (P0012451, The Competency Development Program for Industry Specialist) and the Technology Innovation Program - (20016102, Development of 1.2kV Gallium oxide power semiconductor devices technology) funded by MOTIE

[1] M. Higashiwaki and G. H. Jessen, Appl. Phys. Lett. 112, 060401 (2018)

[2] S. J. Pearton, F. Ren, M. Tadjer, and J. Kim, J. Appl. Phys. 124, 220901 (2018)

[3] N. Allen, M. Xiao, X. D. Yan, IEEE Electron Device Lett. 40, 1399 (2019)

[4] Y. Kokubun, S. Kubo, and S. Nakagomi, Appl. Phys. Express 9, 091101 (2016)

[5] H. H. Gong, Appl. Phys. Lett. 117, 022104 (2020)

[6] M. Tyagi, M. Tomar, IEEE Electron Device Lett. 34, 81 (2013)

P1-36
Electroluminescence Property of New Chrysene Derivatives with High Efficiency and Color Purity for OLED Blue Emitter

Changyu Lee, Sunwoo Park, Joohwan Kim, Hyukmin Kwon, Seokwoo Kang, Hwangyu Shin, Hayoon Lee, Jongwook Park
Khung Hee University, Korea, Republic of (South Korea); sinye375@khu.ac.kr

New blue fluorescent materials of 6-([1,1':3',1''-terphenyl]-5'-yl)-12-(4-(1,2,2-triphenylvinyl)phenyl)chrysene (TPE-C-TP) and 4-(12-([1,1':3',1''-terphenyl]-5'-yl)chrysen-6-yl)-N,N-diphenylaniline (TPA-C-TP) based on core-side concept were successfully synthesized. Chrysene known as deep blue chromophore was used as the central core. Triphenylamine and m-terphenyl groups were introduced as side groups in order to improve the quantum efficiency by using electron donating effect and preventing intermolecular interaction. Also, triphenylethylene group which is one of the conventional aggregation-induced emission moieties was substituted for increasing the photoluminescence efficiency in film state. In film state, photoluminescence maximum wavelengths of TPE-C-DPA and TPA-C-TP are 471 nm and 445 nm, respectively. Both compounds were used as an emitting layer in non-doped OLED device. TPE-C-TP device showed electroluminescence maximum wavelength of 476 nm, current efficiency of 5.92 cd/A. TPA-C-TP device exhibited external quantum efficiency of 4.31% and CIE (x, y) of (0.15, 0.07) which meets the TV requirement specification. The related more results will be discussed.

P1-37 Electrolytic Deposition of Anti-cancer Drug Composites on Metal Implants

Shih-Fan Chen, Shih-Han Chang, Yi-Ting Chen, *Shiow-Kang Yen
Department of Materials Science and Engineering, National Chung Hsing University, Taichung; ttpss94054@gmail.com

The electrochemical depositions of Paclitaxel (PTX)/ Doxorubicin (DOX), Cisplatin (CDDP)/DOX and PTX/ CDDP anti-cancer drug composites on Ti6Al4V specimens are investigated for targeting at the related tumors to provide an innovative treating guideline for some cancers. Ultraviolet/ visible spectroscopy（UV/VIS）was utilized to measure Paclitaxel, Doxorubicin and Cisplatin loading and release, scanning electron microscope（SEM）to observe surface morphology, and osteosarcoma cells (G292) 3-(4,5-Dimethylthiazol-2-yl)-2,5-diphenyltetrazolium bromide (MTT) assay to observe cell viability on and toxicity from drug loaded specimens.

These three drug composites can be electrochemically deposited on Ti6Al4V specimens by the methods of layer by layer. In the MTT test of G292 cells, the cell viabilities directly on Ti6Al4V, Chitosan (Chi) coated and HAp coated specimens increase with the culture duration increasing. On the other hand, those of PTX-Chi/DOX-Chi/HAp coated, DOX-Chi/CDDP/HAp and CDDP/PTX-Chi/HAp coated are in the inverse tendency, corresponding to the cell morphology getting into apoptosis.

In the cytotoxicity test of G292 cells, the cell viabilities in medium extracted from the uncoated, Chi coated and HAp coated Ti6Al4V specimens are approaching 100 % (vs. negative control), all revealing good biocompatibility and nontoxicity. However, the cell viabilities of PTX-Chi/DOX-Chi/HAp coated, CDDP/DOX-Chi/HAp coated, CDDP/PTX-Chi/HAp coated specimens, similar to the positive control (10% DMSO) are approaching to 10 % (vs. negative control), indicating that the drug coated specimens make the cells gradually apoptotic until they die, resulting from drugs retarding cell proliferation. In other words, the anticancer drugs in the composite coatings remain their chemical stability after the electrochemical process.

P1-38
Enhanced energy-storage performance and thermal stability in (Bi0.5Na0.5)0.925Ba0.075Ti(1-x)ZrxO3 relaxor ferroelectric ceramics

Cheng-Sao Chen[1], Jhao-Yuan Liao[2], Pin-Yi Chen[3], Chi-Shun Tu[2]
[1]Hwa Hsia University of Technology, Taiwan; [2]Fu Jen Catholic University,; [3]Ming Chi University of Technology;
rickchen@go.hwh.edu.tw

In this paper, Zr-doped (Bi0.5Na0.5)0.925Ba0.075Ti(1-x)ZrxO3 (BNB100xZT, x=0, 0.02, 0.04, and 0.06) relaxor-ferroelectric ceramics were studied to optimize energy density and storage efficiency. Microstructure and electrical properties were analyzed to explore the influence of ZrO2 dopant in energy-storage performance and temperature-stable dielectric properties of BNB100xZT ceramics. By adding ZrO2 dopant, dielectric breakdown strength (BDS) can be effectively increased, while remanent polarization (Pr) and coercive field (Ec) were evidently reduced. The optimal recoverable energy density (Wrec) of 4.77 J/cm3 and storage efficiency (η) of 73.6% are respectively achieved for BNB4ZT (at E=150 kV/cm and T=25oC) and BNB2ZT (at E=100 kV/cm and T=100oC). Temperature-dependent dielectric permittivities show that BNB100xZT ceramics maintain temperature-stable dielectric properties with low dielectric losses (tan δ < 0.1%) and temperature coefficient of capacitance (TCC). This work demonstrates that relaxor-ferroelectric (Bi0.5Na0.5)0.925Ba0.075TiO3 (BNBT) ceramics doped with proper ZrO2 additives are suitable for using in high-density energy storage.

P1-39
Estimation of the excited CO density in plasma contributing to CO2 methanation by optical emission spectroscopy

Susumu Toko[1], Masashi Ideguchi[2], Taiki Hasegawa[2], Takamasa Okumura[2], Kunihiro Kamataki[2], Kosuke Takenaka[1], Kazunori Koga[2], Masaharu Shiratani[2], Yuichi Setsuhara[1]

[1]Osaka University, Japan; [2]Kyushu University, Japan; susumu.toko@jwri.osaka-u.ac.jp

CO2 methanation can be a key technology for realizing a sustainable society. CH4 is used as an energy carrier and raw material for chemical products, thereby contributing to the reduction of CO2 emissions. The methanation reaction is generally promoted by thermal catalysis at temperatures above 250°C. However, since this reaction is exothermic, it is desirable to promote the reaction at lower temperatures for stability and throughput. Plasma catalysis can accelerate the process at lower temperatures than thermal catalysis. This is mainly due to the formation of excited molecules in the plasma. In this study, we investigated the relationship between the excited CO molecules generated in plasma and methane production. Optical emission spectroscopy is useful for estimating the density of excited molecules from CO. The CO Angstrom band intensities give the information of the density of excited molecules. We controlled the generation rate of excited molecules by controlling the gas residence time and electron density, and improved the CH4 generation rate. We found that the CO Angstrom band is useful as a simple indicator of CO2 methanation. Details will be reported in the presentation.

P1-40
Extreme enhancement of mechanical properties of hetero-network hydrogels composed of PVA-Agar cross-linked with tannic acid

Moustapha Mohamed Mahamoud, Makoto Takafuji

kumamoto University, Japan; harroun92@gmail.com

Versatile hydrogels composed of natural and synthetic polymers have great potential for use in biomedical applications such as wound healing, cartilage replacement, and tissue engineering. primarily due to their combined properties such as low toxicity, biocompatibility, biodegradability, and enhanced strength. Herein, we report the preparation of strong and porous hydrogels composed of polyvinyl alcohol (PVA) intercalated agar polymer networks physically crosslinked with tannic acid (TA). The preparation process consists of an amount of TA with different masses dissolved in distilled water. Subsequently, PVA was added to the TA solution heated at 95°C and stirred at 350 rpm for 4 hours to obtain the PVA-TA mixed solution. Finally, a certain amount of agar was added to the PVA-TA solution. The mixed solution was thoroughly stirred and poured into a square styrene case, frozen at -15 °C for 24 hours, and thawed at room temperature for 4 hours (freeze/thaw cycles were conducted 1 to 3 times for strength and morphology investigation). The effect of multiple freezing and thawing on the hydrogel was studied, and it shows that more freezing and thawing cycles generate numerous crystallites in the hydrogel system that result in strong entanglement of the polymer chain. The highest tensile strength of PVA-agar hydrogel incorporated with TA and 3 times frozen/thawed was 0.55 MPa, and it exhibits a highly porous structure. The mechanical strength of PVA-Agar-TA is almost 2 times stronger than PVA-Agar hydrogel without TA, and similarly frozen/thawed 3 times, which was only 0.3 MPa. The mechanical enhancement recorded on the hydrogel loaded with a small amount of tannic acid while subjected to multiple freeze/thaw cycles ensures hydrogel material safety that is fabricated with low toxicity and has multifunctional characteristics. The developed hydrogel will pave the way for a new approach in hydrogel research and has significant potential for medical applications such as cartilage replacement (especially in the deep zone).

P1-41 Factors Influencing Adhesion of Submicrometer Thin Metal Films

Abdeljalil LAHMAR, Ali ASSAF, Marie-José DURAND, Sulivan JOUANNEAU, Gerald THOUAND

University of Nantes, French (France); abdeljalil.lahmar@univ-nantes.fr

The performance of a coating-substrate system depends on adhesion and this study examine factors influencing the adhesion of sub micrometer thin metal films. The scratch test was used to determine the coating-substrate adhesion of d.c. magnetron-sputtered films on substrates. Several systems were discussed, including Cu, Al, AlN/XC70 steel; Cu, Au/Al2 O3 ; and Cu/Ni as well as the following effects of deposition conditions : (a) the effect of heating the sample during or after deposition, (b) the effect of applying a bias voltage on the substrate during deposition, (c) the effect of ion bombardment etching of the substrate surface, (d) the effect of ageing treatment after deposition, (e) the effect of chemical etching treatment before deposition.

The scratch tracks were observed by scanning electron microscopy (SEM), and some energy-dispersive X-ray spectra were recorded to reveal whether the coating was completely removed from its substrate or not. The adhesion failure probability was estimated for each load (Q) by optically inspecting the channels. A correlation between the thermal contact resistance and the adhesion was found showing the variation of the ratio 1/Rc as a function of Q.

The adhesion considerably affect the heat transfer in the interfacial region and the best results are obtained with high values of Q. The low value of Rc is attributed to the mechanical interlocking effect, which results from the formation of micro-cavities and compact structure at the substrate surface during ion bombardment etching. In addition, at low Ar pressure, the formation of a new compound in the interfacial region enhances both adhesion and heat transfer. To further understand the origin of the mean critical load and interface evolution, observations were made using SEM, Auger electron spectroscopy (AES) and X-ray photoelectron spectroscopy (XPS).

The results show that the structural change of the film and formation of a complex interface appear to be the main reason for interface evolution. In most cases, the widening of the interfacial region offers a better film anchorage to its substrate, which requires a notably high stylus load to produce an adhesion failure.

P1-42 Faster Operation of SrCoOx-based Solid-State Electrochemical Thermal Transistors

Mitsuki Yoshimura[1], Qian Yang[2,3], Zhiping Bian[3], Hai Jun Cho[4], Hiromichi Ohta[4]

[1]School of Engineering, Hokkaido University, Japan; [2]Institute of Quantum and Sustainable Technology, Jiangsu Univsity, China; [3]Graduate School of IST, Hokkaido University, Japan; [4]Research Institute for Electronic Science, Hokkaido University, Japan; mit10king11@eis.hokudai.ac.jp

Very recently, we have realized a solid-state electrochemical thermal transistor using SrCoOx as the active layer and YSZ as the solid electrolyte.[1] The transistor is operated at 280 °C in air by applying negative/positive voltage to Pt/SrCoOx/Gd-doped CeO2/YSZ as reduction/oxidation of the SrCoOx layer. The thermal transistor shows rather high on-to-off thermal conductivity ratio of κON/κOFF ~4 (κON: ~3.8 W m−1 K−1 for oxidized SrCoO3, κON: ~0.95 W m−1 K−1 for reduced SrCoO2). Although the thermal transistor repeatedly works very well, the operation speed is slow; When a constant voltage (±8 V) was applied to the transistor, on-to-off switching took ~5 min. Here, we focused to reduce the resistance of the solid electrolyte, YSZ, since the transistor operation almost perfectly obeys Faraday's law of electrolysis. We investigated the effect of the thickness of YSZ substrate on the transistor operation. When we used the 0.2-mm-thick YSZ as the substrate, the time for the redox reaction with constant ±8 V was reduced to 2 min. On the other hand, change in the required voltage when constant current operation became obvious when the YSZ substrate was thinner. The present results reveal that the use of thinner YSZ substrate is an effective way to increase the operation speed.

[1] YANG, Q., CHO, H. J., BIAN, Z., YOSHIMURA, M., LEE, J., JEEN, H., LIN, J., WEI, J., FENG, B., IKUHARA, Y., & OHTA, H. manuscript in preparation

P1-43 Fe3O4-Embedded Hollow Graphitic Carbon Fibers Interlayer as a Polysulfides Barrier for High-Rate Lithium-Sulfur Batteries

Ying Liu, Dong Jun Lee, Ha Cheol Ju, Jou-Hyeon Ahn

Gyeongsang National University, Korea, Republic of (South Korea); lying@gnu.ac.kr

Recently, lithium-sulfur (Li-S) batteries have received much attention due to their inherent merits of high theoretical energy density, low cost, and eco-friendliness, which are considered as one of promising energy storage systems. However, the serious problems of Li-S batteries result from low electrochemical activity, poor cyclability, and sluggish reaction kinetics. In this study, a novel structural configuration of a multifunctional interlayer, including hollow graphitic carbon fibers (HGCF) and in-situ generated Fe3O4 nanoparticles, is designed via a scalable one-step carbonization method. HGCF derived from waste cotton tissues possesses the advantages of superior conductivity, and hierarchically porous structure, which can greatly enhance the transfer of electrons/ions, accelerating the reaction kinetics. The superior anchoring ability and strong catalytic effect of Fe3O4 can prevent the shuttle effect of polysulfides and enhance the conversion rate, promoting an excellent electrochemical performance at high rates. As a result, the Super-P/S cell with the hybrid interlayer shows a high capacity retention of 700 mAh g-1 at 1 C after 100 cycles, providing excellent rate capability up to 3 C-rate.

P1-44 Fluctuation of plasma and amount of nanoparticles in TEOS amplitude modulated rf discharge

Akihiro Yamamoto[1], Iori Nagao[1], Kunihiro Kamataki[1], Daisuke Yamashita[1], Takamasa Okumura[1], Naoto Yamashita[1], Naho Itagaki[1], Kazunori Koga[1,2], Masaharu Shiratani[1]

[1]Kyushu University, Japan; [2]National Institute of Natural Sciences; a_yamamoto@plasma.ed.kyushu-u.ac.jp

For faster development of ultra-precision nano fabrication methods for 3D devices, effects of amplitude modulated (AM) rf discharge on growth of nanoparticles in the TEOS-plasma and relations among spatial profiles of plasma parameters and growth of nanoparticles must be clarified. We already confirmed the effect of AM rf discharge on growth of nanoparticles and fluctuation of amount of nano-particles in DM - DMOS plasma [1,2]. However, there are few reports on the effects of AM rf discharge in TEOS plasma. Moreover, relation between growth of nanoparticles and plasma generation in amplitude modulated reactive plasma has not been clarified yet.

In this study, we investigated effects of AM rf discharge on fluctuation of plasma and the behavior of nanoparticle in TEOS plasma.

Experiments were performed using a capacitively-coupled rf discharge reactor. TEOS (Si(OC2H5)4) and O2 were supplied to the reactor at a flow rate of 40 sccm and 180 sccm, diluted with Ar at a flow rate of 160 sccm. The total gas pressure was 6 Torr. The rf discharge power was 30W and the frequency was 13.56 MHz for a discharge period of Ton = 8 s.

For obtaining information of nanoparticles, we applied a 2DLLS method [3]. Light scattering intensity from nanoparticles was measured with a high-speed camera (Photron, 1000 fps). The LLS intensity is proportional to nanoparticle density np and the sixth power of their size dp (~npdp6) in the Rayleigh scattering regime. For the study of relations between growth of nanoparticles and plasma, we measured simultaneously both LLS intensity and emission intensity of Ar I (λ=750.4 nm) with two high speed cameras.

We found fluctuations in the time evolutions of LLS intensity and ArI emission intensity at plasma/sheath boundary region. The LLS intensity at plasma/sheath boundary region increases or decreases in positive synchronization with ArI emission intensity. This result suggests that there is a strong spatio-temporal correlation between the growth of nanoparticles and the generation of plasma. We will discuss details at the conference.

This work was partly supported by JSPS KAKEN HI (Grant No. JP19K03809 and JP20H00142)

Keywords: Amplitude modulation, nano-particle, plasma fluctuation

[1] K. Kamataki, et al., Appl. Phys. Express, 4, 105001 (2011).

[2] M. Shiratani, et al., J. Phys.D: Appl. Phys. 44, 174038 (2011).

[3] N. Nunomura, et al., J. Appl. Phys. 99, 08330 (2006).

P1-45
Graded adhesive joints with magnetic thermally expandable particles: mechanical properties and debonding of the adhesive joint

Juana Abenojar[1,2], Miguel Angel Martinez[1], Sara López de Armentia[3], Juan Carlos del Real[3]
[1]Universidad Carlos III de Madrid, Spain; [2]Universidad Pontificia Comillas de Madrid, Spain; [3]Universidad Pontificia Comillas de Madrid, IIT, Spain; mamc@ing.uc3m.es

One of the advantages of adhesive joining over other joining techniques is the reduction of stress concentration thanks to the large continuous bonded area. However, stress concentrations still exist at the edges of the joint, causing initial cracks. Consequently, many researchers are focused on reducing stress concentration by different techniques: gradual curing of the adhesive heating by induction; use of more ductile adhesives at the edge of the overlap or the use of adhesives with magnetic particles [1] that can be placed on the edge of the overlap with magnetics fields.

On the other hand, adhesives need to compliance with regulations on recyclability and sustainability must be guaranteed. It means that adhesive-bonded structures should be able to be debonded. In the last years, new debonding technologies have been developed, being the most common the addition of fillers [2]. Amongst them, thermally expandable particles (TEPs) are formed by a thermoplastic shell filled with liquid hydrocarbon. When they are heated, the shell softens and the gasification and expansion of the hydrocarbon occurs, producing the debonding of the joint. TEPs can also create a tailored particle distribution by applying a magnetic field when they are magnetized. Graded joints and debonding could help to develop more sustainable adhesive joints.

TEPs Expancel 031 DU40 with diameter ranged around 13 µm were used. As adhesive, a 2K Epoxy Araldite□2012 was used. TEPs were magnetized with a previously developed method [3]. The aim of this work is to study the addition of non-magnetized and magnetized TEPs on mechanical properties by single lap and wedge tests, and debonding properties by heating at 100 ºC for 5 min.

Keywords: Multifunctional adhesive, debonding, graduated joint, expandable particles, magnetic particles

[1] DA SILVA, C.I., CUNHA M.R.O., BARBOSA, A.Q., CARBAS, R.J.C., MARQUES, E.A.S. & DA SILVA L.F.M. 2021. Functionally graded adhesive joints using magnetic microparticles with a polyurethane adhesive. J Adv Join Process, 3, 100048.

[2] BANEA, M.D., DA SILVA, L.F.M., CARBAS R.J.C. & CAMPILHO R.D.S.G. 2014. Mechanical and thermal characterization of a structural polyurethane adhesive modified with thermally expandable particles. Int J Adhes Adhes, 54, 191-199.

[3] ABENOJAR, J., LÓPEZ DE ARMENTIA, S., BARBOSA, Q., MARTÍNEZ, M.A., VELASCO, F., DA SILVA, L. F. M. & DEL REAL, J.C. 2020. Coating cork particles with iron oxide: effect on magnetic properties. Wood Sci Technol, 54, 869-889.

P1-46
Hierarchically Structured CuxS@NixS Core-Shell Electrode for High-Performance Supercapacitor

MinKyeong Kim, Dongll Kim, SooHong Lee, HeeBin Jeong, John Hong
Kookmin University, Korea, Korea, Republic of (South Korea); alsrud6108@kookmin.ac.kr

There is a large demand for new energy storage system with a high energy density and power density for future electric vehicles and high-performance portable devices. Supercapacitor system is a suitable application for these needs. In particular, pseudocapacitors usually show a higher energy density than electric double layer supercapacitors due to its additional Faradaic redox mechanism on the surface of electrode materials. Therefore, finding a new electrode material for surface Faradaic redox reactions is important for pseudocapacitors.

Transition metal sulfides have received a great attention as the pseudocapacitive electrode material by overcoming the low electrical conductivity of transition metal oxides. Especially, nickel sulfide (NixS) can provide the high capacitance compared to other sulfide materials. [1] Moreover, copper-based sulfide materials (CuxS) show the high cycling stability. Therefore, combining both NixS and CuxS electrode materials can synergistically improve the overall energy storage performance of pseudocapacitors. Here, we fabricated a high-performance pseudocapacitor electrode with core-shell structures. The shell structure of NixS were coated on the CuxS backbone nanorods by a simple solution sulfurization method. By controlling the synthetic parameters, the core-shell structured electrodes can show the increased capacitance and improved cycling stability for the pseudocapacitor application.

P1-47
Highly Sensitive and Selective Colorimetric Sensing for Iodide Based on Chemical Etching of Triangular Silver Nanoplates

Hyeonbo Shim, Mun Ho Kim
Pukyong National University, Korea, Republic of (South Korea); shb1974@pukyong.ac.kr

Iodide is known as an essential nutrient for the human body. However, long-term deficiency of iodide leads to goiter and thyroid atrophy, while an excess of iodide prevents the ability of thyroxine and triiodothyronine, which control many metabolic activities in the human body. In this present study, a triangular silver nanoplate-based colorimetric sensing system was developed for iodide detection. Since the sharp corners of the triangular silver nanoplates are very unstable, the triangular Ag nanoplates are easily transformed into a spheroidal shape by chemical etchants, accompanying dramatic changes in the Localized Surface Plasmon Resonance (LSPR) properties. Based on this correlation, we developed a novel sensing system for iodide. In detail, we constructed a sensing system that did not react with other halide ions (bromide, chloride), sodium 4-vinylbenzenesulfonate, and hydrogen peroxide, which are known as strong etchants for Ag nanoplates, and selectively reacted only with iodide.

P1-48 Hole generation mechanism in n-type SnOx after N2 post-deposition annealing

Kotaro Watanabe, Takuma Kawaguchi, Ayumu Nodera, Yuki Kumamoto, Shun Mori, Shinya Aikawa
Kogakuin Univ., Japan; cm21060@g.kogakuin.jp

Recently, all oxide CMOS applications have been developed because it has unique advantages, for example low-temperature processability, low-power consumption and optical transparency [1]. Typical p-type oxide TFT shows less electrical properties compared to n-type TFT, such as field effect mobility and on/off current ratio [2]. Thus, development of superior p-type TFTs similar to n-type TFTs is required. Among p-type oxide semiconductors, SnO-based materials are attractive attention because of ambipolar conduction, earth-abundant element and high mobility but the deposition condition in p-type SnO is very narrow compared to n-type SnO2. To convert n-type SnOx to p-type, nitrogen (N) doping is effective method because N incorporation into O-site is expected to act as an accepter without unintentional charge compensation [3]. Although nitridation is usually performed using plasma treatment, this technique induces surface damages. On the other hand, it is known that N2 dissociation is difficult by post-deposition annealing (PDA) due to the high binding energy of ~10 eV. Lee et al. discussed that N2 can be dissociated at 600 °C annealing when N2 incorporated in the bulk. This is understood by the elongation of N2 bond length trapped inside bulk [4]. Based on their results, we have focused on the N doping by PDA to obtain p-type SnOx thin films [5]. The Hall-effect measurement revealed that yield of the SnOx thin films in p-type behavior successfully increased, however, the detailed hole generation mechanism in n-type SnOx film by N2 PDA is still unclear. Here, we discuss the origin of hole generation in N-doped SnOx based on X-ray photoelectron spectroscopy (XPS) analyses.

SnOx thin film (thickness: 100 nm) was deposited on a Si/SiO2 substrate using RF magnetron sputtering at room temperature. A ceramic SnO2 target was used for thin film formation. Then, the film was annealed for 30 min under N2 atmosphere at 600 °C using a rapid thermal annealing equipment (ULVAC, MILA-3000). The electrical properties of the film were measured at room temperature using a Hall-effect measurement system. The binding states were also characterized by XPS (JEOL JPS-9000MC).

Figure 1 shows a typical N1s XPS spectra before and after N2 PDA. As shown in the figure, the N1s can be deconvoluted three peaks. The peak located at 397.8 eV is derived from N-Sn bond, which is considered to be triple bond. In case of triple binding states, N is substituted into VO [6], thus, hole generation is possible to occur on O2p orbitals as shown in the inset of Fig. 1. In addition to the N1s spectrum, peak shift caused by charge transfer was also observed in Sn3d orbitals. Other XPS spectrum including structural characterization by X-ray diffraction will be discussed.

P1-49 Zinc ion batteries with stable capacity behavior by an intercalation of Crystal water in a cathode

Geun Yoo[1], Seoyeong Kim[1], Jaeyeon Lee[1], Geon-Hyoung An[1,2]
[1]Department of Energy System Engineering, Gyeongsang National University, Republic of Korea; [2]Department of Energy Engineering, Future Convergence Technology Research Institute, Gyeongsang National University, Republic of Korea; ghan@gnu.ac.kr

Due to the ever-increasing environmental issues and energy crisis over the use of fossil fuels, solar photovoltaic, wind power and other non-fossil energy that can generate electrical energy have attracted significant attention[1,2]. However, renewable energy, such as solar and wind power sources are strongly dependent on the weather condition. Therefore, it is necessary to develop large-scale energy storage systems (ESS) to accomplish a stable power output. Among various rechargeable batteries, lithium-ion batteries (LIBs) have emerged as the most promising ESS system in the commercial ESS field owing to their attractive advantages, such as high energy density, voltage capacity and lower self-discharge rate than other rechargeable batteries. Nevertheless, the potential of LIBs as ESS applications is limited owing to several problems such as the high cost, environmental pollution, and safety issues of the system. Therefore, research on various energy storage devices such as Na-, Al-, Mg-, and Zn-ion batteries (ZIBs) is needed[3]. ZIBs have attracted rising attention for battery industry due to their satisfactory safety levels, low cost, and eco-friendliness. However, the volume expansion and the irreversible dissolution of vanadium pentoxide (V2O5) during cycling lead to the low electrochemical capacity and poor kinetics of the electrode, which limit its development as a cathode material for ZIBs. In this study, a stable V2O5 with structural stability is prepared as a ZIBs cathode material using an electrochemical activation process. The cycling performance of the stable V2O5 was confirmed, as well as the synergistic effects of the zinc ion diffusion process, increased number of active sites, improved electrical conductivity. As a results, the stable electrode achieved a superior capacity performance, with a superb specific capacity of 457 mAh g-1 at a current density of 0.1 A g-1, a remarkable rate performance of 272 mAh g-1 at a current density of 2.0 A g-1, and an excellent capacity retention of 91% for 200 cycles at current density of 1.3 A g-1.

These results will be discussed in in AFM 2022 in detail, and this work was supported by the National Research Foundation of Korea (NRF) grant funded by the Korea government (MSIT) (NRF- 2020R1C1C1010611).

References

[1] J. Yin, A. Molini, A. Porporato, Nat. Commun. 11 (2020) 4781.

[2] P.E. Bett, H.E. Thornton, Renew. Energy 87 (2016) 110.

[3] G. Yoo, B.-R. Koo, G.−H. An, Chemical Engineering Journal 434 (2022) 134738

P1-50 Piezoelectric Properties of PSN-PMN-PZT Ceramics for Ultrasonic Transducer Application

In Ho IM[1], Ho jun YOO[2]
[1]Shinansan University, Korea, Republic of (South Korea); [2]Jeju University, Korea, Republic of (South Korea); matt7303@naver.com

In this study, PSN-PMN-PZT ceramics were fabricated with the sintering temperature of 1260°C. And their piezoelectric and dielectric properties were investigated according to changes in polarization temperature. In order to search for optimum poling condition of manufactured specimens, the poling temperatures were varied as 25°C, 60°C, 80°C, 110°C, 140°C, respectively. The higher the poling temperature is, the better the piezoelectric properties are. The poling temperature with the best piezoelectric

properties was 140°C. We reported the excellent values of dielectric constant=1306, density= 7.78 g/cm3, kp = 0.545 , Qm = 2,054 in the poling temperature of 140°C. This characteristic is suitable for the application of high power piezoelectric transformer and actuator requiring high Qm.

P1-51 Piezoelectric Properties of PMN-PZT Ceramics and Simulation of Ultrasonic Tooth Cleaner

Juhyun Yoo[1], Sun A Whang[2], Jae Gyu Lee[1], Jonghyeon Lee[1], Sujin Kang[1], Sua Kim[2], Dae Yeol Hwang[2], Ji Hoon Lee[2]

[1]Department of Electrical Engineering, Semyung University, Korea, Republic of (South Korea); [2]Department of Nursing, Semyung University, Korea, Republic of (South Korea); dlworb7101@naver.com

In this paper, in order to develop the composition ceramics for ultrasonic tooth cleaner testing, Pb(Mn1/3Nb2/3)O3-Pb(Zr,Ti)O3 [PMN-PZT] system ceramics were manufactured and their dielectric and piezoelectric properties were investigated. At the ceramics sintered at 920 [℃], the high values of piezoelectric properties were appeared, respectively: the dielectric constant (εr) of 1,689, piezoelectric charge constant (d33) of 433 [pC/N], electromechanical coupling factor (kp) of 0.64, and mechanical quality factor (Qm) of 835 were suitable for the device application such as ultrasonic tooth cleaner. Using this composition ceramics, the ultrasonic tooth cleaner was designed and simulated.

[1] Yoo, J.; Lee, J. The Effects of MnO2 Addition on the Physical Properties of Pb(Ni 1/3Nb 2/3)O3-Pb(Zr,Ti)O3-Pb(Mg 1/2 W 1/2)O3-

BiFeO3 Ceramics. Crystal 2021, 11, 29.

P1-52 Electrodeposited cuprous oxide-based light-addressable potentiometric sensors

Yan-Qi Liang[1], Hui-Ling Liu[1,2], Dorota G. Pijanowska[3], Chia-Ming Yang[1,2,4]

[1]Institute of Electro-Optical Engineering, Chang Gung University, Taoyuan, Taiwan.; [2]Department of Electronic Engineering,Chang-Gung University,Taoyuan, Taiwan; [3]Nalecz Institute of Biocybernetics and Biomedical Engineering, Polish Academy of Sciences, Warsaw 02-109, Poland; [4]Department of Neurosurgery, Chang Gung Memorial Hospital at Linkou, Taoyuan City, Taiwan; poke210113@gmail.com

Cuprous oxide (Cu2O) is a well-proven semiconductor material with microstructures. [1, 2] To evaluate the application of Cu2O [3] to photoelectrochemical and light-addressable potentiometric sensor (LAPS) [4], the electrochemical deposition of Cu2O on indium tin oxide on glass (ITO/glass) was modified in the deposition temperature, deposition time and pH value of deposition solution, under our established 3-eletrodes electrochemical system and self-designed holder. The fabricated Cu2O layers were investigated by using non-destructive and destructive material analysis to collect all relative material information including Ultraviolet–visible spectroscopy (UV-vis), atomic force spectroscopy (AFM), x-ray diffraction spectroscopy (XRD), and scanning electron microscopy (SEM). The AFM and SEM picture of Cu2O layer is shown in the Fig. 1(a) and (b), respectively. It matches to published literatures. [5] Then the photoelectrochemical behaviors were tested under different wavelength and intensity to evaluate the feasibility of light addressable potentiometric sensors. An insulator layer, niobium oxide (NbOx), deposited by a radio frequency (rf) reactive sputtering on electrochemical deposited Cu2O. Then a standard encapsulation with PDMS tank was attached on the surface of NbOx for following standard LAPS measurement. [6] The typical photocurrent versus bias voltage curves under different wavelength and frequency is shown in Fig. 2(a) and (b), respectively. The obtained photocurrent is in the similar level of IGZO-based LAPS [7], but higher than Si-based LAPS [8]. For the basic pH sensing, the pH-dependent PC-V curves are shown in Fig. 2(c) with a pH sensitivity and linearity of 86.3 mV/pH and 96.467%, respectively. The first study of electrodeposited Cu2O layer for the semiconductor layer of LAPS and corresponding material analysis is detail presented for future chemical and biomedical sensing applications.

P10-13

P1-53 Fabrication and Characterization of Synaptic Devices Based on Au/HfxZr1-xO2/Pt Ferroelectric Tunnel Junction

Sejoon Lee[1,2], Deuk Young Kim[1,2], Youngmin Lee[2], Woochul Yang[3], Moon-Deock Kim[4]

[1]Department of Semiconductor Science, Dongguk University, Seoul 04620, Korea; [2]Quantum-functional Semiconductor Research Center, Dongguk University, Seoul 04620, Korea; [3]Department of Physics, Dongguk University, Seoul 04620, Korea; [4]Department of Physics, Chungnam National University, Daejeon 34134, Korea; sejoon@dongguk.edu

The HfxZr1-xO2 thin films were grown onto the (111) Pt substrates at 450 °C by radio-frequency magnetron sputtering, and were annealed at 600 – 800°C. The samples showed a smooth surface and an orthorhombic lattice structure, and exhibited a nonlinear lossy-type ferroelectric characteristic. The memristive devices, which were fabricated in the form of the top-to-bottom two-terminal device scheme of Au/HfxZr1-xO2/Pt, clearly showed the polarization-dependent asymmetric hysteresis behavior in their resistive switching characteristics. At the certain and moderate sweep voltage ranges, the on-state current became taller as the sweep number was gradually increased. This could be attributed to the increased potential gradient in the HfxZr1-xO2 layer because the repeated voltage stresses would tenaciously increase the electrical polarization inside the ferroelectric HfxZr1-xO2 layer. Namely, the increased electrostatic polarization field in HfxZr1-xO2 gives rise to the increase in the tunneling probability through the HfxZr1-xO2 potential barrier; and it eventually results in an increase of the tunneling current. Using these unique characteristics, we demonstrated various synaptic functions such as a long-term potentiation/depression and a spike-timing dependent plasticity.

[1] L. Chen et al., Nanoscale. 10, 15826 (2018).

[2] C. Sung, et al., Appl. Phys. 124, 151903 (2018).

P1-54
Effects of Rapid Thermal Annealing on Dielectric Characteristics of High-k ZrO2 Grown on p-Ge

Youngmin Lee[1], Sejoon Lee[1,2], Deuk Young Kim[1,2], Woochul Yang[3], Moon-Deock Kim[4]

[1]Quantum-functional Semiconductor Research Center, Dongguk University, Seoul 04620, Korea; [2]Department of Semiconductor Science, Dongguk University, Seoul 04620, Korea; [3]Department of Physics, Dongguk University, Seoul 04620, Korea; [4]Department of Physics, Chungnam National University, Daejeon 34134, Korea; ymlee@dongguk.edu

The high-k ZrO2 layers were grown on p-type Ge substrates at 500 °C by RF magnetron sputtering. Subsequently, the samples were then annealed at 600 – 700 °C for 60 s in Ar ambient to improve their structural and dielectric properties. In comparison with the as-grown sample, the annealed samples exhibited both the improved crystal phase and the increased electrostatic capacitance. Particularly, the ZrO2 layer annealed 650 °C showed the high dielectric permittivity (kox ~ 24) and the low equivalent oxide thickness (EOT << 4 nm). Furthermore, the 650 °C-annealed sample revealed the stable electrostatic capacitance characteristics even at the wide frequency range of 5 – 1000 kHz. From the structural and electrochemical characterization results, it was found that the improved dielectric characteristics were attributed to the annealing effect on the crystallographic stabilization of ZrO2, particularly, at the ZrO2/Ge interface. Namely, the metastable bonds of Zr-O-Ge were at created at the interface between ZrO2 and Ge so that the electrostatic coupling strength could be enhanced at the interface.

[1] Z. C. Lei et al., Thin Solid Films 642, 352 (2017).

[2] Y. H. Wong et al., Surf. Interfaces 23, 101007 (2021).

[3] I. Mitevski et al., ECS Trans. 77, 1977 (2017).

[4] T. I. Lee et al., IEEE Electron Device Lett. 40, 502 (2019).

P1-55 A Study of Solid-phase Crystallization of Amorphous ZnON Films

Zhiyuan Shen[1], Yuta Mido[1], Naoto Yamashita[1], Takamasa Okumura[1], Kunihiro Kamataki[1], Kazunori Koga[1,2], Masaharu Shiratani[1], Hisato Yabuta[1], Naho Itagaki[1]

[1]Kyushu University, Fukuoka, Japan; [2]National Institutes of Natural Sciences, Tokyo, Japan; z.shen@plasma.ed.kyushu-u.ac.jp

Aluminium-doped zinc oxide (ZnO:Al) is a promising alternative to tin-doped indium oxide (ITO) as transparent conductive oxides because of the high conductivity and high transparency to the visible light [1-3]. Recently, very thin ZnO:Al films, 20 nm in thickness, with a resistivity of and an optical transmittance higher than 80% have been realized by using ZnO buffer layers fabricated by solid phase crystallization (SPC) [4,5], where the SPC has been realized by deposition of amorphous zinc oxynitride (a-ZnON) films using Ar/N2 magnetron sputtering followed by annealing. Here, aiming to clarify the mechanism of the SPC of a-ZnON, we investigate the desorption behavior of N atoms during annealing by thermal desorption spectrometry (TDS) and discuss the correlation with the crystallization behavior observed by transmission electron microscopy (TEM). Furthermore, we performed extended x-ray absorption fine structure (EXAFS) measurements to investigate the structural ordering of the ZnO films fabricated by SPC.

a-ZnON films were prepared on quartz glass substrates by radio-frequency (RF) magnetron sputtering at room temperature in Ar/N_2 atmosphere. Then, the a-ZnON films were annealed in air at 400℃ and 600℃to perform SPC. The thickness of all the films was 100 nm. Reference ZnO film formed by vapor phase crystallization (VPC) was prepared in Ar/O2 atmosphere. We confirmed from x-ray diffraction (XRD) measurements that the out-of-plane alignment of ZnO film is improved by SPC, where the (002) diffraction peak of SPC-ZnO film is more intense than that of the ZnO film made by VPC.

TDS and TEM results indicate that desorption of N atoms is the trigger for SPC of a- ZnON films. TDS spectrum shows N2 started to desorb around 150℃ and the desorption rate peaked in 360℃. Then it falls sharply to zero at 400℃. TEM observations revealed that a small number of nano-crystallites, less than 10 nm in diameter, are embedded in the amorphous matrix before annealing, while the film annealed at 400℃ are polycrystalline with the crystal grains of 30 nm, and the degree of the crystallinity does not change even after annealing at higher temperature than 400℃ (Fig. 1). These results indicate the desorption of N atoms strongly correlates with the crystallization of a-ZnON films. We found that the SPC brings about an improvement in local structures of ZnO films. The radial-distribution function around Zn atoms, derived from EXAFS signal at Zn K-edge, showed that the third and fourth shell peaks for the SPC-ZnO films are more intense than that for the VPC-ZnO films, indicating more ordered structures of the SPC-ZnO films.

This work was supported by JSPS KAKENHI Grant Numbers JP21H01372, JP21K18731, NTT collaborative research, Toyota Riken Scholar, and The Murata Science Foundation.

P1-56 Synthesis of Highly Stable Metal Halide Perovskite by B-site Passivation

SOOGEUN KIM[1], DOKYUM KIM[1], SEONGON PARK[2], CHANG-LYOUL LEE[1]

[1]Gwangju Institute of Science and Technology (GIST), Republic of Korea; [2]Department of Mechanical Engineering, Kyungpook National University, Daegu, Republic of Korea; vsepr@gist.ac.kr

The common surface defects in metal halide perovskite quantum dots (PQDs, ABX3) are halide vacancies, which lead to the destruction of the BX6 octahedral structure and create uncoordinated B-site defects [1,2]. X-type ligands such as thiol groups can fill halide vacancies and simultaneously bind with uncoordinated B sites. In this study, we investigated a novel synthesis method for realizing surface passivated high-quality PQDs using thiol-based ligands.

P1-57 Mn-Doped Battery-Type CuCo2O4/CuO composite electrodes for All-Solid-State Asymmetric Supercapacitors

RAJASEKHARAREDDY GUTTURU, MOHAN REDDY P, SANG WOO JOO
Yeungnam University, Korea, Republic of (South Korea); grr2021@yu.ac.kr

Introduction of Manganese (Mn) ions (2+ ⇋ 3+ ⇋ 4+) to transition metal oxides proved to be a potential strategy to tailor the redox behavior of these materials for energy storage. We fabricate a lower electronegative element (i.e., Mn) doped copper cobaltite and copper oxide (CuCo2O4/CuO; CCO) heterostructures electrodes through the hydrothermal synthesis route. The ensued electrodes have a more than 2-fold improvement in specific capacity (382.9 C g-1) than the undoped CCO electrode (120.8 C g-1) at 1 A g-1. The all-solid-state asymmetric supercapacitor (ASC) practical device is constructed with higher Mn-doped CCO heterostructures as the positive electrode and activated carbon (AC) as the negative electrode. With a voltage window of 1.5 V, the fabricated ASC device has a high specific energy of 52.6 Wh kg-1 and specific power of 774.3 W kg-1. The long-term cyclic stability of 92% capacity retention after 5000 cycles at the current density of 4 A g-1. Additionally, two ASC devices are series-connected that can power up a red light-emitting diode (LED) display for more than150 s, demonstrating the device's efficient power delivery..

P1-58 Redox-active polymer microgels for electrochemical applications

Elena Yu. Kozhunova[1], Daniil M. Itkis[2,1], Alexander V. Chertovich[2,1]
[1]Moscow State University, Russian Federation; [2]Semenov Research Center of Chemical Physics; kozhunova@polly.phys.msu.ru

Flow batteries are considered promising electrochemical sources and current storage devices with good and separate power and energy scalability. They are especially attractive for use both as in combination with alternative energy sources (wind, solar, geothermal energy) in stationary applications: in private households, in production, and for smoothing fluctuations in energy production and consumption at power plants. In flow batteries, the oxidized and reduced forms of the reagents involved in electrochemical reactions on the electrodes are present in a dissolved form or in the form of a dispersion. First, metal-based redox pairs, such as vanadium or zinc, were used as electroactive components in flow batteries. Now the number of studies in which low molecular weight organic substances and polymers are taken as active compounds has recently increased significantly.

The use of organic compounds (preferably water-soluble) instead of often toxic and expensive metals can simplify and reduce the cost of production of flow batteries, as well as improve their environmental safety. At present, the efforts of many scientific groups from different countries are focused on the search for optimal chemical components for the creation of flow batteries based on polymers and on the development of optimal conformations of polymer carriers.

In our study, we considered electroactive microgels, cross-linked water-soluble polymer networks with sizes less than one micron, as a new class of active component in flow batteries. In order for the resulting microgels to be used as an electroactive working substance, redox groups must be added to their composition. We used the well-known 2,2,6,6-tetramethylpiperidine-1-oxyl (TEMPO) as such groups for the cathode. The TEMPO groups were grafted to microgels based on poly-N-isopropylacrylamide and polyacrylic acid [1], as well as on the basis of poly-N-isopropylacrylamide and poly-N-(3-aminopropyl)methacrylamide hydrochloride. The resulting microparticles were characterized by dynamic light scattering and electron microscopy. It is shown that the resulting microgels have sizes from 100 to 500 nm and form stable aqueous dispersions. Using ESR spectroscopy, the successful incorporation of TEMPO groups into microparticles was confirmed, and their quantitative evaluation was carried out. Cyclic voltammetry confirmed the redox activity of TEMPO-modified microgels. It has been shown that such polymeric microparticles have electrochemical activity and are capable of being reversibly charged and discharged. It should be noted that there are no world analogues of using microgels as redox-active components for aqueous flow batteries.

This work was supported by the Russian Science Foundation (project no. 22-13-00115).

[1] Kozhunova E.Y., Gvozdik N.A., Motyakin M.V., Vyshivannaya O.V., Stevenson K.J., Itkis D.M., and Chertovich A.V. // J. of Phys. Chem. Lett. 2020. V. 11. no. 24. C. 10561. https://doi.org/10.1021/acs.jpclett.0c03164

P1-59 Electrical Characterizations of Nd-doped Bismuth Ferrite for Energy Storage Applications

Subhadeep Saha[1], Sreenu Gomasu[1], Rabindranath Bhowmik[2], Dibakar Das[1]
[1]University of Hyderabad, India; [2]Pondicherry University, India; subhadeep66phy@gmail.com

A long-term temperature goal for limiting the global warming to <1.5°C by the end of this century and net zero carbon dioxide emissions by the year 2050 was set out in the Paris Agreement1. To meet these targets, a heavy reliance on technologies based on renewable energy sources is necessary. Although today an increasing proportion of electricity comes from renewable sources, the intermittent nature of these energy sources poses a huge challenge. Therefore, energy storage is an indispensable requirement for the sustainable renewable technologies to maintain a balance between the production and demand.

There are already existing technologies for energy storage such as batteries, supercapacitors and so on. But modern electrical and electronic systems, especially pulse power devices including directed energy weapon (DEW) systems, hybrid electric vehicles (HEV) and high frequency inverters require energy storage systems with high power density, higher operating voltages and longer working cycles. Among various available options dielectric capacitors have been proven optimal because of their faster charging/discharging abilities and higher power densities compared to batteries and supercapacitors. But their applications are extremely limited because of low energy density (~2 Jcm-3)2 compared to fuel cells and Li-ion batteries (~20 Jcm-3). Therefore, dielectric materials with improved energy density will find extensive applications in pulse power devices. Antiferroelectric (AFE) materials have been found to be very effective in having high energy storage density due to its characteristic double hysteresis P-E loop3. Pure bismuth ferrite is known to have a distorted rhombohedral ferroelectric state with R3c as the predominant phase at room temperature. But a stable AFE Pnma phase with large energy density can be achieved by suitable doping. In this work, lead-free Nd3+ doped bismuth ferrite (Bi1-xNdxFeO3, x = 0.1, 0.2, 0.3, 0.4) was prepared by solid state route using Bi2O3, Fe2O3 and Nd2O3 as the raw materials and sintered at 9000C. In this work, the influence of Nd3+ doping on the structural, microstructural, and electrical properties of bismuth ferrite (BFO) for energy storage application, was studied. XRD pattern revealed a structural

transition of the Nd3+ doped BFO samples. FESEM micrographs showed a decrease in grain size with increasing dopant concentration. An order of increase in current density with increasing electric field up to ~10 KV/cm has been observed for all the samples indicating insulating nature of the samples (Figure 1). Variation of electrical conductivity with respect to temperature up to 200°C is also studied. An order of magnitude increase in resistivity with increasing doping concentration has been observed. The details of the experimental results and analysis will be presented in this paper.

P1-60

Novel Biomarkers for Isolation of Brain Derived Extracellular Vesicles in Plasma for Accurate Diagnosis of brain Diseases

Jisook Moon, Yuri Choi

CHA university, Korea, Republic of (South Korea); antiagingmoon@gmail.com

Abstract

Neurodegenerative disease is diagnosed after brain function is irreversible. Therefore, diagnosing at incipient disease and predicting the disease stage are imperative for prevention and effective treatment. Unfortunately, early and accurate diagnosis are still challenging due to difficult to detect biomarkers such as beta amyloid and Tau proteins secreted from the brain, not other organs. Recently, capture of neuronally derived extracellular vesicle (NDEV) using L1CAM has been suggested as a new diagnostic technology for detection of brain derived biomarkers. However, L1CAM has limitations in isolation of NDEV. Here, we present new markers that can replace L1CAM. In this study, we have further demonstrated in detail the process of selecting novel markers and present evidence that the new markers, X1 and X2, are more sensitive and accurate for isolation of neuron-enriched EVs than L1CAM as well as early biomarkers of Alzheimer's Disease. In addition, we verified the potential of captured EV by X1 and X2 from human plasma through analysis of EV RNA.

Our results demonstrate that X1 and X2 are more sensitive and specific biomarkers for isolating neuron-enriched EVs. Furthermore, our results suggest usefulness as a diagnostic platform for early diagnosis of neurodegenerative diseases through a combination of X1 and another specific neuronal marker such as X2.

This research was financially supported by by the Bio & Medical Technology Development Program of the National Research Foundation (NRF) 2019M3A9H1103765.

P1-61

The well-arrayed ZnO Nanorods Fabricated by Chemical Bath Deposition Applying for Photocatalytic Activity

CHAOYANG LI, Tomoya Ikuta, Htet Wai

Kochi University of Technology, Japan; 230015f@gs.kochi-tech.ac.jp

ZnO as one of the promising semiconductor metal oxides has been considered as an effective alternative to replace TiO2 applying photocatalysis due to its unique properties [1]. It was reported that the photocatalytic efficiency of ZnO was influenced by crystal growth orientation, surface area, particle size, nanostructure, light intensity, etc. Particularly, crystal growth orientation of ZnO along the (0001) crystal plane showed high photocatalytic activity. In this research, we propose a simple and low cost chemical bath deposition method to synthesize well-arrayed ZnO nanostructures and investigate their photocatalytic activity as well. AZO films with 300 nm thickness was deposited on glass by a radio frequency magnetron sputtering method. The obtained AZO film was put into the solution of mixture of Zn(NO3)2•6H2O and hexathylenetetramine, with the concentrations of 0.025 and 0.0125 mol/L. The solution was heated from room temperature to 95 °C and kept at 95 °C for 2.5, 5 ,7.5, 10 and 12.5 hours for comparison. SEM images showed that ZnO nanostructures grown on AZO films with different time. It was observed that well-aligned ZnO nanorods could grow on as-deposited AZO films. The length of ZnO nanorods was growth from 650nm to 2300 nm with the deposition time increase form 2.5 hour to 12.5 hours. The XRD patterns of ZnO nanorodss showed that there was only a single dominant (002) diffraction peak for ZnO nanorods grown with different deposition time. The crystallinity was enhanced with the length of nanorods increased. The dominant (002) peak indicated ZnO rods had highly preferred orientations in the (0001) direction. The photocatalytic measurements of ZnO nanorods/AZO films were carried out at room temperature. The methyl red solution with concentration of 1 × 10−5 mol/L and volume of 70 mL was prepared prior to the UV irradiation. It was found that absorbance was significantly decreased with the with the length of nanorod increase, which meant that photocatalytical efficiency was increased.

In summary, the ZnO nanorods grown on AZO substrate showed vertical alignment growth orientation. The photcatalytic activity was enhanced with the surface area increase and crystallinity improvement.

P1-62

Stabilization of large area M2 Phase in VO2 thin films at room temperature through novel strain engineering

Hardeep Singh1, Minkyun Sohn2, Hayoung Choi1, Seungnam Cha1, Daejoon Kang1

1Department of Physics, Sungkyunkwan University, 2066, Seobu-ro, Jangan-gu, Suwon, Gyeonggi-do 16419, Republic of Korea; 2Department of Physics and Institute of Basic Science, Sungkyunkwan University, 2066 Seobu-ro, Jangan-gu, Suwon, Gyeonggi-do 16419, Republic of Korea; qwe1592@naver.com

Interestingly, VO2 exhibits many competing insulating phases (mainly M1, M2, and T) during the insulator-to-metal transition. The formation mechanism of the metastable M2 phase, which is thought to be a true Mott insulator, has received immense attention for uncovering the fascinating physics of the metal-insulator transition, and the possibility of realization of ultrafast switching applications. Also, the practical detection of antiferromagnetic properties in the M2 phase could help to explain the magnetic aspect of MIT transition in VO2. We here, develop an approach through strain engineering to stabilize the M2 phase over a large area in VO2 thin films at room temperature. The large lattice mismatch between VO2 and GaN substrate and post-annealing for tuning stoichiometry has been utilized to induce tensile strain along the CR axis to meet the stabilization conditions for the M2 phase at room temperature. Raman spectroscopy and XRD (X-ray diffraction) distinguished the M1, T, and M2 phases depending upon the shift in ωv-o and characteristic 2θ peaks, respectively. Besides, large area stabilization of the M2 phase was demonstrated with Raman mapping. By showing excellent controllability and reproducibility to stabilize the large area M2 phase, we lay down the foundation for antiferromagnetism detection to explore magnetic aspects of the MIT mechanism, and realization of high-speed switching MTFET (Mott transition field effect transistor) devices.

Keynote Session-2: Keynote Session

Time: Wednesday, 11/Jan/2023: 8:45am - 10:45am · *Location:* Main Hall

8:45am - 9:15am

Unprecedented Stretchability of Highly Conductive Large-Area Graphene Grown Directly at 100 oC

Soon-Gil Yoon

Chungnam National University, Korea, Republic of (South Korea); sgyoon@cnu.ac.kr

The direct synthesis of inherently defect-free, large-area graphene on flexible substrates is a key technology for soft electronic devices. In the present work, in situ plasma-assisted thermal chemical vapor deposition (PATCVD) is implemented in order to synthesize 4-inch-diameter high-quality graphene directly on 10-nm-thick Ti-buffered substrates at 100 °C. The in situ synthesized monolayer graphene displays outstanding stretching properties coupled with low sheet resistance. Further improved mechanical and electronic performances are achieved by the in situ multi-stacking of graphene. The 4-layered graphene multi-stack is shown to display an ultralow resistance of ~ 6 Ohm per square, which is consistently maintained during the harsh repeat stretching tests and is assisted by self-p-doping under ambient conditions. Graphene-field effect transistors fabricated on polydimethylsiloxane (PDMS) substrates reveal an unprecedented hole mobility of ~ 21,000 cm2V-1s-1 at a gate voltage of -4V, irrespective of the channel length, which is consistently maintained during the repeat stretching test of 5,000 cycles at 140% parallel strain.

9:15am - 9:45am

Nano-Photocatalytic Materials for effective antifouling in ship hull and other marine environments

Dennis Leung

The University of Hong Kong, China, People's Republic of; ycleung@hku.hk

Fouling is a common phenomenon on those objects submerged in seawater due to the deposit and growth of microorganism in the sea. For boat and yacht, antifouling paints are applied so as to avoid fouling on the hull under water. Common practice uses paint containing either tributyltin (TBT) or heavy metals that would kill the microorganisms in seawater exhibiting an anti-fouling effect. However, TBT materials are toxic in nature and therefore was banned for usage. On the other hand, heavy metals are still allowed in antifouling paints that can be as high as or higher than 30% in mass. No doubt these toxic additives continue to pollute our marine environment as well as affect the food-chain. In this keynote speech, general materials for fouling protection and their limitations will first be discussed. Then, newly developed nano-sized photocatalytic coating was introduced, which can effectively control the growth of microorganisms on the hull of yachts. Applying these materials can avoid frequent removal of the deposited microorganisms, saving the maintenance cost and improving the fuel efficiency of the yachts. The prospects of this applying these photocatalytic materials to control antifouling on other marine structures will be discussed at the end of the talk.

9:45am - 10:15am

Immobilization Paclitaxel-loaded Liposomes Using Microbubble-Templated Giant Capsules as Drug Delivery for Cancer Therapy

Liqin Ge[1], Xin Tan[2]

[1]School of Biological Science and Medical Engineering, Southeast University, China, People's Republic of; [2]College of Materials Science and Technology, Nanjing University of Aeronautics and Astronautics, Nanjing 210016, P.R. China.; lqge@seu.edu.cn

Paclitaxel (PTX), a small hydrophobic molecule, is demonstrated to be effective in treating a broad spectrum of human advanced cancer. However, the poor water solubility of PTX results in a relatively low drug concentration in the solution, which significantly reduces the therapeutic effects. The liposome (Lipo) is a successful drug delivery system in the clinic, which can encapsulate both hydrophilic and hydrophobic drugs in the core and the bilayer lipid shell, respectively. However, liposomes have several drawbacks, including rapid clearance in blood, structural instability, and rapid drug leakage. Herein, air microbubbles (MBs) template-mediated layer-by-layer self-assembly technique is reported for immobilizing PTX-loaded Lipo in giant microcapsules with diameters of 74.06±12.06μm (Capsule@Lipo GMs) by absorption of poly (allylamine hydrochloride) (PAH) and poly(styrene sulfonate) (PSS) onto the templates of PTX-loaded Lipo MBs. This method doesn't need template removal due to the spontaneous process of air gas escape, which can avoid template residues, harsh template decomposition conditions, and high internal osmotic pressure issues brought by the template-core decomposition process. The liposomes are firmly encapsulated within GMs by electrostatic interaction and the covered lipids on the surface. The presence of liposomes enables the enhanced encapsulation and controlled release of PTX, while GMs reinforce the structural stability of liposomes. To achieve site-specific release, the GMs are functionalized with Fe3O4 nanoparticles, which can achieve remote control delivery and controlled release via magnetic field gradient and alternating magnetic field. Due to the huge cavity of capsules, Capsule@Lipo GMs present much higher loading contents of 50.56% (equal to 2.73ng per capsule). Compared with PTX-loaded liposomes, PTX-loaded Capsule@Lipo GMs could extend PTX release for over 72h and have remarkable effects against cancer cells viability in vitro. Furthermore, in vitro cell study also revealed that the magnetic-sensitive GMs, which can be ruptured after being exposed to an alternating magnetic field and release PTX rapidly, allow for rapid uptake by 4T1 breast cancer cells. Collectively, this study demonstrates that Capsule@Lipo GMs with high loading ability, as an innovative drug delivery system, can reach targeted sites under magnetic field gradient and achieve site-specific release under alternating magnetic field, which holds tremendous potential for cancer treatment.

10:15am - 10:45am

Transparent Amorphous Oxides Semiconductors Materials Features, Progress and Applications

Hideo Hosono[1,2]

[1]Tokyo Tech, Japan; [2]NIMS; hosono@mces.titech.ac.jp

While amorphous hydrogenated Si (a-Si:H) had been exclusively used as the backplane TFTs to drive flat panel displays, amorphous oxide semiconductor (AOS)-TFTs is becoming a strong alternative due to their high mobility, low off-current, high transparency, and easy fabrication. In particular, AOSs with In-Ga-Zn-O compositions (IGZO) are practically applied as the backplane for high resolution and energy-saving LCDs and large-sized OLED TVs [1]. Oxide semiconductors have rather different characteristics from the traditional semiconductors. In this talk I introduce outline, progress and outlook of AOS i.e., the research history, the general feature of carrier transport properties, electronic structure of AOS materials and their display applications. Recently a comprehensive book on this topic was published. This monograph will be a good reference to know fundamentals and current status of IGZO-TFTs[2]

Keywords: TFT, semiconductor, display, amorphous

[1] H.Hosono "How we made the IGZO transistor." Nature Electronics 1, 428 (2018)

[2] H.Hosono and H.Kumomi (ed.) Amorphous Oxide Semiconductors: IGZO and Related Materials for Display and Memory (Wiley Series in Display Technology, 2022)

Invited Talk-2: Invited Talk

Time: Wednesday, 11/Jan/2023: 11:00am - 11:54pm · *Location:* Main Hall

11:00am - 11:18am

Spintrophoretic Mattertronics for Multiplex Cell Tweezers

Byeonghwa Lim, Hyeonseol Kim, Yumin Kang, Jonghwan Yoon, Keonmok Kim, Sri Ramulu Torati, CheolGi Kim
DGIST, Korea, Republic of (South Korea); cgkim@dgist.ac.kr

The precise delivery of bio-functionalized matters is of great interest in emerging biomedical technologies from the fundamental and applied viewpoints. Particularly, most existing single cell platforms are unable to achieve large scale operation with flexibility on cells and digital manipulation towards multiplex cell tweezers. Recently, the flexibility of magnetic shuttling technology using nano/micro-scale magnets for the manipulation of particles has gained significant advances for a versatile living cell manipulation tasks. Herein, let's call "spintrophoresis" using micro-/nano-sized Spintronic devices rather than "magnetophoresis" using bulk magnet. Especially analogy of IC chip via the electronic carriers of electron and hole has been implemented in the integrated spintrophoretic circuit platform with active and passive circuitry elements and gates based on magnetic and pseudo-diamagnetic carriers (mattertronics; matter+tronics).

In fact, each cells have the different bio-chemical characteristics, as well as different drug resistance. As for the realization of future personalized care considerring the individual cell hetrogeneity, primary hurdle is development of multiexed cell manipulation method. Here, magnetic assisted multiplexed cell array will offer the promising verstile platform for multiplexed cell tweezering, compared with the other methods including current FACS and optical tweezers. Here I will introduce the spintrophoresis devices and integrated platform for versatile multiplexed tweezers of living cells, which enables a novel platform for multiplex cell tweezers.

11:18am - 11:36am

Process control in high frequency technological plasmas by Voltage Waveform Tailoring

Julian Schulze
Ruhr University Bochum, Germany; schulze@aept.rub.de

As process requirements in plasma technology continue to increase, empirical methods of process development/optimization fail and knowledge-based approaches become essential. Based on a fundamental understanding of the charged particle dynamics in capacitive RF discharges, Voltage Waveform Tailoring (VWT) is introduced as a new method to realize ultimate control of energy distribution functions of different particle species in such plasmas to overcome a variety of process limitations.

Multi-frequency power generator and impedance matching technology to upgrade existing RF plasma sources to use VWT without modifying the reactor itself will be described [1,2]. Concepts to control the shape of the Ion Energy Distribution Function (IEDF) by using customized voltage waveforms and their potential advantages for plasma etching will be discussed [3]. Recent results also show that VWT allows for controlling the Electron Energy Distribution Function (EEDF) in the plasma volume and at boundary surfaces [4-8]. Selected examples of EEDF control by VWT will be discussed. Finally, the effects of VWT on plasma uniformity across large electrodes will be presented for selected discharge conditions. By tuning the relative phases between multiple consecutive harmonics used to construct tailored voltage waveforms the plasma uniformity is found to be improved significantly [9,10].

Funding: German Research Foundation (No. 428942393, SFB TR 87 (C1), SFB 1316 (A4)), National Natural Science Foundation of China (No. 12020101005, 11975067).

References:

[1] J. Franek et al. 2015 Rev. Sci. Instr. 86 053504
[2] F. Schmidt et al. 2018 Plasma Sourc. Sci. Technol. 27 095012
[3] P. Hartmann et al. 2022 Plasma Sourc. Sci. Technol. submitted
[4] F. Krüger et al. 2019 Plasma Sourc. Sci. Technol. 28 075017
[5] P. Hartmann et al. 2021 J. Phys. D 54 255202
[6] L. Wang et al. 2021 Plasma Sourc. Sci. Technol. 30 054001
[7] A. Gibson et al. 2019 Plasma Sourc. Sci. Technol. 28 01LT01
[8] I. Korolov et al. 2019 Plasma Sourc. Sci. Technol. 28 094001
[9] K. Zhao et al. 2020 Plasma Sourc. Sci. Technol. 29 124001
[10] E. Schüngel et al. 2015 Appl. Phys. Lett. 106 054108

11:36am - 11:54am

Direct Growth of MoS2 films on hBN Substrates by Chemical Vapor Deposition

Qianwen Zhang, Dae Joon Kang
Department of Physics, Sungkyunkwan University, 2066, Seobu-ro, Jangan-gu, Suwon, Gyeonggi-do 16419, Republic of Korea; djkang@skku.edu

With the rapid development of two-dimensional materials, vertical heterostructures are considered promising materials for fabricating devices due to their flexibility, making it possible to design the material properties. Heterostructures synthesized by conventional transfer methods are processing complex and easy to introduce impurities in the transfer process. Direct synthesis has been reported but shown only limited size. Chemical vapor deposition (CVD) is a readily available, less expensive, and more parametric synthesis method. Here, we studied the direct synthesis of MoS2/hBN heterostructures using CVD. Dual-sulfur-source CVD method, solution precursor method, and space-limited synthesis method were used to study the direct synthesis of MoS2 on hBN-SiO2 substrates. The results indicate that the providing way of the sulfur precursor, the treating way of the Mo precursor, and the size of the reaction space all affect the synthesized heterostructures.

Invited Talk-3: Invited Talk

Time: Wednesday, 11/Jan/2023: 1:15pm – 2:27pm · *Location:* Main Hall

1:15pm – 1:33pm

Promoting Homogeneous Interfacial Li+ Migration by using a Facile N2 Plasma Strategy for All-Solid-State Lithium-Metal Batteries

Feng Liang

Kunming University of Science and Technology, China,; liangfeng@kust.edu.cn

All-solid-state lithium (Li)-metal batteries (ASSBs) are ideal energy storage devices owing to their high energy densities and desirable safety characteristics [1]. Solid electrolytes are vital materials in the development of next-generation ASSBs [2]. In particular, novel hybrid solid electrolytes (HSEs) consisting of active inorganic particles and solid polymer electrolytes have gained considerable attention due to its the high flexibility of the solid polymer electrolyte and improved ionic conductivity at room temperature [3]. However, Li dendrites and sluggish interfacial dynamics of Li+ transfer between the Li metal and HSEs restrict practical applications. Herein, we propose a facile strategy to promote homogeneous interfacial Li+ migration by modifying the surface properties of HSEs through using nitrogen (N2) plasma. N2 plasma not only decreases the crystallinity and glass transition temperature of HSE, but also in-situ generates an ultra-stable and conductive Li3N layer on the HSE surface. This conductive layer promotes interfacial Li+ migration and favourable wettability, thus effectively improving Li+ transfer dynamics and homogeneous deposition. This work provides a new facile strategy to address the interface issues between HSEs and electrodes in all-solid-state batteries.

1:33pm – 1:51pm

Advanced Electrode Materials for High-Rate Aqueous Zinc-Ion Batteries

Geon-Hyoung An[1,2], Seoyeong Kim[2], Jaeyeon Lee[2], Geun Yoo[2]

[1]Department of Energy Engineering, Future Convergence Technology Research Institute, Gyeongsang National University, Republic of Korea; [2]Department of Energy System Engineering, Gyeongsang National University, Republic of Korea; qhan@gnu.ac.kr

Energy storage systems (ESS) have attracted as encouraging technology for controlling the energy output of sporadic renewable energy, such as wind and solar. Recently, lithium-ion batteries (LIBs) have emerged as the promising candidate for the ESS field due to high energy density and long cycling stability. However, the low safety, high cost, and environmental impact have prompted the study of alternative batteries. Due to their acceptable level of safety performances, easy assembly, and low cost, zinc-ion batteries (ZIBs) have emerged to attention as next-generation energy storage devices.

However, the intrinsic limitation of the V2O5 cathode with a high capacity used to enhance the energy storage performances of ZIBs has restricted the further application of ZIBs. However, the volume expansion of V2O5, from the intercalation/de-intercalation of Zn2+ in the initial cycles leads to the generation of voids and cracks in electrode; therfore, leading to an unstable capacity behavior. Consequently, the high capacity potential of V2O5 cathode cannot be utilized. Hence, nano-sized split V2O5 with H2O-intercalated interfaces is fabricated as a ZIB cathode using an electrochemical activation process. These results will be discussed in detail.

These results will be discussed in in AFM 2022 in detail, and this work was supported by the National Research Foundation of Korea (NRF) grant funded by the Korea government (MSIT) (NRF- 2020R1C1C1010611).

1:51pm - 2:09pm

Advanced MXene-Carbon Heterostructures for Energy Applications

Debananda Mohapatra

Yeungnam University, Korea, Republic of (South Korea); debanandaiitb@gmail.com

Since discovering graphene, there has been a tremendous effort for the two-dimensional (2D) nanomaterials to explore their unique planar structure, physiochemical, and electrochemical features. MXenes are a large family of 2D transition metal carbides, nitrides, and carbonitrides, with similar and better overall properties than graphene.

However, its electronic and electrochemical properties are hugely affected by wet chemistry synthesis and processing parameters such as stoichiometry, etchant concentration, cleaning and storing conditions. The two significant issues such as face to face stacking and self-assembly need to be overcome while making the advanced MXene heterostructure.

Recently we attempted to introduce the exohedral carbon nano-onions to MXene's structure to reduce aggregation due to strong van der Waals forces. The CNOs are the fullerene family's critical members that come with exohedral pores without any internal pores, which is advantageous for electrochemical applications, viz; dye-sensitized solar cells (DSSCs), supercapacitors. We will discuss its suitability and applications of those advanced heterostructures as optically transparent DSSCs for windows applications on rooftops and building walls.

2:09pm – 2:27pm

Interfacing Nanostructured Zincite Electron Transport Layer with Newly Derived Small Molecule Squaraine Absorbers for Photovoltaic Devices

Vilko Mandić[1], Ivana Panžić[1], Floren Radovanović-Perić[1], Dragana Vuk[1], Thomas Rath[2]

[1]Faculty of Chemical Engineering and Technology, Croatia; [2]Institute for Chemistry and Technology of Materials, Austria;
vmandic@fkit.hr

Efficiency and high performance of solar cells heavily depend on the ability to successfully generate charge carriers and facilitate their extraction from the active layer, through electron transport layer (ETL) or hole transport (HTL) layer to the electrodes. Since all newer generations of solar cells repose on thin-film configurations this opens up a wide area for upgrades but also comes with the drawback of unidentified mutual dependences of the layers.

In this work we increased the specific surface of the ETL by nano-structuring of the zinc oxide by a low-temperature chemical bath method compatible with flexible polymeric substrates (transparent electrodes). Nanostructured ZnO was interfaced with several newly developed small molecule organic light absorbers form the squaraine group (SQs). The ZnO-SQ interfaced materials were broadly characterized by grazing incidence X-ray diffraction (GIXRD), scanning electron microscopy (SEM) and atomic force microscopy (AFM), spectroscopic (UV-VIS) and electrical (cyclic voltammetry and solid state impedance spectroscopy) methods, confirming neatly ordered nano-features for ZnO and uniform coverage by SQs. Also, the evolution of the bandgap and complex conductivity was elaborated. It was shown that the structural organization of the SQ material (in bulk heterojunction configuration with fullerene-based acceptors) had a large impact on the several parameters that govern the solar cell efficiency and stability. The results ask for further optimization of newly synthesized SQ small molecules (symmetric and asymmetric) for their full utilization in the organic photovoltaic devices.

2:27pm - 2:40pm

Electrically, thermally, mechanically anisotropic gels

Insu Jeon

Chonnam National University, Korea, Republic of (South Korea); i_jeon@chonnam.ac.kr

Next-generation applications such as flexible electronic devices, sensors, actuators, and soft robotics require anisotropic functional soft materials with controlled, directional electrical and heat conductivities, mechanical properties, and responsiveness, as well as shape-morphing capability, complex designability, and wide operational temperature ranges. However, a combination of these extraordinary functions in any single class of materials has hardly been realized to date. In this study, we developed a novel class of multi-anisotropic gels through a new fabrication route to realize all these functions. The gels were synthesized by integrating cellulose, a natural biopolymer, with poly(3,4-ethylenedioxythiophene)-poly(styrenesulfonate) (PEDOT:PSS), an exceptionally conductive and biocompatible synthetic polymer, in tripropylene glycol, a green organic solvent with extremely high boiling and low freezing temperatures. The prepared gels exhibited high electrical and thermal conductivities of ~200 S m−1 and ~1.49 W m−1 K −1, respectively, with a record-breaking Young's modulus and a tensile strength of ~500 and ~55 MPa, respectively, which are much better than the previously reported mechanical properties of PEDOT-based gels (modulus/strength < 10 MPa). Moreover, the gels exhibited self-welding ability and maintained their properties for 14 d over a wide temperature range (from −50 to 35 °C) covering almost the entire atmospheric temperature range on Earth. Due to the combination of these remarkable properties, the developed gels are promising candidates for application in many next-generation flexible devices, some of which have been experimentally demonstrated in this study.

Oral Talk-2: Oral Talk

Time: Wednesday, 11/Jan/2023: 1:15pm - 4:03pm · *Location:* Hall 1&2

1:15pm - 1:27pm

Investigation of the reaction process of carbon material sulfonation via gas-liquid interfacial plasma

Siqi Deng[1], Nozomi Takeuchi[1], Junko Hieda[2], Katsuyuki Takahashi[3], Kosuke Tachibana[4], Oi Lun Li[5]

[1]Tokyo Institute of Technology; [2]Nagoya University; [3]Iwate University; [4]Oita University; [5]Pusan National University; deng@hv.ee.e.titech.ac.jp

Sulfonated carbon catalysts have admirable catalyst performance for biomass transformation so that carbon sulfonation is desirable. Carbon sulfonation is a process to modify carbon materials with sulfonic group (-SO3H), carboxyl group (-COOH), and hydroxyl group (-OH). Besides, a conventional method for carbon sulfonation requires concentrated sulfuric acid at elevated temperatures. Therefore, we used the gas-liquid interfacial plasma (GLIP) process for carbon sulfonation which just requires dilute (1 mol/L) sulfuric acid at room temperature (38 ℃)[1]. Moreover, after the plasma process, the catalytic performance and stability of carbon materials are much better than catalysts produced by the conventional method. In previous research, we found that SO2 gas can be generated by plasma discharge with H2SO4 solution whereas could not be generated with Na2SO4 solution by FT-IR measurement. In addition, SO2 gas also can be generated by plasma discharge with K2S2O7 solution. In this research, we will compare these three kinds of solutions, to confirm the relationship of SO2 generation and carbon sulfonation. In carbon analysis, the typical acid-base titration method and FT-IR measurement will be used.

1:27pm - 1:39pm

The effect of plasma off time on CO2 methanation using pulsed discharge plasma

Taiki Hasegawa[1], Masashi Ideguchi[1], Daisuke Yamashita[1], Susumu Toko[2], Kunihiro Kamataki[1], Kazunori Koga[1,3], Masaharu Shiratani[1]

[1]Kyushu University, Japan; [2]Osaka University, Japan; [3]National Institute of Natural Sciences, Japan; taiki.800224@gmail.com

We are using a capacitively coupled plasma system for CO2 methanation. When the plasma off time is taken as a parameter, the CO2 conversion and CH4 yield/CH4 selectivity improve with shorter plasma off time.

In addition, the energy cost for CO2 decomposition can be significantly reduced by increasing the plasma off time.

1:39pm - 1:51pm

Properties of Ni-Mn-Ga High Temperature Shape Memory Alloys doped with Hf or Zr

Shoukai Xu, Ruben Santamarta, Jaume Pons

Universitat de les Illes Balears, Spain; jaume.pons@uib.es

Alloys with compositions close to the Heusler Ni2MnGa are well known for their outstanding properties for magnetic actuation due to their huge magnetic field-indued strain [1]. Some compositions of this family are also candidates for High Temperature Shape Memory Alloys (HTSMA) due to good shape memory properties and high thermal cycling stability with large recoverable strain in single crystalline specimens [2-3]. In Ni-Mn-Ga polycrystals, a ductile second phase is introduced to improve the mechanical and functional properties through compositional design and thermal treatment [4-5]. Ti addition in Ni-Mn-Ga has been reported to increase the transition temperature accompanied with Ni3Ti precipitation [6], while Zr substituting Cu in Ni-Mn-Ga-Cu can lead to transition temperature variation with formation of γ-phase [7]. To the authors' knowledge, no studies on addition of Hf or Zr to Ni-Mn-Ga have been reported, elements located in the same column of the periodic table as Ti. Therefore, this presentation will report on this topic.

Polycrystalline Ni-Mn-Ga-Hf/Zr alloys with maximum 4 at.% Hf/Zr content have been prepared by two-step induction and arc melting, and characterized by DSC, SEM, EDX, TEM, XRD and thermo-mechanical experiments. The martensitic transformation temperatures are continuously decreasing with increasing the Hf/Zr content and are correlated with the change of e/a ratio. This ratio is affected by the precipitation process and the solubility of Hf/Zr. Alloys with Zr show higher transformation temperature than alloys with Hf for the same addition content due to a lower solubility of Zr in the matrix. The precipitated phase possesses double value of lattice parameter than the common γ-phase. Its complete crystal structure determination indicates a face-centered tetragonal structure. The formation of precipitates causes reduction of martensite volume fraction, so the enthalpy change is gradually decreasing with Hf/Zr addition, as well as the transformation strain obtained from thermo-mechanical experiments. However, the alloys with relatively large Hf/Zr addition surprisingly show a very low hysteresis of only 8 K, which is attributed to a better compatibility between the parent and martensite phases.

1:51pm - 2:03pm

Study of Ferroelectric HfZrO2 FinFET with Trench Structure for Sub-60-mV/Decade Subthreshold Slope

Siao-Cheng Yan, Chen-Han Wu, Yung-Chun Wu

National Tsing Hua University, Taiwan; jeff910029@gmail.com

We fabricated the ferroelectric HfZrO2 (HZO) fin field-effect transistors (FinFETs) with trench structure for sub-60 mV/decade subthreshold slopes (SSs). HZO with a thickness of 5 nm was deposited as gate insulator in the ALD chamber. The atomic force

microscopy (AFM) was conducted to map the devices' surface morphology and three-dimension structure through an interaction between the tip and surface.

Meanwhile, the analysis of HZO thin film was performed to confirm its ferroelectricity. First, X-ray photoelectron spectroscopy of 5 nm HZO thin film was analyzed to determine the chemical bonding of HZO. All the XPS results were calibrated by fixing the C 1S peak at a binding energy of 284.8 eV to compensate for the charge-induced energy shift due to X-ray exposure. From the ratio of relative area fractions of the principal components, the presence of Hf and Zr ratio of 45:55 was confirmed [1]. Furthermore, X-ray diffraction was performed to identify the 5-nm-thick HZO phases as orthorhombic (o) with specific peaks. The non-centrosymmetric o-phase induced polarization characteristic in HZO thin film [2].

To increase the gate control ability and decrease subthreshold swing, an additional mask was performed to define the trench region and the trench was transferred by reactive-ion etching (as shown in Fig.1). The fabricated ferroelectric trench FinFET exhibited a steep SSmin = 35.4 mV/dec for the forward sweep and SSmin = 48.3 mV/dec for the reverse sweep, which was below Boltzmann limit (SS = 60mV/dec). The anticlockwise transferred ID–VG curve was caused by the dipoles flipping in the ferroelectric gate insulator when gate voltage swept from positive to negative [3]. Also, the ferroelectric trench FinFET showed an excellent on/off current ratio and potential to low power applications.

2:03pm - 2:15pm

Synthesis of functional gradient structure in metallic glasses by thermal rejuvenation technique for improved mechanical properties

Junji Saida[1], Rui Yamada[1], Haruka Isano[2], Tomohiro Yoshikawa[2], Wookha Ryu[3]

[1]Frontier Research Institute for Interdisciplinary Sciences, Tohoku University; [2]Graduate School of Engineering, Tohoku University; [3]Seoul National University; jsaida@fris.tohoku.ac.jp

Since metallic glasses have excellent mechanical properties such as high strength, elastic modulus and hardness, originating from an intrinsic random atomic configuration, they are strongly expected to be used for the precise mechanical parts. However, we are concerned about a poor ductility for the industrial use especially in the relaxed metallic glass due to mechanical processing or insufficient cooling rate during a manufacturing process. So, structure controlling of relaxation state in metallic glass has been widely evolved by thermal and physical processes. The authors have found out that the less relaxed state can be recovered (rejuvenated) using a thermal process in Zr-, Cu-, Mg-based metallic glasses.[1-4] We have already reported that the rejuvenated metallic glasses actually exhibit the mechanical softening with improved plasticity, which is correlated to changes of local glassy structure and an amount of local free volume.[5,6] Recently, we succeeded in the introduction of the gradient distribution of rejuvenated structure in the cylindrical metallic glass sample using the newly developed asymmetric heat treatment equipment.[7] In such the unique structure, the shear band angle is sensitive to the relaxation state (i.e., amount of local free volume), which develops the formation and propagation of shear band in a very complex manner during the deformation process. As a result, an intrinsic work hardening and an improvement of plastic strain in metallic glass are obtained.

The results provide a novel way to control the relaxation state (random atomic structure) functionally and beneficial information on the industrial application of metallic glasses.

Keywords: metallic glass, rejuvenation, gradient structure, mechanical property

[1] J. Saida et al., Appl. Phys. Lett., 103(2013)221910.

[2] J. Saida et al., Sci. Tech. Adv. Mater., 18(2017)152-162.

[3] W. Guo et al., J. Non-Cryst. Solids, 498(2018)8-13.

[4] W. Guo et al., Met. Mater. Trans., 50A(2019)1125-1129.

[5] M. Wakeda et al., Sci. Rep., 5(2015)10545.

[6] M. Wakeda and J. Saida, Sci. Tech. Adv. Mater., 20(2019)632-642.

[7] W.H. Ryu et al., NPG Asia Mater., 12(2020)52.

2:15pm - 2:27pm

Vertically Stacked Ge GAAFET by Using Diamond-shape Nanowires for nearly ideal SS, Ozone Treatment for Reducting Interficaial Defects, and Ferroelectric HZO application

Yi-Wen Lin[1], Hao-Hsiang Chang[1], Chong-Jhe Sun[1], Siao-Cheng Yan[1], Shan-Wen Lin[1], Guang-Li Luo[2], Fu-Ju Hou[2], Yung-Chun Wu[1]

[1]National Tsing Hua University, Taiwan; [2]Taiwan Semiconductor Research Institute, Hsinchu, Taiwan; da373816w@gmail.com

We report the vertically stacked diamond-shape Ge nanowires gate-all-around field-effect transistor (Ge-NW GAAFET) with ferroelectric (FE) layer HZO=2nm / Al2O3=4nm. The vertically stacked diamond-shaped Ge NWs were fabricated through simple alternative isotropic (Cl2/HBr) and anisotropic etching (Cl2) sequences. The in-situ ALD ozone (O3) treatment [1] was applied in Ge / GeO2=0.4nm / HZO=2nm / Al2O3=4nm to reduce the interface trap density (Dit). The multi-frequency capacitance-voltage (CV) characteristics of MISCAPs were used to quantify the Dit value [2] with and without O3 treatment. The ferroelectric property of a 2nm-thick HZO / 4nm-thick Al2O3 gate stack through rapid thermal annealing (RTA) of 450℃ was confirmed using polarization-voltage (PV) measurement. Furthermore, the transfer ID-VG curve of the vertically stacked diamond-shape Ge-NW FE-GAAFET shows superior performance with a minimum steep-sub-threshold slope (SSMIN) of 49 mV/dec for PFET. The clockwise curve of forward and reverse sweep of the ID-VG curve indicated the dipole flipping [3] in the ferroelectric HZO layer. The formation of the vertically stacked diamond-shape Ge-NW FE-GAAFETs could be compatibility with the current CMOS technology platform.

2:27pm - 2:39pm

Visible-light-active Polymeric Carbon Nitride for Enhanced Removal of Volatile Organic Compounds (VOCS) in Air

Milad Jourshabani, Mahdieh Razi Asrami, Lee Byeong–Kyu

University of Ulsan, Korea, Republic of (South Korea); milad.shabani90@yahoo.com

Photocatalytic air purification, specifically the removal of volatile organic compounds (VOCS), has emerged as a promising technology, owing to its ability to operate under ambient temperature and pressure conditions. In comparison with commercial methods such as adsorption, the photocatalyst efficiently works under humid condition and enable the removal of sub-ppmv-level concentrations of air pollutants [1].

However, TiO2 has been intensively investigated for indoor environment remediation, the most suitable application is limited due to its UV-active photocatalyst. So, novel discoveries and frontlines in photocatalytic materials science have been focusing on the development of high visible light-active photocatalysts to make the technology more feasible [2].

Without a doubt, carbon nitride (CN) materials have become an interesting visible-light active photocatalyst in many areas. CN is a low-cost and environmentally friendly photocatalyst with unique electronic and photophysical properties. It demonstrated high activity in H2 production, CO2 conversion, and photodegradation of pollutants. However, because of the solid-state polycondensation process, the resulting CN possesses low surface area and poor π-conjugative heptazine units. This shortcoming has been tackled by applying the supramolecular self-assembly through non-covalent bonds and making heterojunction with well-matched WO3 [3].

Herein we demonstrated the preparation of carbon nitride from melamine-cyanuric precursors. The resulting carbon nitride was obtained by thermal polycondensation of the precursor at 540 °C for 4h. Afterward, the CN/WO3 heterojunction was prepared via the impregnation method. The resulting polymeric carbon nitride shows excellent photocatalytic activity for the removal of non-polar and polar VOCs such as acetaldehyde and toluene with a high concentration of 180 ppmv in the air under visible-light irradiation.

Fig. 1. a) The concentration of acetaldehyde and b) toluene over time under visible light irradiation in the reactor; initial gas concentration: 180 ppmv, light source: 300 W Xe lamp with a 400 nm cutoff filter.

As seen in Fig. 1a, and b, the carbon nitride film degraded more than 70% of acetaldehyde and toluene after 3h under visible light. To the best of our knowledge, this is very a promising and breakthrough for carbon nitride materials for indoor air purification.

2:39pm - 2:51pm

Self-induced Ferroelectric Ge-doped HfO2 applied to SiGe/Si Bilayer Channel Gate-all-around Field-effect-transistor

Yi-Ju Yao[1], Chong-Jhe Sun[1], Siao-Cheng Yan[1], Shan-Wen Lin[1], Fu-Ju Hou[2], Guang-Li Luo[2], Yung-Chun Wu[1]

[1]National Tsing Hua University, Hsinchu, Taiwan; [2]Taiwan Semiconductor Research Institute, Hsinchu, Taiwan; yiju0410@gmail.com

Recently, Gate-all-around field-effect-transistors (GAA-FETs) including nanosheet (NS) and nanowire (NW) channel structures are considered as the most promising candidates to replace FinFETs for sub-N3 technology node due to the excellent electrostatic characteristics. In this work, we proposed a novel option of channel structure for GAAFETs by selectively etching on SiGe/Si bilayer, which suspend the bilayer channel and wrap the gate metal all around the channel. In this way, the multi-corner concave polygonal bilayer channel could provide excellent gate control, and the suspended channel also resolves the leakage issue. On the other hand, for ultra-low power consumption applications, the ferroelectric FETs that use HfO2-based ferroelectric film (mostly Hf0.5Zr0.5O2) as the gate oxide was introduced as exhibiting subthreshold swing (SS) value less than 60 mV/dec. In this work, we have entirely investigated the ferroelectric properties of the self-induced HfGeOx in HfO2 film deposited on SiGe substrate and further demonstrated the novel ferroelectric GAAFET with SiGe/Si bilayer channel and applying self-induced ferroelectric Hf-germanate. Our results reveal the proposed device has well suppression on the SCEs and exhibits extremely steep SSavg for five decades, and could be another candidate for sub-N3 technology node ultra-low-power and high-performance applications.

2:51pm - 3:03pm

Electric Field Thermopower Modulation Analyses of High Mobility In-Sn-Zn-O Thin Film Transistors

Hui Yang[1,2], Yuqiao Zhang[3], Yasutaka Matsuo[1], Hiromichi Ohta[1]

[1]Research Institute for Electronic Science, Hokkaido Univ., Sapporo, Japan; [2]Institute of Optoelectronic Technology, Beijing Jiaotong Univ., Beijing, China; [3]Institute of Quantum and Sustainable Technology, Jiangsu Univ., Zhenjiang, China; huiyangphd@gmail.com

Amorphous oxide semiconductor InSnZnOx (In : Sn : Zn = 1.1 : 0.1 : 1, ITZO hereafter) based TFT has attracted increasing attention as the next generation backplane beyond InGaZnOx (IGZO)-TFT because ITZO-TFTs show higher mobility than IGZO-TFTs [1]. Although many results on the high mobility of ITZO have been reported thus far, its origin is still unclear yet. Here, we show that electric field thermopower (S) modulation [2] of ITZO-TFTs is a powerful technique to clarify the origin of high mobility. We fabricated bottom gate top contact ITZO-TFTs using 106-nm-thick ALD-AlOx as the gate insulator. The resultant ITZO-TFTs showed excellent transistor characteristics (μFE ~48 cm2 V−1 s−1, μeff ~58 cm2 V−1 s−1, S.S. ~100 mV decade−1). From the n3D vs. S relationship of the ITZO films with varied n3D, we extracted the density of states effective mass of ITZO (m* ~0.11 m0), which is lighter than that of a-IGZO (~0.3 m0). The estimated effective thickness (n2D/n3D) was always thicker than the ITZO film thickness, suggesting that the bulk part dominantly contributes to the drain current when TFT is on.

3:03pm - 3:15pm

Characterization parameters of wear life of hydrogenated diamond-like carbon films

Zhen Li[1], Zhinan zhang[1], Guozheng Ma[2]

[1]Shanghai Jiao Tong University, Shanghai, People's Republic of China; [2]Army Academy of Armored Forces,Beijing, People's Republic of China; lizhen2019@sjtu.edu.cn

The hydrogenated diamond-like carbon(H-DLC) films have excellent tribological properties, such as high hardness, low coefficient of friction and good anti-wear performance, which makes them widely used in the aerospace field of moving parts to prolong the service life. The mechanical properties and tribological properties of H-DLC films are improved by various methods such as element doping and multi-layer structure. However, there are few studies evaluating the wear life of H-DLC films. At present, the wear rate is the vital index to evaluate the wear resistance of H-DLC films. Nonetheless, the wear characterization parameters, such as wear width, wear depth, wear cross-sectional area and volume, are not constant values. Therefore, it is of great significance to reveal the variation of characterization parameters at different wear test times to ensure the prediction accuracy of the wear life of H-DLC films. In this work, the multi-layered H-DLC films were prepared on GCr15 steel through the unbalanced magnetron sputtering system, which consists of a function layer with chromium and boron doping, Cr-C and Cr-H-DLC transition layer and a Cr bonding layer. The wear characterization parameters of H-DLC films at the different testing time was obtained by the friction and wear tester. The microstructural characterization of the H-DLC films was carried out through Scanning electron microscopy (SEM) and Raman spectroscopy. Besides, the variation of wear mechanism is also studied.

3:15pm - 3:27pm

Effect of Different Dopants on the Performance of Post-Deposited Silicon Carbide Thin Films on Doped Si Substrates

Sree Harsha Choutapalli[1], Prashantha Kumar H. G[1], Emmanuel P[2], Nilesh J Vasa[1], Jayaganthan R[1]

[1]Indian Institute of Technology Madras, India; [2]Anna University, India; ed18d004@smail.iitm.ac.in

Silicon carbide (SiC) is a wide bandgap (~ 3.3 eV) material that can satisfy higher-performance demands and seeks its attention in large-scale futuristic needs in power electronics applications. Such high-performance materials have demand in renewable energies, electric vehicles and power distribution grid sectors (Garimella et al., 2017). However, SiC technology still faces its challenges in defect-free thin films development techniques followed by the device fabrication perspective (Boomer and Scheick, 2020). In this work, SiC targets were fabricated via spark plasma sintering (SPS) at a temperature of 1850°C by using SiC precursor with the average particle size 10.21 µm followed by pulsed laser deposition (PLD) of thin films on Si wafers (1 0 0) at temperatures ranging from 650°C to 800°C. Nd3+:YAG (λ=355 nm, 6 ns) laser source was used to deposit the SiC thin films in an Argon atmosphere. Laser-assisted doping technique was used in aqueous AlCl3 and phosphoric solutions to dope Al and P in the post-deposited SiC thin film selectively and synthesize p-SiC and n-SiC doped areas, respectively. The KrF excimer laser fluence of 2.5 J cm-2 was found to be suitable for simultaneous annealing and doping of post-deposited SiC thin films (Paneerselvam et al., 2021).

The KrF laser (248 nm) assisted doping technique was used to grow p-SiC/n-Si and n-SiC/p-Si heterostructures by using n-Si and p-Si substrates, respectively. I-V measurements clearly showed p-n diode characteristics with a cut-in voltage of 2.8 V. The rectification ratios at ± 5 V were estimated to be 4.32×103, and 8.89×103, for laser doped p-SiC film on n-Si substrate, and laser doped n-SiC film on p-Si substrate, respectively. Currently, the technique is studied by using a 6-ns pulsed Nd3+:YAG laser-assisted doping at the third harmonic generation (355 nm).

3:27pm - 3:39pm

Electric Field Thermopower Modulation Analyses of the Operation Mechanism of Amorphous InGaO3(ZnO)m Thin Film Transistors

Prashant R. Ghediya[1], Hui Yang[1,2], Takashi Fujimoto[1], Yuqiao Zhang[3], Yasutaka Matsuo[1], Hiromichi Ohta[1]

[1]Research Institute for Electronic Science, Hokkaido University, Sapporo, Japan; [2]Institute of Optoelectronic Technology, Beijing Jiaotong University, Beijing, China; [3]Institute of Quantum and Sustainable Technology, Jiangsu University, Zhenjiang, China; prashantghediya@gmail.com

Currently, amorphous InGaZnO4-based TFTs [1] have been widely applied as the backplane of flat panel displays. Since widely spread 5s orbital of In ion makes conduction band bottom, a-IZGO shows rather high mobility. Although homologous series of InGaO3(ZnO)m (m = integer, IGZOm hereafter) are known as the crystal, research on a-IGZOm-TFTs is still rare and the operating mechanism is not clearly explained yet. Here, we attempted the electric field thermopower modulation analysis to clarify the relationship between transistor characteristics of a-IGZOm-TFTs and the m-value. The resultant IGZOm-TFTs showed good transistor characteristics. We measured the thermopower of the TFT channel upon gating and compared the sheet carrier concentration (n2D) with bulk carrier density (n3D) using the thermopower as the measure [2]. We found that the effective channel thickness of the amorphous IGZOm thin film transistors varied from ~0.9 nm to ~50 nm depending on the m-value. The overall tendency of n2D/n3D first decreases with m-value and then increases with m-value. This information may be useful to further improve a-IGZOm-TFT characteristics in the future.

3:39pm - 3:51pm

Electrodeposited hierarchical metal networks for Cu(In,Ga)Se 2 (CIGS) solar cells

Eunyeong Yang, Seoin Kang, Choong-Heui Chung

Hanbat National University, Korea, Republic of (South Korea); didcjswo4931@gmail.com

Indium tin oxide (ITO) with high optical transmittance and electrical conductivity is dominated material for optoelectronic device applications. However, it has problems such as brittleness of the material itself, high cost, and scarcity of indium metal. In particular, since it is difficult to apply to a flexible device due to its brittleness, a material to replace ITO is required. Metal networks are being studied as a strong candidate to replace ITO in that it can be applied to large-area and flexible devices due to its low cost and its own flexibility. In this study, the metal networks were formed using a self-cracking template. Since the thickness of the metal networks are determined by the crack template, a method capable of further improving the electrical properties is required. Since the silver nanowire layer serves as a passage between the metal networks, it is possible to facilitate the movement of electrons and improve electrical properties. In addition, electrodeposition can significantly improve electrical properties through an inexpensive and simple process. We believed that hierarchical metal networks transparent conductive electrodes (TCEs) electrodeposited with a layer of silver nanowires could significantly improve the device performance of CIGS solar cells.

3:51pm - 4:03pm

Figures of merit for the evaluation of Transparent Conductive Films: Influence of resolution on the selection of the best specimen

Arturo Rodríguez-Gómez

Instituto de Física - UNAM, Mexico; arodriguez@fisica.unam.mx

Transparent conductive films (TCF) are essential components in manufacturing electronic and photovoltaic devices such as organic and inorganic solar cells, touch screens, and light-emitting diodes [1–3]. Figures of merit (FOM) are tools that allow measuring the performance or effectiveness of procedures, systems, or devices. For the TCF's case, the purpose of a given FOM is to provide a reliable answer to the questions: (a) which TCF is better? And (b) in what proportion? The most widely used FOMs are Fraser & Cook (T/Rs) [4] and Haacke (T10/Rs) [5]. T refers to transmittance and Rs to the sheet resistance in both definitions. Although both FOMs can answer the question of which TCF is better, neither can correctly say in what proportion. In this work, we evaluate the advantages and disadvantages of Fraser & Cook and Haacke FOMs. Further, we present a slight modification to Haacke's FOM that does not alter its original essence but improves its resolution. With this resolution improvement, our FOM is able to answer the question of which TCF is better?, exactly as Haacke's FOM does, but additionally, our FOM also gives a very precise answer to the question of how much one TCF is better than another.

Oral Talk-4: Oral Talk

Time: Wednesday, 11/Jan/2023: 1:15pm – 4:03pm · *Location:* Hall 3

1:15pm - 1:27pm

2D polymers based on aromatic 1,5-diheterocines with oxygen and nitrogen

Ruslan Kevorkyants

The University of Hong Kong, Hong Kong S.A.R. (China); ruslan.kevorkyants@gmail.com

Novel class of two-dimensional polymers (2DP) formed from aromatic oxygen- and nitrogen-containing 1,5-diheterocines [1] is proposed. The aromatic monomers are interconnected via -N=N-, -C≡C-, -N=CH-, and -CH=CH- linkages that are the same in each spatial dimension. Given this construction principle, 30 2DPs were constructed. Periodic PBE DFT modeling of their crystal structures followed by phonon spectra analysis reveals 7 strictly planar, π-conjugated species of monoclinic symmetry. Their electronic band structures feature either direct or indirect transitions whose HSE06 energies fall in the range [0.01-0.53] eV. The highest charge carrier velocities and respective masses were estimated at 5.79*10*5 m/s and 9.45*10-3 m0, respectively. In addition to possible optoelectronic applications, separation of gases that is due to pores in between the heterocyclic rings is feasible. The proof of concept of N2/O2 separation is presented. Pore sizes of the 2DPs can be increased subject to the type of linkage and monomer thereby expanding separation applications.

[1] KEVORKYANTS, R. and CHIZHOV, Yu. V. 2016. The Structure and Aromaticity

of 1,4 and 1,5-Dihydro Diazocine, Dioxocine, Hydro Oxazocine: Ab Initio CCSD(T)

Singlet Potential Energy Surface Study. Tetrahedron Lett., 57, 340-344.

1:27pm - 1:39pm

Promising heavy-metal free emissive materials based on fluorene derivatives

Anna Pidluzhna[1], Aivars Vembris[2], Raitis Gržibovskis[3], Oleksandr Bezvikonnyy[4], Dmytro Volyniuk[5], Juozas Grazulevicius[6]

[1]Institute of Solid State Physics, University of Latvia, Latvia; [2]Institute of Solid State Physics, University of Latvia, Latvia; [3]Institute of Solid State Physics, University of Latvia, Latvia; [4]Kaunas University of Technology, Kaunas, Lithuania; [5]Kaunas University of Technology, Kaunas, Lithuania; [6]Kaunas University of Technology, Kaunas, Lithuania; anna.pidluzhna@cfi.lu.lv

Organic semiconductor materials became very popular during last decades because of numerous advantages such as low-cost synthesis, good chemical compatibility, relative ease of handling and simpler manufacturing process. Nowadays many emissive materials contain metals and they perform well in different semiconductive devices. Nevertheless, there is a set of issues with metal-containing organic substances which needs to be solved and one of the problems is the application of heavy metals in metal-organic complexes as emissive materials. But most of heavy metals are toxic and some of them are already restricted in EU. Therefore the synthesis of new efficient, heavy metal free electroactive emitters for organic electronics is one of the key tasks nowadays.

Fluorene core-based derivatives recommended themselves as promising emissive substances due to high photoluminescence efficiency and good charge transport properties. Therefore four different fluorene-based emissive substances were synthesized and investigated in the present work. It was determined that all synthesised compounds are optically active, they demonstrate absorption maxima at 320-420 nm, emission maxima at 390-430 nm and around 55% of photoluminescence quantum yield. As the obtained results reveal the synthesized substances are attractive and promising for application in organic electronic devices.

The study was supported by the VIAA project Nr: 1.1.1.2/VIAA/4/20/592

1:39pm – 1:51pm

Solid-state Electrochemical Thermal Transistors using SrCoOy−SrFeOy Solid Solutions

Zhiping Bian[1], Qian Yang[1,2], Mitsuki Yoshimura[1], Hai Jun Cho[3], Hiromichi Ohta[3]

[1]Graduate School of IST, Hokkaido Univ., Sapporo, Japan; [2]Institute of Quantum and Sustainable Technology, Jiangsu Univ., Zhenjiang, China; [3]Research Institute for Electronic Science, Hokkaido Univ., Sapporo, Japan; bianzhiping96@gmail.com

Very recently, we have demonstrated a solid-state electrochemical thermal transistor using SrCoOy as the active layer.[1] The fully oxidized SrCoO3 (perovskite structure) showed high thermal conductivity (κ) of ~3.8 W m−1 K−1 whereas the fully reduced SrCoO2 (defect perovskite structure) showed lower κ of ~0.95 W m−1 K−1. Although rather large κon/κoff ratio of ~4 has been obtained, the detailed κ change mechanism has not been clarified yet. Here, we show that the lattice thermal conductivity (κlat) of the fully oxidized SrCoO3 is ~2.8 W m−1 K−1 whereas the electron thermal conductivity (κele) is ~1 W m−1 K−1. We fabricated several thermal transistors using SrCo1−xFexOy solid solutions as the active layer. The observed κ of the oxidized SrCo1−xFexO3 dramatically decreased with x and became constant (~2.8 W m−1 K−1) when x > 0.3. Since the electrical conductivity drastically decreased with x, we estimated the κlat of the SrCo1−xFexO3 by assuming Wiedemann-Frantz law. We found that the κlat of the SrCo1−xFexO3 is constant (~2.8 W m−1 K−1). In addition, the κ of the reduced SrCo1−xFexO2 was two different values; ~0.98 W m−1 K−1 for x ≤ 0.5 and ~1.3 W m−1 K−1 for x ≥ 0.75, due to the difference in the crystal structure; former is defect perovskite and the latter is infinite layer. This work also provides a guiding idea for improving the on-to-off ratio of thermal transistors.

Keywords: Thermal transistors, SrCoOx, SrFeOx, Wiedemann–Franz law

[1] YANG, Q., CHO, H. J., BIAN, Z., YOSHIMURA, M., LEE, J., JEEN, H., LIN, J., WEI, J., FENG, B., IKUHARA, Y., & OHTA, H. manuscript in preparation

1:51pm - 2:03pm

Spin current generation using a compositional gradient interface between titanium and tungsten layers

Hayato Nakayama[1], Taisuke Horaguchi[1], Kazuto Yamanoi[1], Yukio Nozaki[1,2]

[1]Department of Physics, Keio University, Yokohama, Japan.; [2]Center for Spintronics Research Network, Keio University, Yokohama, Japan.; hiyokomame8810@keio.jp

Recently, it has been demonstrated that a spin current (SC) as large as in Pt can be generated in naturally oxidized Cu films although the understanding of the microscopic mechanism of SC generation is insufficient. One of the potential candidates is that a local angular momentum in a vortical flow caused by a gradient of electrical conductivity can be a source of SC. However, the detail of the coupling between electron spin and vorticity of electric current has not been clarified yet, especially the contribution of spin orbit interaction (SOI) to the coupling. In this study, we have studied the SC generation in a compositional gradient interface between Ti and W layers, both of whose spin Hall angles are negative. According to the difference in the electrical conductivity between Ti and W, a vortical flow of electrons will appear at the interface.

We fabricated multilayered microstrips consisting of Si Sub./Ti(10)/W(ti/2)/Ti(ti/2)/W(10)/Ni95Cu5(10)/SiO2(20) (unit: nm) by magnetron sputtering, where ti, i.e. the thickness of inserted Ti/W bilayer, is 0 or 0.5 nm. We conducted spin-torque ferromagnetic resonance (ST-FMR) measurement for an evaluation of the SC. Here, we applied an AC electric current to the microstrip, which produced not only an AC-SC but also an AC magnetic field. A longitudinal DC voltage, which was determined by an amplitude of magnetization precession, was measured as a function of a DC external magnetic field applied at an angle of $\pi/4$ from the long axis of the strip. We can evaluate a spin-torque efficiency ξFMR by measuring the amplitude ratio of symmetric and antisymmetric components of ST-FMR spectrum.

Figure 1 shows the ST-FMR spectrum for a sample with ti=0.5 nm. We can confirm an SC generation in the sample because the symmetric component of the ST-FMR spectrum appears. The ξFMR evaluated from the ST-FMR spectrum is 0.069, which is much larger than that for another sample with ti=0 nm (ξFMR=−0.0011). Namely, the increase of ξFMR is realized not in a sharp Ti/W interface but a composition-mixed one. This is surprising because a conventional interfacial SOI prefers the sharp interface that leads to a strong symmetry breaking. Moreover, the polarity of ξFMR for the sample with t=0.5 nm is inconsistent with the sign of spin Hall angle for W. Thus, we can neglect the SC generated via a bulk SOI of the W layer.

We demonstrated the improvement of ξFMR by using the Ti/W composition gradient interface although there was little increase for a sharp Ti/W interface. Moreover, the polarity of spin-torque produced by the Ti/W gradient material cannot be explained by the bulk spin Hall effect in the W with the negative spin Hall angle. These results imply the SC generation via coupling between electron spin and vorticity of electric current. For a better understanding of the microscopic mechanism of the SC generation, we will examine the dependence of ξFMR on ti layer which can vary the vorticity of electric current.

2:03pm - 2:15pm

Spin elastodynamic motive force

Takumi Funato[1], Mamoru Matsuo[2]

[1]Keio university, Japan; [2]Kavli-ITS, UCAS, China; t_funato@keio.jp

Spintronics is concerned with the interconversion of charge transport and spin dynamics. The control of magnetization structures by charge current has been extensively investigated for MRAM and spin-torque oscillator applications. The spin-motive force (SMF), known as the inverse effect, is an electric voltage generation in a ferromagnetic metal due to an emergent spin-dependent gauge field driven by the interplay between conduction electron spins and the magnetization dynamics. The conventional SMF requires both non-vanishing time and space derivatives of the magnetization. Therefore, a complicated experimental setup is necessary, such as magnetic domain wall motion and nonuniformly shaped devices. The SMF induced via spin-orbit interaction is proposed theoretically to resolve the restriction. However, these mechanisms require strong spin-orbit materials and restrict the range of material choices. Accordingly, they have not been observed experimentally so far.

We propose the SMF induced by surface acoustic waves (SAWs) via spin-elastodynamics to overcome conventional limitations. Three couplings drive the spin-elastodynamics in a ferromagnetic metal: spin-vorticity coupling (SVC), magnetoelastic coupling, and s-d coupling. In this setup, the injected SAW generates the magnetization dynamics with the non-vanishing time and space derivatives. The advantage of the SAW device is that it does not require nano-fabrications of the magnetic metal itself. In addition, the SVC, the coupling between conduction electron spins and the vorticity field of the lattice, emerges universally in various systems, and thus, it does not restrict material choices. Indeed, SVC has attracted much attention because it generates spin current without spin-orbit interaction. Also, the magnetoelastic coupling has been widely exploited for driving non-equilibrium spin dynamics with a SAW.

This presentation considers the SMF induced by a Rayleigh-type SAW. We calculate the SAW-induced SMF up to second-order in lattice displacement by treating the influence of magnetization dynamics as a unitary transformation of the spin space. We show two mechanisms of the SAW-induced SMF: the first is the SVC-driven SMF, which generates the first harmonic electromotive force due to gradient spin accumulation induced by SVC. The second is the spin-elastodynamic motive force (SEMF), which generates d.c. and the second harmonic electromotive force due to the combination of SVC and magnetoelastic coupling. The results show that the SEMF causes non-reciprocity of the electromotive force. Our estimation suggests that the electric voltage induced by the present SMFs is detectable in polycrystalline nickel. Therefore, the SVC-driven SMF and the SEMF are expected to expand the SMF applications' range significantly.

2:15pm - 2:27pm

Spin Torque Generation using Si/Al Compositional Gradient Material

Taisuke Horaguchi[1], Cong He[2], Zhenchao Wen[2], Tadakatsu Ohkubo[2], Kazuhiro Hono[2], Seiji Mitani[2], Hiroaki Sukegawa[2], Junji Fujimoto[3], Kazuto Yamanoi[1], Mamoru Matsuo[3,4,5,6], Yukio Nozaki[1,7]

[1]Keio University, Japan; [2]Research Center for Magnetic and Spintronic Materials, National Institute for Materials Science,Japan; [3]Kavli Institute for Theoretical Sciences, University of Chinese Academy of Sciences, China; [4]CAS Center for Excellence in Topological Quantum Computation, University of Chinese Academy of Sciences, China; [5]RIKEN Center for Emergent Matter Science (CEMS), Japan; [6]Advanced Science Research Center, Japan Atomic Energy Agency, Japan; [7]Center for Spintronics Research Network, Keio University, Japan; taisuke.horaguchi@keio.jp

Recently, high-efficient spin torque generation using only weak-SOI elements has been demonstrated for an alternative way of the spin-orbit torque generated by strong-SOI elements such as Pt, Ta, and W. For instance, Cu oxides [1,2,3] have attracted much attention as a superior spin torque generator although the origin of spin torque is under debate. One of the possible mechanisms is attributed to a composition gradient from poorly conductive CuOx to highly conductive Cu, which leads to a local angular momentum in a vortical flow of electric current. In this study, we demonstrated an enhancement of spin torque efficiency in Si/Al compositional gradient materials and found that the spin torque efficiency was increased with decreasing the width of the composition gradient interface.

We prepared Si sub./Si(10)/Al(t_i/2)/Si(t_i/2)/Al(10)/Ni95Cu5/SiO2(20) (unit: nm) multilayer by magnetron sputtering, where t_i is the thickness of interfacial insertion of Al/Si bilayer. Figure 1(a) shows the cross-sectional HAADF-STEM images at the interface for the sample with t_i= 2.0 nm. The 2-nm insertion increased the width of mixed interface between 10 nm thick Si and Al. The depth profile of each composition obtained by energy dissipative spectroscopy was well fitted by the tanh function with a transition width of L. As shown in Fig. 1(b), a monotonous increase of L with t_iwas observed. Namely, we succeeded to realize nm-thick Si/Al compositional gradient at the interface.

To evaluate the spin torque efficiency ξ_FMR of the Si/Al gradient materials, we conducted spin torque ferromagnetic resonance(ST-FMR) measurement[4]. Figure 2 shows the value of ξ_FMR, i.e. a conversion ratio from charge current to spin current, for various t_i. We found that the ξ_FMR clearly increased with decreasing t_i, although there was little increase in ξ_FMR for the sample without Al/Si insertion. This result implies that the compositional gradient from Si to Al is the most important factor for the enhancement of ξ_FMR. Namely, an interfacial spin-orbit interaction, such as Rashba-Edelstein effect, is not effective in our sample. Moreover, a strong nonreciprocity of the conversion between charge- and spin-currents appeared, as seen in previous study using Cu oxide[2]. Such a nonreciprocity is considered as an evidence that a spin current is generated from an electric current vorticity which is associated with a compositional gradient. A theoretical work on a coupling between electron spin and vorticity of electric current predicted that the charge to spin conversion efficiency was inversely proportional to the square of transition width. The increase in ξ_FMR with decreasing L observe in the Si/Al gradient material seems to be consistent with the theory. Our findings suggest that nm-scale compositional gradient material is a promising candidate for efficient and sustainable spin torque generator without using rare metals.

2:27pm - 2:39pm

Structural and electrical properties of La0.7Sr0.3MnO3 / La0.85Sr0.15MnO3 heterolayered thin films for IR detectors

Jeong-Eun Lim[1], Byeong-Jun Park[1], Sam-Haeng Yi[1,2], Myung-Gyu Lee[1,2], Joo-Seok Park[2], Sung-Gap Lee[1]

[1]Dept. of Materials Engineering and Convergence Technology, RIGET, Gyeongsang National University, Jinju 52828, S. Korea; [2]Business Support Division, Korea Institute of Ceramic Engineering and Technology, Jinju 52851, S. Korea; cosmosjjh@naver.com

In this study, for application as IR detectors, La0.7Sr0.3MnO3 / La0.85Sr0.15MnO3 heterolayered thin films were fabricated and structural and electrical properties were investigated. La0.7Sr0.3MnO3 (LSMO(70/30)) and La0.85Sr0.15MnO3 (LSMO(85/15)) coating solutions were synthesized by sol-gel method, and LSMO heterolayered thin films were fabricated by spin-coating method on Pt/Ti/SiO2/Si substrate. For the first layer, LSMO(70/30) layer was spin-coated at 4000 rpm and 30 sec, dried at 200°C for 5 min, and pyrolyzed at 400°C for 10 min. And then, the second LSMO(85/15) layer was coated on the first layer with the same conditions. XRD, FE-SEM, and XPS were measured to investigate the structural properties of LSMO heterolayered thin films. And the electrical properties, such as resistivity, TCR, and B-value, were measured to investigated possibility of application as IR detectors.

2:39pm – 2:51pm

Study of Flexible Tactile Sensor Fabricated by Laser Induced Metallization

Yu-Xuan Cho[1], Shang-Ru Wu[1], Yi-Hung Chen[1], Gabriel Vanko[2], Robert Andok[3], Hung-Yin Tsai[1]

[1]Department of Power Mechanical Engineering, National Tsing Hua University, Hsinchu, 30013, Taiwan; [2]Institute of Electrical Engineering, Slovak Academy of Sciences, Dúbravská cesta 9, 841 04 Bratislava, Slovakia; [3]Institute of Informatics, Slovak Academy of Sciences, Dúbravská cesta 9, 841 04 Bratislava, Slovakia; je810759@gmail.com

This study investigates the feasibility of using Laser Induced Metallization (LIM) technology to fabricate flexible tactile sensors and the stability of the sample under repeated pressing and bending. In this study, a polyimide (PI) plastic was used as the substrate and two layers of electrodes were deposited using the LIM method to realize a capacitive sensor structure after the process parameters were evaluated. The experimental results show that the sensor samples with the two-layer electrode array structure, which enables the implementation of projected capacitive sensing, have better flexibility than other similar sensors, achieving a minimum curvature radius of 1 mm without breaking and maintaining the sensing function after 1000 bending cycles. The laser-induced metallization method shows high potential for flexible tactile sensors and has the potential to expand its application areas to motion detection, multi-touch panels, anti-collision systems, etc.

2:51pm - 3:03pm

Using a laser generated shock wave to characterize the strength adhesion of thin lightning strike protection layers of aeronautic composite structures

Audrey Bigand[1,2], Christine Espinosa[1], Jean-Marc Bauchire[3], Michel Boustie[4,5], Didier Zagouri[5]

[1]Institut Clément Ader (ICA), University of Toulouse, ISAE-SUPAERO, INSA, IMT MINES ALBI, UTIII, CNRS, 3 Rue Caroline Aigle, 31400 Toulouse, France; [2]Airbus Operations SAS, 316 route de Bayonne, 31060 Toulouse Cedex 09, France; [3]GREMI, CNRS-University of Orleans, 14 rue d'Issoudun, BP 6744, 45067 Orléans Cedex 2, France; [4]Institut Pprime, CNRS-University of Poitiers, ISAE-ENSMA, Téléport 2, 1 Av. Clément Ader, 86360 Chasseneuil-du-Poitou, France; [5]SimChoc, 64 Rue Galliéni, 92240 Malakoff, France; christine.espinosa@isae-supaero.fr

Aircrafts' structures are exposed to the risk of being damaged during and after a lightning strike which is a natural and unpredictable event. An aircraft is hit once per year as a mean. Lightning strike is a multi-physical intense and harsh event leading to flashes of extremely high current and high voltage pulses of few microseconds to few milliseconds [1]. The low conductivity of Carbon Fiber Reinforced Plastic (CFRP) that composes the aeronautic primary structures enhances the Joule heating generated by the current flow into the structure which can lead to significant core or surface damage [2, 3]. Many Lightning Strike Protection (LSP) layers have been developed for the protection of composite structure against lightning damage. Due to their low mass to conductivity and low cost to high draping capacity ratios, the most common coatings are expanded metallic grids like the Expanded Copper Foil (ECF). Still the dependence of damage generation and final extent in the composite panel on the LSP behavior is complex to handle from lighting test campaigns. Indeed, the lightning damage mechanism for carbon laminate is a complex multi-physical phenomenon. The lightning current entering into the surface metallic protection and the underlying carbon plies generates Joule's effects and magnetic forces which both induce mechanical forces and surface explosion that has produced a significant mechanical impact. Due to the presence of paint, the arc can't spread freely and thus the distribution of current into the LSP and CFRP is disturbed. The first one will change the profile of explosion on the surface due to LSP vaporization and the second one will break the composite fiber due to Joule heating. The combination of these two phenomena can lead to significant delamination into the composite structure. In order to measure the adhesion strength of the LSP under high strain rates due to the different shock waves, a laser shock experiment is used (Figure 1). Laser shock have been generated from the top face and from the rear unpainted face at different intensity levels in order to bracket the tensile stress level at which the LSP or the paint layer are detached from their underlying substrates. The mechanical pressure generated from the laser is evaluated thanks to damage comparisons between the different plates in the test matrix. This work is a new step in the characterization of the damage creation during a lightning strike and in the use of laser induced shock to characterize interface adhesive strengths of multi-layer assemblies [4].

Figure 1 – Post-mortem surface damage after 5mm laser shots at various intensities.

3:03pm - 3:15pm

A new experimental setup to study the effect of adhesive properties on spreading and resultant forces during the approach process

Lorraine Aparecida Silva[1], Christine Espinosa[1], Eric Paroissien[1], Frédéric Lachaud[1], Lucas F.M. da Silva[2], Joseph Morlier[1], Timothée Neveu[3]

[1]Institut Clément Ader (ICA), Université de Toulouse, ISAE-SUPAERO, INSA, IMT MINES ALBI, UTIII, CNRS, 3 Rue Caroline Aigle, 31400 Toulouse, France; [2]Department of Mechanical Engineering, University of Porto, 4200-465, Portugal; [3]Institut Supérieur de l'Aéronautique et de l'Espace (ISAE-SUPAERO), 10 Avenue Edouard. Belin, 31400 Toulouse, France; lorraine.silva@isae-supaero.fr

One of the most well-known problems with assembly by adhesive joints is the difficulty of dismantling the components without damaging them. Yet, in the context of enhancing sustainable design, the structures must be designed to anticipate the possibility of disassembly. If in automotive industry, disassemble on demand (or DoD) is more and more used, the certification of aeronautic structure and the required robustness of satellite require the structures to keep their integrity to ensure safety during their life, which can come in conflict with the need of dissembling. In particular, in space industry, this has become crucial to reduce debris generation with the so-called Design for Demise (D4D) strategy. A controlled disassembly of the substrates at the end of the mission is thought as being a good way to achieve it, transforming the adhesive joint into a structural functional material. This component is required to sustain the loads during the structures' life, and to be a demountable component when it is desired to control the disassembly. One way to demount is to go through usage of Thermally Expandable Particles (TEP) [1]. Addition of TEP is a particularly interesting strategy, because it can be applied without significant modifications of the assembled structure, or of the industrial approach process. However, filling the adhesive with TEP changes its properties, especially the viscosity or spreading capability. It also adds other mechanisms in the optimal approach process, indeed the creation of particles packages [2]. Recent works have allowed to study the effect of adhesive property on spreading both on experimental [3] or numerical [4] point of view. This work presents a new experimental setup that has been designed to observe and measure the spreading of adhesives between different substrates during the approach process. The setup measures directly the resultant forces involved in the process and tracks the spread in real time without the use of mirrors, which can cause distortion when the substrates have different curvatures (Figure 1). With this experimental setup, we are able to study different aspects of the spreading process, indeed the nature and format of the substrates, the conditions of the approach, as the speed and pression applied. The distribution of adhesive in a honeycomb's cells, and the distribution of adhesive and TEP are presented and discussed.

3:15pm - 3:27pm

Alkaline-earth Sulfide Nano-phosphors Template Synthesis and Characterization

Chen-Yu Wu[1], Pei-Tzu Cheng[2], Horng-Yi Chang[2]

[1]Metal Industries Research & Development Centre (MIRDC), Taiwan; [2]National Taiwan Ocean University, Taiwan; hychang@mail.ntou.edu.tw

Alkaline-earth sulfide phosphor doped with Eu2+ is a candidate for red compensation in white light emitting devices (WLEDs) [1,2]. The reason is a great possible alternation to oxides in obtaining saturated red emission. The Eu2+ in alkaline-earth sulfide is difficult formation completely by conventional high temperature and using toxic sulfur-containing atmosphere. The isotropic nano-sized sulfide

phosphors were prepared by carbon-sphere template. A precursor of Eu-doped alkaline-earth sulfide was nucleated and grown on carbon sphere surface. Sulfide nanophosphors were synthesized by carbon decomposed reduction in a nitrogen atmosphere at 800□C in one step without compensated by extra sulfur sources. The formation mechanism of such carbon-sphere template synthesized sulfide nano-phosphors is then studied. The photoluminescence (PL) intensity as a function of crystal structure, microstructure, Eu-dopant contents and environmental temperature are investigated in this work. The concentration and thermal quenching effects are evaluated for the LED applications.

3:27pm - 3:39pm

Amphibious Artificial Compound Eye with the Self-aligned waveguide

Ji-Eun Yeo, Hyuk Jae Jang, Young Min Song

School of Electrical Engineering and Computer Science (EECS), Gwangju Institute of Science and Technology (GIST), 123 Cheomdangwagi-ro, Buk-gu, Gwangju 61005, Republic of Korea.; jieunyeo@gm.gist.ac.kr

1. introduction

Compound eyes of arthropods show outstanding functionalities such as a wide field-of-view and high sensitivity to motion detection due to their unusual optical unit, ommatidium. [1,2] Figure 1a shows the biological structure of the ommatidium which consists of a corneal lens, crystalline cone, and rhabdom. In nature, biological structures of the ommatidium have diversely evolved with their environments, such as a corneal lens for optical power and crystalline cone for optical guidance. [3,4] To mimic these functionalities, artificial ommatidium has been studied using a photosensitive polymer material. [5] However, previous efforts to mimic a natural ommatidium have not focused on the external environment such as weather conditions. Generally, optical systems lose their focusing power since the refractive power of curved lenses is changed with their external refractive index (RI). Therefore, the curved lens does not gather the optical rays efficiently once they are in the changing environment.

Here, we introduce an amphibious artificial ommatidium with the waveguide via a self-writing process and flat micro-lens array (MLA), which enables the same light-gathering efficiency regardless of outer RI. As shown in Fig. 1b, the optical power of the curved lens is changed with the external medium while that of the flat lens is consistent. [6]

2. Fabrication of the self-aligned waveguide

Using the ultraviolet (UV) curing property of the photosensitive polymer (SU-8, Microchem Corporation, Newton, MA) and the light focusing property of MLA, artificial ommatidium with the self-written waveguide was formed.

Figure 2 shows schematic illustrations of the fabrication process of self-aligned waveguides. Prior to the fabrication of the SU-8 MLA, a polydimethylsiloxane (PDMS) mold with a sidewall was fabricated using a quartz MLA mold etched by reactive ion etching. The temperature of SU-8 was gradually increased from 65 ℃ to 120 ℃ to completely evaporate the solvent and the optical adhesive (Norland optical adhesive (NOA), Norland Products, USA) was spin-coated on a fabricated SU-8 MLA. When the UV light source is irradiated, the exposed region is photo-crosslinked through post-exposure baking, which results the RI increase, while the unexposed region is thermal-crosslinked with the RI reduction through hard baking. As a result, the exposed and unexposed regions serve as a core and cladding of the waveguide, respectively.

3. Conclusion

We have implemented the universal self-aligned waveguide by using flat MLA and the difference in RI between the photo/thermal-crosslinked regions. This artificial component allows the optical system to ensure amphibious imaging without non-essential optical loss. Our optical system could be of use in a variety of imaging applications such as medical engineering and light field imaging in all-weather.

3:39pm – 3:51pm

Construct-cDNA for Versatile Biopolymer Functional Material, in Microorganisms: Use of Synthetic Biology

Raul Cuero[1,2], Jhonny Mateo Sanchez[2]

[1]BioCapital Holdings LLC, United States of America; [2]International Park of Creativity, Colombia; olimpa@aol.com

The aim of this investigation was to use synthetic biology for designing and tailoring functional materials in microorganisms for polymer synthesis with versatile bio-applications, hence mimicking the organization of nature with high fidelity. Therefore, different construct-cDNA(s) were designed and cloned into bacteria and/or yeast, using synthetic biology to produce different biodegradable and waterproof functional material, such as bio-foam including drinking cups, replacement of synthetic plastic, non-toxic delivery system for biological material to treat some diseases, and for regenerative agriculture. Thus, different sequences of genes and/or proteins with desired properties were assembled. Sequences of specific proteins such as chitin synthase, chitin deacetylase, and other sequences were arranged along with promoters, terminators, and reporter proteins, and were assembled and cloned in bacteria or yeast, using synthetic biology and other molecular biology techniques. Cell free lysates from these grown transformed microbial cultures were subjected to molecular biology such as ELISA test and physical chemical analysis such as absorption spectrometry, in order to confirm the presence of a biodegradable chitin based natural material for making the foam and/or cups, for treating plants to harness production of hormones, and for producing an encapsulating delivery system.

After ELISA and spectroscopic analysis, results showed a great expression of the recombinant proteins, such as chitin synthase and fluorescent reporter protein which are the main genetic parts of the denoted construct-cDNA in the microbial cultures. Thus, corroborating the success of the genetic assemblage. Laboratory and field tests showed the efficacy of using the final functional material in producing biodegradable and waterproof bio-foams, drinking cups, increase of plant hormones (i.e. auxins, cytokinins, and abscisic acids), and encapsulating materials for delivery of biomolecules. Therefore, the denoted molecular approach presents a good alternative for producing biodegradable functional material for protection of the environment (i.e. alternative for synthetic plastic) and public health, as well as for effective delivery system of therapeutic treatments, and for regenerative agriculture-forestry.

3:51pm - 4:03pm

Evaluating efficacy of different geometries of PDMS for CO2 confinement

Anant Vaishnav1, Aleksandar Staykov2

1Department of Applied Chemistry, Faculty of engineering, Kyushu University, Japan; 2International Institute for Carbon Neutral Energy Research I2CNER, Kyushu University, Japan; vaishnav.anant.363@s.kyushu-u.ac.jp

Oral Talk-10: Oral Talk

Time: Wednesday, 11/Jan/2023: 2:40pm – 4:04pm · *Location:* Main Hall

2:40pm – 2:52pm

2D Hybrid Perovskite for Next Generation Optoelectronic Devices

Karl Jonas Riisnaes[1], Rosanna Mastria[1], Agnes Bacon[1], Hoi Tung Lam[1], Luisa De Marco[2], Monica Craciun[1], Saverio Russo[1]

[1]University of Exeter, United Kingdom; [2]Instetute of Nanotechnology; kr378@exeter.ac.uk

Fast signal processing devices working at the interface between photonic and electronic systems are required to have large bandwidth real time photoresponse, high sensitivity and capable of operating at ambient condition. These performance requirements impose stringent requirements on the electrical and optical properties of materials, with only a few systems passing the threshold. The new emerging class of layered 2D organic-inorganic perovskites are attracting growing attention owing to their unique combination of photophysical and electrical transport properties. [1-5] However, their instability to ambient conditions and solvents used in device fabrication have so far hindered their potential for signal processing technologies. In this talk I will discuss a reliable way to enhance the resilience of these materials and demonstrate top-down semiconductor processing of high-quality nano-scale structures based on them. Hence, I will present a detailed characterization of the opto-electronic properties of 2D perovskite devices, and demonstrate that their performance exceed that of high-end commercial Si and InGaAs-based structures. Finally, I will demonstrate the use of 2D perovskite opto-electronics in a range of imaging applications.

Keywords: 2D Perovskites, opto-electronics, photodetectors

[1] L. Pedesseau et al. ACS Nano. 11, 9776–9786 (2016).

[2] B. Saparov, D. B. Mitzi, Chemical Reviews 116, 4558-4596 (2016).

[3] S.-T. Ha, C. Shen, J. Zhang, Q. Xiong, Nature Photonics 10, 115-121 (2015).

[4] B. R. Sutherland, E. H. Sargent, Nature Photonics 10, 295-302 (2016).

[5] D. Cortecchia, et al. Chemistry of Materials 29, 10088-10094 (2017).

2:52pm – 3:04pm

Figures of merit for the evaluation of Transparent Conductive Films: Influence of resolution on the selection of the best specimen

Arturo Rodríguez-Gómez

Instituto de Física - UNAM, Mexico; arodriguez@fisica.unam.mx

Transparent conductive films (TCF) are essential components in manufacturing electronic and photovoltaic devices such as organic and inorganic solar cells, touch screens, and light-emitting diodes [1–3]. Figures of merit (FOM) are tools that allow measuring the performance or effectiveness of procedures, systems, or devices. For the TCF's case, the purpose of a given FOM is to provide a reliable answer to the questions: (a) which TCF is better? And (b) in what proportion? The most widely used FOMs are Fraser & Cook (T/Rs) [4] and Haacke (T10/Rs) [5]. T refers to transmittance and Rs to the sheet resistance in both definitions. Although both FOMs can answer the question of which TCF is better, neither can correctly say in what proportion. In this work, we evaluate the advantages and disadvantages of Fraser & Cook and Haacke FOMs. Further, we present a slight modification to Haacke's FOM that does not alter its original essence but improves its resolution. With this resolution improvement, our FOM is able to answer the question of which TCF is better?, exactly as Haacke's FOM does, but additionally, our FOM also gives a very precise answer to the question of how much one TCF is better than another.

3:04pm – 3:16pm

Application of Ion-exchanged PEDOT:PSS with Ionic Liquids to Organic Thermoelectric Materials

Ichiro Imae, Hiroki Uehara, Keiichi Imato, Yousuke Ooyama

Hiroshima University, Japan; imae@hiroshima-u.ac.jp

Recently, conducting polymers attracting a high level of interest since they have been found to function as thermoelectric materials, and it was found that they can be applied to not only waste heat recovery systems below 200°C, but also power sources for wearable devices and trillion sensors. Among them, poly(3,4-ethylenedioxythiophene):poly(styrenesulfonic acid) (PEDOT:PSS) has been the most actively investigated as the most promising candidate for commercialization because of its moderate performance. Thermoelectric materials are known to exhibit superior performance when the dimensionless figure-of-merit ($ZT = (S^2\sigma/\kappa)T$), where S is the Seebeck coefficient, σ is the electrical conductivity, κ is the thermal conductivity, and T is the absolute temperature, has a large value. Since conducting polymers are organic materials, thermal conductivities are relatively small. The Seebeck coefficients of most organic thermoelectric materials are about several tens of μV/K. In contrast, the electrical conductivity varies by many orders of magnitude depending on the materials, so it is important to fabricate a sample with high electrical conductivity in order to improve the ZT value.

In this study, the ion exchange reaction between PEDOT:PSS and ionic liquid was performed to improve the electrical conductivity by removing the insulating PSS portion from PEDOT:PSS, and the thermoelectric properties of the resulting films were investigated.

3:16pm – 3:28pm

Bandgap Shrinkage and Charge Transfer in Two-Dimensional Layered SnS2 doped with V for Photocatalytic Efficiency Improvement

Way-Faung Pong

Tamkang University, Taiwan; wfpong@mail.tku.edu.tw

Bandgap Shrinkage and Charge Transfer in Two-Dimensional Layered SnS2 doped with V for Photocatalytic Efficiency Improvement

Abhijeet R. Shelke1, Hsiao-Tsu Wang1, Jau-Wern Chiou2, Indrajit Shown3, Chi-Cheng Lee1, Hung-Chung Hsueh1, Chao-Hung Du1, S. C. Ray4, Shang-Hsien Hsieh5, Chih-Wen Pao5, Huang-Ming Tsai5, Chia-Hao Chen5, Kuei-Hsien Chen3, Li-Chyong Chen6, Way-Faung Pong1

1 Department of Physics, Tamkang University, New Taipei City 251, Taiwan

2 Department of Applied Physics, National University of Kaohsiung, Kaohsiung 811, Taiwan

3 Institute of Atomic and Molecular Sciences, Academia Sinica, Taipei 106, Taiwan

4 Department of Physics, CSET, University of South Africa, Johannesburg 1710,

South Africa

5 National Synchrotron Radiation Research Center, Hsinchu 300, Taiwan

6 Center for Condensed Matter Sciences, National Taiwan University, Taipei 106, Taiwan

wfpong@mail.tku.edu.tw

Effects of electronic and atomic structures of V-doped two-dimensional layered SnS2 have been studied using X-ray spectroscopy for the development of photocatalytic/photovoltaic applications. Extended X-ray absorption fine structure measurements at V K-edge revealed the presence of V–O and V–S bonds which forms the intercalation of tetrahedral O–V–S sites in the van der Waals (vdW) gap of SnS2 layers. X-ray absorption near-edge structure (XANES) reveals not only valence state of V dopant in SnS2 is approximately 4+ but also the charge transfer (CT) from V to ligands, supported by V Lα,β resonant inelastic X-ray scattering. These results suggest V doping produces extra interlayer covalent interactions and additional conducting channels, which increase the electronic conductivity and CT. This gives rapid transport of photo-excited electrons and effective carrier separation in layered SnS2. Additionally, valence-band photoemission spectra and S K-edge XANES indicate that the density of states near/at valence-band maximum is shifted to lower binding energy in V-doped SnS2 compare to pristine SnS2 and exhibits band gap shrinkage. These findings support first-principles density functional theory calculations of the interstitially tetrahedral O–V–S site intercalated in the vdW gap, highlighting the CT from V to ligands in V-doped SnS2.

3:28pm – 3:40pm

Electron tunneling and properties of break-junction interfaces in cuprates and related materials

Toshikazu Ekino[1], Akira Sugimoto[1], Hironori Ohtsubo[1], Kaito Matsumoto[1], Takeshi Saito[1], Masatoshi Iwano[1], Ryuichi Ukita[1], Jun Akimitsu[2], Alexander M. Gabovich[3]

[1]Hiroshima University, Japan; [2]Okayama University, Japan; [3]Institute of Physics, Ukraine; ekino@hiroshima-u.ac.jp

Herewith we report the results of the experimental study of the cuprate ladder and layered materials by mean of break-junction (BJ) and scanning tunneling spectroscopy (STS). From BJ formed by a Ca-doped ladder Sr14Cu24O41 compound, the characteristic gap Σ of ~ 120 ± 20 meV was revealed at low temperature, T, which disappears above Td ≈ 90 K. We attribute this feature to the charge-density wave (CDW) formation, since the ratio 2Σ/Td ≈ 15 is consistent with the often observed ratios for CDWs. The BJ spectra manifest such a CDW-gap signal coexisting with the strong zero-bias peak well inside the CDW coherence gap peak. After mechanically adjusting bending conditions of the break junction, an additional subtle gap feature of 2Δ ≈ 6 ± 2 meV appears below Tc ≈ 7 - 12 K. Both low-T characteristic features are believed to be due to the interface superconductivity of the freshly formed BJ coexisting with CDW. The surface superconducting gap Δ found in the semiconducting ladder compound is consistent with the apparent Tc ≈ 6 - 8 K in either the overdoped Bi2Sr2CuO6 or the classical high-Tc compound La2-xSrxCuO4 possessing intrinsic compositional inhomogeneity as was previously observed in BJ experiments. Therefore, we can attribute such a low Tc as the manifestation of a lower boundary for the cuprate superconductivity. The similar BJ interface Tc observed in the copper-iron layered chalcogenides will be presented and discussed separately together with the STS experimental results.

[1] EKINO, T., IWANO, M., SUGIMOTO, A., AKIMITSU, J. & GABOVICH, A.M. 2021. Tunneling and break junction spectroscopy of the ambient-pressure semiconducting and superconducting gap structures in the ladder compound (Sr, Ca)14Cu24O41. Phys. Rev. B104, 054514 (1-14).

[2] EKINO, T., GABOVICH, A.M., Li. M.S., SZYNCZAK, H. & VOITENKO, A.I. 2020. Break-junction tunneling spectra of Bi2212 superconducting ceramics: Influence of inhomogeneous d-wave-Cooper-pairing and charge-density-wave order parameters. Low Temp. Phys. 46, 400 (1-13).

3:40pm – 3:52pm

Nano-bioremediation: Comparative study of nano-zero valent iron and nano-ferric oxide for remediation of oil contaminated soils

Phenny Mwaanga[1], Niza Kaonga[1], Lubomba Siamuzyulu[1], Matimba Mpundu[1], Adolf Lungu[2], Patrick Musenge[1]

[1]Copperbelt University, Zambia; [2]University of Zambia; phennym@yahoo.co.uk

In this study, nano-zero valent (nZVI) and nano-ferric oxide (nFe3O4) synthesised using banana and mango peel extracts, were used as reductive-catalytic and biostimulatory-augmentation agents in the bioremediation of oil contaminated soils. The polyphenol-rich extracts acted both as stabilizing and reducing agents for ferrous/ferric sulphate solutions in the formation of the nanoparticles (NPs). The resultant nZVI and nFe3O4 were characterized using UV–visible spectroscopy, X-ray diffraction (XRD), Fourier transform infra-red (FTIR) spectroscopy and scanning electron microscopy (SEM). The nZVI and nFe3O4 were compared in their reductive-catalytic and biostimulatory-augmentation ability in the nano-bioremediation of the oil contaminated soils from the mining and metal processing environments. This study further used two other commonly used bioremediation formulas as controls. The oil contaminated soils were optimised for pH, moisture content and temperature for each bioremediation agent and their effectiveness in facilitating the degradation of oils in soils were monitored over a period of 14 weeks. Additionally, the concentrations of relevant heavy metals in the oil contaminated soils were also determined before and after bioremediation. Complementary toxicity tests were conducted on the oil contaminated soils before and after bioremediation using earthworm, Essenia fetida. The endpoints considered were mortality, weight gain and oxidized glutathione (GSSG). The amounts of oils in soils were determined according to the EPA's method 5520 E and the toxicity tests on Essenia fetida were carried out according to the methods specified by OECD.

The SEM characterization confirmed that both nZVI and nFe3O4 were formed, with sizes ranging from 30 nm to 100 nm. FTIR spectra indicated presence of functional groups of polyphenols on surfaces of nanoparticles (NPs). Further XRD indicated that both NPs had crystalline quality structure. The bio-remediation results showed significantly higher degree bio-remediation for NPs compared to the controls. Further, the degree of bio-remediation of nZVI was significantly higher than that of n-Fe3O4. The results suggest that nZVI's exerts a complex interplay between the reductive-catalytic and the biostimulatory-augmentation capability that is much higher than that of n-Fe3O4 as corroborated by the results of complementary toxicity tests conducted on the bio-remediated soils. For instance, whilst there were some observable toxic effects on soils bio-remediated by the two controls and n-Fe3O4, there was virtually no observed toxicity for the soils bio-remediated with nZVI. However, the concentrations of selected heavy metals did not significantly reduce in all the soils after bioremediation, suggesting that the toxicity observed before bio-remediation was mainly due to oils. These results indicate the promise that nanotechnology holds for soil environmental remediation.

3:52pm – 4:04pm

Developing intrinsically strong, flexible, and liquid-free phase change films via dual-crosslinking for advanced thermal management

Bo Zhang, Zhen Li, Liwei Wang

School of Mechanical Engineering, Shanghai Jiao Tong University, Shanghai 200240, China; zhangbo262@sjtu.edu.cn

Phase change materials (PCMs) have attracted tremendous attention as an efficient technology for energy storage, conversion, and management. However, the rigidity of the traditional PCMs has now become a major obstacle towards advanced applications such as wearable devices, flexible electronics, and soft robotics. Although considerable efforts have been dedicated to fabricating flexible PCMs by physical blending or chemical branching, there still exist serious unresolved issues including liquid leakage and mechanical weakness.

Here, a dual-crosslinking strategy is developed to fabricate intrinsically strong and flexible solid-solid phase change films aiming to the advanced thermal management scenarios. As depicted in Fig.1, different from the traditional approaches which directly graft PCMs such as polyethylene glycol (PEG) onto the all-hydroxyl raw cellulose and its derivatives (e.g., cellulose diacetate), TEMPO-oxidation method is firstly adopted to convert a primary hydroxyl of cellulose into a carboxylate. The strong electrostatic repulsive forces generated by the ionized carboxyl is conducive to fibrillate micron-scale cellulose to cellulose nanofiber (CNF), which can expose more hydroxyl on the CNF surface to react with isocyanate to graft more PEG in the next step, and thus the CNF-PEG PCMs show greater energy storage capacity. Meanwhile, compared to the original hydroxyl, the carboxyl is much more active and can combine with cations, which yields the potential to strengthen the CNF-based PCMs by ionic bonding. Therefore, a multivalent cation (the common divalent calcium ion is adopted here) is finally added into the PEG-grafted CNF to chelate with the carboxyl to significantly enhance the strength.

Fig. 1. Dual-crosslinking strategy of the intrinsically strong and flexible phase change films.

Through the dual-crosslinking strategy, CNF and PEG are connected by the glue, isocyanate, where CNF ensures the mechanical flexibility while PEG generates the energy storage ability. Compared with the traditional methods of PCMs, the dual-crosslinking strategy has two main advantages: 1) more PEG can be chemically grafted onto CNF than the micron-scale cellulose because more hydroxyl groups are exposed on the fiber surface. 2) the strength of CNF-PEG PCMs is significantly enhanced because the sperate 2D cellulose fibers are connected to form a robust 3D skeleton by the chelation between calcium ion and carboxyl. Overall, a novel approach is demonstrated to prepare high-performance PCMs and the obtained CNF-PEG PCMs are intrinsically flexible, strong, and liquid-free, showing enormous application potential in advanced thermal management scenarios.

Keywords: Thermal management, phase change, intrinsic strength and flexibility, dual-crosslinking, cellulose nanofiber

[1] SHI, J., QIN, M., AFTAB, W. & ZOU, R. 2021. Flexible phase change materials for thermal energy storage. Energy Storage Materials, 41, 321-342.

Poster Session-2: Poster Session

Time: Wednesday, 11/Jan/2023: 3:30pm - 5:00pm · *Location:* Exchange Hall and Exchange Lobby

P2-1 Hyaluronate-Based Hydrogels for Three-Dimensional Bioprinting

Hyun Seung Kim, Kuen Yong Lee
Hanyang University, Korea, Republic of (South Korea); leeky@hanyang.ac.kr

Three-dimensional (3D) bioprinting is a promising technique to fabricate complex biological structures with living cells. Hydrogels have been widely used as bioinks for 3D printing due to their structural similarity to the natural extracellular matrix. However, the shear force can damage the hydrogel structure when extruded through the nozzle during the printing process. Herein, hyaluronate (HA)-based double-network hydrogels were designed and prepared to have the self-healing ability and their potential use as bioinks was evaluated. Briefly, HA was partially oxidized with sodium periodate to prepare oxidized hyaluronate (oHA). Hydrazide-modified hyaluronate (hHA) was also synthesized by chemical conjugation of adipic acid dihydrazide (ADH) to the backbone of HA. The synthesis of oHA and hHA was confirmed by FT-IR spectroscopy and 1H NMR spectroscopy. Hydrogels were prepared by simply mixing solutions of oHA and hHA, cross-linked by charge interaction (physical cross-linking) and acylhydrazone bond formation (chemical cross-linking). Viscoelastic properties and mechanical properties of the gels were investigated using rotational rheometer and mechanical tester, respectively. The addition of free ADH enabled self-healing of the oHA/hHA hydrogels, which were useful to fabricate various 3D structures using an extrusion-based 3D printer without additional treatment after printing. Cell viability within the constructs was also evaluated and the printing process did not significantly affect their viability.

P2-2 Hydrothermally Synthesized LiNi0.8Co0.1Mn0.1O2 Cathode Material with Structure-Controlled Primary Particles

SooHong Lee, MinKeong Kim, DongIl Kim, HeeBin Jeong, John Hong
Kookmin University, Korea, Korea, Republic of (South Korea); dltnghdpp@kookmin.ac.kr

Lithium-ion batteries (LIBs) have been regarded as the dominant system in energy storage applications. As the large growth of electric vehicle (EV) market, new cathode material with a high energy density is required. Therefore, it is important to increase the energy-storage performance of cathode materials by using high nickel (Ni) contents. In this regard, Ni-rich layered oxide cathodes are a promising material to replace conventionally used LiCoO2 cathodes in terms of energy density and material cost. However, when the content of Ni is higher than 80%, there is a problem during Li intercalation that the sudden c-axis collapse occurs due to the phase transition process of Ni-rich layered oxide cathodes. In this work, we focused on controlling the structure of LiNi0.8Co0.1Mn0.1(NMC811) cathode primary particles by using a solvothermal/hydrothermal method. By introducing the different supersaturation states during the synthesis, the new structure of the primary particles was obtained. Especially, the morphology of the carbonate precursor was controlled by tunning the solvent, reaction temperature, and time parameters. Those new structures can improve the overall stability and energy-storage performance of the LiNi0.8Co0.1Mn0.1(NMC811) cathode.

P2-3 i/n a-Si:H/SiN stack for passivating antireflection of crystalline silicon

Shota Nunomura[1], Isao Sakata[1], Tatsuya Misawa[2], Naho Itagaki[3], Masaharu Shiratani[3]
[1]National Institute of Advanced Industrial Science and Technology, Japan; [2]Faculty of Science and Engineering, Saga University; [3]Graduate School of Information Science and Electrical Engineering, Kyushu University; s.nunomura@aist.go.jp

Passivating antireflection coating of (crystalline silicon) c-Si is experimentally studied by comparing three different structures of samples composed of (i) a single SiN layer, (ii) an i a-Si:H/SiN bilayer and (iii) an i/n a-Si:H/SiN trilayer. The passivation property is examined by the QSSPC minority carrier lifetime measurement, and optical and material properties are analyzed by various characterization methods of SE, FTIR, RBS, HFS and spectrophotometer. The passivation property is strongly improved by the i a-Si:H/SiN bilayer due to the H-mediated chemical passivation effect, compared with a single SiN layer. The passivation is further improved for the i/n a-Si:H/SiN trilayer, due to the field effect, induced by the fixed charges in the n a-Si:H layer. The optical and material analysis show that a SiN layer prepared at 250oC meets the requirement for the antireflection, i.e., n550nm = 2.0. Eventually, the passivating antireflection performance is obtained with the i/n a-Si:H/SiN trilayer as low as 250oC. For such a sample, the carrier lifetime is obtained to be of the order of ms and the reflection is < 2% at 550 nm.

The authors are grateful to K. Koga S. Nagaishi (Kyushu Univ.), A. Sato, and M. Lozac'h (AIST) for fruitful discussions. This work was supported by JSPS KAKENHI (Grant Number 18K03603 and 20H00142) and New Energy and Industrial Technology Development Organization (NEDO).

P2-4 Improvement of high temperature thermal insulation properties of magnesia (MgO) fine particles using surface fluorination

Shogo Matsuoka, Fumihiro Nishimura, Jae-Ho Kim, Susumu Yonezawa
University of Fukui, Japan; mi210406@g.u-fukui.ac.jp

MgO has been used as an insulating material for sheathed heaters due to its excellent insulation and thermal conductivity properties. However, it has been pointed out problems regarding the electric shock due to a sudden drop in insulation at temperatures above 600 °C. It may be caused to the decomposition of impurities (magnesium hydroxide and magnesium carbonate etc.) and/or the desorption of oxygen and so on. In this study, we attempted to improve the high temperature properties of magnesia by surface fluorination.

The surface of MgO particles (magnesium oxide, 0.2 μm, 99.9 %, Wako Pure Chemicals) was fluorinated using fluorine gas (99%). The change in physical properties due to fluorine treatment was confirmed by TG-DTA, XPS, and XRD, and the insulating property with increasing temperature was evaluated by superconducting resistance meter. Figure 1 indicates the results of electrical resistance of various MgO samples according to increasing temperature. Comparing with untreated MgO sample, the insulation of fluorinated MgO samples could be kept even at 1000 ℃. It may be that the MgF2 or MgOF layers coated on MgO can prevent the desorption of oxygen or surface purification of impurities as like Mg(OH)2 on MgO in F2 gas.

P2-5 Improvement of mechanical flexibility using completely amorphous B-doped In2O3 transparent conductive thin films

Shun Mori, Kotaro Watanabe, Kaito Murano, Shinya Aikawa

Kogakuin University, Japan; cm21053@ns.kogakuin.ac.jp

Room-temperature processable highly transparent and flexible conductive films are demanded for next-generation energy and information devices. However, a conventional ITO requires annealing treatment after deposition, which is the limit of room temperature processes. In addition, ITO deposited on a flexible substrate has some problems such as occurring cracks at the grain boundaries when it is deformed. To solve the issue, alternative materials, for example, carbon nanotubes and Ag nanowires have been considered but corrosiveness and complex coating processes are still remaining issues. Thus, we have focused on amorphous transparent conductive oxide films that can be deposited at room temperature. Indium oxide-based materials reduce the electron scattering probability and improve their carrier mobility by decreasing the ionic radius of the dopant. Trivalent B ion with VI coordination has very small ionic radius of 0.027 nm. We found that the mobility of B-doped In2O3 (IBO) was improved than that of non-doped In2O3 even deposited at room temperature. To utilize these features of IBO, we developed the IBO as flexible transparent electrode on a plastic substrate. In this study, we compare the change in the resistance of IBO and ITO deposited on PET substrate and discuss how to improve mechanical flexibility of brittle oxides.

P2-6 IR Transmittance Switching of VOx thin film on TiO2 Buffer Layer

Bunyod Allabergenov[1,3], Sanghun Yun[1], Soo-Keun Lee[2], Byeongdae Choi[1,4]

[1]Division of Electronics and Information System, Daegu Gyeongbuk Institute of Science and Technology (DGIST), Daegu, 42988, Republic of Korea; [2]Division of Energy Technology, Daegu Gyeongbuk Institute of Science and Technology (DGIST), Daegu, 42988, Republic of Korea; [3]Department of Transport Systems, Urgench State University (UrSU), Urgench, 220100, Uzbekistan; [4]Department of Interdisciplinary Engineering, Daegu Gyeongbuk Institute of Science and Technology (DGIST), Daegu, 42988, Republic of Korea; bunyod_kit@dgist.ac.kr

Vanadium dioxide (VO2) based thin film has attracted much attention due to its near-infra-red (NIR) sharp metal-insulator transition (MIT) concerning optoelectronic applications such as energy-saving smart windows and electro-optical thermochromic switching devices [1]. In addition, it has a low phase transition that occurs nearer to room temperature, at approximately 68 ℃, compared to those exhibited by other vanadium oxides such as VO, V2O3, and V2O5 [2]. In this study, we investigated TiO2 buffer layer effects on the electro-optical properties of VOx thin films deposited on glass substrates by a magnetron sputtering system. The VO2 and VO2/TiO2 thin films prepared at room temperature were annealed at the temperature range of 350 to 550 ℃ using a tube furnace under an oxygen atmosphere of 150 mTorr for 60 min to obtain crystallized structure. The samples were analyzed with 4-point probe resistivity, X-ray diffraction (XRD), X-ray photoelectron spectroscopy (XPS), UV-Vis-NIR spectrophotometer, and field emission electron transmission microscope (FE-TEM), respectively. The structural analysis of the pure film exhibited a mixed phase structure of VO2(B), V5O17, and V2O5 was organized. Employing TiO2 as a buffer layer improved the crystallization behavior, and the diffraction peaks associated with V5O17 and V2O5 phases were suppressed. The XRD patterns of the VO2/TiO2 film revealed the preferred orientation of (011) reflection corresponding to the single VO2 monoclinic phase. Compared to pure VO2 the infrared IR transmittance switching (ΔTIR) behavior in the 2000 nm wavelength range for VO2/TiO2 sample is enhanced from 3% to 35 % as shown in Figures 1(a) and 1(b).

Figure 1. The transmittance of VOx thin films annealed at 550 ℃ according to temperature.

(a) Pure VO2, (b) VO2/TiO2

This result means that the optoelectrical characteristics of the VO2 thin films such as ΔTIR can be easily adjusted using TiO2 as a buffer layer, which plays a huge role in the production of economical, energy-saving smart windows. Further, the detailed results on the structural, optical, and electrical properties of the films will be discussed.

Keywords: vanadium dioxide, thin film, phase transition, buffer layer, titanium dioxide

Acknowledgment

This work was supported by the Brain Pool Program of the National Research Foundation of Korea (NRF, Grant number: 2019H1D3A1A01102541) and the Basic Research Program of the DGIST(22-IT-10-01, 22-DPIC-09) funded by the Ministry of Science and ICT.

[1] ALLABERGENOV, B., YUN, S., CHO, H.-S., LYU, H.-K., & CHOI, B. ACS Appl. Electron. Mater. 3, 2021,1142-1150.

[2] MORIN, F. J.. Phys. Rev. Lett., 3(1), 1959, 34-36.

P2-7
Magnetic Resonance Tracking of Copper Ions Fixation on the Surface of Carboxylated Nanodiamonds and Their Location on the Surface

Vladimir Osipov[1], Ekaterina Osipova[2], Yasushi Ishiguro[3], Kazuyuki Takai[4]

[1]Ioffe Institute, St. Petersburg, Russian Federation; [2]Saint-Petersburg State Institute of Technology, St. Petersburg, Russian Federation; [3]Tokyo Denki University, Tokyo, Japan; [4]Hosei University, Tokyo, Japan; katyaossipova@mail.ru

5-nm detonation nanodiamonds (DND) with a carboxylated surface are easily modified by doubly charged copper ions. The main idea of the method is to use pairs of carboxyl groups in the composition of functional groups on the surface to fix doubly charged cations by ion exchange with protons of carboxyl groups. A diluted DND water suspension and a 0.3 wt.% solution of copper nitrate taken in a certain volume were mixed with vigorous stirring. Then the dry product was isolated. The presence of copper cations in the chelate complexes was confirmed by electron paramagnetic resonance (EPR) by observing signals from Cu2+ ions in the 3d9 state and by X-ray photoelectron spectroscopy [1]. The paper analyzes the parameters of the EPR signal depending on the concentration of copper ions on the surface of DND particles. EPR spectra of the Cu2+ DND particles were analyzed for three selected samples with the minimum (~1.1 wt.%), middle (~1.5 wt.%) and maximum (~2.0 wt.%) copper contents. The maximum concentration corresponds to ~46 copper atoms on the surface of a particle.

We found that only the EPR method is able to reliably detect the signal from Cu2+ ions, despite the strong overlap of the high-field part of the Cu2+ EPR signal (from the perpendicular component) with intensive g=2.0027 EPR signal from the spins of dangling bonds in the crystal cores of DND particles. Other methods give an approximate estimate of the total number of copper atoms in different charge states, including the neutral one. The estimated mean distances between the surface copper ions and the shallow/deeper paramagnetic defects in the interior of DND particles are 1.01 and 1.33 nm, respectively. The corresponded depths of occurrence of shallow and deeper paramagnetic defects in the DND are ~0.76 and ~1.08 nm, respectively. These distances were obtained from an analysis of the broadening of the EPR line (from intrinsic DND defects) due to the dipole-dipole interaction of the spins ½ of these defects with the spins ½ of copper ions. The obtained depth of the location of shallow paramagnetic centers is in good agreement with the estimates made by the nuclear magnetic resonance method in other groups.

[1] OSIPOV, V.YU., ROMANOV, N.M., SUVORKOVA, I.E., OSIPOVA, E.V., TSUJI, T., ISHIGURO, Y. & TAKAI, K. 2022. Magnetic Resonance Tracking of Copper Ion Fixation on the Surface of Carboxylated Nanodiamonds from Viewpoint of Changes in Carbon-Inherited Paramagnetism. Mendeleev Commun., 32, 1-4.

P2-8 Magneto-optic waveguides with Si guiding layer fabricated by supersonic free-jet PVD

Tsukasa Michino[1], Atsushi Yumoto[1], Hideki Yokoi[1,2]

[1]Graduate School of Engineering and Science, Shibaura Institute of Technology, JAPAN; [2]International Research Center for Green Electronics, SIT, JAPAN; yokoi@sic.shibaura-it.ac.jp

In optical communication systems, optical nonreciprocal devices are indispensable in protecting active photonic devices from unwanted reflected light. Magnetic garnet crystals are used to construct magneto-optic waveguides in the near infrared region. Optical isolators employing a nonreciprocal phase shift is attractive because they utilize one polarization mode so that no phase matching condition is needed. Large nonreciprocal phase shifts are obtained when magneto-optic waveguides have a core layer with high refractive index and a magnetic garnet cladding layer [1]. The magneto-optic waveguide is realized by deposition of magnetic garnet films on a silicon-on-insulator (SOI) waveguide. In this paper, the authors report on deposition of magnetic garnet films on a silicon substrate by supersonic free-jet PVD.

Yttrium iron garnet (YIG) films were deposited on a Si substrate by supersonic free-jet PVD. Refractive indices of the deposited YIG films were measured by spectroscopic ellipsometer. The nonreciprocal phase shift of the magneto-optic waveguide with the Ce:YIG/Si/SiO2 structure was calculated at a wavelength of 1.55 micron. It was found that the maximum nonreciprocal phase shift was obtained when the Si thickness was 0.20 micron.

[1] YOKOI, H., Calculation of nonreciprocal phase shift in magneto-optic waveguides with Ce:YIG layer. 2008. Opt. Matr., 31, 189-192.

P2-9
Measurement of fluctuation of electric field in Ar plasmas using a fine particle trapped with laser tweezers

Toma Sato[1], Sakyo Okunaga[1], Kunihiro Kamataki[1], Kentaro Tomita[2], Pan Yiming[1], Daisuke Yamashita[1], Takamasa Okumura[1], Naoto Yamashita[1], Naho Itagaki[1], Kazunori Koga[1,3], Masaharu Shiratani[1]

[1]Kyushu University, Japan; [2]Hokkaido University, Japan; [3]National Institute of Natural Sciences, Japan; t.sato@plasma.ed.kyushu-u.ac.jp

High-precision nanofabrication based on plasma processing has been one of the main technology drivers of modern information society. Development of highly sensitive diagnostic methods in process plasmas is imperative for understanding and controlling interactions between the materials and plasma. A diagnostic method using few dust particles in plasma is a possible solution of this problem. In this study, we measured the strength and fluctuation of electric field in Ar plasmas using laser tweezers.

A plasma reaction vessel with a quartz window on the top and a sapphire window on the bottom was used in the experiment, which was set up in an epi-illumination microscope. A perforated metal ground electrode was placed in the center of the vessel, and a ring-shaped electrode with an inner diameter of 15 mm and an outer diameter of 25 mm was placed on the bottom of the vessel. A high-frequency voltage of 13.56 MHz was applied between the electrodes to generate a plasma in the vessel. When an acrylic particle (diameter is 20μm) was introduced into the plasma, it was suspended near the plasma/sheath boundary. In this experiment, a single particle was trapped by the optical tweezers and moved horizontally with the laser until the particle is de-trapped. We measured the levitation positions and the position fluctuation of a fine particle trapped with laser tweezers by high-speed camera.

A fine particle trapped with lazer tweezers flucates minutely. We observed the position fluctuations for 5 seconds while varying the laser power. Time evolution of x-position of the fine particle have fluctuation components. When the laser power increases, the

standard deviation of particle position decreases. The magnitude of this standard deviation indicates the magnitude of position fluctuation. The force of the laser on the particle, which is obtained from an ray optical model, increases while increasing the laser power. It implies that the force of laser is related to the trapping one of the particles. We will discuss details at the conference.

P2-10 Measuring Stiffness of Ovarian Cancer Spheroids using AFM via a novel technique

Tavishi Dutt, Jimpi Langthasa, Prosenjit Sen, Ramray Bhat
INDIAN INSTITUTE OF SCIENCE, India; tavishidutt@iisc.ac.in

Ovarian cancer is the 7th most commonly occurring cancer in women, and 18th most commonly occurring cancer overall. The diagnosis of epithelial ovarian cancer is difficult in the early stages, due to limited screening tests. The peritoneal cavity of a patient with advanced ovarian cancer is observed to house multicellular clusters of disseminated cancer cells, commonly known as spheroids. These spheroids are metastatic to the organs of the abdomen. In addition to that, they are known to display chemo-resistance. These properties make them an interesting subject of research, because not much is known about their origin and how they metastasize.

Cells respond to their microenvironment by sensing mechanical triggers, and respond by changing their shape, or by exerting contractile forces to feel the bulk properties of their surrounding substratum (1)(2). Different cells react in distinct time-scales to substrates of varying stiffness. This spatial-temporal response in turn determines their functions, and the processes that they mediate.

Thus, mechanical properties, such as stiffness, can lend insight to the dynamics, and behaviour of cells in great detail. Since, response of one type of cell to the same immediate environment, may be different from another type, their stiffness can be used as a bio-marker to their invasion, metastatic potential, migration and progression (3)(4).

Mechanical properties of ovarian cancer cells have been reported in previous studies.

However, not much attention has been given to spheroids for the same. There are established

techniques to study biomechanics and measure the mechanical properties of cells and tissues. Of these, Atomic Force Microscopy (AFM), has gained popularity due to its applicability to a variety of cell populations, and because it allows an access to structural as well as mechanical information at nanometer resolution.

This work presents a new technique to measure stiffness of ovarian cancer clusters immobilized on an agar bed, using AFM. Previous studies have reported stiffness of monolayers of cells, which are well adhered to the substratum. However, when considering single / clusters of cells, in suspension, probing the cell surface using AFM is a challenge, due to their slippery nature. Molten noble agar, a biologically inert polymer, when solidifies, fixes the cells along with it. The bottom portion of the cell is embedded in this gel-bed. The cantilever probes the remaining part which is above, to measure the Force-distance (F-d) curves, which are in turn analyzed to calculate their stiffness.

P2-11 Mechanical property modification of “living” networks via PET-RAFT photopolymerization

Patrick Imrie[1,2], Jianyong Jin[1,2]
[1]The University of Auckland, New Zealand; [2]Dodd-Walls Centre for Quantum and Photonic Technologies, New Zealand;
pimr761@aucklanduni.ac.nz

In this work, we employed the PET-RAFT photopolymerization method to modify the mechanical properties of “living” networks in the post-production stage. We used a one-pot tactic to create “living” parent networks from company-bought constituents (N,N-dimethylacrylamide (DMAm) monomer and poly(ethylene glycol) diacrylate (PEGDA) 700 crosslinker) so that no synthesis was involved. Two different RAFT agents were used: asymmetric 2-(n-butyltrithiocarbonate) propionic acid (BTPA) and symmetric S,S-dibenzyl trithiocarbonate (DBTTC). These parent networks were then modified after initial polymerization with three new monomers (acrylamide (AAm), DMAm and methyl acrylate (MA)), which was achieved by restarting the PET-RAFT process. The Fourier transform infrared (FTIR) spectra of the resulting daughter networks confirmed the existence of photo-growth. The daughter networks were subjected to thermogravimetric analysis (TGA), where they displayed thermal stability dependent on both choice of monomer and parent network RAFT agent symmetry. Finally, the daughter networks were mechanically tested by compression, where it was revealed that asymmetric daughter networks were stiffer and symmetric daughter networks were tougher than their respective parent networks. These effects were explained by the pore-filling and pore-expansion models of the microscopic “living” polymer matrices. It is hoped this research will further the development of cheap and easy-to-use sustainable smart materials.

P2-12 Mesoporous Titanium Dioxide/Polyaniline Composite as a Quasi-Solid-State Energy Storage Layer for Photorechargeable Batteries

Shunsuke Maeda[1], Teruaki Nomiyama[1], Yuji Horie[1], Chitose Mihara[2]
[1]Kagoshima University, Japan; [2]Joyson Safety Systems Japan K.K.; k4988960@kadai.jp

A photorechargeable battery, a storage battery charged by sunlight, has been studied.1,2 One of the promising structures to realize photocharge/discharge is a bilayer of photovoltaic and storage layers. In this study, mesoporous TiO2/polyaniline (mpTP) composite2 infiltrating non-aqueous and quasi-solid-state electrolyte, which is favorable for suppressing degradation of the photovoltaic layer and easy fabrication, is applied for the storage layer.

P2-13 Microstructures and dielectric properties of Nb-doped Sr0.9Ca0.1TiO3

Kuei Chih Feng[1], Jhih-Qain Cai[1], Pin-Yi Chen[1], Cheng-Sao Chen[2], Chi-Shun Tu[3]

[1]Ming Chi University of Technology, Taiwan; [2]Ming Chi University of Technology, Taiwan; [3]Ming Chi University of Technology, Taiwan; kwechin@mail.mcut.edu.tw

With increasing application in electronics and automobile industry, demand for passive components is on the rise. This project is aimed to develop Ultra-high dielectric constant ceramic materials (εr>200,000). Literature survey shows that ceramic materials produced from the high temperature sintering of Nb2O5 doped in Sr0.9Ca0.1TiO3 (SCTO) under the oxygen deficit environment are with ultra-high dielectric constant and less likely to be subject to the temperature and frequency, yet relative mechanisms remain incomplete.

The research team has tried to dope SCTO with different ratio of Nb2O5 and to have them burnt under the oxygen deficit environment to conduct study on dielectric properties and microstructure. Firstly, XRD analysis is conducted on synthetic SCTO ceramic materials, of which the microstructure is cubic. Then, small amount of Nb2O5 is added for high temperature sintering for comparison study on air atmosphere and N2-H2 atmosphere. The dielectric constant shows that when 0-2.5wt% Nb2O5 is doped, εr remains at the level of 200~400 under the high temperature sintering in air atmosphere, while εr surges from 300 to 370,000 in N2-H2 atmosphere (with 1.45mol% Nb2O5 doped) and insulation resistance changes from 1012 to 105.

In addition, XRD analysis shows there is no second phase found in different atmospheres. The peak of sample in N2-H2 atmosphere moves to high angle after low angels, showing the entry position of Nb2O5 into TiO2. Besides, Raman spectra analysis shows that with the doping of Nb2O5, oxygen bond becomes weaker. Further synchrotron X-ray absorption spectra observes Ti-L edge of different Nb2O5 ratios. The absorption spectra of Ti have no major changes, while Tg/eg(Ratio) of O-K edge drops from 1.12 to 1.01. This demonstrates that oxygen cannot be bonded with Ti with weaker oxygen bonding. The results of Raman spectra and synchrotron X-ray absorption spectra shows that the high temperature sintering in N2-H2 atmosphere of Nb2O5 doped in SCTO will create mass amount of oxygen vacancy. Following TEM test shows that with the ratio of STN-1.45wt%, there is a large amount of dislocation loop.

In conclusion, the study shows that the sintering of Nb2O5 doped in SCTO in oxygen deficit environment will not only create donor behavior which increases free electron and decreases IR because Nb5+ enters Ti4+, but also creates large amount of oxygen vacancy. The defect dipole increases dielectric constant. Therefore, this material has development potentials to be applied in passive components.

P2-14 N2 concentration dependence of electrical conduction in partially nitrided SnOx thin-films deposited by reactive RF magnetron sputtering

Takuma Kawaguchi, Kotaro Watanabe, Shinya Aikawa

Kogakuin University, Japan; c418031@ns.kogakuin.ac.jp

Recently, all oxide CMOS and solar cell applications have been developed because it has unique advantages, for example low-temperature processability, low-power consumption and optical transparency [1]. Typical p-type oxide TFT shows less electrical properties compared to n-type TFT, such as field effect mobility and on/off current ratio [1-3]. Thus, development of superior p-type oxide TFTs similar to n-type TFTs is required. Generally, oxide semiconductors include large amount of oxygen vacancies (VO). Because VO generates electrons, sputtering conditions for obtaining p-type behavior is very difficult, thus far [4]. To solve the issue, we have focused on nitrogen (N) doping as a VO passivation. Since $N3^-$ has almost same ionic radius and electronegativity as $O2^-$, it can be replaced into O-site in the SnO2 matrix. N substitution leads to decrease the density of VO; thus, improvement of hole mobility is expected [5-7]. In this study, we investigate sputtering conditions in N2 ambient to fabricate p-type N-doped SnOx (SnON) thin films and clarify their electrical properties, crystal structure and binding states.

SnOx thin films was deposited on a Si/SiO2 substrate using an RF magnetron sputtering in Ar/N2 mixed gas atmosphere. The substrate temperature during deposition was set at 300 °C. A ceramic SnO2 target (purity: 99.999%) was used as the starting material. The RF power and the deposition pressure were fixed at 100 W and 0.12 Pa, respectively. The N2 ratio was varied between 25 and 75% for the deposition. The electrical properties of the thin films were measured at room temperature using a Hall-effect measurement system. The crystallographic structure was determined by an X-ray diffractometer (XRD). The composition analysis and binding states of the thin film were characterized by X-ray photoelectron spectroscopy (XPS).

Figure 1 shows the relationship between N2 concentration and the electrical properties (sheet resistance, carrier density, and mobility) of the fabricated SnON films deposited at N2 ratio of 25 - 75%. In 25 to 50% of N2 concentrations, the films were exhibited n-type conductivity. This is because there still have many VO in the SnO2 matrix. On the other hand, the films deposited at 70~75% showed p-type behavior and also the carrier density was found to decrease. This is due to change in the majority carriers to holes with increasing the N concentration in the SnO2 matrix. We analyzed XPS results that N substitution into O-site was occurred and confirmed that the decrease in VO concentration correlates increase in the N concentration during deposition. This revealed that N substitution by reactive sputtering in N2 ambient is effective way to widen the deposition condition of p-type SnOx-based films. Other characterizations such as XRD including XPS spectrum will be discussed.

P2-15 Nanostructured biohybrid composed of recombinant protein/DNA/Au nanoparticle/electrically releasable complex for spatiotemporal control of neuronal differentiation

Joungpyo Lim, Jinho Yoon, Minkyu Shin, Jeong-Woo Choi

Sogang University, Korea, Republic of (South Korea); jwchoi@sogang.ac.kr

Spatiotemporal control of cell differentiation is important issue in biomedical fields such as stem cell therapy and regenerative medicine, as it enables the generation of heterogeneous tissue structures similar to those of their native counterparts. For this reason, the simultaneous control of both spatial and temporal cell differentiation poses important challenges. However, no previous

studies have achieved this goal. Here, we developed a nanostructured biohybrid composed of recombinant proteins, DNA, Au nanoparticles, and electrically releasable complex (ERC) conjugated with retinoic acid (RA) to spatiotemporally control SH-SY5Y cell differentiation. RA was released from the nanostructured biohybrid only when the ERC was electrically stimulated, thus implementing the temporal control of SH-SY5Y cell differentiation. Furthermore, spatiotemporal differentiation of SH-SY5Y cell was demonstrated by introducing a patterned Au substrate that allows adjusting the region where the nanostructured biohybrid is immobilized. In conclusion, the proposed nanostructured biohybrid-mediated differentiation method provides a promising strategy for spatiotemporal cell differentiation control with applications in regenerative medicine and cell therapy.

Acknowledgments: This research was supported by the National Research Foundation of Korea (NRF) grant funded by the Korea government (MSIT) (No.2019R1A2C3002300) and Samsung Research Center Funding for Future Research.

P2-16 Non-Covalently Functionalized Two-Dimensional Nanomaterials Mediated by Self-Assembled Supramolecular Polymer

Chih-Chia Cheng

Graduate Institute of Applied Science and Technology, National Taiwan University of Science and Technology, Taipei 10607, Taiwan; ccheng@mail.ntust.edu.tw

Programmed exfoliation of highly crystalline molybdenum disulfide (MoS2) into water-dispersible exfoliated nanosheets with well-tunable structural characteristics was successfully developed using an environmentally benign solvent (water) and the water-soluble cytosine-functionalized supramolecular polymer (Cy-PPG). Herein, we show MoS2 can be directly dispersed in aqueous solution using ultrasound to obtain dozen-layered MoS2 nanosheets; this process is termed first exfoliation. When Cy-PPG is subsequently incorporated into the MoS2 solution (i.e., second exfoliation), ordered hierarchical lamellar nanostructures form through self-assembly of Cy-PPG on the surface of the metallic 1T and semiconducting 2H phases of the exfoliated MoS2 nanosheets due to the high-affinity interaction between Cy-PPG and MoS2. Furthermore, after second exfoliation, the resulting MoS2/Cy-PPG composites exhibit long-term dispersion stability in water. Broad, tunable MoS2 exfoliation can be achieved by systematically adjusting the content of Cy-PPG within the composites to obtain the desired structural, physical, conductive performance; these exceedingly rare features offered by programmed exfoliation hold great potential for achievement of high-quality, custom-made MoS2 nanomaterials. Thus, this newly developed system offers a myriad of potential uses for fabrication of fully aqueous solution-processed MoS2-based thin films for optoelectronic and biomedical applications.

P2-17 Numerical Study on the Phase Change Material Applied Flow in a Microchannel

Safi Ahmed Memon, Cheol Woo Park

Kyungpook National University, Korea, Republic of (South Korea); safibta@gmail.com

As the electronic devices being micro-structures, the thermal management and cooling performance have been very important issues in point of energy enhancement. Currently, the phase change material (PCM) applied flow has been suggested as an effective solution for micro-scale device cooling. In this study, a phase change material heat sink has been investigated numerically, analyzing the thermal performance feature in a microchannel.

P2-18 Optoelectronic properties of back-gated SnSe2/WSe2 van der Waals heterostructure

PIL JU KO[1], Abdelkader Abderrahmane[1], Pan-Gum Jung[2], Changlim Woo[1]

[1]Chosun University, Korea, Republic of (South Korea); [2]Green Energy Institute, Korea, Republic of (South Korea); pjko@chosun.ac.kr

Transition metal dichalcogenides (TMDCs) have attracted tremendous interest for many applications, such as Memories and Logic Circuits, photocatalytic water splitting devices, field-effect transistors, tunneling transistors, bipolar junction transistors, ferroelectric field-effect transistor (FE) transistors, and ferromagnetic transistors, and sensors. In this research, we made novel low power consumption gate tunable WSe2/SnSe2 van der Waals tunnel field effect transistor. For the fabrication process, we used black phosphorous as gate contact and hexagonal boron nitride as the insulator layer for between the gate and the channel. Black Phosphorus was chosen as gate contact because it shows promising application for low-power consumption electronic device [1]. We carried out morphological characterizations, as well as the electrical and optoelectronic properties for the gated WSe2/SnSe2 tunnel field effect transistor. Figure 1 represents scanning electron microscopy and atomic force microscopy images, and schematic of the fabricated device.

The device showed p-type behavior with good dependence of the gate voltage, and trend toward negative differential resistance (NDR) originated from the band-to-band tunneling. We succeeded to control the tunneling effect by changing the applied gate voltage and valley voltage shift was observed. The maximum photoresponsivity of the device was around 11 mAW-1. Results presented in this study promote the fabrication of tunneling effect transistors based only on two-dimensional materials.

Figure 2. (a) SEM image and (b) AFM image, of the BP gated WSe2/SnSe2 van der Waals heterostructures, and (c) schematic of the fabricated WSe2/SnSe2 van der Waals heterostructures.

Keywords: transition metal dichalcogenides (TMDCs), black-phosphorous, hexagonal BN (h-BN), tungsten diselenide (WSe2), tin diselenide (SnSe2)

Funding:This work was supported by Brain Pool Program through the National Research Foundation of Korea (NRF) funded by the Ministry of Science and ICT (NRF-2019H1D3A1A01102658). This study was supported by research fund from Chosun University, 2022.

This work was supported by the Gwangju.Jeonnam local EnergyCluster Manpower training of the Korea Insitute of Energy Technology Evaluation and Planning(KETEP) grant funded by the Korea government Ministry of Knowledge Economy (No. 20214000000560)

This work was supported by the Promotion of Innovative Businesses for Regulation-Free Special Zones funded by the Ministry of SMEs and Startups(MSS, Korea) (P0020888)

[1] ABDERRAHMANE, ABDELKADER, CHANGLIM WOO, PIL JU KO. (2021) Black Phosphorus/Molybdenum Diselenide Heterojunction-Based Photodetector. Journal of Electronic Materials, 50(10), pp.5713-5720. DOI: 10.1007/s11664-021-09097-y.

P2-19
Perovskite-Type LaSrCoFeO3 Nano-Fibrous Web Interlayer for High-Performance Lithium-Sulfur Batteries

Ha Cheol Ju[1], Dong Jun Lee[2], Liu Ying[2], Jou-Hyeon Ahn[1,2]

[1]Department of Materials Engineering and Convergence Technology, Gyeongsang National University, 501 Jinju-daero, Jinju 52828, Republic of Korea; [2]Department of Chemical Engineering, Gyeongsang National University, 501 Jinju-daero, Jinju 52828, Republic of Korea.; cjfl0118@naver.com

Lithium sulfur (Li-S) batteries have received much attention as next generation power sources. Elemental sulfur is a promising cathode material that possesses not only a high theoretical capacity (1675 mAh g-1) and high energy density (2600 Wh kg-1) but also the advantages of low cost and environmental friendliness. However, the issues that arise from the insulating nature of sulfur, dissolved lithium polysulfide intermediates, and volume expansion of the electrodes during the lithiation process can lead to low utilization of the active material, severe capacity fading, and safety hazards. In this study, a novel interlayer was constructed by designing LaSrCoFeO3 perovskite nano-fibrous web for advanced Li-S batteries, which can enable to effectively immobilize the soluble polysulfides and further accelerate the reaction kinetics. Perovskite-type oxides can tolerate an appreciably high concentration of anion vacancy in their crystal structures, which can provide a large number of active sites to anchoring polysulfides, and further enhance the electrochemical performance of Li-S batteries. Therefore, Li-S batteries with the perovskite-type LaSrCoFeO3 interlayer not only can improve the specific capacity but also can guide an excellent rate capability for Li-S batteries.

P2-20
pH Responsive Polymer Dots Based Strain-Pressure Sensitive Hydrogel Sensor for Cancer Detection

Kaustuv Roy[1], Tae Min Kim[2], Sung Young Park[1,2]

[1]Department of IT and Energy Convergence (BK21 FOUR), Korea National University of Transportation, Chungju, 27469, Republic of Korea; [2]Department of Chemical and Biological Engineering, Korea National University of Transportation, Chungju, 27469, Republic of Korea; kaustuv9323@gmail.com

Quick and accurate cancer screening tests are essential for determining appropriate treatment and preventing advanced stage cancers. However, current detection methods like magnetic resonance imaging (MRI), computed tomography (CT), etc., suffer from limitations like radiation exposure and complicated handling methods which limit their use in the event of prompt cancer detection. Herein, a wireless pH responsive polymer dot (PD) based hydrogel (P-Hydrogel) sensor was designed for the electrochemical distinction of cancer and normal condition in-vitro and in-vivo. The differential extracellular pH in the normal and cancer condition is the main impetus behind the working of the strain and pressure sensitive electrochemical sensor. The boronate ester in the P-Hydrogel undergoes cleavage in the cancer condition which disrupts the crosslinking between the pH responsive PDs and the non-conducting polymer (NCP) which causes an increase in the conductivity of the P-Hydrogel sensor. This increase in conductivity arising due to an increase in the ionic conductivity and change in charge transfer causing a differentiated response when applied with a strain and pressure in cancer and normal condition as highlighted by the in-vitro studies using HeLa and PC-3 as the cancer cells and MDCK, CHO-K1 as the normal cells. This phenomenon is highlighted by the 2-fold increase in the ΔR/R0 value under applied strain and pressure (125% and 56% for HeLa; 133% and 63% for PC-3) when compared to MDCK (70% and 33%, respectively) and CHO-K1-treated P-Hydrogel (70% and 34%, respectively). Furthermore, in-vivo studies in tumor-bearing mice revealed that the implanted P-Hydrogel performed exceptionally well in detecting tumor in an in-situ and ex-situ setting, with a more sensitive response to tumor than to normal tissue. The P-Hydrogel was then attached to a wireless sensing system that provided real-time conductivity and strain-pressure responses via a smartphone to make the detection process much easier. Therefore, this cancer environment specific strain-pressure responsive P-Hydrogel sensor provides a simple method for sensitive and selective cancer detection and holds great promise for its use in point-of-care diagnostics.

P2-21
pH-Responsive Disulfide Core-Crosslinked Poly Carbon Dots-PTX Loaded for Tumor Targeting and Drug Delivery

A Hyun Kim[1], Seul Gi Kim[2], Kaustuv Roy[3], Ha Yeon Jo[2], Sung Young Park[2,3]

[1]Department of Polymer Science & Engineering, Korea National University of Transportation, Korea, Republic of (South Korea); [2]Department of Chemical and Biological Engineering, Korea National University of Transportation, Korea, Republic of (South Korea); [3]Department of IT and Energy Convergence (BK21 FOUR), Korea National University of Transportation, Korea, Republic of (South Korea); dkgusaks@gmail.com

Targeted drug distribution for cancer therapeutic performance based on systems has been investigated in studies. However, due to limitations of current drug delivery systems with lack of high dosage release, low ability in realizing tumor sites, it is therefore an urge to develop a desired system with high sensitivity and selectivity for tumor detection which facilitates drug transfer effectively to targeted areas. Herein, a pH/redox responsive fluorescent ON/OFF system based on disulfide core-crosslinked poly carbon dots (PCD) encapsulated with fluorescent dye for cancer targeting was fabricated and characterized. PTX was then constituted into dye-conjugated PCD by the interaction of the aromatic group of PTX and sp2 group of dye-conjugated PCD to form PTX loaded matrix that demonstrated dual functions in cancer diagnosis and therapeutic selectivity. It was expected that high concentration of GSH in tumors (at least four time as high as GSH in normal cells) amplified the cascade release of loaded PTX by breaking the disulfide

bonds of the system, leading to the efficient cancer therapy. Simultaneously, due to the acidic microenvironment in tumors, the boronate ester bonds of the nano particle were disintegrated resulting in the discharge of the dye conjugated in the system to make the fluorescence recover again. No significant increase exhibited in the fluorescent intensity of PTX loaded matrix and PTX cascaded under the physiological environment with pH 7 even after GSH treatment demonstrated the stability of the quenching behavior and drug leakage prevention of the system. This system offered a promising versatile model for cancer diagnosis and treatment relied on the interaction of pH/redox responsive loaded PTX into dye-conjugated PCD drug delivery system with pH and GSH level in microenvironment which enabled to distinguish between normal cells and cancer cells by bioimaging ability as well as deliver drug to targeted tumor sites.

P2-22 Pharmaceutical cocrystal formation using lipid media in supercritical CO2

Yuna Tatsumi, Yasuhiko Orita, Yusuke Shimoyama

Tokyo Institute of Technology, Japan; scccss2011@gmail.com

Pharmaceutical cocrystal has been investigated for increasing the dissolution rate and amounts of pharmaceuticals in human body. The cocrystal is composed of the active pharmaceutical ingredient (API) molecule and coformer molecule combined by non-ionic bonding, such as hydrogen bonding. The dissolution of API cocrystal in the body leads to the rapid increase of API concentration and then the large decrease of that. The cocrystal of API and coformer is need to form and design as achieving a sustainable release of API. There is also a problem of using the large amounts of organic solvents on the cocrystal formation processes. In this work, a lipid media in supercritical CO¬2 is applied for the API cocrystal formation toward the enhancement of cocrystallization and development of the cocrystal formation process without a toxic organic solvent.

Theophylline and nicotinamide were used as API and coformer for its cocrystal formation. After the cocrystal formation, supercritical CO2 extraction was applied for removing the linoleic acid from the cocrystal of theophylline and nicotinamide. The cocrystal formed lipid media in supercritical CO2 were characterized by Particle X-ray diffraction (PXRD) method and the morphologies from an optical microscope. The results of PXRD give that lipid-media in supercritical CO2 promote the formation of cocrystal for theophylline and nicotinamide compared with those formed in pure CO2. The amorphrization degree of the cocrystal formed in lipid media in supercritical CO2 from XRD patterns decreases by increasing the time of supercritical CO2 extraction after the cocrystal formation. This means the amount of linoleic acid in the theophylline / nicotinamide cocrystal are reduced by the supercritical CO2 extraction. The dissolution of theophylline from its cocrystal would be controlled by the amount of linoleic acid in the cocrystal. It is found that linoleic acid covers the theophylline / nicotinamide cocrystal formed in lipid media without supercritical CO2 extraction. The morphologies of cocrystal formed with supercritical CO2 extraction provides the results of removing linoleic acid from the theophylline / nicotinamide cocrystal by supercritical CO2 extraction.

P2-23 Phase engineering of heteroepitaxially grown α-Ga2O3 solar blind photodetector using mist chemical vapor deposition

Joonhui Park, Youseung Rim

Sejong University, Korea, Republic of (South Korea); julia980406@gmail.com

Due to its nature wide bandgap (4.4~5.3eV), gallium oxide has attracted attention as a next-generation power semiconductor material than conventional wide bandgap material such as SiC and GaN [1]. Gallium oxide has five phases (α, β, γ, δ, and ε) having different energy band gaps and crystal structures, and it is applied according to various uses of solar blind photodetector [2]. However, existing studies have been conducted on Ga2O3 photodetector with only one phase.

In this study, different phases of high crystalline Ga2O3 was hetero-epitaxially grown on sapphire substrate at 400-900°C range of growth temperature using low cost, non-vacuum and non-toxic mist chemical vapor deposition (MIST-CVD). At less than 500°C (especially at 400°C) single crystalline α-Ga2O3 was grown on a sapphire substrate, and in the 500-800°C range, α, β, and ε phases were combined in the form of polycrystalline structures. Above 800 degrees, preferred orientation of β-Ga2O3 phase was investigated,

We fabricated an α-Ga2O3 interdigitated solar-blind photodetectors (PDs) by depositing Ti/Au as an electrode. To improve the optoelectronic device properties, doping control for α-Ga2O3 was performed. The responsivity and detectivity under ultraviolet C(UVC) wavelength and dark state of Sn-doped PDs were almost increased by one orders of magnitude.

As a result, we successfully controlled the phase of Ga2O3 using MIST-CVD and fabricated Ga2O3 photodetectors for various phases to demonstrate structural, optical, and electrical properties.

Reference

[1] D. Shinohara, S. Fujita, Heteroepitaxy of corundum-structured α -Ga2O3 thin films on α -Al2O3 substrates by ultrasonic mist chemical vapor deposition, Jpn. J. Appl. Phys. 47 (2008) 7311.

[2] Zhao B, Wang F, Chen H, et al. Solar-blind avalanche photodetector based on single ZnO–Ga2O3 core-shell microwire. Nano Lett, 2015, 15(6), 3988

Acknowledgment

This work was supported by the National Research Foundation of Korea (NRF) grant funded by the Korea government (MSIT) (No. 2020R1A2C1013693), Korea Institute for Advancement of Technology (KIAT) grant funded by By the Ministry of Trade, Industry & Energy (MOTIE, Korea) (P0012451, The Competency Development Program for Industry Specialist) and the Technology Innovation Program - (20016102, Development of 1.2kV Gallium oxide power semiconductor devices technology) funded by MOTIE.

P2-24 Polydopamine-Coating Porous Carbon Fiber as Interlayer for Lithium-Sulfur Batteries

Dong Jun Lee[1], Ying Liu[1], Ha Cheol Ju[2], Jou-Hyeon Ahn[1,2]

[1]Department of Chemical Engineering, Gyeongsang National University, Republic of Korea; [2]Department of Materials Engineering and Convergence Technology, Gyeongsang National University, Republic of Korea; donjun0625@gnu.ac.kr

Lithium sulfur (Li-S) batteries will open a new era for energy storage due to their high theoretical capacity of 1675 mAh g-1 and high energy density of 2600 Wh kg-1, which is six-fold specific energy compared with conventional lithium-ion batteries. In addition, Li-S batteries also have the advantages of abundant sulfur in nature and environmental friendliness. However, a series of problems are hindering progress of commercialization of Li-S batteries, such as the poor electrical conductivity of elemental sulfur, the soluble lithium polysulfides and huge volumetric expansion. In this work, polydopamine-coating porous carbon fibers as an interlayer for advanced Li-S batteries have been designed, which takes into account the advantages of physical structure and chemical adsorption. The porous structure not only can effectively confine the dissolution of polysulfides, but also provide enough space for the volume expansion. Polydopamine coating not only can improve the wettability and accessibility of electrolyte, but also strengthen the chemical interaction between polysulfides and carbon. Therefore, polydopamine-coating porous carbon fibers composite is expected to be a superior interlayer material for improving the electrochemical performance of lithium sulfur batteries.

P2-25
Preparation and characterization of Al-doped zinc oxide thin films by mixed powder targets with different states

Tamiko Ohshima[1,3], Yusuke Hibino[1], Takeshi Ihara[1], Yoshihito Yagyu[1], Takahiko Satake[1,2], Hiroharu Kawasaki[1], Naho Itagaki[3], Kazunori Koga[3], Masaharu Shiratani[3]

[1]National Institute of Technology, Sasebo College, Japan; [2]Sojo University, Japan; [3]Kyusyu University, Japan; ohshima@sasebo.ac.jp

In the conventional sputtering method, solid targets are generally used. Solid targets are mainly fabricated using the sintering method, but it is difficult to fabricate solid targets for materials with low melting points. It is also time-consuming and expensive to fabricate solid targets of multi-element composites. In this study, we have used powder as the target in the sputtering method. The use of powder targets makes it possible to fabricate thin films of low-melting point materials, and also makes it possible to fabricate multi-element composite material thin films inexpensively and easily. However, there are few reports on the fabrication of thin films by sputtering method using powder targets [1]. This work fabricates Al doped zinc oxide (AZO) thin films, that is an attractive candidate for transparent conducting oxides (TCOs) instead of indium tin oxide (ITO), by using mixed powders of zinc oxide (ZnO) and aluminum oxide (Al_2O_3). We have prepared four kinds of powder targets (1) untreated, (2) dried at 150 °C, and pressed at (3)15 MPa and (4) 230 MPa. AZO thin films have been prepared using four kinds of powder targets and the structural, electrical and optical properties of the deposited films were investigated. The data obtained from this experiment will clarify the relationship between the state of the powder and the film properties, and will provide knowledge the film deposition process of powder sputtering.

P2-26
Preparation of hierarchical recycled-carbon fiber/aramid nanofiber composites using centrifugal spinning

Jung Eon Lee, Jung Jae Hoon, Jae Min Park, Tae Young Kim, Jeong Hyun Yeum

Kyungpook national university, Korea, Republic of (South Korea); dlwjddjs2@gmail.com

Carbon fiber reinforced plastic is a composite material manufactured using carbon fibers. It is a type of fiber-reinforced plastic. Also, it is lightweight and has high durability and mechanical properties. As one of the new materials attracting the most attention in improving fuel efficiency through weight reduction of transport aircraft such as airplanes and automobiles, the field of use is gradually expanding. Recently, for environmental and economic reasons, the problem of waste treatment related to carbon fiber products has become a big issue, and various methods for recycling carbon fiber have been announced. Centrifugal spinning is a new practice that employs centrifugal forces to shape nano- and microfibers both from a solution and a melt. Compare to electrospinning, is has lot of advantages such as easy orientation control, material selection, and remarkable production speed. When aramid nanofibers are used as reinforcing materials, the physical properties of composite materials such as tensile strength and impact strength can be improved. Multiscale composite materials are prepared by centrifugal spinning of polymer nanocomposites filled aramid nanofiber on the top of the nonwoven fabricated by recycled carbon fibers. In this study, mechanical properties of prepared composite materials were analyzed. This research was supported by Basic Science Research Program through the National Research Foundation of Korea (NRF) funded by the Ministry of Education (2020R1I1A3075002).

P2-27 Preparation of syndiotactic-poly(vinyl alcohol) nanofiber using heterogeneous saponification

Jung Eon Lee, Jung Jae Hoon, Jae Min Park, Tae Young Kim, Jeong Hyun Yeum

Kyungpook national university, Korea, Republic of (South Korea); dlwjddjs2@gmail.com

Poly(vinyl alcohol) (PVA) has excellent biocompatibility, chemical resistance, thermal stability, and physical properties, so it is a material that has been actively researched in cosmetics and medical fields. PVA is classified into three types, isotactic, atactic, and syndiotactic, according to the stereoregularity of its hydroxyl groups. The syndiotactic PVA with the highest syndiotactic diad content was obtained using VPi, owing to the strong steric effects of the tertbutyl group. Nanofibers have been the subject of vigorous experimentation because they exhibit distinctive characteristics such as a large surface-area-to-volume ratio, flexible surface functionalities, and superior mechanical properties. Representative methods of manufacturing nanofibers include electrospinning and centrifugal spinning. Centrifugal spinning is a method of manufacturing nanofiber through a jet formation process by centrifugal force, and it is possible to control the shape of nanofibers by adjusting process variables such as rotational speed, tip-collector disctance, and spinning solution viscosity. It has been operated in both melt and solution state fabrication of a wide range of polymeric, composites, and inorganic fibers. In this study, poly(vinyl acetate-co-vinyl pivalate) nanofibers were prepared by electrospinning and centrifugal spinning, and then converted into a syndiotactic PVA nanofibers by a heterogeneous

saponification of poly(VAc-co-VPi). This research was supported by Basic Science Research Program through the National Research Foundation of Korea (NRF) funded by the Ministry of Education (2020R1I1A3075002).

P2-28
Rabies Virus Glycoprotein-Mediated T Cell Infiltration to Brain Tumor By Magnetoelectric Gold Yarnballs

Shang-Hsiu Hu

National Tsing Hua University, Taiwan; shhu@mx.nthu.edu.tw

T lymphocyte infiltration with immunotherapy potentially suppresses most devastating brain tumors. However, local immune privilege and tumor heterogeneity usually limit the penetration of immune cells and therapeutic agents into brain tumors, leading to tumor recurrence after treatment. Here, a rabies virus glycoprotein (RVG)-camouflaged gold yarnball (RVG@GY) that can boost the targeting efficiency at brain tumor via dual hierarchy- and RVG- mediated spinal cord transportation, facilitating to perish tumor heterogeneity for T cell infiltration, is developed. Upon a magnetoelectric irradiation, the electron currents generated on the GYs activates the electrolytic penetration of palbociclib-loaded dendrimer (Den[Pb]) deep into tumors. In addition, the high-density GYs at brain tumor also induces the disruption of cell-cell interactions and T cell infiltration. The integration of the electrolytic effects and T cell infiltration promoted by drug loaded RVG@GYs deep in the brain tumor elicits sufficient T cell numbers and effectively prolongs the survival rate of mice with orthotopic brain tumors.

P2-29
Reactive oxygen species-sensitive nanoparticles for tumor-specific delivery of photosensitizer and photodynamic treatment of oral carcinoma cells

Chang-Young Kim[1], Seong-Won Yang[2], Young-IL Jeong[1], Byung-Hoon Kim[1]

[1]Department of Dental Materials, Chosun University College of Dentistry, Republic of Korea; [2]Department of Ophthalmology, Chosun University College of Medicine, Gwangju 61452, Korea; kco5055@naver.com

Photodynamic therapy (PDT) using photosensitizers has been extensively investigated for cancer treatment because photosensitizers generate reactive oxygen species (ROS) under light irradiation [1]. We synthesized phenyl boronic acid pinacol ester (PBAP)-conjugated chitosan using thioketal group (ChitotkPBAP) for ROS-sensitive delivery of chlorin e6 (Ce6) against cancer. For synthesis of ChitotkPBAP copolymer, PBAP was conjugated with one of carboxyl group of thioketal dicarboxylic acid (HOOC-tk-COOH) and then remained carboxylic acid was conjugated again with amine group of chitosan to make ChitotkPBAP. YD38 human oral cancer cells were used to evaluate PDT efficacy of nanoparticles. Ce6-incorporated ChitotkPBAP (Ce6-ChitotkPBAB) nanoparticles has spherical morphology and small particle sizes less than 200 nm. Ce6-ChitotkPBAP nanoparticles showed ROS-sensitive release behavior of Ce6. Ce6-ChitoPBAP NP resulted in increased Ce6 uptake ratio and ROS production in YD38 cells compared to free Ce6. Ce6-ChitotkPBAP nanoparticles efficiently inhibited the viability of YD38 cells under light irradiation, i.e. Ce6-ChitotkPBAP nanoparticles suppressed viability of cancer cells less than 30 % at 2 μg/ml Ce6 concentration while free Ce6 treatment resulted in higher than 50 %. Ce6-ChitotkPBAP nanoparticles released Ce6 with ROS-sensitive manner through disintegration of nanoparticles in the presence of hydrogen peroxide.

Keywords: Photodynamic therapy, chlorin e6, nanophotosensitizer, chitosan, oral cancer cells

Acknowledgement: This study was supported by the National Research Foundation of Korea (NRF) grant funded by the Korea government (MSIT) (No. 2020R1A2C1102850).

[1] SAINI, R., LEE, N.V., LIU, K.Y., POH, C.F. 2016. Prospects in the Application of Photodynamic Therapy in Oral Cancer and Premalignant Lesions. Cancers (Basel). 8, 83.

P2-30
Scanning tunneling spectroscopy and break junction spectroscopy on the impurity transition-metal doped iron 11 superconductors

Takeshi Saito[1], Hironori Ohtubo[1], Akira Sugimoto[1], Toshikazu Ekino[1], Alexander M. Gabovich[2]

[1]Graduate School of Advanced Science and Engineering, Hiroshima University,, 1-7-1, Kagamiyama, Higashi-Hiroshima 739-8521, Japan; [2]Institute of Physics, National Academy of Sciences of Ukraine, 46 Nauka Ave., Kyiv 03028, Ukraine; m214729@hiroshima-u.ac.jp

The iron-based 11 superconductor Fe (Se, Te) has the simplest crystal structure among iron-based superconductor family possessing only 2D superconducting layers of iron-chalcogen network. We have performed the scanning tunneling microscopy/spectroscopy (STM/STS) and break junction tunneling spectroscopy (BJTS) measurements of the doped Fe (Se, Te) superconductors doped by various kinds of the transition metal impurities. The single crystals Mx-Fe1.01-x (Se, Te) (M = Ni, Cu, Co, Zn; x =1 %) were fabricated by the self-flux method using double sealed quartz tubes. The onset critical temperatures (Tc onset) were suppressed by those dopants, in particular, being 15.1 K for Zn, 14.2 K for Co, 12.7 K for Cu, and 10.4 K for Ni. The STM images (surface topography) showed the clear basic lattice structure with a period of about 0.37 nm in all the samples. There were no significant change of the STM topography due to the dopant atoms, while the spatial distribution of the electron local density of states (LDOS map) obtained by the dI/dV measurements showed qualitative differences depending on the dopant atom types. Especially, the LDOS map for M = Zn showed various kinds of the characteristic spot structures, such as circular shaped ones, simple bright spots, and simple dark spots, which are not seen in the STM image. Those results suggest that dopant atoms significantly alter the surface electronic states.

P2-31 Sol-Gel Multilayer Coatings for Thermal Radiation Control

Takashi Yasuda, Taiki Takeuchi, Akito Kinoshita

Kyushu Institute of Technology, Japan; yasuda@phys.kyutech.ac.jp

Spectral control of infrared thermal radiation is promising energy-saving technology in a variety of industries that use electric heaters for drying or baking. If the radiation is concentrated on the wavelength ranges where an object to be heated has high absorbance, heater power can be transmitted effectively to the object. To achieve this goal, applications of plasmonic or photonic materials have attracted much attention. However, these approaches are not entirely cost-effective, because they require numerous processes of high precision. In this study, TiO2-SiO2 sol-gel coatings were applied to radiation control. As the main issue in this case, we focused on preventing crack formation that inevitably occurs in sol-gel thick films during heat treatment.

Precursor sols of TiO2 and SiO2 were prepared by hydrolyzing ethanolic solutions of alkoxides using acid catalysts. These sols were spincoated on quartz glass substrates and heat treated under a stepwise increase of temperature from 60 °C to 800 °C. After the heat treatment, rutile phase TiO2 and amorphous SiO2 were obtained and refractive indices of TiO2 and SiO2 films were 2.33 and 1.40, respectively, at a wavelength of 800 nm. Critical cracking thickness for single spincoated films was examined by changing the amount of polymer added as a crack-preventing agent [1]. As a result, the critical thickness of TiO2 films heated at 130 °C increased monotonically with increasing polymer content. The maximum thickness was more than 600 nm, which was approximately three times that for polymer-free samples. This prevention of cracking coincided with a decrease in residual tensile stress measured by warp analysis. If the films were heated at 130 °C for a sufficiently long time, no crack growth occurred after the subsequent heat treatment up to 800 °C. After heating at 800 °C, the thickness of the TiO2 film decreased to less than half of that at 130 °C.

As a test sample for radiation control, a triple layer TiO2/SiO2/TiO2 film was prepared. The optical lengths of TiO2 and SiO2 layers were set to λ/4 and λ/2, respectively, to obtain a peak at λ = 800 nm in the emissivity spectrum. Radiation experiments were performed on the film attached to a black-painted plate heater. The emissivity spectrum measured at 800 °C showed fair agreement with the transmittance data, indicating a peak at 780 nm with FWHM of 180 nm and an emissivity suppression of about 50% at neighboring minimums. A further increase in critical thickness will allow us to develop the spectral shape and operating wavelength ranges.

P2-32 Sputtering deposition of single crystalline Zn1-xMgxO films on sapphire substrate via inverted Staranski-Krastanov mode: effects of substrate temperature

Kotaro Yataka[1], Naoto Yamashita[1], Daichi Takahashi[1], Takamasa Okumura[1], Kunihiro Kamataki[1], Kazunori Koga[1,2], Masaharu Shiratani[1], Naho Itagaki[1]

[1]Kyushu University, Japan; [2]National Institutes of Natural Sciences, Japan; k.yataka@plasma.ed.kyushu-u.ac.jp

Zn1-xMgxO has attracted much attention as a candidate material for ultraviolet optoelectronic devices due to the large exciton binding energy and the tunable direct band gaps (3.3–4.5 eV)[1]. However, the large lattice mismatch of 18% between Zn1-xMgxO and commonly used sapphire substrates makes it challenging to fabricate single crystalline films at low cost. In this context, we have performed growth of single crystalline Zn1-xMgxO films ($x \leq 0.33$) on sapphire substrates via inverted Stranski-Krastanov (inverted SK) mode[2]. In this mode, a buffer layer consisting of strain-relaxed 3D islands is initially grown using insoluble impurities that decrease the surface energy. Then we stop the impurity supply and make the islands coalesce to form a 2D layer, and finally, a single crystalline film is formed[3]. Here, we demonstrate the inverted SK growth of Zn1-xMgxO films of $x > 0.33$ on sapphire substrates using nitrogen. Furthermore, we investigate the effects of substrate temperature during 2D layer growth on the structural properties of Zn1-xMgxO films.

All the films were fabricated by radio frequency magnetron sputtering. First, 10-nm thick buffer layers were deposited on c-plane sapphire substrates at 780°C using ZnO targets. N2/Ar gas was used, and the pressure was 0.35 Pa. Next, on the buffer layers, Zn1-xMgxO films were fabricated at 600–800°C using ZnO and MgO targets. O2/Ar gas was used, and the pressure was 0.70 Pa. We have succeeded in the inverted SK growth of atomically-flat single-phase Zn1-xMgxO films even for large Mg content of $x \sim 0.36$. Figures 1 (a) and (b) show atomic force microscope (AFM) images of the Zn0.64Mg0.36O films fabricated at 800 and 650°C, respectively, on the buffer layers. For comparison, an AFM image of Zn0.79Mg0.21O film fabricated at 800°C without buffer layer is shown in Fig. 1 (c) (normal SK mode). Comparing between the films fabricated at 800°C, we found that the RMS roughness is drastically decreased from 11.6 to 0.6 nm by inserting the buffer layer, though the film on the buffer has higher Mg content. The higher crystal quality of the film on the buffer layer was also observed: the full widths at half maximum (FWHM) of the (0002) x-ray rocking curve (XRC) of the films with and without buffer layers are 0.17° and 0.34°, respectively. These results indicate the clear advantages of inverter SK mode. However, we failed to the inverted SK growth at somewhat low temperature of 650°C, where the RMS roughness and the FWHM of (0002) XRC of the film are large of 11.5 nm and 0.41°, respectively, even on the buffer layer.

According to the results, we conclude that combination of the buffer layer and enhancement of adatom migration during 2D layer deposition is a key for inverted SK growth of high quality Zn1-xMgxO films on large lattice mismatched substrates.

This work was supported by JSPS KAKENHI Grant Numbers JP21H01372, JP21K18731, NTT collaborative research, Toyota Riken Scholar, and The Murata Science Foundation.

P2-33
Sputtering Deposition Using Several Kinds of Mixture Powder Targets For Elemental Gradiented Functional Thin Film

Hiroharu Kawasaki, Tamiko Ohshima, Yoshihito Yagyu, Takeshi Ihara, Yusuke Hibino, Takayuku Satake
National Institute of Technogogy, Sasebo College, Japan; h-kawasa@sasebo.ac.jp

Gradient functional thin films simultaneously provide bonding surfaces similar to the base material and hard cutting surface to address this problem. We have previously reported the preparation of A6061 thin films on JIS-S25C steel via sputtering deposition. Furthermore, we reported that A6061 plasma coating was highly effective in reducing hydrogen entry into materials in a corrosive environment. However, the A6061 plasma coating on stainless steel (SUS304) did not markedly increase the hydrogen-entry resistance under corrosive environments; we attribute this result to the difference in the crystal structure between the base material and the film. We also found that the hydrogen embrittlement prevention was improved by doping of small amounts of Ni. Therefore, gradient functional thin films that have an greater Ni contents at the surface of the thin film in contact with the hydrogen gas, and a greater SUS304 content at the boundary with the base SUS304 may be an effective and low-cost strategy to prevent hydrogen embrittlement. In this study, we prepared gradient functional thin films for hydrogen entry prevention by a sputtering deposition method with powder targets. The composition ratio of nickel (Ni) and SUS304 was varied over the film thickness using 11 types of nickel oxide (NiO) and SUS304 mixed powder targets.

Gradient functional thin films were deposited by sputtering from 11 types of mixed powder targets. In these films, the composition varies through the film cross section from the film surface to the bulk/film boundary. At first, the 100% SUS304 powder was used as the sputtering deposition target. Next, the target was changed to 10%NiO/90%SUS304, and the deposition was performed on the same substrate under the same conditions. Then, gradient functional thin films were prepared by sequentially switching the mixed powder targets from 20%NiO/80%SUS304 to 100%NiO. The RF power of the deposition was 100 W, and the deposition time was 1 h. The substrate surface was maintained at room temperature. An XPS depth profile of the prepared film with Ar ion etching suggest that the Ni concentration ratio of the prepared film increased as the NiO content of the target was increased. As the results, thin films with variable Ni and SUS304 compositions were prepared by a sputtering deposition method with the use of NiO and SUS304 mixed-powder targets. The Ni and SUS304 thin films had a smooth surface morphology. The elemental concentration ratio of the prepared films was controlled by the NiO/SUS304 ratio of the mixed powder target. We used this method to deposit gradient functional thin films with variable Ni and SUS304 compositions from 11 powder targets. XPS depth profile results confirmed the composition change.

P2-34
Structural Characteristics of Carbon Sphere Composite Deposited by Ar+CH4 Plasma Chemical Vapor Deposition Method

Kazunori Koga[1,2], Sung Hwa Hwang[1], Shinjiro Ono[1], Daichi Yoshikawa[1], Takamasa Okumura[1], Kunihiro Kamataki[1], Naoto Yamashita[1], Naho Itagaki[1], Masaharu Shiratani[1]
[1]Kyushu University, Japan; [2]NINS, Japan; koga@ed.kyushu-u.ac.jp

Carbon spheres (CSs) have been attracted huge attention due to their unique properties compared to bulk materials [1]. Plasma is the most promising method of CS production because it can reduce impurity by using the dry processes and avoids their unexpected coagulation due to charging and neutralizing processes in plasmas. So far, we have produced CSs above 20 nm in size using a multi-hollow discharge plasma chemical vapor deposition (MHDPCVD) method. The MHDPCVD method can control fluxes of CSs and radicals independently by distance L between the plasma and the substrate. In this study, we fabricated CS composite using the MHDPCVD and analyzed their structure using Raman spectroscopy as a parameter of the L.

For the MHDPCVD, a multi-hollow electrode had 8 holes with a diameter of 5 mm. Ar and CH4 were supplied from the backside of electrode with 86 sccm and 14 sccm respectively [1,2]. The mixture gas passed through the holes. The working pressure was kept at 2 Torr. The discharge frequency and power were 60 MHz and 40 W, respectively. A mesh grid for transmission electron microscopy (TEM) and a silicon (100) substrate for Raman spectroscopy were set in the downstream region. The L was from 60 mm to 140 mm. For the Raman spectroscopy (Jasco, NRS-3000), the wavelength of the excitation laser was 532 nm.

We measured Raman spectra of the CS composite as a parameter of L. For L= 60 mm and 80 mm, the Raman spectra of deposited films showed polymer-like carbon structure. For L≥ 100 mm, both D band and G band were narrower in bandwidth than that for L≤ 80 mm. The G band position was around 1600 cm-1 with a full width at half maximum (FWHM) of 50 cm-1. From the relation between the G band position and the FWHM of G band suggested the clustered nanocrystalline-graphite structure [3]. For the conventional method, this nano-graphite is generally formed by post annealing process after carbon film deposition [3-5]. From TEM observation, CSs of 24 nm in size were clearly for L≥100 mm. These results suggest that the one-step deposition of nanocrystalline-graphite can be realized by using MHDPCVD method.

Keywords: Raman, Plasma CVD, nanocrystalline-graphite

References :

[1] S.H Hwang, et al., J. PFR. 14, 4406115 (2019).

[2] S.H. Hwang, et al., Processes 9, 1 (2021).

[3] A. Merlen, J. Buijnsters, C. Pardanaud, coatings. 7, 1-55 (2017).

[4] A. C. Ferrari, J. Robertson, Phil. Trans. R. Soc. Lond. A. 362, 2477-2512 (2004).

[5] C. Pardanaud, C. Martin, P. Roubin, G. Giacometti, C. Hopf, T. Schwarz-Selinger, W. Jacob, Diam Relat Mater. 34, 100-104 (2013).

P2-35
Structure-Controlled Zinc Metal Electrode for High-Performance Aqueous Zinc Ion Energy Storage System

Hee Bin Jeong, Dong Il Kim, Min Kyeong Kim, Soo Hong Lee, John Hong
Kookmin University, Korea, Korea, Republic of (South Korea); koco0113@kookmin.ac.kr

Lithium-ion battery is the most notable secondary battery for energy storage application. However, lithium-ion batteries have some problems such as the lack of lithium resources, stability problems, and toxicity. Many next-generation batteries are being developed to replace them. Zinc ion battery can solve all the drawbacks of lithium-ion batteries. Especially, it is safe and eco-friendly as well as zinc ion battery can provide high energy density and stability compared to lithium-ion battery. However, zinc-ion batteries could not avoid the problem of dendrite formation on the zinc electrode. The flat zinc foil (electrode) is usually used as the electrode, and the dendrite after cycling can cause a short circuit and decrease the overall power and energy density due to the limited movement path of ions and electrons. It also causes the poor wettability between the electrolyte and zinc anode. In this work, to solve the dendrite formation on the zinc electrode, the surface structure of the zinc electrode was successfully modified by the chemical etching procedure using a piranha solution. The piranha solution is a mixture of sulfuric acid and hydrogen peroxide, which is a powerful oxidant to modify the metal surface. The surface of zinc electrode is changed into a porous structure due to the exposure of the piranha solution. It is expected that the porous structure will increase the accessibility between electrolyte and electrode. Moreover, the dendrite will grow firstly in the pores to prevent protruding dendrite formation and the short ion diffusion path will be provided.

P2-36
Surface modification of nickel coated carbon fiber reinforced PEEK composites using SiO2/Ag and MWCNTs for multi-functional of superhydrophobic and electrothermal

Van-Tho Hoang, Jun-Sung Lee, Hyeon-Seok Choe, Rho-Shin Myong, Young-Woo Nam
Gyeongsang National University, Korea, Republic of (South Korea); thohv@gnu.ac.kr

Ice could be formed during operation in the cold-wet environmental condition leading to resist aircraft aerodynamics. It is essential to remove the ice (de-icing) as fast as possible even avoid ice forming (anti-icing). As the conventional solution for de-icing, the outer structure of aircraft is heated by supplying an electric current through the structure. A sufficient given electric current could completely remove the ice. However, in another way, ice cannot be formed if there is not any liquid on the outer structure of the aircraft. It is such a more efficient method for anti-icing solution. Recently, several materials with extremely low wettability (superhydrophobic) and high electrothermal properties have been found. It could be a great chance to apply these materials to obtain and/or improve the anti-icing performance of structures. In this study, different contents of multi-walled carbon nanotubes (MWCNTs) and a fixed amount of SiO2/Ag microsphere were utilized to enhance electrothermal properties and obtain the superhydrophobic surface of nickel-plated carbon fabric (NPCF) reinforced thermoplastic composites, respectively. Excellent results were achieved by higher than 150º in contact angle using SiO2/Ag microsphere and 48.6% higher in heating performance using MWCNTs. This fundamental investigation indicates a high potential method for de-icing and/or anti-icing functions that could be applied for further applications in the industry.

P2-37
Synthesis and luminescence properties of new blue polymer using carbazole and triazine groups based on bipolar effect

Seunghyeon Jo, Sunwoo Park, Sangwook Park, Joohwan Kim, Nikita A. Khairnar, Hayoon Lee, Jongwook Park
Kyung Hee University, south of Korea, Korea, Republic of (South Korea); pswook@khu.ac.kr

White organic light-emitting diodes (WOLEDs) have recently received a lot of attention because of their potential in display backlighting, full-color display, and solid-state lighting.[1] Generally, white-light emission can be implemented as the composition of three primary emission colors such as red, green, and blue colors. In this study, blue polymer based on carbazole with high quantum efficiency and thermal propery was synthesized using Yamamoto reaction. 9-phenylcarbazole (PCZ) and 9-(4-(4,6-diphenyl-1,3,5-triazin-2-yl)-2,5-dimethylphenyl)-9H-carbazole (DTPCZ) were used as blue monomer unit, respectively. DTPCZ, single molecule showed photoluminescence maximum (PL max) of 419 nm, violet color, in evaporated film state but poly(DTPCZ) had real blue emission due to strong charge transfer effect. Two polymers of poly(PCZ) and poly(DTPCZ) exhibited PL max peaks of 424 and 464 nm, respectively and could be applied to the solution process for white emission due to the violet and real blue colors. The solution process can provide simple manufacturing process compared to the evaporation process for WOLED devices. The related experimental results regarding PLQY, transient life-time, and the stacked devices as well as the single emission devices using new polymer will be discussed.

Keywords: polymer emitting layer, bipolar property, WOLED, solution process

[1] W. D'ANDRADE, B., E. THOMPSON, M., & R. FORREST, S. 2002. Controlling Exciton Diffusion in Multilayer White Phosphorescent Organic Light Emitting Devices. Adv. Mater, 14, 147-151.

P2-38 Synthesis of composite particles and separation of metal ions

Yayoi Yoshioka, Takuya Ehiro
Osaka Research Institute of Industrial Science and Technology, Japan; yoshioka@tri-osaka.jp

Functional particles have been used as separation carriers, adsorption carriers, and medical carriers in various fields. One of them is core-shell type composite particles consisting of polymer and ceramic particles. Porous silica particles having a large surface area and excellent shape stability are very useful as a separation carrier. Aromatic polyamides have been previously reported to show excellent separation ability. Also, they are easier to introduce various functional groups than ceramics.

In this study, composite particles, in which silica particles are coated with aromatic polyamides having carboxyl groups, were synthesized and evaluated for their structure and characteristics including separation ability. For example, two types of composite particles were obtained by polymerizing 1,3,5-benzenetricarbonyl chloride and 3,5-diaminobenzoic acid (SiO2-PA1) or 1,3-

diaminobenzene (SiO2-PA2) in solutions in the presence of silica particles (SiO2) (Fig. 1). Both the polyamides had crosslinked structures, but the introduction numbers of carboxyl groups were different. The morphology did not change significantly by the coating of polyamide. For both the SiO2-PA1 and SiO2-PA2 particles, the coating amounts of polyamide were estimated to be ca. 4 wt% using TG measurements. Next, the separation ability of metal ions (Ni2+, Co2+, Cu2+, B3+, La3+) in aqueous solutions (pH=5.5) was evaluated. The SiO2-PA1 particles showed higher removal ratios for Cu2+ and La3+ than the SiO2-PA2 particles. Meanwhile, they did not remove Ni2+, Co2+, and B3+. Thus, it is found that the composite particles have specific separation characteristics. Also, it is thought that the removal ratio is closely related to the number of carboxyl groups in the polyamide.

P2-39
Synthesis of Porous Ag–Ag2S@Ag–Au Hybrid Nanostructures with Broadband Absorption Properties and Their Photothermal Application

Astrini Pradyasti, Mun Ho Kim

Pukyong National University, Korea, Republic of (South Korea); apradyasti@pukyong.ac.kr

Hybrid nanostructures composed of a plasmonic noble metal and a semiconductor have been studied intensively because of their unusual properties and wide range of potential applications. However, preparing these hybrid nanostructures with a precisely controlled shape, composition, heterostructure, and internal structure remains a challenge. Here, we describe a method for synthesizing new metal–semiconductor@bimetal hybrid nanostructures. Specifically, Ag–Ag2S nanoplates were first prepared by site-controlled sulfidation of hexagonal Ag nanoplates. Ag–Ag2S nanoplates were then used as seeds for seed-mediated growth synthesis to obtain Ag–Ag2S@Ag core@shell metal–semiconductor@metal hybrid nanostructures. Thus, these nanoparticles were employed as templates for galvanic replacement reaction to synthesize Ag–Ag2S@Ag–Au hybrid nanostructures with unique porous architectures. The composition of the ternary alloy combined with the porous structure of the hybrid nanostructures resulted in excellent broadband absorption in the UV–Vis–NIR region (300–1100 nm), and hence a black color, without an additional post-treatment process. When used as photothermal conversion materials, the hybrid nanostructures showed good photothermal conversion activity, with a maximum efficiency of 76.1% under irradiation with an 808 nm near-infrared laser. A mechanism for the high photothermal conversion activity is proposed on the basis of experimental and simulation results.

P2-40
The effect of cold atmospheric plasma on the Inflammation of human gingival fibroblast cells for application in periodontal disease

Young-IL Jeong[1], Ji-Hoon Suk[1], Hee-Jung Kim[2], Min-Suk Kook[3], Byung-Hoon Kim[1]

[1]Department of Dental Materials, Chosun University College of Dentistry; [2]Department of Prosthodontics, Chosun University College of Dentistry; [3]Department of Maxillofacial Oral Surgery, Chonnam National University School of Dentistry;
jeongyi@chosun.ac.kr

The aim of this study is to study the anti-inflammatory effects of cold-atmospheric plasma (CAP) against human gingival fibroblast-1 (HGF-1) cells for application in periodontitis treatment. Customized CAP apparatus was designed for periodontal study in vitro. For inflammation study, HGF-1 cells were treated with lipopolysaccharide (LPS) and then cell viability was determined using MTT cell proliferation assay. The inflammatory response was evaluated with the levels of inflammatory cytokines including interleukin (IL)-6, 8, and TNF-α using enzyme-linked immunosorbent assay. The CAP treatment against HGF-1 cells was not significantly affected to the viability of cells until 30 s and cell morphology was not significantly modified. When LPS was treated to HGF-1cells, secretion of inflammatory cytokines such as IL-6, IL-8 and TNF-α was increased compared to the control group. Furthermore, cell viability was also decreased by treatment of inflammatory cytokines. However, the secretion of inflammatory cytokines from LPS-treated HGF-1 cells was significantly decreased when CAP was treated to cells. Furthermore, cell viability was also increased compared to LPS-treated cells. We suggest CAP as a promising candidate to control inflammatory reaction in periodontal disease.

Keywords: Cold atmospheric plasma, inflammation, human gingival cells, periodontitis

Acknowledgement: This work was supported by the National Research Foundation of Korea (NRF) grant funded by the Korea government (MSIT) (No. 2020R1A2C2008540).

[1] SUN, T., YU, S., SONG, X., ZHANG, J., BAO, Q., MEI, Q., SHEN, Q., WANG, D., NI G. 2022. Cold Plasma Irradiation Regulates Inflammation and Oxidative Stress in Human Bronchial Epithelial Cells and Human Non-Small Cell Lung Carcinoma. Radiat. Res. 197, 166-174.

P2-41
The effect of diverse structural variation of the interlayer on the properties of the polymer solar cells

SABRINA AUFAR SALMA, RAHMATIA FITRI BINTI NASRUN, DONG HWAN SON, QURROTUN AYUNI KHOIRUN NISA, INDAH SALMA SAUSAN, HYEONBO SHIM, JOO HYUN KIM

PUKYONG NATIONAL UNIVERSITY, Korea, Republic of (South Korea); sabrinasalma@pukyong.ac.kr

In this study, we prepare small molecules based on PDI with amino N-oxide (PDIN-O), dimethyldipropylenetriamino, (PDIN-N), and ethyl tosylate (PDIN-OTs) as the cathode buffer layer (CBL) in inverted type OSCs. The application of PDIN-O as CBL inverted-type devices becomes challenging due to PDIN-O being unstable under heat treatment and tending to degrade. To enhance the thermal stability in the inverted type of devices we introduce the side group dimethyldipropylenetriamino and tosylate. The PCE of the device based on PDIN-O, and PDIN-OTs were 12.5%, 13.3%, and 14.2%, respectively. This paper provides the ability to modulate CBL in non-fullerene organic solar cells by introducing a side group to tune the work function at the cathode interface. The PDIN-OTs is a promising material for the CBL in the inverted type of device and become the vanguard for the next exploration by changing the counterion or side group side

P2-42
The Ionic Liquid Modified PtCo/C Catalysts for Cathode of High-Temperature Polymer Electrolyte Membrane Fuel Cell

Dong Hee Kim, Hyeon-Seung Jung, Jong Gyeong Kim, Chanho Pak

Graduate School of Energy Convergence,Institute of Integrated Technology,Institute of Integrated Technology; kdhlonarun@gm.gist.ac.kr

The Ionic Liquid Modified PtCo/C Catalysts for Cathode of High-Temperature Polymer Electrolyte Membrane Fuel Cell

Dong Hee Kim, Jong Gyeong Kim, Chanho Pak1

Graduate School of Energy Convergence, Institute of Integrated Technology, Gwangju Institute of Science and Technology, Gwangju 61005, Republic of Korea

chanho.pak@gist.ac.kr

High-temperature polymer electrolyte membrane fuel cell (HT-PEMFC) is operate at over 150 °C, at which the water in the fuel cell cannot exist in the liquid phase. That is why the PBI-based membrane with phosphoric acid is used in HT-PEMFC. Phosphoric acid is as an electrolyte to carry hydrogen ions in the form of phosphate ions. However, phosphate ions are attached to the surface of the platinum catalyst and inhibit the catalytic activity [1]. In particular, phosphate ions attached to the cathode prevent oxygen from reacting to platinum and become a major resistance factor [2,3]

In this study, the [MTBD][beti] ionic liquids were modified PtCo/C according to loading amounts. The synthesized catalysts were characterized through TEM and XPS by identifying sulfur elements in [beti]. In addition, changes due to modification of ionic liquid in the pore volume and surface area of the catalyst surface were identified through nitrogen adsorption and desorption. The ionic liquid modified catalyst shows a reduced park in the low voltage range of 0 V-0.4 V and high voltage above 0.8 V on the cyclic voltammogram in 0.1 M HClO¬4. In 1 M H3PO4, as the loading amount of ionic liquid increases, the peak intensity at the 0.25 V region decreases on the cyclic voltammogram. This is the result of adsorption of ionic liquid to the active site on the PtCo/C catalyst, and inhibits the binding of phosphoric acid on the catalyst. Also, linear sweep voltammetry was conducted in in 0.1 M HClO4 electrolyte, the oxygen reduction reaction rate decreased as the ionic liquid loading increased. However, the rate reduction due to phosphoric acid poisoning in 1 M H3PO4 electrolyte decreases as the amount of ionic liquid loading increases. Furthermore, all ionic liquid modified PtCo/C have improved oxygen reduction rate than commercial PtCo/C in 1 M H3PO4.

Keywords: High-temperature polymer electrolyte membrane fuel cell, Oxygen reduction reaction, ionic liquid

[1] Bevilacqua, N.; George, M. G.; Galbiati, S.; Bazylak, A.; Zeis, R. Phosphoric Acid Invasion in High Temperature PEM Fuel Cell Gas Diffusion Layers. Electrochimica Acta, 2017, 257, 89–98.

[2] He, Q.; Shyam, B.; Nishijima, M.; Ramaker, D.; Mukerjee, S. Mitigating Phosphate Anion Poisoning of Cathodic Pt/C Catalysts in Phosphoric Acid Fuel Cells. The Journal of Physical Chemistry C, 2013, 117, 4877–4887.

[3] Kaserer, S.; Caldwell, K. M.; Ramaker, D. E.; Roth, C. Analyzing the Influence of H3PO4 as Catalyst Poison in High Temperature PEM Fuel Cells Using in-operando X-ray Absorption Spectroscopy. The Journal of Physical Chemistry C, 2013, 117, 6210–6217.

P2-43
The photovoltaic performance of conjugated polyelectrolytes as a cathode interlayer material by modifying side chain functionalities.

QURROTUN AYUNI KHOIRUN NISA, SABRINA AUFAR SALMA, RAHMATIA FITRI BINTI NASRUN, DONG HWAN SON, JOO HYUN KIM

Pukyong National University, Korea, Republic of (South Korea); ayuni@pukyong.ac.kr

In a polymer solar cell, the cathode interlayer material (CIM) is a quaternized conjugated polymer based on poly[(9,9-bis(3'-(N,Ndimethylamino)propyl)-2,7-fluorene]-alt-2,7-(9,9-dihexylfluorene)] (PFN) were examined. Dihexyl fluorene and dimethyl aminopropyl fluorene backbones are alternately used in the interlayer. By adding quaternized compounds, such as bromoethane or bromoethanol, as side chains to the PFN precursor polymer, the corresponding quaternized conjugated polyelectrolytes, known as PFN salt and PFN-OH salt, were created. ZnO/interlayer/PTB7-Th:PC71BM/MoO3/Ag were made to evaluate the inverted polymer solar cells (iPSCs). By using PFN, PFN salt, and PFN-OH salt as the CIM, the efficiency of the iPSCs was improved. When using bromoethanol as an interlayer to modify side-chain functionality, the results are superior to those obtained with bromoethane.

P2-44
The Synergetic effect of dual electrodeposition and coupled CoFe-LDH/CoMoP on nickel foam for boosting electrocatalytic hydrogen evolution reaction

Yasamin Shajirati[1], Mohamad Mohsen Momeni[2], Meysam Tayebi[3], Byeong-Kyu Lee[1]

[1]Department of Civil and Environment Engineering, University of Ulsan, Republic of (South Korea); [2]Department of Chemistry, Isfahan University of Technology, Isfahan, Iran; [3]Advanced Industrial Chemistry Research Center, Advanced Convergent Chemistry Division, Korea Research Institute of Chemical Technology (KRICT); Yasminshadjirati@gmail.com

Recently, layered double hydroxides (LDHs) with tunable elemental composition and diverse nanostructure are considered to be admirable materials for various applications(Chen et al. 2018; Shamloofard and Shahrokhian 2021). In this work, A-LDHs electrocatalyst (A= CoNi, FeNi and CoFe) were been electrodeposited on the highly porous cobalt molybdenum phosphate (CMP) electrocatalyst by using the dual electrodeposition method. Utilizing the activated A-LDHs as an HER electrocatalyst, small overpotential of CoFe-LDH/CMP (22.4 mV) is required to reach a 30 mA Cm-2 current response, while much higher overpotential is needed for NiFe-LDH/CMP (383 mV), CoNi-LDH/CMP (117 mV) than the CoFe-LDH/CMP. This work not merely reports the design of a stable and efficient HER electrocatalyst but also demonstrates the elemental doping effects in phosphide electrocatalysts. Also, this study analyzes the effect of second electrodeposition of three different LDH at the constant time. The second electrodeposition significantly decreases Tafel slope and overpotential in comparison to the first electrodeposition.

P2-45 Thermo-Responsive Cell Filtration Membrane Hydrogel Based Pressure Sensor

Benny Ryplida[1,2], Ga Young Seo[2], Ha Yeon Jo[3], Sung Young Park[1,2,3]

[1]Department of Green Bio Engineering, Korea National University of Transportation, Chungju, 27469, Republic of Korea; [2]Chemical Industry Institute, Korea National University of Transportation, Chungju, 27469, Republic of Korea; [3]Department of Chemical and Biological Engineering, Korea National University of Transportation, Chungju, 27469, Republic of Korea; ryplida@gmail.com

Recently, there has been a significant amount of interest in adaptive hydrogel membranes that are responsive to environmental factors such temperature, electric field, magnetic force, and redox environment. Thermo-responsive hydrogel has been thoroughly explored as one of the "smart" hydrogels because it can undergo volume transition between the lower critical solution temperature (LCST) and upper critical solution temperature (UCST). Herein, a thermo-responsive and conductive hydrogel (TR-gel) sensor with a conductive membrane for cell filtration and water purification, which can determine the volume transition while cooling and heating. The electroconductivity of the carbon dot (CD) was improved further by the conjugation of calcium ions (Ca2+), which caused a reduction in the resistivity from 1624 Ω to 527 Ω after fabrication of the TR-gel. Furthermore, following heating to 45 oC, the pore size of the hydrogel fell from an average of 12 m (25 oC) to an average of 2μm. Surprisingly, the mechanical characteristics of the hydrogel were altered by external temperature, which caused a reduction in the capacity of the TR-gel to absorb water by about 50% while increasing the storage modulus by two folds. The TR-gel functioned as a conductive membrane filter of cells with filtration efficiencies of 22.96 % and 71.83 % at 25 oC and 37 oC, respectively, owing to changes in the shape and size of the membrane brought about by the volume transition. Furthermore, the TR-gel displayed pressure responsiveness yielding a different result (52% at 25 oC) when applied with 200 g worth of pressure and only 19% at 55 oC. The thermo-responsive conductive hydrogel membrane demonstrated excellent performance for water filtration and purification by means of an in-situ wireless system and can separate water from bacteria-contaminated water (100 % efficiency of bacteria filtration at 45 oC) and oil and water mixtures (oil absorption efficiency at 24.81 %). As a versatile membrane sensor adaptable for a multitude of applications, the TR-gel offers a convenient and effective solution.

P2-46
Time resolved optical emission spectroscopy in Ar and Ar/Ne capacitively coupled radio frequency plasma.

Michihiro Otaka[1], Daiki Nagamatsu[1], Toshiaki Arima[1], Kunihiro Kamataki[1], Daisuke Yamashita[1], Naoto Yamashita[1], Takamasa Okumura[1], Naho Itagaki[1], Kazunori Koga[1,2], Masaharu Shiratani[1]

[1]Kyushu-university, Japan; [2]National Institutes of Natural Sciences, Japan; m.otaka@plasma.ed.kyushu-u.ac.jp

Semiconductors play major roles in many fields such as IoT and automatic driving [1]. Plasma processes are used more than 70% of the front-end processes of the modern semiconductor manufacturing. For ultra-precision nano-fabrication for 3D semiconductor devices, spatio-temporal structures of processing plasmas must be clarified and controlled. In such CCRF discharges, high-energy electrons contribute to the gas separation and ionization. There are two main patterns of high-energy electron production: α-action and γ-action. There are rather few reports of measurements of the production and behavior of these high-energy electrons. In this study, an image intensified charge-coupled device (ICCD) camera (minimum gate width: 2ns) was used to obtain information on plasma behavior with a high temporal and spatial resolution during the RF periods (several ns to tens of ns). The phase resolved optical emission spectroscopy (PROES) is a non-intrusive method that allows us to study behavior of high-energy electrons during the rf period with high spatial and temporal resolution by observing optical emission in discharge [2, 3].

A capacitively coupled plasma reaction vessel was used for PROES measurements of CCRF discharges. The reaction vessel contained two parallel plate electrodes with a diameter of 85 mm. The distance between the electrodes was set at 20.5 mm. Plasma was sustained between the electrodes by applying an RF voltage of 6, 10, and 13 MHz. The flow rate of Ar and Ne were 5 sccm and 5sccm, respectively. The pressure was 37.5, 100, 600 and 1200 mTorr. The ICCD camera had a gate width of 3 ns, and emission intensity of Ar I 750 nm and Ne I 585 nm were integrated with a repetition rate of 1-10 kHz. To perform the phase-resolved measurements, the camera was synchronized with the RF power supply for the plasma generation, and phase scanning was performed by setting a delay between the synchronization signal and the camera gate.

The present results confirm the behavior of plasma in the RF cycle. The generation region of high-energy electrons shifts toward the discharge electrode as the pressure increases from 37.5 to 1200 mTorr. In addition, dominant excitation by thex α-action is confirmed between 37.5 to 1200 mTorr. The excitation by γ-action is observed at 600 and 1200 mTorr. As for the frequency dependence, the generation region of the high-energy electrons shifts toward the discharge electrode as the frequency increases from 6.78 to 13.56 MHz. The excitation rate due to high-energy electrons increases with the frequency. Details will be presented at the conference.

Acknowledgement

This study was partly supported by JSPS KAKENHI Grant Number 20H00142.

References

[1] WSTS, Japan council (2021). https://www.jeita.or.jp/japanese/stat/wsts/docs/20210608 WSTS.pdf

[2] J. Schulze, et ai., J. Phys. Appl. Phys. 43 124016 (2010)

[3] B. Bruneau, et al, Phys. Rev. Lett. 114 125002 (2015)

P2-47
Tumor site-specific PEG detachment and active tumor homing of therapeutic PEGylated chitosan/folate-decorated polydopamine nanoparticles to augment antitumor efficacy of photothermal/chemo combination therapy

Wen-Hsuan Chiang
National Chung Hsing University, Taiwan; whchiang@dragon.nchu.edu.tw

To effectively promote tumor-targeted delivery of photothermal/chemo combined therapy for boosted antitumor efficacy, the versatile photothermal hybrid polymeric nanoparticles capable of detaching poly(ethylene glycol) (PEG) segments and exposing tumor-targeting folate (FA) moieties in response to tumor extracellular acidity (pHe) are developed to selectively deliver doxorubicin (DOX), a chemotherapy drug, to the tumor sites. Through one-pot co-deposition of dopamine molecules with acidity-responsive benzoic imine-containing PEGylated chitosan (BI-PC) adducts, the hybrid BI-PC/polydopamine (PDA) nanoparticles were attained as DOX vehicles and characterized to have a spherical structure composed of a PDA core surrounded by hydrophilic BI-PC shells. The DOX@BI-PC/PDA nanoparticles not only showed prominent colloidal stability in serum-containing environment and photothermal conversion efficiency, but also exhibited acidity/photothermal-activated drug release. The PEG detachment and FA exposure of FA-DOX@BI-PC/PDA nanoparticles in weak acidic environment appreciably promoted their uptake by FA receptor-overexpressed CT-26 colon cancer cells, thus largely augmenting anticancer potency based on the photothermal/chemo therapy. Importantly, the pHe-responsive FA-DOX@BI-PC/PDA nanoparticles markedly accumulated in CT-26 tumor sites in vivo and inhibited tumor growth without significant systemic toxicity upon the near infrared (NIR)-triggered hyperthermia integrated with DOX chemotherapy. This work presents a practical strategy for improved antitumor potency of photothermal/chemo combination therapy.

P2-48 Wireless Cancer Sensing Platform Based on Surface Coated MnO2-Polymer dots

Hyeong Jun Jo[1], Sunu Hangma Subba[1], Tae Min Kim[2], Sung Young Park[1,2]
[1]Department of IT and Energy Convergence (BK21 FOUR), Korea National University of Transportation, Chungju, 27469, Republic of Korea; [2]Department of Chemical and Biological Engineering, Korea National University of Transportation, Chungju, 27469, Republic of Korea; jhg4629@ut.ac.kr

Studies have shown investigation in cancer sensing, however, due to drawbacks of current methods such as low sensitivity, selectivity and time-consuming process, it is thus an urgent demand for the ideal sensor for cancer diagnosis with rapid selectivity and high sensitivity. Herein a wireless electrochemical cancer detection platform based on manganese oxide (MnO2) immobilized polymer dots complex by carbonized catechol conjugated poly ethylene glycol (C-PEG) was fabricated, which exhibited high selectivity and sensitivity for cancer detection due to the electrochemical response of cancer cells to the novel polymer dots coated surfaces. The system utilized the quenching effect of manganese oxide toward fluorescence of polymer dots by fluorescence resonance energy transfer, thus increased the electro-conductivity of the bio-sensing system that approached dually fluorescence-based materials and electrochemical properties of polymer dots. Engagingly, MnO2-mediated quenching effect was found to be able to recover by the reduction of MnO2 to Mn2+ by ascorbic acid leading to the disintegration of the MnO2 integrated polymer dots. Therefore, it was hypothesized that in the tumor environment with high concentration of extracellular alkaline phosphatase, the formation of ascorbic acid by bio-catalyzed hydrolysis process of 2-phospho-L-ascorbic acid by ALP could decompose the polymer dots/MnO2 releasing Mn2+ which resulted in the fluorescence recovery of the biosensing system. Not only did this phenomenon change in fluorescence bioimaging but it also caused an increase in resistance of the biosensing platform. In contrary, the normal cells treated with MnO2/polymer dots did not show any significant changes in electrochemical signal and optical which proved the superiority in selectivity of the synthesized carbon dots for cancer detection. The MnO2/polymer dots biosensor also showed greater sensitivity compared with the colorimetric method as the limitation of detection of MnO2 biosensor was 10^0.6 cells/mL while for the fluorescence method was 10^3.3 cells/mL. Furthermore, that the electrochemical signals could be collected by a smartphone enabled the process of detecting cancer to be rapid, simple and sensitive. In conclusion, with its high sensitivity and efficient selectivity, including time-saving feature, the synthesized MnO2/polymer dots biosensor indicated its potential in cancer detection and a promising material in future medical application.

P2-49
Zn Metal Electrode with Hexagonal Boron Nitride Nanosheets Layers for High-Performance Aqueous Zinc Ion Capacitors

Dong Il Kim, Min Kyeong Kim, Soo Hong Lee, Hee Bin Jeong, John Hong
Kookmin University, Korea, Korea, Republic of (South Korea); rasbora0@kookmin.ac.kr

Aqueous zinc ion capacitors (AZICs) are a promising new candidate for future electrochemical energy storage application. Zinc is an earth-abundant element and the aqueous condition of AZIC is beneficial for low-cost and safety operation as well as large-scale production. However, the major challenge for AZICs is the dendrite growth of Zn on the surface of Zn metal electrodes, which can decrease the long-term cyclability and induce the structural deformation of Zn metal electrodes. Here, to protect the surface of Zn metal electrodes and suppress the growth of Zn dendrite, we introduced hexagonal boron nitride (h-BN) nanosheets and the h-BN nanosheets were coated on the Zn metal. The thin layers of h-BN allow the penetration and flat deposition of Zn ions on the surface of Zn metal electrodes. Moreover, the thin layers of h-BN can be used as the large energy barrier to block the excess electron tunneling [1]. In this work, the h-BN nanosheets were synthesized by a simple solution method and uniformly coated on the Zn electrode material. Accordingly, we can demonstrate the effective control of Zn dendrite growth and the improved electrochemical energy storage performance with the h-BN layers.

P2-50
Fluorine and nitrogen co-doped mesoporous carbon fiber electrodes for flexible supercapacitors with high capacitance

Jaeyeon Lee[1], Geun Yoo[1], Seoyeong Kim[1], Geon-Hyoung An[1,2]

[1]Department of Energy System Engineering, Gyeongsang National University, Republic of Korea; [2]Department of Energy Engineering, Future Convergence Technology Research Institute, Gyeongsang National University, Republic of Korea; ghan@gnu.ac.kr

Internet of things industry expansion caused market growth of wearable electronic devices [1,2]. Wearable devices require independent energy storage devices with high portability and long operating time [1,2]. Due to the structure and material characteristics of existing energy storage devices, it was difficult to satisfy the conditions. Consist of flexible fiber textile energy storage devices has been proposed as an alternative for wearable devices [3,4]. The properties of the fiber-based flexible supercapacitors can maintain their performance when bent, twisted, and tied up[3,4]. However, due to the low surface area and electrical conductivity of carbon fiber electrodes occur poor electrochemical performance. To overcome these problems, applied nitrogen and fluorine co-doped activated carbon fiber electrodes contribute to energy capacity and conductivity improvement. In this study, the outcome supercapacitor shows a high specific capacitance of 243.9 mF cm−2 at a current density of 10.0 μA cm−2 and good ultrafast cycling stability with capacitance retention of 91.3% for up to 10000 cycles at a current density of 250.0 μA cm−2[1].

These results will be discussed in AFM 2022 in detail, and this work was supported by the National Research Foundation of Korea (NRF) grant funded by the Korea government (MSIT) (NRF- 2020R1C1C1010611).

P2-51
Fluorine-doped manganese oxide as cathode for aqueous zinc ion batteries with improved rate capacity

Seoyeong Kim[1], Jaeyeon Lee[1], Geun Yoo[1], Geon-Hyoung An[1,2]

[1]Department of Energy System Engineering, Gyeongsang National University, Republic of Korea; [2]Department of Energy Engineering, Future Convergence Technology Research Institute, Gyeongsang National University, Republic of Korea; ghan@gnu.ac.kr

A lithium-ion battery (LIB) has high energy density and thus occupies the battery market from small mobile devices to large-scale applications, but it is necessary to develop an alternative battery technology with high safety and low cost due to extrinsic limitations of lithium, such as limited lithium supply, high price, and stability [1,2]. The aqueous Zinc-ion battery (ZIB) is attracting candidate for next-generation energy storage technology to replace LIBs, have many advantages such as low cost, low combustibility, high theoretical capacity, inherent safety, and compatibility with water [3]. Normally, ZIBs composed of four main components: the anode, cathode, aqueous electrolyte, and separator. Among these, the research of cathode materials will be key technologies in order to enhance the performance of energy storage of ZIBs. However, β-MnO2 which is used as a cathode material, exhibits low capacity and rate capabilities due to the relatively narrow tunnel structure (1×1) limiting the dynamics of ion insertion and transport. Therefore, a high-performance zinc-ion battery may be realized by making a lattice and defect structure in β-MnO2 by the chemical doping process to promote an energy storage performance. Herein, a β-MnO2 cathode with a hierarchical porous structure designed by the valence engineering using fluorine (F)-doping, thus leading to improved electron transfer kinetics and ionic diffusion along with an enhanced electrical conductivity. As a result, the optimized MnO2 cathode was shown to deliver a remarkable energy-storing performance with a high capacity of 320 mA h g-1 at a current density of 0.1 A g-1, a superior rate capability of 165 mA h g-1 even at 2.0 A g-1 in comparison to the existing ZIB cathodes, and an outstanding cycling retention of 85%. The present study demonstrated that defect engineering via fluorine (F)-doping and oxygen vacancies has the potential of the development of advanced cathodes for rechargeable aqueous batteries.

These results will be discussed in in AFM 2022 in detail, and this work was supported by the National Research Foundation of Korea (NRF) grant funded by the Korea government (MSIT) (NRF- 2020R1C1C1010611).

References

[1] Chem. Rev., 2020, 120, 7795–7866

[2] J. Mater. Chem. A, 2019, 7, 18209–18236

[3] J. Mater. Chem. A, 2021, 9, 17211–17222

P2-52
Fabrication and Evaluation of a Powder-type Adhesive Hemostatic Agent Containing Blood Coagulation Agents

Dong Hun Kang, Young-Gwang Ko, Oh Hyeong Kwon

Kumoh National Institute of Technology, Korea, Republic of (South Korea); ohkwon@kumoh.ac.kr

Severe bleeding from a variety of factors can lead to death. Hemostasis is particularly important in an operating room where bleeding is frequent, and the development of a hemostatic agent with improved adhesion is essential. In this study, DAS (dialdehyde starch)/HA (hyaluronic acid) powder-type adhesive hemostatic agents cross-linked with glyoxal were prepared by introducing calcium ions and thrombin, which are blood coagulation agents. The introduction of blood coagulation agents was confirmed through ICP/OES, Bradford assay, and chromogenic assay with S-2238 substrate. Crosslinking was confirmed by FT-IR and XPS. Blood absorption capacity was controlled by DAS/HA composition, amount of crosslinking agent and particle size. As a result of in vitro whole blood coagulation test, DAS/HA/CaCl2/thrombin powder showed a faster coagulation effect than the control. In the in vivo experiment using the rat hepatic hemorrhage model, DAS/HA/CaCl2/thrombin powder showed less bleeding time and amount compared to the control and commercial products. DAS/HA powder introduced with calcium ions and thrombin will be a useful hemostatic agent for laparoscopic and endoscopic surgery.

P2-53
Highly redox- responsive fluorescent carbon nanogel (FNG)-MnO2 mediated nanocarrier for paclitaxel release for breast carcinoma cells

Sunu Hangma Subba[1], Hyeong Jun Jo[1], Seul Gi Kim[2,3], Sung Young Park[1,2,3]

[1]Department of IT and Energy Convergence (BK21 FOUR), Korea National University of Transportation, Chungju, 27469, Republic of Korea; [2]Chemical Industry Institute, Korea National University of Transportation, Chungju, 27469, Republic of Korea; [3]Department of Chemical and Biological Engineering, Korea National University of Transportation, Chungju, 27469, Republic of Korea; sunuhangma23@gmail.com

A highly selective paclitaxel (PTX)-loaded redox- sensitive fluorescent carbon nanogel was designed for breast carcinoma cell-targeting based on disulfide crosslinked hyaluronic acid for the fluorescence's "on" state and manganese oxide (MnO2) nanosheets attached to induce the fluorescence quenching. Owing to high levels of glutathione (GSH) in tumor cells, the disulfide bond is cleaved and MnO2 is reduced to Mn2+ thereby increasing the fluorescence intensity of PTX-loaded MnO2-FNG nanocarrier and consequently paclitaxel is released at the targeted site. Under normal circumstances, the existence of disulfide bonds and the MnO2 attachment, which only reacts to high potential, prevents the premature release of paclitaxel from the drug delivery system after it has entered the human body. PTX-loaded MnO2-FNG nanocarrier initiates the drug release by opening the structure in response to high concentration of GSH in the cancer cell microenvironment.

The outstanding biocompatibility of PTX-loaded MnO2-FNG with normal cells and its ability to target only tumor cells demonstrate the therapeutic potential of the system. With excellent potential for biomedical applications, the proposed PTX-loaded MnO2-FNG system may be used as a smart drug delivery system with diagnostic and therapeutic properties, strong selectivity, and compatibility.

P2-54
GSH-sensitive PDA-loaded disulfide crosslinked conductive hydrogel as a strain-pressure sensor for cancer detection

Akhmad Irhas Robby[1,2], A Hyun Kim[3], Sung Young Park[1,2]

[1]Department of Green Bio Engineering, Korea National University of Transportation, Chungju, 27469, Republic of Korea; [2]Chemical Industry Institute, Korea National University of Transportation, Chungju, 27469, Republic of Korea; [3]Department of Polymer Science & Engineering, Korea National University of Transportation, Chungju 3880-702, Republic of Korea; ahmadir93.ai@gmail.com

A wireless hydrogel-based pressure and strain sensor that can distinguish between cancer and normal cells using various strain-pressure responses and self-healing phenomena was developed based on glutathione (GSH)-sensitive polydopamine (PDA)-loaded disulfide-crosslinked polymer dot in PAAm hydrogel matrix. The glutathione levels in cancer cells are four times higher than in normal cells, and this difference in glutathione concentration acts as a biomarker for identifying cancer cells and causes various conformational changes in GSH-responsive polymer dots in the hydrogel matrix. Additionally, the availability of CD44 receptor in the cancer cell microenvironment facilitates PD uptake owing to their specific interactions with residual hyaluronic acid moieties in the system. In response to expressed GSH in cancer cells, the disulfide bond is broken, and PDA is released, which leads to a higher electrical response ($\Delta R/R0 \approx 23\%$) compared to normal cell-treated hydrogel ($\Delta R/R0 \approx 15\%$) and the onset of self-healing and selective strain-pressure responses. The catechol groups on PDA provides high interfacial hydrogen bond interaction, which is essential for promoting self-healing phenomena and further facilitates electron transfer and hence, increase in electrical conductivity. In contrast, there is no release of PDA in case normal cell treated hydrogel and no self-healing was observed. Moreover, the higher strain-pressure response and the self-healing phenomena in response to higher concentration of GSH in the cancer cell microenvironment confirms the selectivity and sensitivity of the system towards cancer cells. Additionally, a real-time wireless sensing can be carried out by directly monitoring self-healing and pressure response via a smartphone. As a result, our system offers considerable potential for point-of-care diagnostics applications that require sensitive and selective cancer detection.

P2-55 Squaraine fullerene bulk heterojunction solar cells: A performance enhancement study

Floren Radovanović-Perić[1], Ivana Panžić[1], Thomas Rath[2], Vilko Mandić[1]

[1]University of Zagreb, Faculty of Chemical Engineering and Technology, Croatia; [2]Technical University Graz, Institute for Chemistry and Technolofy of Materials; fradovano@fkit.hr

Organic photovoltaic devices are receiving increased attention over the last decade for their potential to be fabricated into light weight, flexible large area organic photovoltaic devices (OPV) at a low cost [1]. Donor materials, such as squaraines (SQ), are actively being investigated in a bulk heterojunction (BHJ) thin film setup with acceptor materials, such as fullerene derivatives (PCBM) as they show great preference for superstructural assembly, tunable bandgaps and high absorption coefficients [2]. Developing a clear and straightforward methodology for understanding and control of morphology and aggregation/phase separation phenomena is of utmost importance for upgrading performance properties of these OPV devices. In this study, we investigated the effects of two physical processes that occur during solvent or thermal annealing of spin cast SQ:PCBM BHJ thin films; crystallization of SQ and phase separation of SQ from the PCBM matrix. Morphology of self-assembled and post processed samples was obtained by AFM, while the size domains of SQ in the PCBM matrix were determined in cross section by TEM analysis. The organization phenomena investigated by GISWAXS was, with microscopy data, correlated to performance properties (JSC, VOC, EQE) of assembled devices. The results provided a clear insight on the importance of squaraine superstructural organization for OPV device upgrading.

P2-56
Fabrication and study of diamond-based rf MEMS microheaters for insects behavior monitoring

Gabriel Vanko[1], Robert Andok[2], Martin Tomáška[3], Marián Vojs[3], Boris Hudec[1], Tibor Izsák[1], Hung-Yin Tsai[4]

[1]Institute of Electrical Engineering SAS, Slovak Republic; [2]Institute of Informatics SAS, Slovak Republic; [3]Faculty of Electrical Engineering and Information Technology STU, Slovak Republic; [4]Department of Power Mechanical Engineering, NTHU, Taiwan R.O.C.; gabriel.vanko@savba.sk

Drosophila is the most commonly used model organism in cranial neuroscience. It has complex social interaction behavior which is an important feature of many organisms that can be defined for two or more biological individuals interacting with each other and initiated by showing some reactions including courtship, fighting or oviposition behavior, etc. In addition, fruit flies have shorter lifespan compared to humans and other model organisms. The advantages of short cycle, low cost and easy gene manipulation allow brain researchers to use drosophila brain to study human-related diseases (such as Alzheimer's disease, Huntington's and Parkinson's disease) and neural networks. Recently, many testing devices were designed and fabricated to observe the olfactory [1], visual [2] or thermally stimulated memory [3] of drosophila. Further, advanced insect behavior monitoring systems were fabricated and tested [4, 5]. The thermal stimulation effect has been proven. In our approach, a wireless heater is fabricated and installed onto the back of the flies that enables to stimulate any individual subject of desire throughout the experimental process. The existing camera monitoring systems can reach a 99.8% accuracy of locating the flies but for more precise measurements and monitoring, development of a micro-technologically fabricated positioning system is required.

In this work, we propose a suitable technological process that allows the fabrication of a micro-heater based on a diamond film and a resonant LC circuit. In the future, we intend to use the hybrid integration of either supplementary resonant circuit on the same chip with the micro-heater for wireless monitoring of the tiny insects.

Taking into account the requirements above, we propose a simple LC resonant circuit (Fig. 1) that can be fabricated by planar technology small enough to be carried by a tiny insect such as drosophila. The micro-heater is placed on a 3-5µm free standing diamond membrane that will serve as the supporting layer and as biologically acceptable material for tiny insets on one hand, but on the other hand as most suitable material also for its thermal properties (controlled heat transfer when the above LC circuit is intentionally brought into resonance by outside rf field). The rf coil and the electrodes of the capacitor were deposited using electron beam evaporation of thin Ti(10nm)/Au(50nm) metal layers. For the creation of the thin Al2O3 (30nm) dielectric layer between the electrodes of the capacitor, atomic layer deposition (ALD) technique was used.

Preliminary simulation results of such a concept are shown in Figure 2. We expect the insects being influenced by thermal effect of particular rf tag due to thermal loss selectively increased at resonant frequency of the tag. The resonance frequency determination (from the measured s-parameters) exhibits some differences between simulation and real measurement that will be further investigated.

P2-57
Optical properties of nanostructured liquid crystal alignment film produced by brush coating

DongHyun Kim, Dae-Shik Seo

Yonsei University, Korea, Republic of (South Korea); kdh2975698@naver.com

A liquid crystal (LC) alignment layer was efficiently generated through brush coating, and the LC alignment ability was confirmed. After brush application to the indium-tin oxide substrate, the coating was allowed to solidify at various curing temperatures. The directional micro/nanostructure was formed differently depending on the curing temperature due to the shear stress caused by the movement of the brush bristles. Surface chemistry changes were analyzed using X-ray photoelectron spectroscopy and contact angle measurements. The anisotropic boundary of the microgroove and the van der Waals force due to the increase in surface energy are the alignment mechanisms of LC molecules. The LC alignment due to this surface modification was confirmed by a polarized optical microscope and pretilt angle measurement. This confirmed the effectiveness of the brush coating method, which dramatically simplified the LC alignment layer process. Uniform LC alignment properties through brush coating with curing temperature provide an innovative approach for LC alignment.

P2-58
Sensitivity Enhancement of Localized Surface Plasmon Resonance Sensors: Mathematical Approach in Single Gold Nanostructure

Ji Won Ha

University of Ulsan, Korea, Republic of (South Korea); jwha77@ulsan.ac.kr

Localized surface plasmon resonance (LSPR) sensors using metallic nanoparticles are extensively used for refractive index (RI) measurements in chemical and biological studies, and their sensitivity is highly influenced by the material and structure of the nanoparticle. Despite the great advantages of LSPR sensors using frequency shifts, there are still major challenges in terms of detection sensitivity as well as the broadening and asymmetry of LSPR peaks. In this presentation, I provide a general background of the fundamentals of LSPR and RI-based LSPR sensing.[1] Thereafter, I present recent studies using a simple mathematical approach with LSPR inflection point to improve the RI sensitivity in gold nanoparticles with different shapes, sizes, shells, etc.[2,3]

P2-59
Structural and Electrical Characteristics of a novel Lead-free Ferroelectric (1-x)BiFeO3 –xCaTiO3 Ceramics for High Temperature Energy Storage Application

SREENU GOMASU[1], SUBHADEEP SAHA[1], RN BHOWMIK[2], DIBAKAR DAS[1]

[1]UNIVERSITY OF HYDERABAD, India; [2]PONDICHERRY UNIVERSITY, India; sreenu.giiit@gmail.com

Even though promising results have already been obtained in lead titanate-based dielectrics, lead-free alternatives are strongly desirable due to the environmental concerns. Development of advanced ceramics with large energy storage has seen a surge in research interest because of their capacitive energy storage potential in modern electrical and electronic devices. (1-x)BiFeO3 - xCaTiO3 (x = 0.6, 0.7, and 0.8) composites were prepared by direct mixing the powders of BiFeO3 (BFO) and CaTiO3 (CTO) in stoichiometric amount synthesized by the standard auto combustion route. Structural and electrical properties were explored. Rietveld analysis results of XRD patterns revealed that all the compositions indicated single-phase perovskite structure for x = 0.6, 0.7, 0.8, and 1 with space group symmetry of Pbnm [1]. Fabricated samples were sintered using microwave sintering furnace and dense ceramics (sintered density ≥ 95% of the theoretical density) were obtained. Grain size distribution revealed that the average grain size of (1-x)BiFeO3 - xCaTiO3 for x = 0.6 was ~0.9 µm and for x = 0.7 was ~5.5 µm. Electrical measurements show that the

leakage current density J of (1-x)BiFeO3 - xCaTiO3 (x = 0, 0.6, 0.7, and 0.8) was reduced by almost four orders of magnitude with increasing CTO content, 1.9 □ 10-1 A cm-2 for x = 0 (pure BFO) to 7.4 □ 10-5 A cm-2 for x = 0.8 as shown in fig. 1a.[2] and electrical conductivity diminished from 1.04 □ 10-5 S cm-1 to 4.9 □ 10-8 S cm-1 at room temperature for the same sample (x = 0.8). A stable electrical conductivity up to 200 oC and current density up to 16.7 kV were observed for all the samples. But, a surge in the leakage current above 150 oC was observed for all the three samples.

Incorporation of CaTiO3 into BFO suppress the Fe ions fluctuations, formation of Oxygen vacancies, reduces the impurity phases and porosity in BFO-CTO ceramics. In the present investigation enhanced properties with significant decrease in the leakage current (compared to pure BFO) and electrical conductivity and increase in the density, structural stability, and electrical insulation have been observed and the best properties were obtained for x = 0.8 at room temperature and x = 0.7 at higher temperatures up to 200 oC.

P2-60 Syntheses of Low-oxygen Ti3AlC2 MAX Phase by Using Deoxidized Titanium

Jae-Won Lim, Taeheon Kim

Jeonbuk national university, Korea, Republic of (South Korea); jwlim@jbnu.ac.kr

MAX phase is a material with excellent electrical, thermal conductivity, thermal shock, and chemical shock resistance because of metal-like bonding properties. When the oxygen content of the Ti3AlC2 MAX phase is high, TiO2 and Al2O3 are formed. These oxides cause a problem in which Al is lost and TiC is formed. Impurities such as oxides and TiC derived from the Ti3AlC2 MAX phase remain in the MXene and have a great influence on electrical conductivity and chemical stability, so it is important to control these impurities. To synthesis low-oxygen Ti3AlC2 MAX phase, the deoxidized titanium powder was applied to synthesize Ti3AlC2 MAX phase with aluminum and graphite powders. The deoxidation of titanium powder was conducted at the temperature of 800 °C in argon condition. Ti3AlC2 MAX phase was synthesized at the temperature range of 1350 °C to 1450 °C for 5 hours. Oxygen/Nitrogen analyses, X-ray diffraction, and secondary electron microscopy were performed before and after syntheses of Ti3AlC2 MAX phase. It was found that the oxygen concentration of the Ti3AlC2 MAX phase with the deoxidized titanium powder was below 4,000 ppm, whereas the Ti3AlC2 MAX phase without the deoxidized titanium powder showed higher oxygen of 6,000 ppm. Detailed results will be announced at the conference.

P2-61 The well-arrayed ZnO Nanorods Fabricated by Chemical Bath Deposition Applying for Photocatalytic Activity

Tomoya Ikuta [1], Htet Su Wai[1], Chaoyang Li[1]

[1]School of Systems Engineering, Kochi University of Technology, 230015f@ugs.kochi-tech.ac.jp

ZnO as one of the promising semiconductor metal oxides has been considered as an effective alternative to replace TiO_2 applying photocatalysis due to its unique properties [1]. It was reported that the photocatalytic efficiency of ZnO was influenced by crystal growth orientation, surface area, particle size, nanostructure, light intensity, etc. Particularly, crystal growth orientation of ZnO along the (0001) crystal plane showed high photocatalytic activity. In this research, we propose a simple and low cost chemical bath deposition method to synthesize well-arrayed ZnO nanostructures and investigate their photocatalytic activity as well. AZO films with 300 nm thickness was deposited on glass by a radio frequency magnetron sputtering method. The obtained AZO film was put into the solution of mixture of $Zn(NO_3)_2$•$6H_2O$ and hexathylenetetramine (HMTA), with the concentrations of 0.025 and 0.0125 mol/L. The solution was heated from room temperature to 95 °C and kept at 95 °C for 2.5, 5 ,7.5, 10 and 12.5 hours for comparison.

Fig. 1: ZnO nanorods grown on AZO substrates from 2.5, 5,7.5, 10 and 12.5 hours.

SEM images of ZnO nanostructures grown on AZO films with different time, showed that well-aligned ZnO nanorods could grow on asdeposited AZO films. The length of ZnO nanorods was growth from 650nm to 2300 nm with the deposition time increase form 2.5 hour to 12.5 hours.

The XRD patterns of ZnO nanorodss showed that there was only a single dominant (002) diffraction peak for ZnO nanorods grown with different deposition time. The crystallinity was enhanced with the length of nanorods increased. The dominant (002) peak indicated ZnO rods had highly preferred orientations in the (0001) direction.

The photocatalytic measurements of ZnO nanorods/AZO films were carried out at room temperature. The methyl red solution with concentration of 1×10^{-5} mol/L and volume of 70 mL was prepared prior to the UV irradiation. It was found that absorbance was significantly decreased with the with the length of nanorod increase, which meant that photocatalytical efficiency was increased.

In summary, the ZnO nanorods grown on AZO substrate showed vertical alignment growth orientation. The photcatalytic activity was enhanced with the surface area increase and crystallinity improvement.

[1]FRANCO, P.; SACCO, O.; DE MARCO, I.; VAIANO, V. 2019. Zinc OxideNanoparticles Obtained by Supercritical Antisolvent Precipitation for 295 the Photocatalytic Degradation of Crystal Violet Dye. Catal., 9, 346.

P2-62 Mechanical Properties of Polymer Nanocomposite Reinforced by Hydrophobic-Modified Cellulose Nanofibers

Yubin Kim, Seong Il Yoo

Pukyong National University, Korea, Republic of (South Korea); sea_through@naver.com

Mechanical Properties of Polymer Nanocomposite Reinforced by Hydrophobic-Modified Cellulose Nanofibers

In developing eco-friendly polymer nanocomposites, nanocellulose is one of the promising reinforcements and fillers, which can improve the mechanical properties of polymers. However, the intrinsic hydrophilicity of nanocellulose originating from an abundance of surface hydroxyl groups strongly restricts the dispersion of the nanocellulose in hydrophobic polymer matrix. In this study, we present that a hydrophobic-surface modification of nanocellulose can induce uniform dispersion of nanocellulose in organic solvent as well as polymer matrix without noticeable aggregation. With the inclusion of surface-modified nanocellulose, tensile modulus and ultimate tensile strength of the polymer nanocomposites were strongly improved, in comparison with the nanocomposites with pristine nanocellulose. In addition, the interaction between nanocellulose and polymer chains has been discussed with the results of differential scanning calorimetry and dynamic mechanical analysis.

P2-63 Partial Covalent Interactions Effect on Oxygen Diffusion in CeO2, ZrO2, and Bi2O3

Nguyen Xuan Thi, Aleksandar Staykov

International Institute for Carbon Neutral Energy Research (WPI-I2CNER), Kyushu University, Japan; nguyen.thi.796@s.kyushu-u.ac.jp

Reducing the dependence on fossil fuels requires more efficient Solid Oxide Fuel Cells (SOFCs). One of the determining factors of SOFCs' efficiency is the oxide ion conductivity within the electrolyte. Each electrolyte material has different oxide conductivity because of varying interactions between the oxide ion and surroundings cations. Understanding how oxygen interacts with these cations can guide the choice of electrolyte material and will lead to accurate models of oxide ion diffusion.
Two models of oxygen diffusion can be investigated: the classical ionic model and the partial covalent conduction model. The conventional model assumes that all ions in the lattice are fully ionized, and oxygen conduction is hindered by steric effects from cations and electrostatic interactions. According to this model, the most favorable scenario is oxygen traveling through cations with small radius and small positive charge. Such theory ignores oxygen-cation electronic interactions and the effect of the polarizability of cations. The partial covalent model involves partially ionized atoms with some degree of covalent bonding. This theory considers electronic interactions along with steric hindrance and electrostatic force. Including these partial covalent bonds is likely to produce different conclusions to those of the conventional ionic model [1]. The model has shown already its potential in the simulation and understanding of oxygen reduction reaction on oxide surfaces [2,3,4].
We examined the effect of partial covalent interactions on oxygen migration in CeO2, ZrO2, and Bi2O3. Activation energy and electron density of all possible migration pathways were calculated using plane-wave Density Functional Theory. The results proved that the oxygen migration is influenced by the oxygen-cation partial covalent interaction in a non-intuitive manner. If oxygen at the transition state is stabilized by partial covalent interaction, the activation energy is decreased. When oxygen at the initial state had higher partial covalent interaction with cations compared to the transition state, initial energy is stabilized, thus increasing bond breaking energy penalty and activation energy.
The electron density data showed nonlinear oxygen migration trajectory of the oxygen inside δ-Bi2O3. It moves in curved pathway, breaking bond with one Bi and forming bond with another Bi simultaneously. Oxygen also breaks bonds in succession in Y doped ZrO2 and propagates in diagonalized pathway. These results indicate that maximizing partial covalent interaction in the vicinity of cations is preferable for oxygen migration.

P2-64 YAG:Tb-YAG:Pr single crystal-thin film hybrid luminescence thermometer

Joanna Jedoń1, Justyna Zeler1, Eugeniusz Zych1, Yuriy Zorenko2

1University of Wroclaw, Faculty of Chemistry, 50-383 Wroclaw, 14 F. Joliot-Curie Street, Poland; 2Kazimierz Wielki University, Institute of Physics, PL-85090 Bydgoszcz, 2 Powstańców Wielkopolskich Street, Poland; joanna.jedon@chem.uni.wroc.pl

Luminescence thermometry is considered one of the most forward-looking techniques for semi-contact remote temperature measurements. Development of high-quality luminescent thermometers pose a challenge, as meeting the demands of specific applications appears tough. One of common issues concerns broadening the thermometers operating range, while still preserving decent values of relative sensitivity and temperature uncertainty. We present an original approach to overcome these constraints using a hybrid fully inorganic oxide phosphor, whose core part is YAG:Tb single crystal on which single-crystalline thin film of YAG:Pr (fig.1) was grown. Both impurities (Tb^{3+} and Pr^{3+}) can be effectively excited by their allowed 4f 5d absorption transitions showing quite similar energies. Hence, we expected that both Pr^{3+} and Tb^{3+} ions may, in principle, be excited simultaneously or separately upon a deliberate choice of the excitation energy/wavelength. This, in turn, was supposed to give the opportunity to use both intra- and interconfigurational transitions of the two ions for thermometric purposes. Detailed studies on spectroscopic properties related to the thermometric parameters will be discussed and the thermometer performance will be presented.
The work is Supported by The Polish National Science Centre (NCN) under grant No. UMO-2018/29/B/ST5/00420.

Keynote Session-3: Keynote Session

Time: Thursday, 12/Jan/2023: 8:45am - 10:45am · *Location:* Hall 1&2

8:45am - 9:15am

Electric Field Control by Multi-dimensional Functionally Graded Materials for DC-GIS Spacer

Boxue Du, Hang Yao, Hucheng Liang, Jianan Dong

Tianjin University, 92 Weijin Road, Tianjin, China.; hcliang@tju.edu.cn

This study discusses the application of the multi-dimensional functionally graded materials (MDFM) for relaxing the electric field concentration around the epoxy-based spacer in high voltage direct current gas insulated transmission lines (HVDC GIL). Based on the ±500 kV HVDC GIL model, the iterative method was applied to optimize the permittivity gradient inside the spacer bulk (ε-FGM) as well as the conductivity gradient on the spacer surface (σ-SFGM). A group of functional spacers, i.e, ε-FGM, σ-SFGM and MDFM, were fabricated by electrospinning and gradient casting methods. It is proved that the ε-FGM spacers can reduce the transient electric field by up to 33.6%, and the σ-SFGM spacers can reduce the DC steady electric field by up to 23.6%. The MDFM spacers combine the advantages of ε-FGM and σ-SFGM, which can relax the electric field concentration under both steady and transient conditions.

9:15am - 9:45am

CMOS MEMS as the Platform Technology for More-than-Moore Applications

Weileun Fang

National Tsing Hua University, Taiwan; fang@pme.nthu.edu.tw

The complementary metal oxide semiconductor (CMOS) transistor is the key building block for the microelectronic devices and systems. Presently, various standard CMOS processes have been established, and these CMOS platforms are mature and available in many existing foundries. Moreover, the situation of no depreciation cost for most of the 8-inch foundries is another advantage to adopt the related CMOS processes. It would be a cost-effective approach to leverage the CMOS fabrication technologies to implement MEMS devices. Thus, the CMOS-MEMS can serve as the platform technology to extend CMOS processes for More-than-Moore applications [1].

The CMOS back-end-of-line processes are consisted of multiple metal and dielectric layers which could enable the design flexibility for MEMS devices and their electrical routings [1-4]. Moreover, various sensing mechanisms (e.g. piezoresistive, capacitive, and inductive) can be achieved by using thin film materials inherent in the CMOS processes [2-4]. Thus, the CMOS-MEMS approach could serve as the process platform to implement sensors and sensing hub. Presently, many CMOS-MEMS devices such as pressure sensors, inertial sensors, humidity sensors, chemical sensors, microphones, resonators, and so on have been demonstrated.

As the CMOS processes approaching the physical limit of Moore's law, the technologies to implement and integrate micro sensors, actuators, and ICs attract a lot of attentions from academia and industry. This talk presents the approach to implement and integrate various MEMS transducers by using the standard CMOS processes plus the in-house post-CMOS processes. Moreover, the CMOS/MEMS networks at Taiwan is also introduced. As a future perspective, the mature semiconductor ecosystems established at Taiwan could make contributions for the commercialization of MEMS products.

Funding: The National Science and Technology Council (NSTC) of Taiwan under grant number NSTC 110-2218-E-007-032-, NSTC 110-2923-E-007-009-, and NSTC 110-2926-I-007-506-.

References:

[1] W. Fang et al., "3D and circuit integration of MEMS," Chapter 6, Wiley VCH, Germany, 2020

[2] W. Fang et al., "CMOS MEMS: A key tech towards the more than Moore era," Transducers, Barcelona, Spain, 2013

[3] Y.-C. Lee et al., "CMOS-MEMS technologies for the applications of environment sensors and environment sensing hubs," J. Micromechanics and Microengineering, 2021

[4] S.-K. Yeh et al., "CMOS-based tactile force sensor: a review," IEEE Sensors J., 2021

9:45am - 10:15am

Microfluidic devices for drug screening and in vitro diagnostics

Sungsu Park

School of Mechanical Engineering, Sungkyunkwan University (SKKU), Suwon, South Korea; nanopark@skku.edu

Microfluidic chips are highly useful for studying drug resistance because they can manipulate and control fluids and particles at the micron level. For an example, we obtained clinically meaningful giant cancer cells in the chip to mimic the spatiotemporally heterogeneous ecosystem of cancer cells in the tumor tissues of patients receiving chemotherapy by integrating concentration gradients and microfabricated habitat in a microfluidic chip. Using the same chip, we have been studying virus propagation pattern and herd immunity. These microfluidic chips can be potential platforms for drug screening and in vitro diagnostics.

10:15am - 10:45am

Sn perovskite solar cells following Pb perovskite solar cells

Shuzi Hayase

I-PERC, The University of Electro-Communications; hayase@uec.ac.jp

The efficiency of the Lead perovskite solar cell (Pb-PVK PV) reached to 25.7%, which is close to that of single crystalline Si solar cells (26.7%). The focus is now shifting to the development of the large modules and stability issues. As the next research items, Tin based perovskite solar cells (Tin perovskite solar cells (Sn PVK PV) and Tin-Lead alloyed perovskite solar cells (SnPb PVK PV) have attracted attention. The former is a Pb free PVK PV and the latter is a narrow band gap PVK PV which is expected as the bottom cells of all perovskite tandem solar cells. The efficiency of these Tin based PVK PV were low at first. This is explained by high carrier trap density associated with various lattice defects and large carrier densities brought about by the self-doped Sn4+(1). We have reported that the Sn4+ concentration was suppressed by the addition of GeI2 and the grain boundary defects were passivated by ethylenediamine (EDA) (1). The EDA passivation facilitated the electron injection from the Sn-PVK layer to the n-type layer (fullerene) by around 10 times. The efficiency of the Sn-PVK PV was enhanced to 13.2% (1). In addition, we found that SnOx (x=1.7-1.8, 10 nm thickness) prepared by plasma-oxidized Sn metal layer worked as the HTL of the Sn-PVK PV. These heterointerface engineering enhanced the efficiency of the Sn-PVK PV to 14.1% (2). These defect suppression engineering were also effective for enhancing the SnPb-PVK PV efficiency. By introducing mixed monolayer HTL layer which increases the surface coverage on the TCO layer, the efficiency of the SnPb-PVK PV was enhanced to 23.3% (3).

Keywords: perovskite, tin, interface, defect, Lead free

Reference

[1] HAYASE, S., Sn-based Halide Perovskite Oolar Cells, Chapter 10, 293-319, 2021, Perovskite Photovoltaics and Optoelectronics, Edited by Miyasaka, T., Eiley-VCH.

[2] WANG, L., CHEN, M., YANG, S., UEZONO, N., MIAO, Q., KAPIL, G., BARANWAL, A., SANEHIRA, Y., WANG, D., LIU, D., MA, T., OZAWA, K., SAKURAI T., ZHANG, Z., SHEN, Q., HAYASE, S. 2022. SnOx as Bottom Hole Extraction Layer and Top In-situ Protection Layer Yields over 14% Efficiency in Sn-based Perovskite Solar Cells, ACS Energy Lett., Just Accepted.

[3] KAPIL, G., BESSHO, T., SANEHIRA, Y., SAHAMIR, S. R., CHEN, M., BARANWAL, A., LIU, D., SONO, Y., HIROTANI D., NOMURA, D., NISHIMURA, K., KAMARUDIN, M. A., SHEN, Q., SEGAWA, H., HAYASE, S. 2022. Tin-lead perovskite solar cells fabricated on hole selective monolayers, ACS Energy Lett., 7, 3, 966-974.

Oral Talk-5: Oral Talk

Time: Thursday, 12/Jan/2023: 8:45am - 10:45am · *Location:* Hall 3

8:45am - 8:57am

Anti-inflammatory activity of onion peel derived gold nano bioconjugate

Devasish Chowdhury, Kabayshree Phukan, Rajlakshmi Devi

Institute of Advanced Study in Science and Technology, India; devasish@iasst.gov.in

Plant secondary metabolites such as flavonoids demonstrate high degrees of antioxidant, anti-inflammatory, and anticancer activities. Among flavonoids, quercetin plays an important role in inflammation by downregulating the level of various cytokines. Thereby, in this work, onion (Allium cepa) peel was successfully utilized for the synthesis of gold nano-bioconjugates acting as a natural therapeutic drug. In this process, crude onion peel extract was first divided into different fractionates, namely, ethyl acetate, butanol, methanol, and water, and they were subjected to various preliminary studies of antioxidant activities. The ethyl acetate fractionate shows high antioxidant activities in all the assays. The bioactive components were identified and found to contain a high amount of quercetin as confirmed by liquid chromatography with tandem mass spectrometry and high-performance liquid chromatography. Three gold nano-bioconjugates were prepared with different concentrations of the ethyl acetate fractionate. Various biochemical anti-inflammatory assays were carried out and compared with the active ethyl acetate fraction of the onion peel drug (OPD). The cytotoxicity of the nano-bioconjugate system and the OPD was checked in the myoblast L6 cell line from skeletal muscle tissues to evaluate the toxicity. All the three nano-bioconjugates A, B, and E demonstrated high percentages of cell viability, viz., 73.07, 72.3, and 69.15%, respectively, at their highest concentration of 200 µg/mL. The OPD also showed 88.56% cell viability with no toxic effects in the myoblast L6 cell line from skeletal muscle tissues. The reactive oxygen species reduction of nano bioconjugate B showed a marked reduction of 76.77% at a maximum concentration of 200 µg/mL, whereas the OPD showed 68.17%. Then the prepared gold nano bioconjugates (GNBCs) from the ethyl acetate fraction of onion peels with best results were investigated their anti-inflammatory activity in lipopolysaccharide-stimulated RAW 264.7 macrophages. Comparative studies have been conducted among GNBCs, fractionate alone [onion peel drug (OPD)], and the standard drug dexamethasone in various anti-inflammatory assays. It was observed that GNBCs showed comparatively good therapeutic efficacy than the fractionate alone. At the lowest 10 µg/ mL concentration, the GNBC and OPD exhibited 70.86 and 91.98% of reactive oxygen species production, 10.88 and 20.97 ng/µL of nitrite production, 337 and 378 pg/mL of TNF-α production, 27.1 and 30.64 pg/mL of IL-6 production, respectively, by maintaining a satisfactory cell viability. Moreover, to understand the mechanistic pathway of GNBCs in their entry into the macrophages, their localization, and duration, uptake studies have been performed where a caveolar-mediated endocytosis pathway is found to be prominent. Hence, this study will lead to the development of cheap, green synthesis of nano bioconjugates and their role in inflammation.

8:57am - 9:09am

Living Polymer Networks

Chris Bainbridge[1,3], Jianyong Jin[1,3], Neil Broderick[2,3]

[1]School of Chemical Sciences, The University of Auckland, New Zealand; [2]Department of Physics, The University of Auckland, New Zealand; [3]Dodd-Walls Centre for Quantum and Photonic Technologies, New Zealand; cbai804@aucklanduni.ac.nz

The introduction of controlled polymerization techniques to polymer networks has allowed us to create “Living polymer networks (LPNs)”. These combine the versatile and adaptable nature of methods such as RAFT and ATRP with macro-scale 3D networks to produce materials capable of undergoing various 4D transformations. Typically 4D materials are restricted to particular transformations; however, these LPNs can perform either a single or multiple transformations, both sequentially and simultaneously.

Our focus has been on creating RAFT networks and demonstrating a number of the potential transformations. We use visible light photo-RAFT techniques to both produce and modify our networks, with the process driven by either photocatalysts or direct activation of the RAFT agent. Some of our published work includes 3D/4D printing, surface modification, stimulus-response, size and mass growth, physical property modification, self-healing, and growth-induced bending. Furthermore, the use of light allows us a great deal of spatial and temporal control over the growth process. Together this demonstrates the use of living polymer networks as a platform for performing 4D transformations.

9:09am - 9:21am

Doping epitaxial Pb(Zr,Ti)O3 thin films

Lucian Pintilie, Georgia Boni, Cristina Chirila, Iuliana Pasuk, Lucian Trupina, Cristian Radu, Lucian Filip, Ioana Pintilie

National Institute of Materials Physics, Romania; pintilie@infim.ro

Undoped, p-doped (Fe) and n-doped (Nb) epitaxial Pb(Zr,Ti)O3 (PZT) films were grown on (001) orientated SrTiO3 (STO) substrates with bottom SrRuO3 (SRO) electrodes. The doping was of about 1 % atomic. The films were grown from nominally undoped, Fe-doped (PZT-Fe) and Nb-doped (PZT-Nb) targets, respectively. Further on, p-n PZT homojunctions were grown by successive deposition of PZT-Nb and PZT-Fe layers on SRO/STO substrates.

The structural and electrical properties of the deposited layers were thoroughly investigated and the following important results were obtained:

- The structural differences between undoped, Fe-doped and Nb-doped films are minor, but the differences in the electrical properties are significant. Notably, the leakage current is lower with more than two orders of magnitude in PZT-Nb compared to PZT-Fe and undpoed PZT, which is correlated to a larger potential barrier at the electrode interfaces (about 0.3 eV, compared to 0.1-0.15 eV).

- The polarization orientation can be controlled through doping. By careful PFM experiments, it was found that PZT-Nb has upward polarization in the as-grown state, while PZT-Fe has downward polarization (see figure 1). This behavior can be explained by the change in the sign of the charges involved in the compensation of the depolarization field during polarization switching (electrons and positive donors versus holes and negative acceptors).

- The p-n homojunctions have an abnormal behavior, showing well defined hysteresis loops although the current-voltage characteristics are nearly linear, as for a resistor. The capacitance of the p-n PZT homojunction is larger than that of the component layers, indicating a possible steady state negative capacitance effect. These findings may be explained by different polarization orientations in the component layers.

9:21am - 9:33am

Novel ferroelectric materials of kappa-Al2O3

Shintaro Yasui[1], Tsukasa Katayama[2], Yosuke Hamasaki[3], Jianding Yu[4], Mitsuru Itoh[5]

[1]Tokyo Institute of Technology, Japan; [2]Hokkaido University, Japan; [3]National Defense Academy, Japan; [4]Chinese Academy of Science, China; [5]National Institute of Advanced Industrial Science and Technology, Japan; yasui.s.aa@m.titech.ac.jp

Perovskite type structured ferroelectric materials such as BaTiO3 and Pb(Zr,Ti)O3 and related compounds have been used for memory, sensor and various applications since they are found around 70 years ago. Since Perovskite-type ferroelectrics are found, they have been used until now because of their superior ferroelectric and piezoelectric properties. To evolve forward from this situation, we would like to suggest novel ferroelectric/ferrimagnetic ferroelectric which has k-Al2O3 type crystal structure classified as polar Pna21 space group. This structure consists of the corundum-type and spinel-type staking layers along c-axis. The corundum and spinel layers consist of only oxygen-octahedra, and mixture of oxygen-octahedra and oxygen-tetrahedra, respectively. Spontaneous polarization direction is c-axis. It is note that coordination recombination from octahedra to tetrahedra (6 to 4) and tetrahedra to octahedra (4 to 6) in spinel layer is occurred during polarization switching. At the same time, corundum layer moves right and left alternately along in-plane a-axis which is like shear motion. This polarization switching system is optimized by first principal calculation. However, almost all of the materials with k-Al2O3 type crystal structure are metastable phase, which is difficult to prepare conventional technique in chemical equilibrium. Here, we succeeded to prepare this structure's materials by physical vapor deposition technique. We would like to introduce novel ferroelectricity of this material's family.

[1] Hamasaki et al., APL 104, 082906 (2014), [2] Hamasaki et al., Cry. Growth. Des. 16, 5214 (2016), [3] Hamasaki et al., APL 109, 162901 (2016), [4] Hamasaki et al., JAP 122, 015301 (2017), [5] Katayama et al., APL 110, 212905 (2017), [6] Katayama et al., Adv. Funct. Mater. 28, 1704789 (2018), [7] Yasui et al, J. Ceram. Soc. Jpn, 127, 474 (2019), [8] (12) Rao et al., J. Mater. Chem. C, 8, 706-714 (2020), [9] Rao et al., ACS Appl. Electro. Mater. 2, 1065-1073 (2020).

9:33am - 9:45am

Manufacturing with light: multimaterial 3D printing through selective crosslinking and metallization

Jose Marques-Hueso, Adilet Zhakeyev, Mansour Abdulrhman

Heriot-Watt University, United Kingdom; J.Marques@hw.ac.uk

The astonishing growth that the additive manufacturing sector has experienced has been fostered by two pillars: engineering innovation and improved materials. However, integration of different materials is still limited, both in techniques and materials, which reveals one of the growth areas in the next few years.

In this work we present different approaches to tackle the problem of multimaterial additive manufacturing, with an emphasis in techniques that use light as a driver, such as laser writing and stereolithography.

First, a method for the direct light writing of metallic microtracks on different 3D printed materials is presented [1]. The method relies on the synthesis of silver nanoparticles on the surface of the polymer substrates through direct laser writing, and their use as seeds for metal plating. Catalytic techniques, including the use of plant extracts [2], accelerates the nanoparticle formation by up to two orders of magnitude. Polymers of interest to the microelectronics and 3D printing industries, including biodegradable materials and elastomers [3], are patterned by light using this photography-inspired technique with high throughput, and track widths of 25 µm.

Next, an approach to overcome printing depth by stereolithography is presented. Photopolymer resins used in stereolithographic 3D printing are limited to penetration depths of only a few millimetres, which suppose additional limitations, such as only being able to write in a 2D contour at a time. The use of non-linear effects, namely upconversion [4], is used here to enhance the penetration depth. This approach uses near-infrared (NIR) to ultraviolet-blue upconversion emissions from NaYF4:Yb3+,Tm3+ phosphors to initiate monomer crosslinking at a much higher depth. This concept relies on the use of invisibility windows and non-linear optical effects to achieve selective crosslinking in photopolymers. This opens a myriad of possibilities to create samples with different materials.

REFERENCES

[1] MARQUES-HUESO, J., JONES, T.D.A., WATSON, D.E., ET AL., 2018, A Rapid Photopatterning Method for Selective Plating of 2D and 3D Microcircuitry on Polyetherimide, Advanced Functional Materials 28 (6), 1704451

[2] MARQUES-HUESO, J., JONES, T.D.A., WATSON, D.E., ET AL., 2020, Spinach-based photo-catalyst for selective plating on polyimide-based substrates for micro-patterning circuitry, Chemical Engineering Research and Design 153, 839-848

[3] RYSPAYEVA, A., JONES, T.D.A., NEKOUIE ESTAFAHANI., ET AL., 2019, Selective Metallization of 3D Printable Thermoplastic Polyurethanes, IEEE Access 7, 104947-104955

[4] JONES, C.M.S., GAKAMSKY, A., MARQUES-HUESO, J., 2021, "The upconversion quantum yield (UCQY): a review to standardize the measurement methodology, improve comparability, and define efficiency standards", Science and Technology of Advanced Materials, 22:1, 810-848, doi.org: 10.1080/14686996.2021.1967698

9:45am - 9:57am

Naphthol-based phenolic polymer modified silica as a multi-mode chromatographic stationary phase

永シン 胡, 誠 高藤
Kumamoto University, Japan; huyongxing210@gmail.com

We try to introduces a novel phenolic resin-coated silica stationary phase grafted from the surface of amino-functionalized silica through copolymerization of 1,5-dihydroxynaphthalene and 1,3,5-trioxane in the dispersed state, followed by low-temperature calcination at 200 °C [1]. The new stationary phase was evaluated by elemental analysis, scanning electron microscopy, thermogravimetric analysis, Brunauer Emmett-Teller analysis and Fourier-transform infrared spectroscopy. The new column has the capability to separate different types of compounds. When utilizing hydrophilic interaction liquid chromatography, sulfonamide drugs and nucleosides/nucleobases could be separated with good resolution even if there were no buffer salts in the eluent. In reversed-phase liquid chromatography, the column indicated satisfactory separation abilities for positional isomers, alkylbenzenes and polycyclic aromatic hydrocarbons. The selectivity and retention of the new column for PAHs were higher than those for alkylbenzene, which may be affected by the π–π interactions between the PAH analytes and naphthalene ring from the surface of the silica. Depending on the retention mode, the elution order can be reversed using this column. Thus, the stationary phase was intended as a novel mixed-mode column. Meanwhile, the retention and selectivity can be adjusted very flexibly by changing the chromatographic conditions.

9:57am - 10:09am

Network Relaxation in Ion Conducting Polymers: A Study based on the BSCNF Model

Masaru Aniya[1], Masahiro Ikeda[2]
[1]Kumamoto University, Japan; [2]National Institute of Technology, Oita College, Japan; aniya@gpo.kumamoto-u.ac.jp

The understanding of fundamental materials properties is a key factor for the development of functional materials. In a recent study, the Bond Strength-Coordination Number Fluctuation (BSCNF) model of structural relaxation developed in our group was applied to understand the Li+ ion concentration dependence of the fragility in Li+ ion conducting polymers [1]. The analysis based on the model also revealed that the degree of cooperativity or the number of correlated structural units involved in the network relaxation decreases with the Li+ ion content. These studies suggest that our BSCNF model could provide a framework to understand the correlation between the molecular mobility and the fragility index of the system. In the present contribution, such a possibility will be explored. On the other hand, many studies have recognized that an important characteristic of ionic conducting disordered systems is the decoupling between the structural and electrical relaxations [2]. The decoupling in polymer electrolytes will be also discussed based on the same BSCNF model.

[1] ANIYA, M. & IKEDA, M. Network Relaxation and Cooperativity in Ion Conducting Polymers PEO-Li: An Analysis based on the BSCNF Model. Key Eng. Mater., accepted.

[2] WANG, Y. & SOKOLOV, A.P. 2015. Design of superionic polymer electrolytes. Curr. Opin. Chem. Eng., 7, 113-119.

10:09am - 10:21am

Novel carboxymethyl chitosan Zn-doped hydroxyapatite scaffold for bone tissue engineering

Ayoub GROULI, Yahya Bachra, Mohammed Talbi, Mohammed Berrada
Faculty of Sciences Ben M'Sick, University Hassan II of Casablanca, Morocco; grouliayoub@gmail.com

In recent years, chitosan (CS) has attracted great interest from scientists as a functional polymer due to its remarkable intrinsic properties: biodegradability, biocompatibility, non-toxicity, antibacterial, mucoadhesive, analgesic and anti-inflammatory activities [1].

We have developed a new CM-CS/ZnHA biocomposite using Carboxymethyl-Chitosan and Zinc doped hydroxyapatite (ZnHA). Zinc doped Hydroxyapatite was synthesized using a calcium precursor derived from eggshells obtained by the precipitation method.

The uniform mixture of Carboxymethyl-chitosan and ZnHA was freeze-dried to obtain a porous biocomposite. The fabricated biocomposite was characterized by FTIR, XRD and SEM. In addition, the antibacterial, swelling, biodegradation, viability and cell proliferation capacity of the fabricated biocomposite was evaluated [2]. The biocomposite showed improved swelling and antibacterial activities. The Zn doped Hydroxyapatite (HA) improved the antibacterial activity. Biocompatibility studies were performed using osteoblast cells and proved the non-toxic nature of the biocomposite. The osteoblast cell adhesion studies demonstrated that the cells were attached and infiltrated within the biocomposite. The results obtained encourage the use of this Biocomposites for different types of wounds with infection and bleeding and especially in bone tissue repairing.

10:21am - 10:33am

Molecular Junction Built in Nanowires and Electrical Characterization

Ramazan KIZIL

Istanbul Technical University, Turkey; kizilr@itu.edu.tr

Electron transport through molecular junction is the most fundamental characteristic for molecular electronic devices. Molecular junctions can be prepared using a prior sophisticated break junction methods, such as mechanically or scanning probe controlled break junctions or electromigration, to create nanometer scale separated metallic contacts and self-assembly of a molecule in the gap. Electrical coupling between the molecule and the contact is another concern when charge transfer of a molecular circuit is considered. A molecular junction built in hybrid nanostructure in a form of metal-molecule-metal however will provide a useful interconnect for molecular electronics enabling a reliable and strong metal-molecule coupling.

This talk will cover synthesis of a novel self-assembled polymeric molecular junction of biphenyl dithiol (BPDT) in the middle of a Au nanowire with a total length of 7.5 - 8.0 micrometer and 300 nm diameter. The extent of the polymeric BPDT molecular section in the hybrid nanowire was made in 20 to 30 nm to study length dependent charge transport through DC mode room temperature I-V measurements. A single hybrid nanowire was trapped across a lithographically defined microelectrode pair using AC dielectrophoresis. The current carrying capacity of the molecular junction were determined in the nano and microamper regimes with interesting I-V characteristics, showing repeatable conductance switching and hysteresis. The first voltage sweep led to a change in the conduction state of the molecular junction from insulating to conducting around 1.4- 1.6 Volt. A sudden increase in the current was characteristics of most of the hybrid nanowires with a few exception of negative differential conductance behavior. Continuing voltage sweep from -4 to 4 V led to nonlinear response with hysteresis once conductive state was achieved for the molecular junction.

This novel nanowire with molecular junction was characterized using SEM and EDS and its electron transport characteristics studied thoroughly to produce repeatable and interpretative I-V measurements.

10:33am - 10:45am

Development of tin(IV) oxide nanorods as potential layer in solar cells

Arijeta Bafti[1], Ivana Panžić[1], Luka Pavić[2], Vilko Mandić[1]

[1]Faculty of Chemical Engineering and Technology, Croatia; [2]Ruđer Bošković Institute, Croatia; abafti@fkit.hr

Tin(IV) oxide is an earth-abundant, important, and widely used semiconductor with a bandgap of 3.6 eV and known as part of the transparent conductive oxide (TCO) family used in solar cells. [1] Synthetic wise, various routes to fabricate SnO2 nanostructures and nanocrystals have been investigated, including hydrothermal synthesis, thermal evaporation, and various sol-gel methods.

In this work, we report a chemical method for synthesis of nanostructured SnO2 nanoparticles and thin-films. We display the control of nanoparticle size and morphology by varying the reaction conditions and attempt to elucidate the processes behind the formation of the domains. The prepared samples were thoroughly (micro)structurally characterized using XRD, AFM, KPFM and SEM. We observed that by varying the synthesis temperature and tin(iv) chloride concentration, we have prepared films and bulk materials with diverse morphology and other properties, such as the electrical ones, i.e. activation energy for the conduction process. For the potential application of tin(IV) oxide films as a layer in solar cells, the electrical characterization of prepared samples was carried out using impedance spectroscopy (IS) in a wide range of temperature and frequency in attempt to fully control the features of SnO2 surface, including thin-film quality, homogeneity, defects, and surface states. Characterizations indicate chemically and structurally homogeneous samples suitable for facilitating the charge transfer and mitigation of recombination.

Oral Talk-11: Oral Talk

Time: Thursday, 12/Jan/2023: 11:00am - 12:36pm · *Location:* Hall 1&2

11:00am - 11:12am

Gamma-ray induced room temperature ferromagnetism in few layered MoS2 thin films prepared by magnetron sputtering

Aswin kumar Anbalagan, Fang-Chi Hu, Chao-Chin Wang, Hsin-Yi Chen, Chih-Hao Lee

National Tsing Hua University, Taiwan; chlee@mx.nthu.edu.tw

Defect engineering is of great interest to the 2D materials community. If a nonmagnetic TMDs monolayer could possess room temperature (RT) ferromagnetism (FM), then it will not only act as an option for ideal spintronic materials for nanodevices, but also for understanding the relation existing between electronic and magnetic properties of quantum-confined structures. Thus, in this work, we aim to study gamma-irradiation effects on MoS2, which is diamagnetic in nature. We observed that gamma-ray exposure up to 9 kGy on few layered MoS2 films will induce FM behavior at RT with a magnetic moment around 600 emu/cm3 and the highest saturation magnetization has been observed at 10 K indicating the long range ordering of FM behavior. It only can be found at a few layer of MoS2. For hundred of layers of MoS2, no appreciate ferromagnetism can be measured after gamma ray irradiation. Raman spectroscopy results revealed a drastic drop in the intensity of E12g and A1g peaks for the few layered films implying that the defects or lattice distortions have been created in the MoS2 structure after gamma-ray exposure of 9 kGy. X-ray photoelectron spectroscopy (XPS) showed the disappearance of S (2s) bonding peak with Mo (3d5/2). In addition, XPS spectra of Mo 3d doublet shifted towards higher binding energies attributing to an increase in the Mo6+ peak by about 2.5 times after gamma-ray exposure of 9 kGy. These results imply that the MoS2 structure was partial disordered after high dose gamma ray irradiation. Furthermore, to figure out the possible origin of the FM behavior in gamma-irradiated MoS2, DFT calculations have been performed. Among all the different possible scenarios, V(1Mo+2S) seems to be the dominant defects that is responsible for inducing the FM at RT in MoS2. Overall, this study suggests that the occurrence of magnetism in gamma irradiated MoS2 films can be attributed to the combination of defect moments arising from vacancies, lattice deformation and partial destruction of the lattice structure. The few layers of MoS2 which allow the Mo segregated and sulfur removed from the top surface might be the reason that only a few layer of MoS2 possesses ferromagnetism.

11:12am - 11:24am

Liquid Metal-Semiconductor 3D Heterostructured Networks: A New Paradigm in Artificial Neural System

Mohammad Karbalaei Akbari[1,2], Serge Zhuiykov[1,2]

[1]Ghent University Global Campus, Korea, Republic of (South Korea); [2]Ghent University, Faculty of Science, Belgium; serge.zhuiykov@ugent.be

3D tortuous networks endowed with capability of tuning the parallel analysis of informative signals are the critical units for development of artificial enteric neuron system (ENS). Here we report a principally new concept of the artificial afferent ENS with extremely low femto-joule energy processing. The ENS contains inter-connected 3D liquid metal-semiconductor network. The chemo-voltaic driven reactions enabled the micro-fluidity of hydrophobic liquid metal galinstan into porous Ni-TiO2 matrix. The fluidity of liquid alloy facilitated the development of shapeable liquid metal-semiconductor hetero-interface with its characteristics of Ga2O3 surface oxide films [1]. In this configuration, the impregnated liquid metal nodes stand as signal transforming centres and two-dimensional (2D) heterostructured Ga2O3-TiO2 performs as synaptic junction. Through combined conductance imaging spectroscopy and electrical measurements it was demonstrated that the dynamic conductance in synaptic junctions can be modulated to mimic the signal communication and bio-functionalities of ENS, including slow and fast inhibitory and excitatory post-synaptic responses of uniaxonal and multipolar neurons. The ultra-low energy tunable synaptic events (20~ 70 fJ), and notably the coordinated signal recognition at the end of axons of the developed multi-synaptic nodes are the distinguished characteristics of this device. This novel design of 3D liquid metal-semiconductor structure opens up completely new opportunities in development of neuromorphic units and further facilitates the realization of the liquid metal-semiconductor interactions at 2D hetero-interfaces.

11:24am - 11:36am

SNDM Investigation of Carrier Density Distribution in Black Silicon Solar Cell

Yasuo Cho[1], Beniamino Iandolo[2], Ole Hansen[2]

[1]Tohoku University, Japan; [2]Technical University of Denmark,Denmark; yasuocho@riec.tohoku.ac.jp

Black silicon (Si) is a nanostructured type of Si capable of near-total absorption of light. Therefore, the use of black Si can lead to highly efficient solar cells. The performance of Si solar cells is dependent on the active dopant carrier distribution in emitters. The carrier distribution in black Si solar cells has been difficult to measure, and thus to optimize, due to the irregular, nano-scaled structure of the emitter.

On the other hand, one of the authors previously succeeded in quantitatively analyzing such distributions in monocrystalline Si solar cells using scanning nonlinear dielectric microscopy (SNDM) [1][2].

In this paper, we investigated quantitatively the carrier distribution in a phosphorous (P) diffused black Si solar cell using SNDM. As a reference, we also measured the carrier distribution on a flat Si sample fabricated under the same P diffusion conditions. The precise carrier distributions in the emitter were visualized, which revealed the feature of carrier distribution in the emitter of black Si solar cell. The results indicate that the lateral inhomogeneous carrier distributions may influence the power conversion efficiency of black Si solar cell. Moreover, super-higher-order-SNDM [3] was also employed to perform a quantitative analysis of the depletion layer thickness

distribution. It was found that fluctuation of depletion layer thickness of black Si solar cell is much larger than that of flat Si solar cell. This fluctuation may also influence the power conversion efficiency of black Si solar cell.

From above mentioned results, we confirmed that SNDM was a very useful means of investigating carrier distributions in the nano-scaled emitter of black Si solar cell.

[1] HIROSE, K., TANAHASHI, K., TAKATO, H., CHO, Y. 2017. Quantitative Measurement of Active Dopant Density Distribution In Phosphorus-Implanted Monocrystalline Silicon Solar Cell Using Scanning Nonlinear Dielectric Microscopy. Appl. Phys. Lett., 111, 032101.

[2] CHO, Y., JONAI, S., MASUDA, A. 2020. A Scanning Nonlinear Dielectric Microscopic Investigation of Potential-Induced Degradation in Monocrystalline Silicon Solar Cell. Appl. Phys. Lett., 116, 182107.

[3] CHINONE, N., NAKAMURA, T., CHO, Y. 2014. Cross-Sectional Dopant Profiling and Depletion Layer Visualization of Sic Power Double Diffused Metal-Oxide-Semiconductor Field Effect Transistor Using Super-Higher-Order Nonlinear Dielectric Microscopy. J. Appl. Phys., 116, 084509.

11:36am - 11:48am

Scanning Tunneling Microscopy and Spectroscopy of the 2D Layered Nitride Chloride superconductor alpha-TiNCl

Akira Sugimoto[1], Kaito Matsumoto[1], Toshikazu Ekino[1], Masashi Tanaka[2], Alexander M. Gabovich[3]

[1]Hiroshima University, Japan; [2]Kyushu Institute of Technology, Japan; [3]National Academy of Sciences of Ukraine; asugimoto@hiroshima-u.ac.jp

The layered nitride superconductors MNCl (M=Zr, Hf, Ti) are the unique kinds of materials which possess the maximum Tc ~25.5 K, with the two-dimensional (2D) conducting layers of rectangular lattice (alpha- type) or honeycomb lattice (beta-type) of MN networks[1][2].

Here we present the scanning tunneling microscopy and spectroscopy (STM/STS) measurements on both superconducting alpha-NaxTiNCl (x~0.2, Tc~18 K) and semiconducting pristine-TiNCl compounds. The STM topography of both compounds showed the rectangular atomic lattice patterns with the spacing of ~0.38 nm (= a0) and ~0.31 nm (= b0). The averaged dI/dV curves of the superconducting alpha-NaxTiNCl show the superconducting gap value of 2Delta ~12 meV, yielding a gap ratio 2Delta/kBTc ~7.7, while that of e pristine-TiNCl show no gap structure around these several mV bias voltage region. The estimated superconducting gap ratio of alpha-NaxTiNCl (~7.7) is quite resemble in that of the cuprate superconductors, indicating that is the common properties of the layered 2D superconductivity.

11:48am – 12:00pm

The effect of insertion of an ultrathin HfO2 interlayer on Ni/β-Ga2O3 Schottky barrier diode

Madani Labed[1,2], Ji Young Min[1], Juyeon Lee[1], Kyung Hwan Kim[3], You Seung Rim[1]

[1]Department of Intelligent Mechatronics Engineering and Convergence Engineering for Intelligent Drone, Sejong University, Seoul 05006, Republic of Korea.; [2]Laboratory of Semiconducting and Metallic Materials, Algeria; [3]Department of Electrical Engineering, Gachon University, Seongnam-si, Gyeonggi-do 13306, Republic of Korea.; madani.labed@gmail.com

Schottky barrier height control, low leakage current and minimize Fermi level pinning effect are critically important to the design of high performance Schottky barrier diodes. In this work, the effect of insertion of HfO2 with different cycle number on forward current reverse, capacitance and MOSSBD parameters such as ideality factor, on-resistance, threshold voltage and Schottky barrier height…etc. Firstly, we observed that, Schottky barrier heights of Ni/HfO2/β-Ga2O3 Schottky barrier diodes was adjusted in range of 1.04-1.48 eV, in which it was increased by repeated atomic layer deposition cycles from 2 to 8 cycles with different annealing temperature. Thanks to the increase in negative fixed charge with increasing HfO2 cycles number. A high decrease in interfacial state density from 5x1012 (eV-1.cm-2) to 2.74x1011 (eV-1.cm-2) when 2-cycle HfO2 deposited for as-deposited device. Therefore, the Fermi pinning level effect is reduced when an ultrathin HfO2 layer was inserted. In addition, a low leakage current was reported by studying the effect of insertion of an ultrathin HfO2 layer by atomic-layer deposition (ALD) with different cycle number at the interface between Ni and β-Ga2O3 at different annealing temperatures. A leakage current decrease from 5.68x10-3(A/cm²) to 2.97x10-6(A/cm²) at -300 V and a breakdown voltage increase, from 467 V to 556 V, is found when two cycles of HfO2 are inserted and annealed at 400 C.

12:00pm – 12:12pm

Washing and drying of surface modified magnetite nanoparticles using supercritical CO2

Yasuhiko Orita, Kai Ikeda, Wijakmatee Thossaporn, Yusuke Shimoyama

Department of Chemical Science and Engineering, Tokyo Institute of Technology, Tokyo, 152-8550, Japan; orita.y.aa@m.titech.ac.jp

Surface-modified metal oxide nanoparticles (NPs) have attracted major attention because surface modification significantly reduces the surface energy and improves their dispersity in the solvent, which has promoted the development of its direct-synthesis method such as heat-up and hydrothermal methods. Although these methods can control the size, shape and surface property of the NPs, they require the washing and drying operation to purify them. In washing step, remained surfactant between NPs is dissolved into organic solvent using sonication operation and is removed using centrifugation and decantation manner, causing a large amount of liquid waste and complicated operation. In drying step, an evaporation is popular approach that removes the solvent, while it causes the interfacial tension between the liquid and gas, possibly inducing the problem of particle agglomeration. Washing and drying technology using supercritical CO2 are expected to overcome these serious problems. Supercritical CO2 has high solubility of surfactant that is typically used as surface modifier and very high diffusibility, which could allow the high-speed washing without liquid waste. Furthermore,

supercritical CO2 has the merit that there is no interfacial tension to solvent due to the loss of the interface, which could prohibit the particle agglomeration in drying step.

In this work, we aimed to apply the supercritical washing and drying technology to surface modified NPs. To investigate its potential, the surface-modified magnetite NPs were washed using supercritical CO2 at the pressure from 0.1 to 20.0 MPa, N2 at 20.0 MP and ethanol. Additionally, the NPs were dried by vacuum and supercritical drying operation. Surface modified NPs were prepared by hydrothermal method at 200℃ using Fe(OH)2 as a precursor and decanoic acid as a surfactant. Washing efficiencies of the NPs were evaluated by comparing the weight losses of as synthesized and washed sample for TGA analysis. The hydrodynamic diameter of NPs dispersed in hexane with a concentration of 0.01 wt% was measured using DLS method to evaluate the re-dispersity of dried NPs.

In supercritical washing, the increase in the pressure from 0.1 to 20.0 MPa led to the increase in the washing efficiency, which reached 99 % at 20.0 MPa. This washing efficiency is significant higher value than those obtained from ethanol and N2 washing, suggesting the superiority of supercritical CO2 as a washing solvent. Additionally, the NPs, which were washed by ethanol and dried in the vacuum chamber, were not dispersed in hexane while the NPs washed and dried by supercritical CO2 at 20.0 MPa showed good dispersity in hexane and showed the hydrodynamic diameter of 89 nm that was equivalent to twice the primary particle size or less. These results indicate that supercritical CO2 drying effectively prohibits the particle agglomeration and improves their re-dispersity in organic solvent comparing the conventional vacuum drying.

12:12pm - 12:24pm

Ba1/3CoO2: A Thermoelectric Oxide Showing a Reliable ZT of ~0.55 at 600 °C in Air

Xi Zhang[1], Yuqiao Zhang[1], Liao Wu[2], Akihiro Tsuruta[3], Masashi Mikami[3], Hai Jun Cho[1], Hiromichi Ohta[1]

[1]RIES, Hokkaido University, Japan; [2]IST, Hokkaido University, Japan; [3]AIST, Japan; hiromichi.ohta@es.hokudai.ac.jp

Oxide-based thermoelectric materials that show a high figure of merit (ZT) are promising because of their good chemical and thermal stability as well as their harmless nature compared to chalcogenide-based state-of-the-art thermoelectric materials. Here, we show a reliable high-ZT thermoelectric oxide, Ba1/3CoO2. We fabricated Ba1/3CoO2 epitaxial films by the reactive solid-phase epitaxy method (Na3/4CoO2) followed by ion exchange (Na+ → Ba2+) [1] treatment and performed thermal annealing of the film at high temperatures and structural and electrical measurements. The crystal structure and electrical resistivity of the Ba1/3CoO2 epitaxial films were found to be maintained up to 600 °C. The power factor gradually increased to ~1.2 mW m–1 K–2 and the thermal conductivity gradually decreased to ~1.9 W m–1 K–1 with increasing temperature up to 600 °C. Consequently, the ZT reached ~0.55 at 600 °C in air [2].

[1] TAKASHIMA, Y., ZHANG, Y. & OHTA, H. et al. 2020. Layered Cobalt Oxide Epitaxial Films Exhibiting Thermoelectric ZT = 0.11 at Room Temperature. J. Mater. Chem. A, 9, 274-280.

[2] ZHANG, X., ZHANG, Y., WU, L., TSURUTA, A., MIKAMI, M., CHO, H. J. & OHTA, H. et al. 2022. Ba1/3CoO2: A Thermoelectric Oxide Showing a Reliable ZT of ~0.55 at 600 °C in Air. ACS Appl. Mater. Interfaces, 10.1021/acsami.2c08555.

12:24pm - 12:36pm

In situ mechanical testing of nanostructured zinc oxide thin films

Ivana Panzic[1], Michael Wurmshuber[2], Daniel Kiener[2], Vilko Mandić[1]

[1]Faculty of Chemical Engineering and Technology, Marulicev trg 20, 10000 ZagrebCroatia; [2]Department of Materials Science, Chair of Materials Physics, Montanuniversität Leoben, Franz Josef-Straße 18, 8700 Leoben, Austria.; ipanzic@fkit.hr

Zinc oxide is a well know semiconducting metal oxide with high electron mobility, wide bandgap, and large exciton binding energy. Due to its beneficial properties and the vast array of physical and chemical deposition methods that can be used for deriving various nanostructured forms it has been applied in solar cells, sensors, photocatalysis, electronics, etc.

Here we prepared ZnO in the form of thin-film with vertically ordered nanorods by a simple chemical method on different substrates firstly with the aim to elucidate the effect of synthesis and deposition conditions on their mechanical properties. Secondly, the influence of the type of substrate on their mechanical properties was investigated. Shedding more light on both aspects is crucial for further applications. To establish that, we used advanced microscopy (SEM) in combination with in situ mechanical testing in combination with nanoindentation. Samples were additionally characterized by XRD, AFM, KPFM, and bending tests. Sample preparation was aided by the use of a focused ion dual-beam microscope equipped with a femtosecond laser system.

Obtained results were used to quantify the mechanical properties and failures such as cracks, which will enable us to optimize the synthesis and mitigate such events for further applications in flexible solar cells or gas sensors.

Oral Talk-6: Oral Talk

Time: Thursday, 12/Jan/2023: 11:00am - 12:36pm · *Location:* Hall 3

11:00am - 11:12am

Polarization-sensitive UVA photodetector based on heterojunction of ITO and rare-earth doped bismuth ferrite ceramics

Haidee Mana-ay[1,2,3], Cheng-Sao Chen[4], Xin-Hao Wang[5], Chi-Shun Tu[5,2], Pin-Yi Chen[1,2,6]

[1]International Ph.D. Program in Innovative Technology of Biomedical Engineering and Medical Devices, Ming Chi University of Technology, New Taipei City, Taiwan; [2]Research Center for Intelligent Medical Devices, Ming Chi University of Technology, New Taipei City, Taiwan; [3]Department of Physics, Silliman University, Dumaguete City, Philippines; [4]Department of Mechanical Engineering, Hwa Hsia University of Technology, New Taipei City, Taiwan; [5]Department of Physics, Fu Jen Catholic University, New Taipei City, Taiwan; [6]Department of Mechanical Engineering, Ming Chi University of Technology, New Taipei City, Taiwan; haideeimana-ay@su.edu.ph

Ferroelectric photovoltaic materials have been subjected to intensive research in view of their applications for high-performance self-biased UV photodetectors. This work reports the ferroelectric polarization-enhanced near-UV (λ=405 nm) and UVA (λ=360 nm) photoresponse of the indium-tin-oxide (ITO)/(Bi0.93Sm0.07)FeO3/Pt and ITO/(Bi0.93Gd0.07)FeO3/Pt heterostructures. A superior photoresponse was observed in the ITO/(Bi0.93Gd0.07)FeO3/Pt device with photoresponsivity of ~7.3×10^(-2) A/W, specific detectivity of ~2.5×10^11 Jones, and response times of τ_r~1 ms and τ_d~1 s under 360-nm light illumination. The photocurrent generation is facilitated by the interfacial E fields and ferroelectric polarization-induced E field. The improved photosensing ability is ascribed to the collective effect of the electric field-enhanced interaction between oxygen 2p and Fe 3d orbitals and the interconnection of grain boundaries and domain walls that plays roles of charge transport paths. (Bi0.93Gd0.07)FeO3 exhibited a more superior photoresponse than (Bi0.93Sm0.07)FeO3 due to its more complex domain structure, smaller bandgap, and stronger orbital hybridization. These results demonstrate the feasibility of utilizing the ferroelectric polarization and domain structure in (Bi0.93Gd0.07)FeO3 to enhance photodetection, thus providing a route for the realization of a highly sensitive and self-biased visible-UVA photodetector.

11:12am - 11:24am

Synthesis of metal and metal oxide particles via atmospheric-pressure plasma processing with inkjet droplets

Kaishu Nitta[1], Takeru Hato[1], Tomoki Sakai[2], Hitoshi Muneoka[1], Yoshiki Shimizu[3], Kazuo Terashima[1,2,3], Tsuyohito Ito[1,2,3]

[1]Grad. Sch. of Frontier Sci., The Univ. of Tokyo, Japan; [2]Faculty of Eng., The Univ. of Tokyo, Japan; [3]AIST-UTokyo OPERANDO-OIL, AIST, Japan; nitta@plasma.k.u-tokyo.ac.jp

Synthesis of inorganic particles by atmospheric-pressure plasma processing with highly reproducible inkjet droplets will be demonstrated. Microdroplets with a diameter of 20–30 μm containing various metal ions were ejected from an inkjet device and exposed to radio-frequency argon plasma. Particles of gold, zinc oxide (ZnO), and zirconium dioxide (ZrO2) were obtained from chloroauric acid (HAuCl4), zinc acetate (Zn(Ac)2), and zirconium oxychloride (ZrCl2O) solutions. Their diameters can be controlled in the range of sub-microns to several microns by adjusting the concentration of the solution. Because of the high reproducibility of the inkjet droplet diameters (standard deviation of 1–2%), the synthesized particles also had a narrow size distribution, for example, the standard deviation of the synthesized submicron gold particles was in the range of 3–9%. Furthermore, it is suggested that by adjusting the parameters of the solution and plasma, not only dense spherical particles but also hollow or clashed particles can be uniformly obtained. Further Details will be presented at the conference.

11:24am - 11:36am

Zeolite ceramics with ordered microporous structure and high crystallinity prepared by cold sintering process

Jun Zuo Shi, Xiao Li Zhu, Lei Li, Xiang Ming Chen

Zhejiang University, China, People's Republic of; 11926043@zju.edu.cn

4A [Na96(Al96Si96O384)•216H2O] and 13X [Na2(Al2Si3.3O10.6)•7H2O] zeolite ceramics were prepared by cold sintering processes, and the physical properties were investigated together with the structure characterization. There were four primary parameters controlling the preparation process: content of NaOH, pressure, temperature, and holding time. Zeolite ceramics with the idea ordered microporous structure and high crystallinity were obtained at 393 K under 450~550 MPa with a holding time of 5 min from the solution with 20wt% NaOH. A high compressive strength up to 60 MPa and low Young's modulus down to 76 MPa were achieved in 13X zeolite ceramics, and the present ceramics might pride the great application potential as damping materials. Also, the present approach might be used to prepare the zeolite ceramics with idea microporous structure and high crystallinity for other applications.

11:36am - 11:48am

Boosting oxygen evolution reaction performance of Ir/Ta2O5 by synergistic effects of electronic structure modulation and structural design

Chaekyung Baik, Jeong In Cha, Chanho Pak

Gwangju Institute of Science and Technology, Korea, Republic of (South Korea); bck0312@gist.ac.kr

For the efficient utilization of intermittent electricity produced by renewable energies, the proton exchange membrane water electrolyzer (PEMWE) has been attracting significant attention by converting surplus electric energy into a form of transportable hydrogen energy [1]. Since the oxygen evolution reaction (OER), which occurs at the anode of the water electrolyzer, is sluggish and proceeds under harsh conditions (e.g., low pH, high V), noble metals have been used as OER active materials [2]. It is a challenging issue to improve OER catalytic activity while decreasing the amount of the noble metal to the level of 0.01 g kW-1 in the membrane-electrode-assembly (MEA) to commercialize PEMWE at a GW per year scale in the near future [2]. Since iridium oxide (IrO2) catalysts are stable and fairly active in the water oxidation reaction, researchers have been focusing on increasing the activity and stability of iridium-based catalysts [2, 3]. One of the most effective strategies is to develop Ir-supported catalysts. It improves the OER catalytic activity and stability by increasing the active sites and restraining Ir agglomerations while reducing Ir loading level [3]. In this study, mesoporous Ta2O5 with a high surface area (>100m2/g) was synthesized through the soft-template method. The Ir nanoparticles were supported on porous Ta2O5 by the formic reduction method. The mesoporous structure of support and layered structure of Ir are attributed to the uniform dispersion of Ir on Ta2O5. XPS and XAS analysis showed the oxidation states of Ir(0) with Ta(IV) with peak shift owing to strong metal-support interaction (SMSI). The uniform Ir dispersion on the support improved electrical conductivity and electrochemically active surface area (ECSA). The uniform dispersion of Ir and SMSI effect between Ir and Ta improved OER activity (288 mV/cm2) and mass activity (876.1 A/g at 1.55 V). The enhanced OER performance toward Ir Black was further demonstrated in PEMWE single cell analysis and exhibited stable operation over 120 h at 1 A cm-2.

[1] GAHLEITNER, G. 2013. Hydrogen from renewable electricity: An international review of power-to-gas pilot plants for stationary applications. International Journal of hydrogen energy, 38, 2039-2061.

[2] SHIRVANIAN, P. & VAN BERKEL, F. 2020. Novel components in Proton Exchange Membrane (PEM) Water Electrolyzers (PEMWE): Status, challenges, and future needs. A mini review. Electrochemistry Communications, 114, 106704.

[3] VAN PHAM, C., BþHLER, M., KNøPPEL, J., BIERLING, M., SEEBERGER, D., ESCALERA-LõPEZ, D., MAYRHOFER, K. J., CHEREVKO, S. & THIELE, S. 2020. IrO2 coated TiO2 core-shell microparticles advance performance of low loading proton exchange membrane water electrolyzers. Applied Catalysis B: Environmental, 269, 118762.

11:48am - 12:00pm

Development of High-efficiency Si Tandem Solar Cells for Vehicle Integrated Photovoltaics

Masafumi Yamaguchi[1], Kyotaro Nakamura[1], Ryo Ozaki[1], Nobuaki Kojima[1], Yoshio Ohshita[1], Taizo Masuda[2]

[1]Toyota Technological Institute, Japan; [2]Toyota Motor, Japan; masafumi@toyota-ti.ac.jp

Development of high-efficiency solar cell modules and expanding their application fields are significant for the further development of photovoltaics (PV) and the creation of new clean energy infrastructure based on PV. Notably, the development of PV-powered electric vehicle (EV) applications is desirable and very important for this end. Previously, the authors presented impacts of solar cell module efficiency upon CO2 emission reduction, battery storage cost saving and driving distance increase of vehicles [1, 2]. In addition, the authors have shown that 2, 3, 4, 5 and 6-junction solar cells have potential efficiencies of 36.6%, 44.0%, 48.8%, 50.4% and 51.4%, respectively [3]. However cost reduction of solar cell modules is also very important for VIPV (vehicle integrated photovoltaics). The Si-based tandem cells [4] that combine Si with other materials such as III-V compound, II-VI compound, perovskite chalcopyrite, and so forth are desirable for realizing super high-efficiency and low cost.

This analytical results shows that the 2-juncton and 3-junction Si tandem solar cells have potential efficiencies of 36% and 42%, respectively. Based on driving test data for Toyota Prius demonstration car [1], driving range for PV-EV powered by various solar cells and modules were analyzed. The PV-EV powered by the Si tandem solar cell modules with an efficiency of more than 35% is shown to have potential of driving distance of more than 30 km/day average and more than 50 km/day on a clear day.

In this paper, our recent approaches are also shown The Toyota Prius demonstration car powered by using Sharp's high-efficiency III-V 3-junction solar cell modules with module efficiency of more than 30% (output power of 860W) has shown actual driving distance of 29.1 km/day at 4.1 kWh/m2/day irradiation and 36.6 km/day at 6.2 kWh/m2/day irradiation conditions, respectively. Properties of single crystalline Si heterojunction (SHJ) solar cell fabricated in this study were also analyzed in this study. The SHJ cells fabricated in this study have shown 23.3% under 1-sun illumination. Because the Si bottom solar cells operate under lower illumination intensity condition compared to Si solar cells under 1-sun illumination, illumination intensity properties of solar cells were analyzed in this study. The current status of efficiencies of our Si bottom cell, upper III-V 2-junction solar cell and III-V//Si 3-junction tandem solar cell are shown to be 5.2% and 28.6% and 33.8%. Some ways such as improving external radiative efficiencies of sub-cells, optimization of bandgap energies of sub-cells and photon management to realize more than 40% efficiency are discussed.

References

[1] M. Yamaguchi et al., Prog. Photovolt. 29, 684 (2021).

[2] M. Yamaguchi et al., Energy and Power Engineering 13, 147 (2021).

[3] M. Yamaguchi et al., J. Appl. Phys. 129, 240901 (2021).

[4] M. Yamaguchi et al., J. Phys. D. Appl. Phys. 51, 133002 (2018).

12:00pm - 12:12pm

Enhancing the Performance of Quasi-Solid Dye-Sensitized Tandem Solar cells Under Low-Concentrated Light

Fadzai Lesley Chawarambwa, Masaharu Shiratani, Erna Tika Putri
Kyushu University, Japan; lesleychawaz@gmail.com

Dye-sensitized tandem solar cells (DSTC) with various dyes are a promising approach that provides broader harvesting efficiency of the solar spectrum. However, the reduced transparency of the DSSCs limits the performance of the solar cells. Such a challenge can be addressed by utilizing optical concentrators to enhance the performance of solar cells. However, the performance of liquid dye-sensitized solar cells (DSSCs) under concentrated light is normally limited by temperature. Increments in temperature in the DSSCs produce large variations in energy conversion efficiency, which decreases at a constant rate. Liquid electrolytes are also volatile, leading to leakage, which in turn reduces the long-term stability of the DSSC. To circumvent these challenges, printable polymer gel electrolytes (PGEs) can be utilized. In this study, PGEs with TiO2 nanofillers were utilized in the fabrication of two quasi-solid dye-sensitized solar cells (QSDDSC) with two different organic dyes (Z709 and N749).

To construct the quasi-solid dye-sensitized tandem solar cell (QSDSTC) with a broader and more integrated absorption band, two QSDSSCs of organic dyes (N749 and DN709) were stacked together in parallel connection. The results indicated that QSDSTC exhibited enhanced conversion efficiency compared to a single QSDSSC. The efficiency of the QSDSSCs with the N749 and Z907 dyes were 3.95% and 4.55% respectively. Under focused light, the system efficiency of a QSDSTC was 24.08%, a performance enhancement above 5 times that of a single QSDSSC. Furthermore, we studied the impact of light soaking time on the photovoltaic performance of QSDSSCs under focused, concentrated light. The QSDSTC has exhibited higher predominant stability due to the 3-D frame formed by the nanofillers and polymers, which effectively prevent evaporation and leakage of the electrolyte. Hence, our QSDSTC retains high efficiency at a higher temperature.

12:12pm - 12:24pm

Highly Stable Perovskite QDs for Light-Emitting Diode Applications

CHANG-LYOUL LEE
Gwangju Institute of Science and Technology (GIST), Republic of Korea; vsepr@gist.ac.kr

Perovskite QDs have attracted lots of attention due to their outstanding opto-electrical properties. However, poor structural instability under environmental conditions are fetal problems to be solved for commercialization. The high structural instability for perovskite QDs can be realized by preventing ligand dissociation and defect generation. In this work, highly stable perovskite QDs were realized by introducing (1) cross-linkable ligand, (2) core-shell structure and (3) alkali metal doping.

12:24pm - 12:36pm

Stable High-Performance 3D Supercapacitor Electrodes by Templaring Polypyrrole on Cellulose Nanocrystals

Zuxin Sun[1], Samuel Eyley[1], Yongjian Guo[2], Reeta Salminen[1], Wim Thielemans[1]
[1]KU Leuven, Belgium; [2]Ghent University, Belgium; wim.thielemans@kuleuven.be

Porous three-dimensional (3D) structures generally improve the performance of electrodes by increasing the active surface area and the diffusion speed of electrolyte ions during charging/discharging. In past work, we created thick 3D electrode materials by electropolymerizing pyrrole (Py) in the presence of carboxylated cellulose nanocrystals.1,2 To investigate the effect of supporting electrolyte and ions on the preparation of these electrode materials, we electrodepositied polypyrrole in the presence of varying amounts of chloride anions (Cl-) and carboxylated cellulose nanocrystals (CNC-COO-). The deposited structure is formed by a combined effect of different nucleation and growth mechanisms induced by CNC-COO- and by Cl- during electropolymerization. The result is that the 3D porous structure of the PPY supported on the CNC-COO- scaffold can be modulated by controlling the Cl- to CNC-COO- ratio, with a direct effect on its performance as supercapacitor electrode material.

The highest area capacitance reached was 1.34 F cm-2 (142.9 F g-1) at a current density of 2 mA cm-2 (0.2 A g-1). More importantly, at a high current density of 20 mA cm-2 (2.2 A g-1), thick (ca.130 µm), 3D, and high mass loading (9.2 mg cm-2) Cl-:CNC-COO-/PPy films exhibited a high areal capacitance of 0.85 F cm-2 (70.8 F g-1), increasing about 16 % over CNC-COO-/PPy films prepared in the absence of Cl- present during electrodeposition. In addition, an aqueous Cl-:CNC-COO-/PPy (with Cl-:CNC-COO- = 2.0) symmetric supercapacitor had a high areal capacitance of 0.60 F cm-2 (55.02 F g-1) at 1 mA cm-2 (0.10 A g-1), an energy density of 83.38 µWh cm-2 (7.64 Wh Kg-1) and good cycling stability, indicating their potential in energy storage devices. In my presentation, I will go into detail into the mechanisms, characterisation, and performance of electrode materials made with different Cl-:CNC-COO- ratios.

Oral Talk-7: Oral Talk

Time: Thursday, 12/Jan/2023: 2:00pm - 3:36pm · *Location:* Hall 1&2

2:00pm – 2:12pm

High Performance Evaporative Cooling Using Biomass-based Hierarchically Porous All-Day Evaporator

Jihun Choi, Bokyeong Sohn, Minjae Song, Sangmin Jeon

Pohang University of Science and Technology, Korea, Republic of (South Korea); jhchoi4@postech.ac.kr

We developed a 3D solar steam generator with the highest evaporation rate reported so far using a carbonized luffa sponge (CLS). The luffa sponge consisted of entangled fibers with a hierarchically porous structure; macropores between fibers, micro-sized pores in the fiber-thickness direction, and microchannels in the fiber-length direction. The microchannels in the fiber-length direction transported water to the top surface of the CLS by capillary action, and the micro-sized pores in the fiber-thickness direction delivered water to the entire fiber surface. The water evaporation rate was 14.5 kg m−2 h−1 under 1-sun illumination and 2 m/s wind that corresponded to the highest evaporation rate ever reported under the same condition. In addition, it was found that the air temperature dropped by 3.6 °C when the wind passed through the CLS because of the absorption of the latent heat of vaporization. The heat absorbed by the CLS during water evaporation was calculated to be 9.7 kW/m2 under 1-sun illumination and 2 m/s wind, which was 10 times higher than the solar energy irradiated on the same area (1 kW/m2).

2:12pm – 2:24pm

Highly efficient moisture-driven power generators using laser induced graphitization of sodium chloride-impregnated cellulose nanofiber films

Jakyung Eun, Seonghye Ha, Sangmin Jeon

POSTECH, Korea, Republic of (South Korea); eun1806@postech.ac.kr

High performance moisture-driven power generators were developed by laser induced graphitization (LIG) of sodium chloride-impregnated cellulose nanofiber films (CNFs). CNFs impregnated with different amounts of NaCl were obtained by immersing CNFs in NaCl solutions of various concentrations. A CO2 laser engraver was employed to convert the CNFs to porous graphitic carbon films (GCFs) under ambient conditions. By focusing the laser beam on the top surface of the CNF, the laser intensity was the highest on the top surface and gradually decreased toward the bottom surface. Since the focal temperature of the laser beam was higher than the boiling point of NaCl, the NaCl particles near the top surface evaporated more rapidly, creating a NaCl concentration gradient along the thickness direction. When the GCF was exposed to moisture, the dissociated ions migrated between the top and bottom surfaces, producing an electrical current. The maximum voltage and current outputs were 0.65 V and 550 μA/cm2, respectively, at 90% relative humidity (RH). Due to abundant dissociated ions, the current output was produced continuously rather than pulsed, and was the highest current reported so far. We demonstrated that six vertically stacked GCFs (each 3 mm × 3 mm × 240 μm in size) at 75% RH were sufficient to turn on green light emitting diodes (LEDs) operating at an onset potential of 2 V for 48 h without any auxiliary devices, such as rectifier circuits and capacitors.

2:24pm - 2:36pm

High-efficiency energy storage in Nd-doped BiFeO3–BaTiO3 dielectric capacitor

Chi-Shun Tu[1], Shu-Yu Chen[1], R.R. Chien[2], Cheng-Sao Chen[3], Pin-yi Chen[2]

[1]Fu Jen Catholic University, Taiwan; [2]Ming Chi University of Technology,Taiwan; [3]Hwa Hsia University of Technology, Taiwan; chishun.tu@gmail.com

Dielectric capacitors as energy storage electronics have attracted attention because they exhibit high power density due to their fast charge-discharge rates. This study highlights the high energy-storage performance using MnO2–added (1-x)(Bi0.7Nd0.3FeO3)-x(BaTiO3) (x=0.2-0.45) ceramics through tailoring microstructures and local polar order. Substitution-driven structural transitions were identified from a co-occurrence of nonpolar pseudo-cubic Pm-3m and ferroelectric rhombohedral R3c symmetries to antipolar/nonpolar orthorhombic symmetries as BaTiO3 increases. Recoverable energy densities (Wrec) of 2.6 J/cm3 and efficienchy (η) of 89% were achieved at x=0.45. The improved energy storage is associated with microstructure modification and complex grain matrix, consisting of grain boundaries, and nanocluster structures (or core-shell structures). The nanocluster structures act as barriers to suppress polar order and to enhance dielectric breakdown strength. This work provides an efficient route to utilize BiFeO3-BaTiO3 ceramics for dielectric capacitors.

2:36pm - 2:48pm

Optimized electric-energy storage in BiFeO3–BaTiO3 ceramics via microstructure tailoring

Rhys Hinampas Montecillo[1,2], Cheng-Sao Chen[3], Yi-Tsung Lee[4], Pin-Yi Chen[1,4], Chi-Shun Tu[1,5]

[1]International Ph.D. Program in Innovative Technology of Biomedical Engineering and Medical Devices, Ming Chi University of Technology, New Taipei City 24301, Taiwan; [2]Department of Physics, Silliman University, Dumaguete City, 6200, Philippines; [3]Department of Mechanical Engineering, Hwa Hsia University of Technology, New Taipei City 23567, Taiwan; [4]Department of Mechanical Engineering, Ming Chi University of Technology, New Taipei City 24301, Taiwan; [5]Department of Physics, Fu Jen Catholic University, New Taipei City 24205, Taiwan; rhyshmontecillo@su.edu.ph

This study demonstrates the high energy-storage performance using 0.1 wt.% MnO2–added 0.7(Bi(1- x)Sm(x)FeO3)-0.3(BaTiO3) (x = 0-0.3) ceramics through tailoring microstructures and polar order. Sequentially substitution-driven structural transitions were identified from a co-occurrence of nonpolar pseudo-cubic Pm-3m and ferroelectric rhombohedral R3c symmetries to antipolar orthorhombic Pbam and nonpolar orthorhombic Pnma symmetries as Sm substitution increases. Recoverable energy densities (Wrec) of ~4.5 J/cm^3 and ~4.1 J/cm^3 with efficiencies (η) of ~62.1% and 78.1% can be achieved respectively for x = 0.15 and 0.2 at a field of 220 kV/cm. The improved energy storage can be associated with microstructure modification and complex grain matrix, consisting of grain boundaries, nanocluster structures (or core-shell structures), and polar nano-regions. The nanocluster structure may act as a barrier to suppress polar order and to enhance dielectric breakdown strength. This work provides an efficient route to utilize binary BiFeO3-BaTiO3 ceramics for electrical energy storage.

2:48pm - 3:00pm

PERFORMANCE CHARACTERISTICS OF BIFACIAL DYE-SENSITIZED SOLAR CELLS WITH A V-SHAPE LOW CONCENTRATING LIGHT SYSTEM

Tika Erna Putri[1], Fadzai Lesley Chawarambwa[2], Attri Pankaj[3], Kunihiro Kamataki[4], Naho Itagaki[5], Kanuzori Koga[6], Masaharu Shiratani[7]

[1]kyushu university, Japan; [2]kyushu university, Japan; [3]kyushu university, Japan; [4]kyushu university, Japan; [5]kyushu university, Japan; [6]kyushu university, Japan; [7]kyushu university, Japan; p.tika@plasma.ed.kyushu-u.ac.jp

The abundance of solar energy shows the significant role of solar cell technology in solving global energy crises and environmental problems caused by the depletion of fossil fuel reserves. Among available solar cells, dye-sensitized solar cells (DSSCs) are attractive due to their simple fabrication process, low cost, performance stability, and eco-friendly. Despite these advantages, the low power output and efficiency of less than 10% still becomes a major bottleneck in DSSCs. On the other hand, the bifacial structure can utilize the front and rear surface illumination to enhance the light-harvesting of DSSCs. Besides, the light-harvesting can be further increased by adding a concentrator to capture direct sunlight as well as diffused light. Here, we successfully increased the power output (Pout) of bifacial DSSCs by applying a V-shape system of concave mirror concentrators.

Bifacial DSSCs were fabricated using the doctor blade method. The effect of the measurement time, tilt angle, and mirror distance were investigated with the V-shape concentrator as a parameter of mirror tilt angle (15°, 30°, 40°, 45°, 60°, 75°) and mirror distance x (0, 1, 2, 3, 4) cm between the mirrors and the solar cells. The power density (mW/cm2) depends on the mirror tilt angle. At some tilt angles, the light passes through solar cells in multipath ways, significantly enhancing the Pout and the apparent efficiency.

The result shows that the concave concentrator is more effective than the plane concentrator to boost the Pout of bifacial DSSCs. The temperature raised by the applied concave concentrator can be controlled by adjusting the distance between mirrors and the solar cells. The V-shape plane mirror concentrator could produce 6.42 mW/cm2 in Pout with optimum tilt angles of 60° and a stable temperature at 57 °C for 2.5 h measurement. The concentrated irradiation light with a V-shape concave mirror concentrator could produce 24.3 mW/cm2 Pout with a rapid increase in temperature to more than 80 °C after 30 min of operation. The distance adjustment to 1 cm between concave mirrors and solar cells can reduce the temperature effect to 60 °C for a 3 h measurement with an average Pout ~17 mW/cm2. This condition successfully boosts 4 times more than without the mirror condition.

.

3:00pm – 3:12pm

Performance enhancement of dye-sensitized solar cells via stepwise co-sensitization of two metal-based sensitizers

Fadzai Lesley Chawarambwa, Erna Tika Putri, Masaharu Shiratani

Kyushu University, Japan; lesleychawaz@gmail.com

Co-sensitization is an excellent technique to enhance the performance of a dye-sensitized solar cell (DSSCs) using a stepwise co-sensitization approach. Herein a ruthenium-based sensitizer (Z907) and an organic sensitizer (SQ2) with complementary absorption spectra (300-750nm) have been selected to investigate how the dye loading procedure and dye soaking time would influence the photovoltaic performance of the co-sensitized DSSCs. Interestingly, the results indicate an increase in the IPCE of the co-sensitized DSSCs in the 620-720 nm range. From Fig.1 it can be observed that there is a general increase in overall IPCE as the soaking time in SQ2 dye is increased from 0 to 1 hr. However, a further increase in SQ2 dye soaking time results in significant IPCE reduction between the 400-620 nm range. Energy dispersive spectrometry indicates that the loading amounts of pre-adsorbed Z907 are replaced by post-adsorption of SQ2. However, the replacement adsorption is not observed when the two dyes are loaded in reverse, which is ascribed to their different binding energies and adsorption configurations. Upon optimization, the co-sensitized DSSC exhibits efficiency (5.75%) enhancement of 12% and 462% compared with the DSSC with single Z907 (5.12%) and SQ2 (1.06%), respectively. The results indicate that by choosing appropriate dye loading procedure and soaking time, stepwise sensitization of the TiO2 films with co-sensitizers with different adsorption properties can lead to enhanced spectral absorption and cell performance

3:12pm – 3:24pm

Modulation of contact barrier between two-dimensional material and transparent electrode for high performance transparent Schottky solar cells

Xing He, Toshiro Kaneko, Toshiaki Kato

Tohoku University, Japan; he.xing.b1@tohoku.ac.jp

Transition metal dichalcogenide (TMD) is one of the most attractive materials for future transparent and flexible optoelectrical devices due to their atomically thin structure, band gap in visible light range, and high optical transparency. Those merits of TMD have not been applied for transparent and flexible solar cell, which is attracted intense attention as a next-generation energy harvesting technology. Recently, we have developed a new fabrication process of TMD-based solar cell. In our process, Schottky type device configuration is utilized, which can be simply formed by asymmetrically contacting electrodes and CVD grown TMD. The power conversion efficiency (PCE) can be reached up to 0.7 %, which is the highest value for solar cell with similar TMD thickness.

In order to apply this Schottky type device to the highly transparent solar cell, it is required to use transparent electrode such as ITO in both carrier generation and collection side, which is required high and low Schottky barrier, respectively. Thus, controlling Schottky barrier height (SBH) is important. To control SBH, in this study, we tried to directly measure the band structure around the contact region of our solar cell by using spatially resolved photoexcited charge-carrier mapping (SPCM). The SBH was also controlled by tuning the work function of ITO by covering its surface with various thin metals (Mx = Ag, Au, Cu, Ni). Based on this study, it was revealed that SBH can be drastically changed by thin metal coating. Mx = Cu includes weaker Fermi level pinning (FLP) effect and higher SBH, resulting in better PCE compared with other metals (Mx = Ni, Ag, Au). Inserting an insulating oxide film material WO3 was found to reduce the FLP, obtaining the drastic improvement of SBH and PCE. This finding is important to realize highly transparent solar cell with TMD.

3:24pm – 3:36pm

Prediction of bandgap in transition metal oxide double perovskites using data-driven machine learning models with the help of instrumental variables

Omkar subhasish Khuntia[1], Siddharth Sradhasagar[2], Amritendu Roy[3]

[1]IIT Bhubaneswar, India; [2]IIT Bhubaneswar, India; [3]IIT Bhubaneswar, India; osk10@iitbbs.ac.in

Rising carbon footprint and environmental pollution due to traditional, fossil fuel-based

technologies have resulted in a paradigm shift in the energy sector and moved the focus to cleaner and renewable energy such as solar, wind, tidal and geothermal technologies. Of these, solar energy-based technologies, especially solar photovoltaic (PV) technology, turns out to be extremely promising. Therefore, harnessing it with utmost efficiency through different types of solar photovoltaic cells is the need of the hour. Lead halide-based perovskites have recently demonstrated large conversion efficiency, albeit lead toxicity and materials instability and degradation [1]. This leaves huge incentives for the search of novel, affordable and efficient PV materials. Transition metal oxide (TMO) -based perovskites and double perovskites with superior stability and innocuousness could be viable alternatives. However, suitable material selection should be made to realize their potential as efficient PV material. In this regard, the most important screening parameter is the nature and magnitude of the band-gap of the material.

Finding prospective solar cell materials using the advanced data-driven technology has

gained popularity due to its fast and reliable approach to materials discovery and improved property prediction compared to previously used resource-intensive methods such as density functional theory (DFT) calculations. However, predicting the bandgap of materials is challenging as typical electronic structure calculations based on DFT often make inaccurate predictions. Keeping this in mind, in our work, we have proposed a machine learning model to predict the nature and magnitude of electronic bandgap of transition metal oxide double perovskites. A progressive learning method with instrumental variables, i.e., formation energy, unit-cell volume, structural parameters (a, b, c, α, β, γ), space group, number of constituent atoms, and standard atomic properties, has helped to produce a ML model with significant.

accuracy and enhanced prediction performance [2, 3]. The ML model with the minimal dataset

using an optimal set of features was used to validate and test the developed model to predict and

further analyze the bandgap of double perovskite TMOs.

Oral Talk-8: Oral Talk

Time: Thursday, 12/Jan/2023: 2:00pm - 3:36pm · *Location:* Hall 3

2:00pm – 2:12pm

Theoretical and experimental validation on effectiveness of radiative cooler for solar cells

Gil Ju Lee[1], Se-Yeon Heo[2], Do Hyeon Kim[2], Young Min Song[2]

[1]Pusan National University; [2]Gwangju Institute of Science and Technology (GIST); gjlee0414@pusan.ac.kr

The power-conversion efficiency of solar cells (SCs) is reduced at high temperatures. The radiative cooling process can be implemented to overcome this issue. The radiative cooler (RC) presents considerable potential in the design of an ideal broadband emitter, which emits heat through the entire atmospheric transmittance window (wavelength ~ 8-13 μm) for devices with operating temperatures that significantly exceed the ambient temperature (298 K). However, the performance of these devices varies based on the type of solar cells. This study aims to determine the dependency of the radiative cooling power for various types of solar cells and proposes the multi junction solar cell (MJSC), which is the SC that benefits the most from RCs. The integrated cooler is designed with a micro-grating which can enhance the emissivity within entire atmospheric transmittance window and can also improve the light-trapping (LT) aspect. A solar simulator is employed in the integrated device to improve the cell efficiency from 25.4% to 26.7 %. Additionally, outdoor field tests demonstrate both the enhanced cooling performance and the power conversion efficiency of the proposed MJSC when compared to conventional glass-mounted MJSC under direct sunlight of ~900 W/m2 including a temperature drop of ~5°C and minimization of the variation of the open-circuit voltage to ~6%. Future research includes the development of a theoretical bridge between the field of SCs and radiative cooling.

2:12pm – 2:24pm

Toward efficient solid oxide protonic electrolysis cells for large scale hydrogen production

Leonard Kwati[1], Wilhelm A. Meulenberg[2], Tatsumi Ishihara[3], Hiroshige Matsumoto[4]

[1]WPI-I2CNER KYUSHU UNIVERSITY, Japan; [2]Institute of Energy and Climate Research, Materials Synthesis and Processing (IEK-1), Forschungszentrum Jülich; [3]WPI-I2CNER KYUSHU UNIVERSITY, Japan; [4]WPI-I2CNER KYUSHU UNIVERSITY, Japan; kwati@i2cner.kyushu-u.ac.jp

Toward efficient solid oxide protonic electrolysis cells for large scale hydrogen production

1 Kwati Leonard 1, Wilhelm A. Meulenberg2, Tatsumi Ishiraha1, Hiroshige Matsumoto 1

1 International Institute for Carbon Neutral Energy Research (I2CNER), Kyushu University 744 Motooka, Nishi-ku, Fukuoka 819-0395, Japan

2 Institute of Energy and Climate Research, Materials Synthesis and Processing (IEK-1), Forschungszentrum Jülich GmbH, Leo-Brandt-Str., D-52425 Jülich, Germany

E Mail;kwati@i2cner.kyushu-u.ac.jp

Proton-conducting solid-oxide electrolyzer and fuel cells are promising viable, intermediate temperature technologies for H2 production and energy conversion. Despite progress made with small-scale laboratory-type cells in recent years, a significant challenge continues to be upscaling robust and affordable planar-type devices. In the present contribution, 5 × 5 cm2 planar cathode-supported protonic electrolysis half-cell consisting of newly developed Ba(Zr0.5Ce0.4)8/9Y0.2O2.9 electrolyte, NiO-SrZr0.5Ce0.4Y0.1O3-δ cathode functional layer, and NiO-Ba(Zr0.5Ce0.4)8/9Y0.2O2.9 substrate (Figure.1) were successfully processed using sequential tape casting. The sintering parameters of the half-cells were analyzed and adjusted to obtain defect-free half-cells with diminished warping. The smooth tri-layered green tapes yielded suitably dense and gas-tight electrolyte layers after co-sintering at 1350 ºC/5h. Current-voltage characteristics and hydrogen evolution rates measured in the temperature range 500-600°C, using Ba0.5La0.5CoO3−δ as the anode, demonstrate excellent performance and durability

Keywords: proton conducting ceramics, steam electrolysis, hydrogen production, upscaling, tape casting

[1] KWATI, L., YUJI, O., MATSUMOTO, H., “Efficient intermediate-temperature steam electrolysis with proton-conducting perovskites.,” J. Mater. Chem. A, 2018.

2:24pm - 2:36pm

Portable Biosensors for Chlorpyrifos Detection using NFC Smartphones

Angkana Phongphut[1], Seeroong Prichanont[2], Amorn Jiraseree-amornkun[3], Aricha Olarnwanich[3], Chanchana Thanachayanont[1]

[1]National Metal and Materials Technology Center, Thailand; [2]Department of Chemical Engineering, Faculty of Engineering, Chulalongkorn University, Thailand; [3]Silicon Craft Technology PLC, Thailand; chanchm@mtec.or.th

Enzyme-electrochemical sensors based on near field communication (NFC) enabled smartphone to detect chlorpyrifos, an organophosphate pesticide were investigated. The system was composed of an electrochemical NFC tag sensor, a smartphone and an acetylcholinesterase (AChE)-modified screen-printed carbon electrode (SPCE). The NFC potentiostat (SIC4341: ISO14443A) and an android application were designed by Silicon Craft Technology PLC, Thailand, to be used as an NFC-enabled smartphone to wirelessly power the sensor and receive detection results through inductive coupling. Montmorillonite/gold nanoparticle composite (Mt/AuNPs) was used as AChE carrier. The Mt/AuNPs was synthesized using the chemical reduction of gold precursor with anchoring 3-aminopropyl triethoxysilane (APTES) on the Mt surface. AChE was immobilized on Mt/AuNPs (denoted as Mt/AuNPs/AChE), then the Mt/AuNPs/AChE was dropped cast onto the SPCE surface and covered by chitosan (CS) denoted as SPCE/Mt/AuNPs/AChE/CS [1].

The NFC-based electrochemical biosensors quantified chlorpyrifos concentration using amperometric technique, i. e., measuring the anodic current from thiocholine before and after chlorpyrifos inhibition. The initial response of the biosensors was tested in a 0.1 M phosphate buffer solution (PBS, pH 9.0) containing acetylthiocholine chloride (ATCh). Then the electrode was rinsed once with the 0.1 M PBS and incubated in a chlorpyrifos for 10 minutes. Finally, the electrode was then tested in the same ATCh solution for the second amperometric measurement. The inhibition percentage of AChE by the pesticide was calculated as Inhibition (%) = [(ΔI1 - ΔI2)/ΔI1] x 100. Under an optimum condition [1], linear calibration curves were obtained in two ranges, i. e., 0.01-0.5 ppm and 0.5-5.0 ppm, with a detection limit of 0.002 ppm. The performance of the biosensors was verified in real samples such as celery juice, cherry tomato juice, and Chinese kale juice which were the most reported pesticide residual in Thailand [2]. The chlorpyrifos was added in the juice samples and the recovery ratios were all within the range (0.01-5.0 ppm) of 93.72±17.13%, 89.97±10.07%, and 95.52±23.87% for celery juice, cherry tomato juice, and Chinese kale juice, respectively. After 4 weeks of storage at 4 °C, the current was 81.8% of its original value.

[1] PHONGPHUT, A., CHAYASOMBAT, B., CASS, A. E. G., SIRISUK, A., PHISALAPHONG, M., PRICHANONT, S. & THANACHAYANONT, C. 2020. Clay/au nanoparticle composites as acetylcholinesterase carriers and modified-electrode materials: A comparative study. Applied Clay Science, 194, 105704.

[2] THAI-PAN, T. P. A. N. 2020. Surveillance results of pesticide residues in vegetables and fruits in 2020. 4 December 2020 ed.

2:36pm - 2:48pm

Bio-fluorometric imaging system for volatile organic compounds in breath and transdermal gas

Kenta Iitani[1], Geng Zhang[2], Koji Toma[1], Takahiro Arakawa[1,3], Kohji Mitsubayashi[1,2]

[1]Institute of Biomaterials and Bioengineering, Tokyo Medical and Dental University (TMDU), Japan; [2]Graduate School of Medical and Dental Sciences, Tokyo Medical and Dental University (TMDU); [3]Department of Electric and Electronic Engineering, Tokyo University of Technology, Japan; i.bdi@tmd.ac.jp

Highly frequent assessment of biomarkers needs to realize early detection of diseases and disorders. Although the blood test is the gold standard for measuring biomarkers, it is not optimal for routine and facile testing of biochemical status because of its invasiveness. In contrast, breath and transdermal gas contain a trace amount of volatile organic compounds (VOCs) derived from blood, and also can be collected noninvasively. Therefore, continuous measurement of those VOCs enables disease screening and metabolism monitoring1,2. In this study, we developed a gas-phase biosensor system that allows quantitative measurement and imaging of specific VOC in breath and transdermal gas by utilizing enzymatic reaction with high substrate specificity.

Ethanol (EtOH) was selected to develop the gas-phase biosensor system for model VOC. Amount of gaseous EtOH was transduced to intensity of visible fluorescence (wavelength of 490 nm) via enzymatic reaction of alcohol dehydrogenase (ADH, from Saccharomyces cerevisiae). ADH was immobilized to 90 mm × 90 mm of a cotton mesh substrate by 2.5% glutaraldehyde solution. When gaseous EtOH was applied to the ADH-immobilized mesh, the distribution of fluorescence intensity was represented as concentration distribution of gaseous EtOH. A highly sensitive camera captured fluorescence change in real-time. Quantitative imaging of gaseous EtOH was possible by analyzing sequential images of fluorescence on the ADH-immobilized mesh. In the experiment, 100 ppm of standard EtOH gas was applied to the ADH-immobilized mesh with the coexistence of oxidized form of nicotinamide adenine dinucleotide (NAD+) under irradiation of 340 nm light. The gas application time was 20 sec with a flow rate of 200 mL/min.

When gaseous ethanol was applied to the ADH-immobilized mesh wetted with NAD+ solution, an increase of fluorescence intensity at the gaseous EtOH application area was observed. The fluorescence intensity immediately converged to a constant value after stopping gaseous EtOH application. Generally, the reaction speed of the enzyme is increased linearly according to the substrate concentration substrate during the first-order phase3. Therefore, we applied time-domain image differential analysis using a custom python script in ImageJ to calculate the change rate of fluorescence intensity. As a result, spatiotemporal changes in response to the gaseous EtOH application was obtained. Finally, we achieved imaging ethanol in the breath and skin gas emitted from subject who taking alcohol beverage (experiments approved by Tokyo Medical and Dental University, #M2018-160).

2:48pm – 3:00pm

Biochemical monitoring of external ear-derived ethanol vapor after drinking

Geng Zhang[1], Shota Suzuki[1], Kenta Iitani[2], Koji Toma[2], Takahiro Arakawa[2,3], Kohji Mitsubayashi[1,2]

[1]Graduate School of Medical and Dental Sciences, Tokyo Medical and Dental University (TMDU), Japan; [2]Institute of Biomaterials and Bioengineering, Tokyo Medical and Dental University (TMDU), Japan; [3]Department of Electric and Electronic Engineering, Tokyo University of Technology, Japan; ma201102@tmd.ac.jp

Measurement of volatile organic compounds (VOCs) released from a human body holds a great potential for non-invasive and simple assessment of metabolisms or diseases screening. A suitable part of a body for real-time VOC monitoring should release VOCs continuously with minimum interference by, e.g., sweat or physical burdens. In this contribution, we introduce a biochemical monitoring system for external ear-derived ethanol vapor.

The monitoring system comprised of an over-ear gas collection cell and a biochemical gas sensor (bio-sniffer) for ethanol. Purified-air carrier gas was injected to the inlet and transported the ear-derived gas from the outlet to the bio-sniffer. Ethanol bio-sniffer was composed of a bifurcated optical fiber, which was connected to a UV-LED (λ=340 nm) and a photomultiplier tube, and an alcohol dehydrogenase (ADH)-immobilized membrane. Gaseous ethanol was oxidized through ADH-catalyzed reaction together with reduction of co-enzyme, β-nicotinamide adenine dinucleotide (NAD). Ethanol was finally measured by detecting the autofluorescence of a product of this reaction, reduced form of NAD (NADH), at the wavelength of 490 nm.

Characterization of the monitoring system demonstrated the high sensitivity with a broad dynamic range (26 ppb–554 ppm), high selectivity to ethanol and capability of continuous measurement, which allowed us for application of the monitoring system to external ear-derived ethanol vapor after drinking alcohol. The experiment revealed that there was little interference from sweat in sensor signals at the external ear; similar temporal change of ethanol concentration to that of breath with delayed peak time (avg. 13 min); the

concentration of 148 ppb. These features indicate the suitability of external ears for non-invasive blood VOCs monitoring and the high degree of usefulness of the developed monitoring system.

3:00pm – 3:12pm

Development of magnetophoretic cell clustering device for intercellular interactions

Byeonghwa Lim, Jonghwan Yoon, Yumin Kang, Hyeonseol Kim, Sri Ramulu Torati, Keonmok Kim, CheolGi Kim
DGIST, Korea, Republic of (South Korea); limbh@dgist.ac.kr

Cell clustering is one of the important methods to analyze intercellular interactions at the single-cell level. Although cell clustering technologies based on microfluidics, dielectrophoresis, and acoustics have been well developed, it is still difficult to accurately manipulate cells in consideration of physical characteristics such as cell shape and size. Therefore, in this study, based on the magnetophoretic circuit technology, we developed a simple device called a “micro-distributor” that can manipulate cells according to the physical characteristics of the cells and composed a desired combination of groups. The magnetophoretic micro-distributor, consisting of trampoline micromagnets and active elements, enables automatic cell separation based on numerical simulations under various conditions and enables selective clustering according to the size by parallel control and programmable manipulation, which provide an efficient lab-on-a-chip platform for intercellular interaction analysis.

3:12pm – 3:24pm

Fabrication of Biosensing Film Robot Based on Kinetic Electronics

Shiyi Zhang[1], Kenshi Hayashi[1], Joseph Wang[2], Fumihiro Sassa[1]
[1]Kyushu University, Japan; [2]University of California San Diego, USA; zhang.shiyi.721@s.kyushu-u.ac.jp

In the current research on wearable biosensors, the characteristics of no wearing feeling, low-invasion and real-time monitoring have been fully realized[1-4]. However, the use and control of biosensors requires professional researchers to setup, which is an urgent problem to be solved in the popularization of wearable biosensors. Soft materials, which matches the mechanical properties and versatility of natural biological tissues, used in soft robots to achieve flexible and lightweight. By integrating biosensor and soft robot, it provides biosensing functions for the next generation of soft robot integrated systems, making wearable biosensors more flexible and controllable.

A new monolithic fabrication process for mass production of soft film robots that are highly compatible with integrated circuits was developed in our past research, which can be used for the fabrication of new “kinetic electronics” for applications such as active mechanical sensors, and disposable medical device end-effectors[5-6]. In order to demonstrate the integrability of biosensor and soft robot, a soft film robot based on kinetic electronics for active electrochemical biosensing was proposed(Figure 1). The film robot is composed of a bimorph actuator layer and a biosensing function layer. Sputtering technology was adopted to form gold electrodes on the sensor functional layer, and a Nafion-coated glucose oxidase and lactate oxidase electrodes were processed to form. By controlling the expansion and bending of the bimorph actuator layer, the film robot can realize flexible movement and high degree of freedom at a specific frequency or displacement distance, and has a durability of more than 8000 times. The enzymatic biosensing film robots connected to potentiostat were evaluated with standard solutions of each substrate substance. This film robot can also be used as a kinetic printed circuit for probe chips for biological and chemical experiments, and provide many opportunities and possibilities for personal health monitoring, remote diagnosis, treatment and management.

3:24pm - 3:36pm

Gas visualization by hyperspectral imaging of 2D Au/Ag core shell plasmonic device

Masato Matsuoka, Kousuke Oohiro, Fumihiro Sassa, Kenshi Hayashi
Department of Electronics, Graduate School of Information Science and Electrical Engineering, Kyushu University, Japan;
matsuoka.masato.380@s.kyushu-u.ac.jp

Visualization of chemical substances, such as odor, is an important technology that can lead to the detection of people at disaster sites and the identification of gas sources of hazardous materials. Oxide semiconductor sensors have been used as alternative sensors for olfactory sensation, but these sensors have disadvantages such as the inability to discriminate the type of odorants, slow response, and time-consuming recovery of sensor output. On the other hand, gas sensors using localized surface plasmon resonance (LSPR) of metal nanoparticles show a fast response in real time to changes in the dielectric properties of the surrounding medium and are capable of fast recovery. Using 2 dimensional LSPR substrate with Au/Ag core-shell structure, the change in optical response to gases can be checked (Fig.1). The objective of this study is to visualize the spatial distribution of two gases by transforming images using principal component analysis (PCA) on information obtained from a hyperspectral camera using the LSPR substrate.

First, response intensities for 16 different gas sources were measured using the LSPR substrate and a hyperspectral camera. The images were taken in the wavelength range from 400 nm to 900 nm, and images were taken every 5 nm. In other words, a total of 101 images were acquired. From these results, six characterized gas sources were selected, and PCA was performed on them (20 areas × 6 gases). Based on the results, two types of gases were selected to be blown. Pentadecane and geraniol were used as gas sources in this experiment. The differential image by hyperspectral camera were obtained by subtracting the image at the time of gas exposure from the image at 10 minutes after exposure. Fig.2 shows the sequence of gas visualization. This image was created by multiplying hyperspectral image data by the eigenvectors obtained by the PCA. Furthermore, each principal component was assigned as RGB values. PC1 was assigned to red, PC2 to green and PC3 to blue. As can be seen, geraniol is blown on the left side of the image as blue, and pentadecane on the right side as red. Thus, the distribution of the two gases can be clearly recognized by the difference in color.

These results show that the spatial distribution of gases can be visualized by using color transformation of hyperspectral image based on PCA using LSPR substrates with Au/Ag core-shell structure.

Tuesday, 10/Jan/2023

	Main Hall	Hall 1&2	Hall 3	Exchange Lobby
8:45	8:50am - 9:00amOpening Ceremony			
9:00	9:00am - 9:45am Plenary Session P1			
9:15				
9:30				
9:45				
10:00	10:00am - 12:06am Invited Talk-1 P2-4			
10:15				
10:30				
10:45				
11:00				
11:15				
11:30				
11:45				
12:00				8:40am - 3:00pm Registration-1
12:15	12:00pm - 1:15pm Lunch Break			
12:30				
12:45				
1:00				
1:15	1:15pm - 2:15pm Keynote Session-1 P5			
1:30				
1:45				
2:00				
2:15				
2:30	2:30pm - 4:18pm Oral Talk-9 P6-9	2:30pm - 4:18pm Oral Talk-3 P10-13	2:30pm - 4:18pm Oral Talk-1 P14-17	
2:45				
3:00				
3:15				
3:30				3:30pm - 5:00pm Poster Session-1 P18-38
3:45				
4:00				
4:15				
4:30				
4:45				
5:00				

Wednesday, 11/Jan/2023

	Main Hall	Hall 1&2	Hall 3	Exchange Lobby
8:45	8:45am - 10:45am Keynote Session-2 P39-40			
9:00				
9:15				
9:30				
9:45				
10:00				
10:15				
10:30				
10:45				
11:00	11:00am - 11:54pm Invited Talk-2 P41			
11:15				
11:30				
11:45				
12:00	12:00pm - 1:15pm Lunch Break			8:40am - 3:00pm Registration-2
12:15				
12:30				
12:45				
1:00				
1:15	1:15pm - 2:27pm Invited Talk-3 P42-43	1:15pm - 3:51pm Oral Talk-2 P44-48	1:15pm - 3:51pm Oral Talk-4 P49-53	
1:30				
1:45				
2:00				
2:15				
2:30				
2:45	2:40pm - 4:04pm Oral Talk-10 P54-56			
3:00				
3:15				
3:30				
3:45				
4:00				3:30pm - 5:00pm Poster Session-1 P58-77
4:15				
4:30				
4:45				
5:00				

Thursday, 12/Jan/2023

	Main Hall	Hall 1&2	Hall 3	Exchange Lobby
8:45		8:45am - 10:45am Keynote Session-3 P78-79	8:45am - 10:45am Oral Talk-5 P80-83	8:40am - 12:00pm Registration-3
9:00				
9:15				
9:30				
9:45				
10:00				
10:15				
10:30				
10:45				
11:00		11:00pm - 12:36pm Oral Talk-11 P84-86	11:00pm - 12:36pm Oral Talk-6 P87-89	
11:15				
11:30				
11:45				
12:00				
12:15				
12:30				
12:45		12:40pm - 2:00pm Lunch Break		
1:00				
1:15				
1:30				
1:45				
2:00		2:00pm - 3:36pm Oral Talk-7 P90-92	2:00pm - 3:36pm Oral Talk-8 P93-95	
2:15				
2:30				
2:45				
3:00				
3:15				
3:30				

− Centennial Hall Floor Plan

1F
Floor Plan

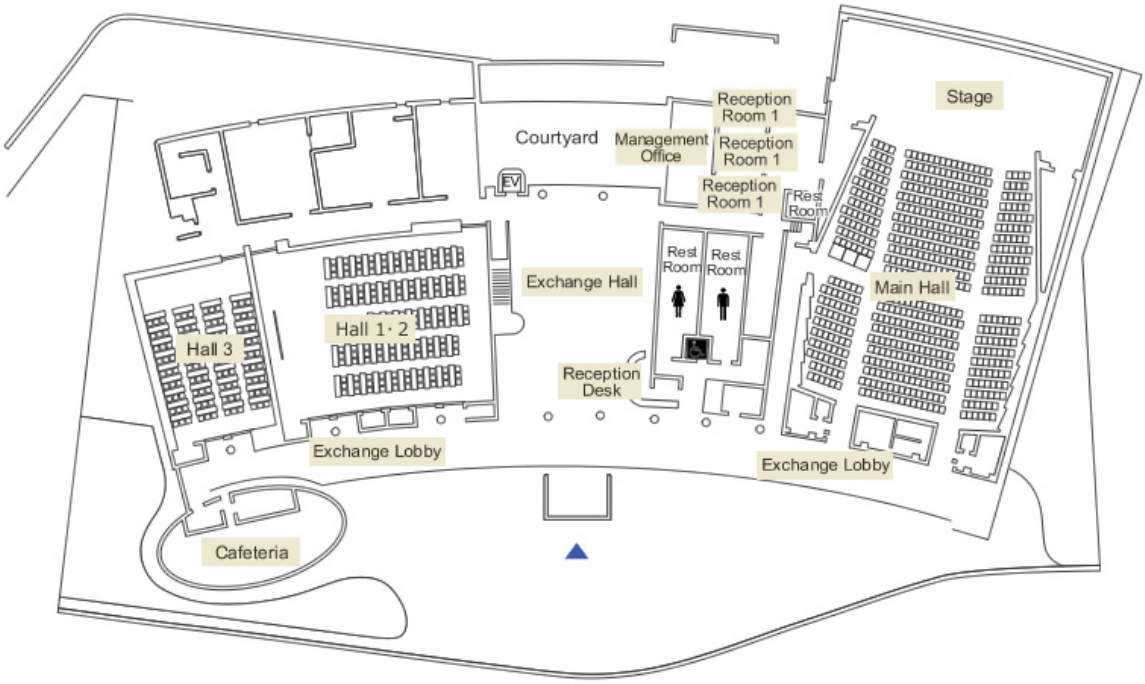

2F
Floor Plan

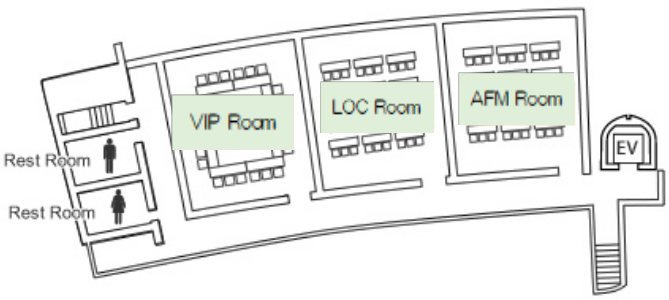

Smoking is not permitted on the grounds of Kyushu University, both indoors and outdoors.

There is no dedicated parking lot. Please use public transportation.

To prevent corona, only bottled beverages will be provided.
Please refer to the map and use nearby restaurants for meals.